U.PORTO

DOUTORAMENTO
BIOLOGIA MOLECULAR E CELULAR

UNDERSTANDING THE MOLECULAR BASES DICTATING TUBERCULOSIS SEVERITY

Ana Isabel Fernandes

D 2025

U.PORTO

Ana Isabel Fernandes. Understanding the Molecular Bases Dictating Tuberculosis Severity

D.ICBAS **2025**

Understanding the Molecular Bases Dictating Tuberculosis Severity

Ana Isabel Fernandes

SEDE ADMINISTRATIVA INSTITUTO DE CIÊNCIAS BIOMÉDICAS ABEL SALAZAR
FACULDADE DE CIÊNCIAS

ANA ISABEL MARTINS FERNANDES

UNDERSTANDING THE MOLECULAR BASES DICTATING TUBERCULOSIS SEVERITY

Tese de Candidatura ao grau de Doutor em Biologia Molecular e Celular;
Programa Doutoral da Universidade do Porto (Instituto de Ciências Biomédicas de Abel Salazar e Faculdade de Ciências)

Orientadora – Doutora Margarida Sofia da Silva Santos Saraiva
Categoria – Líder de Grupo, Investigadora Principal
Afiliação – Instituto de Investigação e Inovação em Saúde (i3S), Universidade do Porto

Coorientador – Doutor Hélder Novais e Bastos
Categoria – Investigador Principal, Professor Auxiliar Convidado
Afiliação – Faculdade de Medicina (FMUP), Universidade do Porto; Unidade de Estudos de Pneumologia, Centro Hospitalar de São João

Declaro que a presente tese é de minha autoria e não foi utilizada previamente noutro curso ou unidade curricular, desta ou de outra instituição. As referências a outros autores (afirmações, ideias, pensamentos) respeitam escrupulosamente as regras da atribuição, e encontram-se devidamente indicadas no texto e nas referências bibliográficas, de acordo com as normas de referenciação. Tenho consciência de que a prática de plágio e auto-plágio constitui um ilícito académico.

Assinado por: **Ana Isabel Martins Fernandes**
Num. de Identificação: 15141533
Data: 2025.07.21 15:05:08 +0100

CHAVE MÓVEL

The experimental work presented in this thesis was undertaken under the Ph.D. programme in Molecular and Cell Biology (MCBiology), hosted by the University of Porto, Porto, Portugal. The experimental work was mainly performed in the Immune Regulation group at the *Instituto de Investigação e Inovação em Saúde* (i3S), Porto, Portugal.

This work was funded by National Funds through *Fundação para a Ciência e a Tecnologia* (FCT) under the project PTDC/SAU-INF/1172/2021 and by the La Caixa Foundation (HR21-00415). This work was also funded by a European Society of Clinical Microbiology and Infectious Diseases (ESCMID) Research Grant 2022 awarded to Ana Isabel Fernandes.

Ana Isabel Fernandes was supported by a Ph.D grant from FCT, reference 2020.05949.BD; a Ph.D fellowship from *Instituto de Biologia Molecular e Celular* (IBMC), Porto, Portugal; a Keystone Symposia Future of Science Fund Scholarship; a *Sociedade Portuguesa de Imunologia* travel grant; and an Aegean Conference Trainee / Young Investigator Award.

LIST OF PUBLICATIONS

Publications

1. **Fernandes AI**, Pinto AJ, Silvério D, Zedler U, Ferreira C, Duarte IF, Silvestre R, Dorhoi A, Saraiva M. "Genetically diverse *Mycobacterium tuberculosis* isolates manipulate inflammasome and IL-1β secretion independently of macrophage metabolic rewiring". J Infect Dis. 2024. https://doi.org/10.1093/infdis/jiae583

2. **Fernandes AI**, Beites T, Saraiva M. "A diversidade genética do *Mycobacterium tuberculosis* e a sua contribuição para a tuberculose". Anais do IHMT. 2024. https://doi.org/10.25761/anaisihmt.463

3. Gomes AC, Sousa DM, Oliveira TC, Fonseca Ó, Pinto RJ, Silvério D, **Fernandes AI**, Moreira AC, Silva T, Teles MJ, Pereira L, Saraiva M, Lamghari M, Gomes MS. "Serum amyloid A proteins reduce bone mass during mycobacterial infections". Front Immunol. 2023. https://doi.org/10.3389/fimmu.2023.1168607

4. Gonçalves R, Couto J, Ferreirinha P, Costa JM, Silvério D, Silva ML, **Fernandes AI**, Madureira P, Alves NL, Lamas S, Saraiva M. "SARS-CoV-2 variants induce distinct disease and impact in the bone marrow and thymus of mice". iScience. 2023. https://doi.org/10.1016/j.isci.2023.105972

Oral Communications

1. **Fernandes AI.** Jan 2025. "Understanding the molecular bases dictating tuberculosis severity". i3S - Young Scientists Seminar, Porto, Portugal.

2. **Fernandes AI**, Pinto AJ, Silvério D, Zedler U, Ferreira C, Duarte IF, Silvestre R, Dorhoi A, Saraiva M. Dec 2024. "Genetically diverse *Mycobacterium tuberculosis*

isolates manipulate inflammasome activation and IL-1β secretion independently of macrophage metabolic rewiring". ADVANCE-TB, Online.

3. **Fernandes AI**, Pinto AJ, Silvério D, Zedler U, Cardoso M, Ferreira C, Duarte IF, Silvestre R, Dorhoi A, Saraiva M. Apr 2024. "Disentangling inflammasome activation and metabolic reprogramming in *Mycobacterium tuberculosis* infected macrophages". 10th MCBiology Symposium: A Decade Building Science, Porto, Portugal.

4. **Fernandes AI**, Silva ML, Gonçalves R, Silvério D, Ferreira C, Zedler U, Silvestre R, Dorhoi A, Saraiva M. Oct 2022. "Inflammasome activation and glycolytic reprogramming are uncoupled in *Mycobacterium tuberculosis* infected macrophages". 5th PhDay: Building Paths: The Science Behind Us, Porto, Portugal.
   Awarded Best Oral Communication.

Poster Communications

1. **Fernandes AI**, Pinto AJ, Silvério D, Zedler U, Cardoso M, Ferreira C, Duarte IF, Silvestre R, Dorhoi A, Saraiva M. Mar 2024. "Disentangling inflammasome activation and metabolic reprogramming in *Mycobacterium tuberculosis* infected macrophages". Keystone Symposia – Tuberculosis: The Host-Pathogen Interface, Colorado, USA.
   Awarded a Keystone Symposia Future of Science Fund scholarship and a travel grant from *Sociedade Portuguesa de Imunologia*.

2. **Fernandes AI**, Silvério D, Cardoso M, Gonçalves R, Santos RF, Saraiva M. Oct 2023. "Understanding the molecular bases dictating tuberculosis severity". 6th PhDay: Brilliant PhDs, Brighter Future: Shaping Science Together, Porto, Portugal.

3. **Fernandes AI**, Silvério D, Silva ML, Gonçalves R, Cardoso M, Ferreira C, Zedler U, Duarte IF, Silvestre R, Dorhoi A, Saraiva M. May/Jun 2023. "Breaking the link: Disentangling inflammasome activation and glycolytic reprogramming in *Mycobacterium tuberculosis* infected macrophages". 18th International Conference on Innate Immunity, Crete, Greece.
   Awarded an Aegean Conference Trainee / Young Investigator Award.

4. **Fernandes AI**, Silvério D, Silva ML, Gonçalves R, Cardoso M, Ferreira C, Zedler U, Duarte IF, Silvestre R, Dorhoi A, Saraiva M. Mar 2023. "Dissecting the dynamic interplay between inflammasome activation and glycolytic reprogramming in *Mycobacterium tuberculosis* infected macrophages". ImmunoHub Annual Meeting: Infection & Immunity, Porto, Portugal.

   Awarded Best Poster.

5. **Fernandes AI**, Silvério D, Cardoso M, Gonçalves R, Santos RF, Saraiva M. Feb 2023. "Understanding the molecular bases dictating tuberculosis severity". 9th MCBiology Symposium: Science: Everything, Everywhere, All at Once, Porto, Portugal.

6. **Fernandes AI**, Silva ML, Gonçalves R, Silvério D, Ferreira C, Zedler U, Silvestre R, Dorhoi A, Saraiva M. Sep 2022. "Inflammasome activation and glycolytic reprogramming are uncoupled in *Mycobacterium tuberculosis* infected macrophages". EMBO workshop: Tuberculosis 2022, Paris, France.

7. **Fernandes AI**, Silva ML, Gonçalves R, Silvério D, Ferreira C, Zedler U, Silvestre R, Dorhoi A, Saraiva M. Apr 2022. "Glycolytic reprogramming of *Mycobacterium tuberculosis* infected cells is uncoupled from differential inflammasome activation". XLVII Annual Meeting of the Portuguese Society for Immunology, Lisboa, Portugal.

8. **Fernandes AI**, Gonçalves R, Ferreira C, Zedler U, Silvestre R, Dorhoi A, Saraiva M. Sep 2021. "Metabolic reprogramming of *Mycobacterium tuberculosis* infected cells is uncoupled from differential inflammasome activation". EMBO workshop: The inflammasomes: The Next Frontier, Online / Martinsried, Germany.

9. **Fernandes AI**, Gonçalves R, Ferreira C, Zedler U, Silvestre R, Dorhoi A, Saraiva M. May 2021. "Understanding the metabolic reprogramming of macrophages upon infection with clinical isolates of *Mycobacterium tuberculosis*". XLVI Annual Meeting of the Portuguese Society for Immunology, Online.

Cover artwork

1. Mar 2024. Original artwork. Journal of Infectious Diseases, Volume 229, Number 3. https://academic.oup.com/jid/issue/229/3

“Effort makes you. You will regret someday
if you don’t do your best now.”

방탄소년단

ACKNOWLEDGMENTS

First and foremost, I owe my deepest gratitude to my supervisor, Margarida Saraiva, whose guidance, wisdom, and unwavering support made this journey not only possible but truly rewarding. Her mentorship shaped every aspect of this work, and her kindness and belief in me extended far beyond the lab. I am endlessly grateful to have had her as both a mentor and a friend. I would also like to thank my co-supervisor, Hélder Novais e Bastos, for his support and for being part of this academic endeavour.

I'm deeply grateful to the outstanding collaborators who helped make this work what it is. To Anca Dorhoi, for her expertise, support, and the countless ways she inspired this project. To Ricardo Silvestre, whose thoughtful discussions on metabolism were invaluable in driving this work forward. And to Iola Duarte, for the crucial help with metabolomics, which opened new avenues in my research. A special thanks goes to Anne O'Garra, for her thoughtful advice as I consider my next steps.

A special thanks to the Immune Regulation group, past and present members, for being my academic home over these years. I've been incredibly lucky to share the lab with all of them. From the intense BSL3 work to the everyday moments, this group has been a constant source of support. A particular thanks to Catarina, Diogo, Marta, Rute, Marco, Joana, and Alex whether troubleshooting experiments, venting about failed ones, or laughing through late nights in the lab, they kept me grounded, motivated, and (relatively) sane. I couldn't have asked for better colleagues and friends, and I couldn't have done this without them.

Finally, to my family for their unwavering support, love, and patience. This achievement is as much theirs as it is mine.

TABLE OF CONTENTS

LIST OF PUBLICATIONS V

ACKNOWLEDGMENTS IX

TABLE OF CONTENTS XI

LIST OF FIGURES XIII

LIST OF TABLES XVI

LIST OF ABBREVIATIONS XVII

RESUMO XXI

ABSTRACT XXIII

CHAPTER 1: INTRODUCTION 1

1.1. TUBERCULOSIS THROUGHOUT HISTORY 3

1.2. THE GLOBAL BURDEN OF TUBERCULOSIS 4

1.3. CORE STRATEGIES IN TUBERCULOSIS CONTROL 5

1.4. THE DYNAMIC SPECTRUM OF TUBERCULOSIS 7

1.5. IMMUNE MECHANISMS IN TUBERCULOSIS PATHOGENESIS 10

1.5.1. INNATE IMMUNITY: EARLY DEFENCE WITH LASTING CONSEQUENCES 12

- MACROPHAGES, THE FIRST LINE OF DEFENCE 14

- NEUTROPHILS AND THEIR DUAL ROLE 15

1.5.2. ADAPTIVE IMMUNITY: A DELAYED BUT ESSENTIAL DEFENCE 16

- $CD4^+$ T CELLS AND THEIR CENTRAL ROLE IN TUBERCULOSIS PROTECTION 18

- THE ROLE OF $CD8^+$ T CELLS 19

- B CELLS AND ANTIBODIES 19

1.5.3. IMMUNE MEDIATORS IN TUBERCULOSIS 20

1.6. THE PATHOGEN BEHIND TUBERCULOSIS 23

1.6.1. THE EVOLUTION AND DIVERSITY OF THE *MYCOBACTERIUM TUBERCULOSIS* COMPLEX 23

1.6.2. THE IMPACT OF BACTERIAL DIVERSITY ON TUBERCULOSIS OUTCOMES 24

- IMPACT ON TUBERCULOSIS PRESENTATION AND TRANSMISSION 25

- IMPACT ON THE IMMUNE RESPONSE 26

1.7. FUELLING THE FIGHT: HOW METABOLISM SHAPES IMMUNITY 28

1.7.1. MACROPHAGE METABOLISM AND TUBERCULOSIS CONTROL 29

1.7.2. THE IMPORTANCE OF BACTERIA VIABILITY IN IMMUNOMETABOLIC REPROGRAMMING 33

CHAPTER 2: AIMS 67

CHAPTER 3: EXPERIMENTAL RESULTS

GENETICALLY DIVERSE *MYCOBACTERIUM TUBERCULOSIS* ISOLATES MANIPULATE INFLAMMASOME AND INTERLEUKIN 1β SECRETION INDEPENDENTLY OF MACROPHAGE METABOLIC REWIRING 71

CHAPTER 4: EXPERIMENTAL RESULTS

TWO MICE, TWO FATES: HOW HOST DIVERSITY SHAPES IMMUNE RESPONSES TO *MYCOBACTERIUM TUBERCULOSIS* 97

CHAPTER 5: GENERAL DISCUSSION 141

APPENDIX 148

LIST OF FIGURES

Chapter 1 – Introduction

Figure 1. Estimated tuberculosis incidence rates, 2023 4
Figure 2. Timeline of tuberculosis treatments 7
Figure 3. Dynamic spectrum of infection and containment of *M. tuberculosis* 9
Figure 4. Immune response to *M. tuberculosis* infection 12
Figure 5. Innate immune defences against *M. tuberculosis* infection 13
Figure 6. *M. tuberculosis* subverts adaptive immunity through multiple mechanisms 17
Figure 7. Immune mediators involved in the regulation of IL-1β production 22
Figure 8. Phylogeny of *M. tuberculosis* lineages 24
Figure 9. Macrophage metabolic dynamics during *M. tuberculosis* infection 32

Chapter 3 – Genetically Diverse *Mycobacterium tuberculosis* Isolates Manipulate Inflammasome and Interleukin 1β Secretion Independently of Macrophage Metabolic Rewiring

Figure 1. Glucose consumption contributes to IL-1β production by infected macrophages 76
Figure 2. Glycolysis does not differ between the 2 *Mycobacterium tuberculosis* clinical isolates 78
Figure 3. DMM inhibits inflammasome activation and IL-1β production independently of mitochondrial ROS and mTOR 79
Figure 4. The impact of metabolic inhibitors on IL-1β is not cell specific 80
Figure 5. NMR-based metabolomic analysis of macrophages infected with *Mycobacterium tuberculosis* clinical isolate 4I2 and 6C4 reveal similar metabolic profiles 81
Figure 6. IL-1β production by *Mycobacterium tuberculosis*-infected macrophages is independent of HIF-1α and IRG1 activity 82
Figure 7. Infection of macrophages with *Mycobacterium tuberculosis* 4I2 exposed to DMM results in reduced inflammasome activation and IL-1β production 83

Supplementary Figure 1. 87
Supplementary Figure 2. 88
Supplementary Figure 3. 89
Supplementary Figure 4. 90
Supplementary Figure 5. 92

Chapter 4 – Two Mice, Two Fates: How Host Diversity Shapes Immune Responses to *Mycobacterium tuberculosis*

Figure 1. The impact of *M. tuberculosis* 4I2 and 6C4 infection in the lungs of infected susceptible and resistant mice 111
Figure 2. Immune cell recruitment in the lungs of C3HeB/FeJ and C57BL/6 mice upon infection with *M. tuberculosis* 114
Figure 3. IL-1β production in C3HeB/FeJ and C57BL/6 mice 117
Figure 4. Potential candidates for the modulation of IL-1β in C3HeB/FeJ macrophages 121

Supplementary Figure 1. Representative images obtained during morphometric analysis of lung histopathology 130
Supplementary Figure 2. Gating strategy for analysis of mature immune cell populations in the lung and bronchoalveolar lavage by flow cytometry 131
Supplementary Figure 3. Bacterial burdens and weight variation over time in C3HeB/FeJ and C57BL/6 mice following *M. tuberculosis* infection 132
Supplementary Figure 4. Total cell numbers in the lungs of C3HeB/FeJ and C57BL/6 uninfected mice 133
Supplementary Figure 5. The immune cell recruitment in the bronchoalveolar lavage of C3HeB/FeJ and C57BL/6 mice following *M. tuberculosis* infection mirrors alterations observed in the lung 134
Supplementary Figure 6. C3HeB/FeJ macrophages show increased viability compared to C57BL/6 macrophages and no differences in bacterial burden 135
Supplementary Figure 7. C3HeB/FeJ macrophages exhibit a lower pro-inflammatory cytokine profile 137

Chapter 5 – General Discussion

Figure 1. IL-1β modulation by the pathogen and the host shapes tuberculosis severity 146

Appendix

Figure 1. NMR-based metabolomics reveals increased levels of trehalose in *M. tuberculosis* 6C4 conditions. 148

LIST OF TABLES

Chapter 3 – Genetically Diverse *Mycobacterium tuberculosis* Isolates Manipulate Inflammasome and Interleukin 1β Secretion Independently of Macrophage Metabolic Rewiring

Supplementary Table 1.	List of materials and resources	93
Supplementary Table 2.	List of oligonucleotide sequences	95

Chapter 4 – Two Mice, Two Fates: How Host Diversity Shapes Immune Responses to *Mycobacterium tuberculosis*

Supplementary Table 1.	List of materials and resources	138
Supplementary Table 2.	Histological features used for qualitative analysis of the lung pathology	140
Supplementary Table 3.	List of oligonucleotide sequences	140

LIST OF ABBREVIATIONS

2-DG	2-deoxy-D-glucose
6AN	6-animonicotinamide
ACK	Ammonium-chloride-potassium
AIM2	Absent in melanoma 2
ANOVA	Analysis of variance
APCs	Antigen-presenting cells
ARRIVE	Animal research: reporting of in vivo experiments
ASC	Associated speck-like protein containing caspase recruitment domains
ATP	Adenosine triphosphate
au	Arbitrary units
B6	C57BL/6 mice
BCG	Bacillus Calmette-Guérin
bdl	Below detection level
BMDM	Bone marrow-derived macrophages
C3H	C3HeB/FeJ mice
CCL2	C-C motif chemokine ligand 2
CD	Cluster of differentiation
cDNA	Complementary deoxyribonucleic acid
CFU	Colony-forming units

cGAS	Cyclic GMP-AMP synthase
CID	PubChem compound identification
CLR	C-type lectin receptor
DGAV	*Direção Geral de Alimentação e Veterinária*
DMEM	Dulbecco's modified medium
DMM	Dimethyl malonate
DNA	Deoxyribonucleic acid
ECAR	Extracellular acidification rate
EDTA	Ethylenediaminetetraacetic acid
ELISA	Enzyme-linked immunosorbent assay
ESAT-6	Early secreted antigenic target 6 kDa
ESX-1	ESAT-6 secretion system
ETC	Electron transport chain
FAO	Fatty acid oxidation
FBS	Foetal bovine serum
GFP	Green fluorescent protein
GM-CSF	Granulocyte-macrophage colony-stimulating factor
H&E	Haematoxylin and eosin
HIF-1α	Hypoxia-inducible factor 1 alfa
HIV	Human immunodeficiency virus
HPLC	High-performance liquid chromatography
IFN	Interferon
IGRA	Interferon gamma release assay
IL	Interleukin

iNOS	Inducible nitric oxide synthase
IRG1	Immune responsive gene 1
LCCM	L929 cell-conditioned medium
LPS	Lipopolysaccharide
MHC-II	Major histocompatibility complex class II
MOI	Multiplicity of infection
Mtb	*Mycobacterium tuberculosis*
MTBC	*Mycobacterium tuberculosis* complex
mTOR	Mammalian target of rapamycin
NETs	Neutrophil extracellular traps
NF-κB	Nuclear factor kappa B
NI	Non-infected
NLR	NOD-like receptor
NLRP3	NLR family pyrin domain–containing-3
NMR	Nuclear magnetic resonance
NS	Non-stimulated
o/n	Overnight
OADC	Oleic albumin dextrose catalase
OXPHOS	Oxidative phosphorylation
p.i.	Post-infection
PAMPs	Pathogen-associated molecular patterns
PBS	Phosphate buffered saline
PCA	Principal component analysis
PCR	Polymerase chain reaction

PDIM	Phthiocerol dimycocerosate
PFA	Paraformaldehyde
PMA	Phorbol 12-myristate 13-acetate
PRR	Pattern recognition receptor
RD1	Region of difference 1
RNA	Ribonucleic acid
ROS	Reactive oxygen species
RPMI	Roswell Park Memorial Institute
SD	Standard deviation
SDH	Succinate dehydrogenase
SEM	Standard error of the mean
TbD1	Tuberculosis-specific deletion 1
TCA	Tricarboxylic acid
TGFβ	Transforming growth factor beta
T_H	T helper
TLR	Toll-like receptor
TNF	Tumour necrosis factor
TST	Tuberculin skin test
WHO	World Health Organization

RESUMO

A tuberculose permanece uma das principais causas de morte a nível mundial, com cerca de 1,25 milhões de óbitos registados anualmente. Esta doença, causada pela bactéria *Mycobacterium tuberculosis*, resulta de uma interação complexa e heterogénea entre o hospedeiro, o agente patogénico e o ambiente. Acredita-se que os eventos imunitários iniciais desempenham um papel determinante na progressão para doença ativa e na gravidade da infeção. No entanto, os mecanismos moleculares subjacentes à evolução para diferentes formas clínicas da tuberculose permanecem, em grande parte, desconhecidos.

O nosso laboratório demonstrou previamente que isolados clínicos obtidos de doentes com apresentação clínica de tuberculosis severa conseguem evadir os sistemas citosólicos de vigilância em macrófagos, resultando numa reduzida ativação do inflamassoma e produção de interleucina (IL)-1β. Dado o papel central da IL-1β na resistência do hospedeiro a *M. tuberculosis* e a sua associação frequente à reprogramação metabólica dos macrófagos, nós investigámos a relação entre a modulação diferencial do inflamassoma e o metabolismo dos macrófagos. Os nossos resultados indicam que o perfil metabólico dos macrófagos permanece inalterado independentemente do isolado de *M. tuberculosis* envolvido. Tal como observado em macrófagos ativados por lipopolissacárido (LPS), a inibição da glicólise durante a infeção comprometeu a secreção de IL-1β. No entanto, contrariamente aos modelos baseados na ativação de recetores Toll-like (TLR), nos macrófagos infetados, a secreção de IL-1β revelou-se independente de alterações no metabolismo mitocondrial, sendo maioritariamente dependente de mecanismos específicos da bactéria. Adicionalmente, identificámos um efeito inesperado de um inibidor metabólico do hospedeiro sobre *M. tuberculosis*, demonstrando que a ativação do inflamassoma e a produção de IL-1β pelos macrófagos requerem bactérias metabolicamente ativas. Estes resultados destacam o potencial impacto dos inibidores metabólicos do hospedeiro na resposta a *M. tuberculosis* e evidenciam a dissociação entre a modulação do inflamassoma pela bactéria e a reprogramação metabólica do hospedeiro.

Para além de investigarmos o impacto da diversidade bacteriana na resposta imunitária à tuberculose, analisamos o papel do perfil genético do hospedeiro na modulação da resposta imunitária à infeção por *M. tuberculosis*. Para isso, recorremos a ratinhos C3HeB/FeJ, suscetíveis à doença, e C57BL/6, mais resistentes. Como esperado, C3HeB/FeJ infetados com *M. tuberculosis* apresentaram lesões pulmonares mais organizadas, dominadas por neutrófilos, e uma carga bacteriana superior 30 dias após a infeção, enquanto C57BL/6 desenvolveram lesões mais difusas e um recrutamento aumentado de células imunitárias adaptativas. Este perfil divergente de resposta imunitária em ratinhos suscetíveis e resistentes revelou-se independente da diversidade genética de *M. tuberculosis*. Além disso, ao comparar a resposta imunitária destas duas estirpes de ratinho a diferentes isolados clínicos de *M. tuberculosis*, verificámos que, em comparação com C57BL/6, a produção de IL-1β encontrava-se comprometida em C3HeB/FeJ. Este défice na resposta de IL-1β poderá contribuir para a maior suscetibilidade dos C3HeB/FeJ à infeção. Mecanisticamente, os nossos dados sugerem um papel da sinalização de IL-27, IL-10 e/ou óxido nítrico na supressão de IL-1β nesta estirpe de ratinhos.

No seu conjunto, os nossos resultados evidenciam a relação complexa entre a genética do hospedeiro, a diversidade do agente patogénico e as respostas imunitárias na progressão da tuberculose, destacando a complexidade no desenvolvimento de estratégias terapêuticas direcionadas para a tuberculose.

PALAVRAS-CHAVE: *Mycobacterium tuberculosis*, imunometabolismo, inflamassoma, interleucina 1β, macrófago, severidade da doença, resposta imunitária.

ABSTRACT

Tuberculosis remains a leading cause of death worldwide, with around 1.25 million deaths reported annually. This disease, caused by *Mycobacterium tuberculosis*, is driven by a complex and heterogeneous interplay between host, pathogen, and environmental factors. Upon *M. tuberculosis* infection, early immune events are thought to be crucial in determining progression to tuberculosis disease and subsequent severity of the disease. Nevertheless, the molecular mechanisms that promote and lead to tuberculosis of varying severities remain largely unexplored.

We have previously shown that clinical isolates recovered from patients with severe forms of tuberculosis evade cytosolic surveillance systems in macrophages and trigger reduced inflammasome activation and interleukin (IL)-1β production. Given the key role of IL-1β in host resistance to *M. tuberculosis* and its common association with the metabolic reprogramming of macrophages, we assessed whether the differential inflammasome modulation was linked to macrophage metabolism. We found that the macrophage metabolic landscape was similar regardless of the infecting *M. tuberculosis* isolate. Paralleling lipopolysaccharide (LPS)-activated macrophages, glycolysis inhibition during infection impaired IL-1β secretion. However, unlike single toll-like receptor (TLR)-based models, in infected macrophages, IL-1β secretion was independent of mitochondrial metabolic changes and primarily relied on bacteria-specific mechanisms. Additionally, we discovered an unappreciated impact of a host metabolic inhibitor on the pathogen and showed that inflammasome activation and IL-1β production by macrophages require metabolically active bacteria. Our study highlights the potential confounding effect of host metabolic inhibitors on the pathogen and the uncoupling of *M. tuberculosis*-inflammasome modulation from the host metabolic reprogramming.

In addition to exploring the role of the pathogen's diversity in the immune response during tuberculosis, we also investigated how the host's genetic background can shape immune responses to *M. tuberculosis* infection using tuberculosis-susceptible C3HeB/FeJ mice and the more resistant C57BL/6 mice. As expected, while *M. tuberculosis*-infected C3HeB/FeJ mice exhibited more organised lung lesions dominated by neutrophils, with

higher bacterial loads 30 days post-infection, C57BL/6 mice had more diffuse lesions and higher recruitment of adaptive immune cells. This divergent immune response profile in susceptible and resistant mice was independent of the *M. tuberculosis* genetic background. Additionally, by comparing the immune response of these two strains of mice to distinct *M. tuberculosis* clinical isolates, we found that as compared to C57BL/6 mice, IL-1β production appeared to be impaired in C3HeB/FeJ mice. This defective IL-1β response likely contributes to the higher susceptibility of the C3HeB/FeJ mice. Mechanistically, our data so far point to a possible role of IL-27, IL-10, and/or nitric oxide signalling in limiting IL-1β responses in C3HeB/FeJ mice.

Overall, our study underscores the intricate relationship between host genetics, pathogen diversity, and immune responses in determining tuberculosis outcomes, emphasising the intricacies involved in developing targeted therapies for tuberculosis.

KEYWORDS: *Mycobacterium tuberculosis*, immunometabolism, inflammasome, IL-1β signalling, macrophage, disease severity, immune response.

CHAPTER 1

INTRODUCTION

Part of this chapter has been adapted and disseminated in Portuguese as part of an outreach output:

A DIVERSIDADE GENÉTICA DO *MYCOBACTERIUM TUBERCULOSIS* E A SUA CONTRIBUIÇÃO PARA A TUBERCULOSE

Ana Isabel Fernandes[1,2], Tiago Beites[1], Margarida Saraiva[1,3]

[1] Instituto de Investigação e Inovação em Saúde, Universidade do Porto, Porto, Portugal

[2] Programa Doutoral em Biologia Molecular e Celular, Instituto de Ciências Biomédicas Abel Salazar, Universidade do Porto, Porto, Portugal

[3] Instituto de Biologia Molecular e Celular, Universidade do Porto, Porto, Portugal

Published in:

https://doi.org/10.25761/anaisihmt.463 **Anais do IHMT** 2024

A section of this chapter is in preparation for publication:

THE IMPORTANCE OF BEING ALIVE: DIVERGING METABOLIC OUTCOMES IN TUBERCULOSIS RESEARCH

Ana Isabel Fernandes[1,2], Anca Dorhoi[3,4], Margarida Saraiva[1]

[1] Instituto de Investigação e Inovação em Saúde, University of Porto, Porto, Portugal

[2] Doctoral Program in Molecular and Cell Biology, Instituto de Ciências Biomédicas Abel Salazar, University of Porto, Porto, Portugal

[3] Institute of Immunology, Friedrich-Loeffler-Institut, Greifswald-Insel Riems, Germany

[4] Faculty of Mathematics and Natural Sciences, University of Greifswald, Greifswald, Germany

CHAPTER 1

INTRODUCTION

1.1. TUBERCULOSIS THROUGHOUT HISTORY

Tuberculosis, also historically known as consumption, phthisis, and the white plague, is one of the oldest known infectious diseases[1]. Evidence of its existence dates back thousands of years. Archaeological findings, such as skeletal remains from ancient Egypt and historical records from Greek, Chinese, and Indian civilisations, attest to tuberculosis's millennia-long impact on human society[2–5]. By the 19th century, tuberculosis peaked, establishing it as a leading cause of death, particularly in industrialised nations where overcrowding and unsanitary living conditions facilitated its spread[6].

The initial understanding of tuberculosis was filled with misconceptions, with many attributing it entirely to inherited predispositions or unhealthy lifestyles[7]. While some believed in its contagious nature, it wasn't until 1865 that Jean Antoine Villemin demonstrated its transmissibility in animals through inoculation[4]. Despite this discovery, without a clear understanding of the causative agent, available treatment options were limited, and the primary approach to disease management was the isolation of patients in sanatoriums, where fresh air, rest, and nutrition were prescribed[8].

The identification of *Mycobacterium tuberculosis* by Robert Koch in 1882[9] marked a turning point in the fight against tuberculosis, not only confirming its infectious nature but also laying the foundation for modern bacteriology[7]. This breakthrough spurred the development of early diagnostics, such as the tuberculin skin test (TST)[10], and the tuberculosis vaccine Bacillus Calmette-Guérin (BCG)[11]. The subsequent discovery of streptomycin in the mid-20th century revolutionised treatment, offering the first effective antibiotic against tuberculosis[7,12]. This was soon complemented by other critical drugs, including isoniazid and rifampicin, which formed the cornerstone of tuberculosis therapy[12]. These advancements, along with improved hygiene conditions and socioeconomic development, contributed to a marked decrease in the number of tuberculosis cases[13].

Despite these advancements, tuberculosis remains a persistent global health challenge. The emergence of multi-drug-resistant strains, the human immunodeficiency

virus (HIV) pandemic, and socioeconomic factors such as poverty and homelessness have hindered progress[14–16]. More recently, the COVID-19 pandemic further disrupted tuberculosis control efforts, diverting resources and compromising access to diagnosis and treatment, thereby undermining global targets such as the World Health Organization's (WHO) END TB Strategy[17]. Thus, tuberculosis, an ancient disease, remains a contemporary problem, with medical advancements often unable to match the disease's ability to adapt and persist. This persistence is reflected in its overwhelming global burden, as tuberculosis reclaimed its position as the world's leading cause of death from a single infectious agent in 2023[18].

1.2. THE GLOBAL BURDEN OF TUBERCULOSIS

Despite being a preventable and usually curable disease, in 2023, tuberculosis caused an estimate of 1.25 million deaths worldwide[18]. Among these, 161,000 occurred in people living with HIV[18]. Over 10 million individuals developed tuberculosis in 2023, marking a concerning increase in cases since 2021[18].

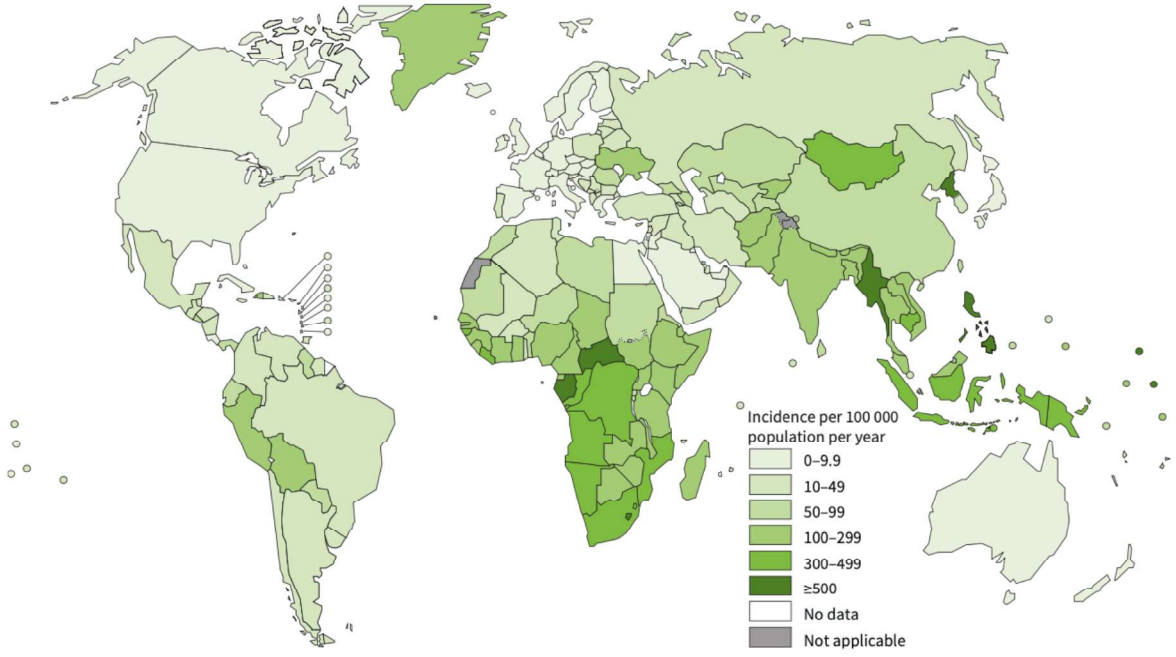

Figure 1. Estimated tuberculosis incidence rates, 2023. Reproduced from *the Global Tuberculosis Report 2024* (World Health Organization, 2024)[18].

The burden of tuberculosis is not evenly distributed. In 2023, more than half (56%) of the global cases were concentrated in five countries: India (26%), Indonesia (10%), China (6.8%), the Philippines (6.8%), and Pakistan (6.3%), reflecting the impact of socioeconomic and environmental factors such as overcrowding, poor ventilation, and limited healthcare access (*Figure 1*)[18]. Disparities in tuberculosis incidence are also evident in gender and age[19]. Men are disproportionately affected, accounting for 55% of cases, compared to 33% in women and 12% in children and young adolescents[18].

Several risk factors increase susceptibility to tuberculosis, including malnutrition, diabetes, smoking, and excessive alcohol consumption[20–22]. Individuals living with HIV are particularly vulnerable, facing a 20–30 times greater likelihood of developing tuberculosis compared to HIV-negative individuals[23]. Settings with close contacts, such as households, hospitals, and prisons, are particularly high-risk environments for tuberculosis transmission[24].

1.3. CORE STRATEGIES IN TUBERCULOSIS CONTROL

Tuberculosis requires a multifaceted approach to control its spread and impact. Effective management of this disease relies on three key strategies: prevention through vaccination, accurate and timely diagnosis, and comprehensive treatment regimens[18]. Despite significant advancements, gaps in each of these areas persist, stressing the need for continued innovation to reduce the global burden of this disease.

The prevention of tuberculosis primarily relies on vaccination, with BCG being the only available vaccine[25]. Developed over a century ago, BCG is a live attenuated strain of *Mycobacterium bovis* and lacks the region of difference 1 (RD1) locus, which encodes virulence factors present in pathogenic mycobacteria[26,27]. While BCG is highly effective in preventing severe forms of tuberculosis, such as meningitis and miliary tuberculosis in infants and children, its efficacy in adults, particularly against pulmonary disease, is variable and often limited (0-80%)[28–30]. Despite its shortcomings, BCG remains the basis of tuberculosis prevention, especially in high-burden regions[18]. Efforts to develop more effective vaccines are ongoing, with several candidates currently in clinical trials (e.g. MTBVAC)[31,32]. These new vaccines aim to provide more consistent protection across all age groups and tuberculosis manifestations[26].

Diagnosis of *M. tuberculosis* infection relies on immune-based approaches, such as the TST and interferon-gamma release assay (IGRA), which are commonly used to detect

exposure to *M. tuberculosis*[21]. The TST measures a delayed hypersensitivity reaction to mycobacterial proteins, including the purified protein derivative (PPD), but can yield false-positive results in individuals vaccinated with BCG or exposed to non-tuberculous mycobacteria[33,34]. In contrast, IGRA detects the release of interferon (IFN)-γ from T cells in response to *M. tuberculosis*-specific antigens, such as RD1, offering greater specificity by distinguishing between BCG vaccination and true *M. tuberculosis* infection[21]. However, both tests have reduced sensitivity in immunocompromised individuals, such as those with HIV, and cannot distinguish between latent tuberculosis infection (individuals exposed to *M. tuberculosis* without evidence of disease) and active disease[35].

For active tuberculosis diagnosis, a combination of microscopy (e.g., sputum smear), culture, and molecular tests is employed, often supplemented by imaging techniques like X-rays and positron emission tomography-computed tomography (PET-CT)[21,36]. Among molecular methods, the Xpert MTB/RIF assay, based on polymerase chain reaction (PCR), has revolutionised tuberculosis diagnostics[10,37]. This test simultaneously detects *M. tuberculosis* deoxyribonucleic acid (DNA) and the presence of rifampicin resistance, making it a valuable tool for rapid diagnosis and treatment guidance, particularly in low-resource settings[38]. It is now recommended by the WHO as a first-line diagnostic tool[39].

Treatment of active tuberculosis requires a lengthy antibiotic regimen, typically lasting at least six months[21]. The standard treatment regimen, developed during the golden age of tuberculosis drug discovery (1940s-1960s; *Figure 2*), involves an initial two-month intensive phase with isoniazid, rifampicin, pyrazinamide, and ethambutol, followed by a four-month continuation phase of isoniazid and rifampicin[40]. Similarly, preventive therapy for latent tuberculosis may include isoniazid alone or combined with rifampicin or rifapentine over several months[34]. These extended treatment durations stem from the need to eliminate non-replicating dormant *M. tuberculosis*[41], which exhibit intrinsic antibiotic tolerance, contributing to persistent infections[42–44]. However, these lengthy treatments often lead to poor patient adherence (due to treatment length, cost, and side effects), thereby contributing to the emergence of drug-resistant strains[45]. In response to the rise of multidrug-resistant tuberculosis (MDR-TB), renewed investment in tuberculosis drug development (2000s) has yielded novel drugs: bedaquiline, delamanid, and pretomanid (*Figure 2*)[40,46]. Alarmingly, recent clinical reports have already documented *M. tuberculosis* resistance to these new drugs[40,47], emphasising the urgent and continued need for new and effective antimicrobial agents and shorter treatment strategies[48,49].

While significant progress has been made in diagnosing, preventing, and treating tuberculosis, critical gaps remain. To overcome these challenges and reduce the global

burden of this disease, the development of more effective vaccines, shorter treatment regimens, and a deeper understanding of tuberculosis pathogenesis are essential. These scientific advances must be coupled with strengthened healthcare systems and equitable access to ensure their global impact[18,30].

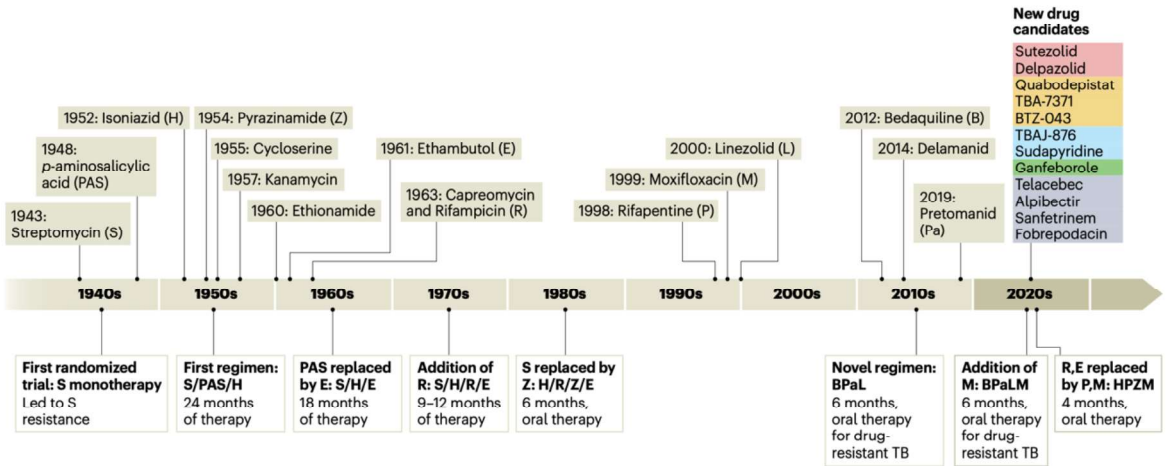

Figure 2. Timeline of tuberculosis treatments. Reproduced from Nuermberger & Chaisson (2024)[40].

1.4. THE DYNAMIC SPECTRUM OF TUBERCULOSIS

Tuberculosis primarily presents as a pulmonary disease, but it can affect multiple organs, such as the lymph nodes, pleura, bones, and central nervous system, with tuberculous meningitis being one of the most severe manifestations[50,51]. While *M. tuberculosis* is not highly infectious compared to other pathogens, an individual with active pulmonary tuberculosis can infect an average of 3 to 10 people annually[21]. The infection begins when aerosolised droplets containing *M. tuberculosis* are inhaled into the alveoli of the lungs[52]. Through epidemiological data, it is speculated that in some individuals, innate and adaptive immune mechanisms successfully eliminate the pathogen[53–55]. In others (20–50%), the bacteria persist[56–58].

This state of contained bacterial persistence, known as latent tuberculosis infection, is characterised by immunological evidence of exposure to *M. tuberculosis* (TST/IGRA+) without clinical symptoms or radiological evidence of disease[21]. Approximately 25% of the global population (around 2 billion people) is considered latently infected[59]. However, a recent estimate suggests that most individuals clear the pathogen over time, with only 2% carrying viable *M. tuberculosis*[60]. In this small subset, the bacteria may evade immune control, leading to active tuberculosis disease, which is marked by symptoms such as

persistent cough, fever, night sweats, haemoptysis (coughing up blood), and unintended weight loss, which weaken the patient and cause their gradual deterioration[21,24]. The risk of progressing to active tuberculosis is highest within the first two years after contact with an active case (approximately 5-10%) and declines significantly thereafter[61–63]. Several risk factors can favour this progression to active disease, including HIV co-infection, diabetes, immunosuppression, and aging[21,64]. Without treatment, active tuberculosis can cause severe tissue destruction, systemic complications, and a staggering mortality rate of ~50%[65].

Historically, tuberculosis has been classified into these two distinct states: latent (asymptomatic, non-infectious) and active (symptomatic and transmissible)[66]. However, this binary classification is increasingly recognised as an oversimplification. Tuberculosis is better understood as a spectrum (*Figure 3*), shaped by host immunity, bacterial virulence, and environmental factors[67,68]. At one end of the spectrum are individuals with a resister phenotype, who remain TST and IGRA negative despite continued exposure to *M. tuberculosis*[53,69,70]. Next is latent tuberculosis infection, where individuals (TST/IGRA+) harbour *M. tuberculosis* without symptoms or radiological evidence of disease[71]. Progressing along the spectrum, incipient tuberculosis represents an early stage of infection with an elevated risk of progression to active disease[71]. Next is subclinical tuberculosis, a state in which macroscopic pathology is present, but individuals remain asymptomatic[71]. Subclinical tuberculosis can be further categorised into non-infectious and infectious, challenging the assumption that asymptomatic individuals cannot transmit the disease[71]. Finally, at the other end of the spectrum lies active tuberculosis, which can also be classified as non-infectious or infectious depending on the extent of pathology and the host's immune response[71]. Active tuberculosis itself also encompasses a spectrum of clinical presentations that can vary from mild to severe pulmonary infection to disseminated forms of the disease (*Figure 3*)[68]. This understanding of the disease spectrum has important implications for tuberculosis control, as subclinical tuberculosis's contribution to transmission may represent a missed opportunity for early intervention[72].

This disease spectrum can also be dissected at the molecular level. Whole blood transcriptomic analyses have correlated the extent of radiological disease with immune pathways associated with tuberculosis pathogenesis, such as a type I interferon (IFNs)-dominant signature (*Figure 3*)[73]. Additional research into these signatures has allowed the distinction of blood transcriptional patterns between latent infection and active tuberculosis[74], with a subsequent study revealing transcriptional shifts in tuberculosis progressors as the disease progressed from incipient to subclinical to clinical[75]. Beyond

transcriptomics, serological profiling has revealed distinct glycosylation patterns of anti-*M. tuberculosis* antibodies in latent vs active tuberculosis patients. Together, these molecular approaches allow for better patient stratification and offer potential biomarkers for disease progression[76].

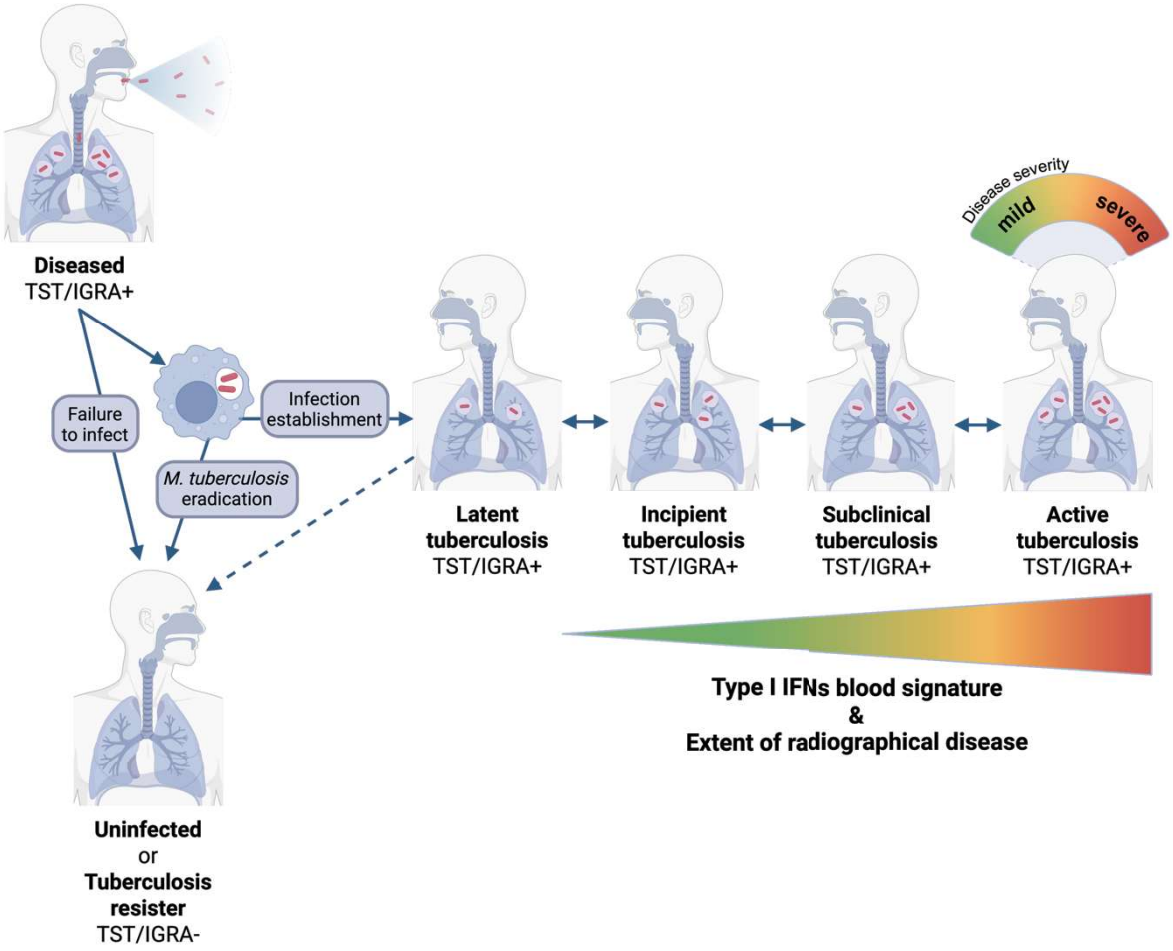

Figure 3. Dynamic spectrum of infection and containment of *M. tuberculosis*. Upon exposure, the immune response can either lead to the elimination of the pathogen or the establishment of infection. In cases where the infection is not eradicated, it may result in a latent infection, which has been further classified into latent infection, incipient, and subclinical disease. At the end of the spectrum is active disease, which also encompasses a spectrum of clinical presentations. Disease progression has been correlated with a type I IFNs blood signature[73,75]. Created in BioRender and Adobe Illustrator.

To build on these advances and standardise the way we study this spectrum, the International Consensus for Early Tuberculosis (ICE-TB) recently proposed a new framework for distinguishing tuberculosis states. This framework emphasises the non-linear nature of tuberculosis progression based on three key dimensions: macroscopic pathology,

infectiousness, and symptoms, identifying four disease states: subclinical tuberculosis (non-infectious and infectious) and clinical tuberculosis (non-infectious and infectious), between which individuals can fluctuate[77]. Moving beyond the latent-active dichotomy allows a more nuanced understanding of tuberculosis and highlights the need for targeted interventions at different stages of the disease.

1.5. IMMUNE MECHANISMS IN TUBERCULOSIS PATHOGENESIS

Tuberculosis pathogenesis relies on a complex interplay between the host immune system and the pathogen's evasion strategies[78]. The immune response to *M. tuberculosis* can be a double-edged sword: while it aims to control and eliminate the infection, excessive or dysregulated immunity can lead to tissue damage and disease progression[51]. The outcome of infection, whether it results in latent infection, active disease, or sterilisation, depends on the balance between protective immunity and pathological inflammation[79]. Although *M. tuberculosis* can disseminate into other organs[50,51], this section will focus exclusively on pulmonary tuberculosis.

Infection begins with the inhalation of aerosolised *M. tuberculosis* droplets through person-to-person contact[79]. Larger *M. tuberculosis* droplets will not reach the distal lung, but bacteria uptake may occur via microfold or M cells, a rare and specialised cell type found in the upper airways, responsible for delivering mucosal particles to submucosal antigen-presenting cells (APCs)[80]. Smaller droplets reach the alveoli, where *M. tuberculosis* encounter alveolar macrophages, the primary sentinels of the lung[81]. These macrophages are the dominant cell type in the early stages of *M. tuberculosis* infection and internalise the bacteria through receptor-mediated phagocytosis[81,82]. This response is amplified as infected alveolar macrophages invade the lung interstitium[83].

In the early stages of infection, *M. tuberculosis* may be found in the cytosol of the infected alveolar macrophages[84,85], where elimination is possible depending on the bacteria's virulence factors and the host's intrinsic microbicidal capacity[86,87]. If the bacteria are not eliminated, *M. tuberculosis* will multiply, disrupt the macrophage and gain access to the lung interstitium, either by infecting the epithelial cells (such as alveolar epithelial type II cells and, to a lesser extent, alveolar epithelial type I) or by transmigration of infected alveolar macrophages across the epithelium[88,89]. This triggers the recruitment of various immune cells, including eosinophils, neutrophils, interstitial macrophages, and dendritic cells, to the site of infection[81,90,91].

Eosinophils are also among the first cells recruited to the airways, and although their exact role in tuberculosis remains poorly understood, eosinophil deficiency is associated with increased susceptibility to tuberculosis[92,93]. The other main granulocytes involved, neutrophils, are the most abundant cells to infiltrate the lung upon *M. tuberculosis* infection, constituting a potent population of effector cells that can mediate both antimycobacterial activity and immunopathology[94].

As the infection progresses, dendritic cells migrate from the site of infection to the pulmonary draining lymph nodes for T cell priming[95–97], marking the initiation of the adaptive immune response. Upon antigen presentation, naïve cluster of differentiation (CD)4^+ T cells differentiate into effector T helper (T_H) cells subsets, primarily T_H1 and T_H17, which produce IFN-γ and interleukin (IL)-17, respectively[98]. These cytokines further activate macrophages and induce microbicidal mechanisms aimed at bacterial control at the site of infection[99]. $CD8^+$ T cells also contribute by producing cytokines and lysing infected cells[99].

The concerted action of these cellular and immune mediators during *M. tuberculosis* infection leads to the formation of the granuloma, the hallmark lesion of tuberculosis[100,101]. Granulomas play a dual role: they limit bacterial dissemination while also providing a niche for bacterial persistence and replication[100,101]. Although granulomas can be morphologically diverse, most share a typical structure: a central core of infected macrophages, multinucleated giant cells, epithelial cells, foamy macrophages, and neutrophils, surrounded by $CD4^+$ and $CD8^+$ T cells, B cells, and an outer fibrotic capsule formed by fibroblasts[102,103].

Granulomas may follow distinct fates even in the same host, depending on the local balance of pro- and anti-inflammatory signals[68,101]. If inflammation is resolved and the granuloma sterilised, the infection is effectively cleared, eliminating the risk of reactivation[68]. In the absence of sterilisation and owing to the granuloma's tight structure, a hypoxic environment may be created[104], which can evolve into a necrotic granuloma[68]. If the granuloma necrotic centre ceases, calcification can ensue[68]. However, expansion of the granuloma and cavitation can also occur, facilitating pathogen dissemination and progression from latent infection to active disease[68]. *M. tuberculosis* can be aerosolised from eroded granulomas via coughing, increasing the bacteria's transmission potential[102,105]. It has also been suggested that granulomas can only accommodate a finite bacterial burden, beyond which bacterial containment fails due to immune and physical constraints, leading to disease progression[106]. In this stage of the infection, the bacteria can re-enter the pulmonary tract and be released, promoting the infection of new hosts[101]. A summary of the immune response to *M. tuberculosis* infection is represented in *Figure 4*.

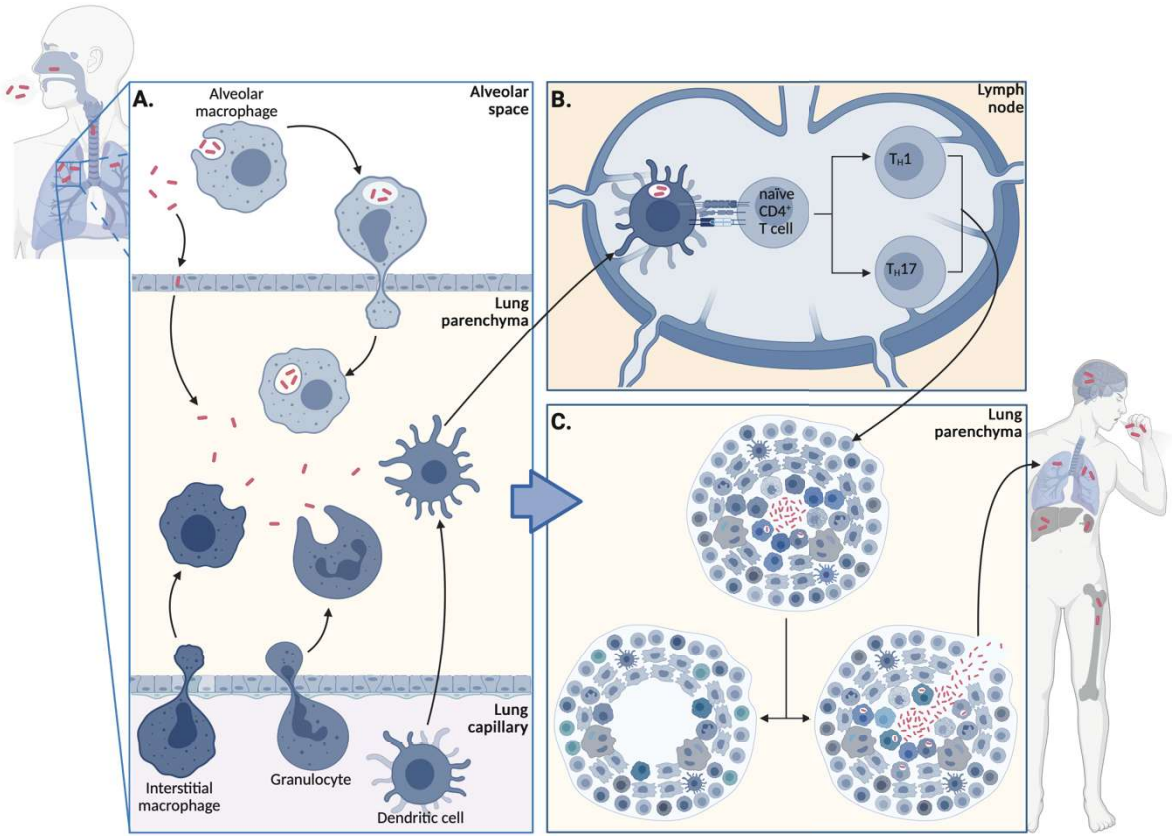

Figure 4. Immune response to *M. tuberculosis* infection. After contact with *M. tuberculosis*, **A.** it infects alveolar macrophages, which move to the lung interstitium, allowing the bacteria to infect other immune cells like macrophages, dendritic cells, and neutrophils. Some individuals may clear infection at this stage. **B.** APCs migrate to the lymph nodes, where they activate T cells. **C.** These T cells migrate to the lung to control infection. Granulomas form during infection, and their outcomes can vary (sterilisation, necrosis, cavitation) depending on the balance of pro- and anti-inflammatory immune signals. While most individuals develop latent infection, 5-10% progress to active tuberculosis, often with cavitary lung lesions that facilitate bacterial transmission. Created in BioRender.

1.5.1. INNATE IMMUNITY: EARLY DEFENCE WITH LASTING CONSEQUENCES

The innate immune system serves as the first line of defence against *M. tuberculosis*, initiating a rapid and coordinated response to contain the pathogen upon infection (*Figure 5*)[107]. Central to early control and shaping subsequent immune defences are macrophages and neutrophils. Innate immune cells recognise *M. tuberculosis* through pattern recognition receptors (PRR), including Toll-like receptors (TLR), NOD-like receptors (NLR), and C-type lectin receptors[108]. Among TLR, TLR2, TLR4, and TLR9 are the most extensively studied in the context of tuberculosis[109–113]. These receptors detect mycobacterial components like

lipoproteins, peptidoglycans, and lipoarabinomannan, triggering signalling pathways that activate immune defenses[114]. These pathways ultimately lead to the production of cytokines such as tumour necrosis factor (TNF)-α, IL-1β, IL-12, and type I IFNs, as well as critical processes like phagosome-lysosome fusion, the generation of reactive oxygen and nitrogen species, autophagy, and apoptosis, all essential for controlling bacterial growth[108,111,115]. Additionally, mycobacterial DNA and ribonucleic acid (RNA) are sensed by cytosolic surveillance systems, such as the cyclic GMP-AMP synthase (cGAS), retinoic acid-inducible gene I (RIG-I), and NLR family pyrin domain containing 3 (NLRP3), further amplifying the immune response[116–118]. Despite these robust defences, *M. tuberculosis* has evolved sophisticated mechanisms to evade and disrupt host immunity[56,119,120]. Most notably, *M. tuberculosis* inhibits phagosome-lysosome fusion and disrupts the phagosomal membrane via the early secreted antigenic target 6 kDa (ESAT-6) secretion system (ESX-1), enabling its survival and replication within host cells[121].

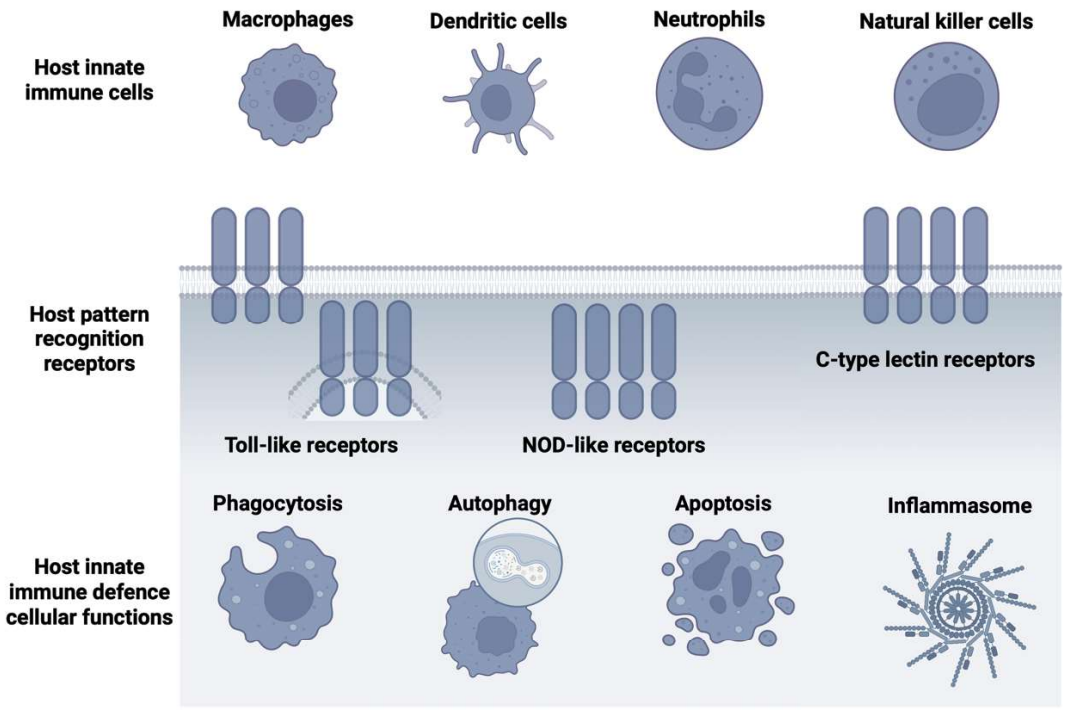

Figure 5. Innate immune defences against *M. tuberculosis* infection. *M. tuberculosis* primarily infects innate immune cells such as macrophages, dendritic cells, neutrophils, and natural killer cells, which recognise the pathogen through multiple classes of PRR. These include TLR, NLR, and CLR. Upon recognition, these receptors initiate signalling cascades that activate critical antimicrobial defence mechanisms, including phagocytosis, autophagy, apoptotic pathways, and inflammasome formation, all of which contribute to the host's ability to control or eliminate *M. tuberculosis* infection. Adapted from Liu et al. (2017)[107].

Given their central role in the immune response to *M. tuberculosis*, macrophages and neutrophils will be further explored in this section, with a focus on their contributions to protective immunity and immunopathology.

Macrophages, The First Line of Defence

Macrophages are central to the innate immune response against *M. tuberculosis*, serving as both defenders against infection and, paradoxically, as reservoirs for bacterial survival[122]. These cells detect, phagocyte, and destroy pathogens but also present antigens to T cells and release cytokines and chemokines that regulate microbicidal mechanisms in other cells[123]. In the lung, two of the main macrophage populations, alveolar and interstitial macrophages, play distinct roles in the response to *M. tuberculosis*. The macrophages' differences are shaped by their ontogeny, metabolic states, and strategies that *M. tuberculosis* employ to evade immune control[123–125].

Alveolar macrophages are long-lived, self-renewing cells that originate from foetal monocytes during embryogenesis and reside in the alveolar space[126,127]. There, they maintain lung homeostasis through immune surveillance, debris clearance, and surfactant regulation[128,129]. These macrophages provide an environment that supports bacterial replication[123]. Alveolar macrophages are inherently poor at antigen presentation and produce limited amounts of antimicrobial molecules, such as reactive oxygen and nitrogen species[130]. Moreover, their metabolic reliance on fatty acid oxidation (FAO) and oxidative phosphorylation (OXPHOS) aligns with *M. tuberculosis'*s ability to exploit host lipids for survival[123,131,132]. Depletion of alveolar macrophages in mice has been shown to reduce bacterial burden and improve survival, reinforcing their detrimental role as a primary niche for *M. tuberculosis*[123].

Interstitial macrophages are derived from circulating blood monocytes recruited to the lung parenchyma during *M. tuberculosis* infection, a process driven by chemokines like C-C motif chemokine ligand 2 (CCL2)[123,131]. In contrast to alveolar macrophages, interstitial macrophages mount a stronger inflammatory response to *M. tuberculosis*, rely on glycolysis, and exhibit a more restrictive environment for bacterial growth[123,131,132]. In line with this protective role, the depletion of interstitial macrophages in mice resulted in increased bacterial burdens[123]. During disease progression, macrophages can undergo profound functional and morphological changes[122]. Within granulomas, macrophages can differentiate into multinucleated giant cells. While these cells are characteristic of granulomas, their role in bacterial clearance remains ambiguous as they may contribute to

immune containment or serve as a niche for *M. tuberculosis* persistence[122]. Additionally, *M. tuberculosis* drives macrophages to accumulate lipids, forming foamy macrophages that provide a nutrient-rich reservoir for bacterial survival[122]. The transition to foamy macrophages is driven by the uptake of host-derived lipids such as cholesterol and low-density lipoproteins, which *M. tuberculosis* can exploit as a carbon source[122]. The presence of foamy macrophages within granulomas is associated with bacterial persistence, as these cells exhibit impaired antimicrobial functions and contribute to the chronic nature of tuberculosis lesions[122].

Despite their potential to eliminate pathogens, macrophages often fail to control *M. tuberculosis* due to the pathogen's sophisticated evasion mechanisms[120]. *M. tuberculosis* can inhibit phagolysosome acidification and maturation[133]; lyse the phagosomal membrane and translocate into the cytosol[84,134], where it can replicate[135]; and modulate programmed cell death[135], all of which contribute to immune evasion[136,137]. As a result, macrophages become long-term reservoirs for persistent bacteria within granulomas, sustaining infection over time[120,137].

Neutrophils and Their Dual Role

Neutrophils are essential components of the innate immune response to *M. tuberculosis*, playing a complex and dual role in tuberculosis pathogenesis[138–141]. As one of the most abundant immune cells in bronchoalveolar lavage and sputum of tuberculosis patients, neutrophils are among the first responders to infection, migrating to the lung in response to inflammatory cytokines, increased expression of adhesion molecules, and activation of the complement cascade[90,107,139,141]. Upon arrival, neutrophils phagocytose bacteria directly or through opsonisation and release antimicrobial enzymes such as elastase, collagenase, and myeloperoxidase to restrict bacterial growth[107,139,141–143]. They also secrete chemokines and cytokines, which recruit additional immune cells, such as blood monocytes, and amplify the inflammatory response.

In the early stages of infection, neutrophils exert a protective role by limiting bacterial replication and promoting macrophage apoptosis, which can enhance pathogen clearance. However, their highly cytotoxic content and short lifespan pose a significant risk[139,143,144]. If not promptly cleared, dying neutrophils can release their cytotoxic granules, leading to tissue damage and exacerbating inflammation[139,143,144]. This dual nature is further complicated by the bacteria's ability to manipulate neutrophil responses[78]. The pathogen induces neutrophil necrosis while inhibiting apoptosis, a strategy that increases

inflammation and lung damage[145]. Studies in both mouse models and humans have shown that excessive neutrophilia during tuberculosis is associated with delayed bacterial clearance, severe tissue damage, and poorer disease outcomes[110,144,146–151]. In fact, a defining feature of tuberculosis pathogenesis and disease severity is the neutrophil-driven type I IFN-inducible blood signature, first identified in active tuberculosis patients[73,74] and later recapitulated in *M. tuberculosis*-infected C3HeB/FeJ mice[152–154].

Furthermore, neutrophils contribute to tuberculosis pathogenesis through the formation of neutrophil extracellular traps (NETs)[155]. While NETs can trap and kill pathogens, they also promote inflammation and tissue damage[155]. During *M. tuberculosis* infection, type I IFNs have been shown to induce NETs formation, which can enhance bacterial replication within neutrophils[110,156]. This process underscores the complex interplay between neutrophils and the immune response, where their protective functions can be subverted to favour bacterial survival and dissemination.

During chronic infection, neutrophils interact with other immune cells through the release of cytokines, chemokines, and enzymes, creating a feedback loop that amplifies the immune response[157]. However, these interactions can also drive pathological inflammation, particularly in advanced stages of disease[157]. For example, neutrophil-derived metalloproteinases (MMPs) contribute to tissue remodelling and damage, further complicating the host's ability to control infection[158]. The balance between the protective and pathological roles of neutrophils is influenced by the stage of infection, the host's immune status, and the virulence of the infecting *M. tuberculosis* strain[139].

In summary, neutrophils play a dual role in tuberculosis, acting as both defenders and contributors to pathology. Their early recruitment and antimicrobial activity are critical for controlling initial infection, but their cytotoxic potential and susceptibility to manipulation by *M. tuberculosis* can exacerbate tissue damage and disease progression.

1.5.2. ADAPTIVE IMMUNITY: A DELAYED BUT ESSENTIAL DEFENCE

One of the defining characteristics of adaptive immunity in tuberculosis is its delayed onset. Unlike other infections where T cell responses are detected within days, in *M. tuberculosis* infection, adaptive immunity takes 8 to 12 days to be initiated in the mouse models[79]. This delay provides the pathogen with a crucial window to establish infection before the host can mount an effective immune response. *M. tuberculosis* not only benefits from this delay but actively extends it through a range of immune evasion strategies,

particularly targeting dendritic cells[78]. These include downregulation of major histocompatibility complex class II (MHC-II) expression[159], along with diverting antigens from major MHC-II presentation to $CD4^+$ T cells via kinesin-2 vesicles[160], enzymatic degradation of bacterial antigens[161], and presentation of decoy antigens[162]. Additionally, *M. tuberculosis* NADH-quinone oxireductase subunit G (NuoG) inhibits apoptosis in infected neutrophils, thereby delaying the transfer of antigens to dendritic cells and their migration to the lymph nodes, where T cell priming occurs[163]. Even after T cell priming, the granuloma architecture physically separates $CD4^+$ and $CD8^+$ T cells from infected macrophages[164,165], limiting their effector functions (*Figure 6*). Despite this delay, the adaptive immune response is crucial for pathogen control and long-term immunity. Although it takes longer to develop than the innate response, adaptive immunity provides specificity and immunological memory, enhancing protection against future infections[79]. $CD4^+$ and $CD8^+$ T cells, along with B cells, play distinct roles in shaping the immune response to tuberculosis[79]. These three lymphocyte populations will be discussed below, with particular emphasis on $CD4^+$ T cells.

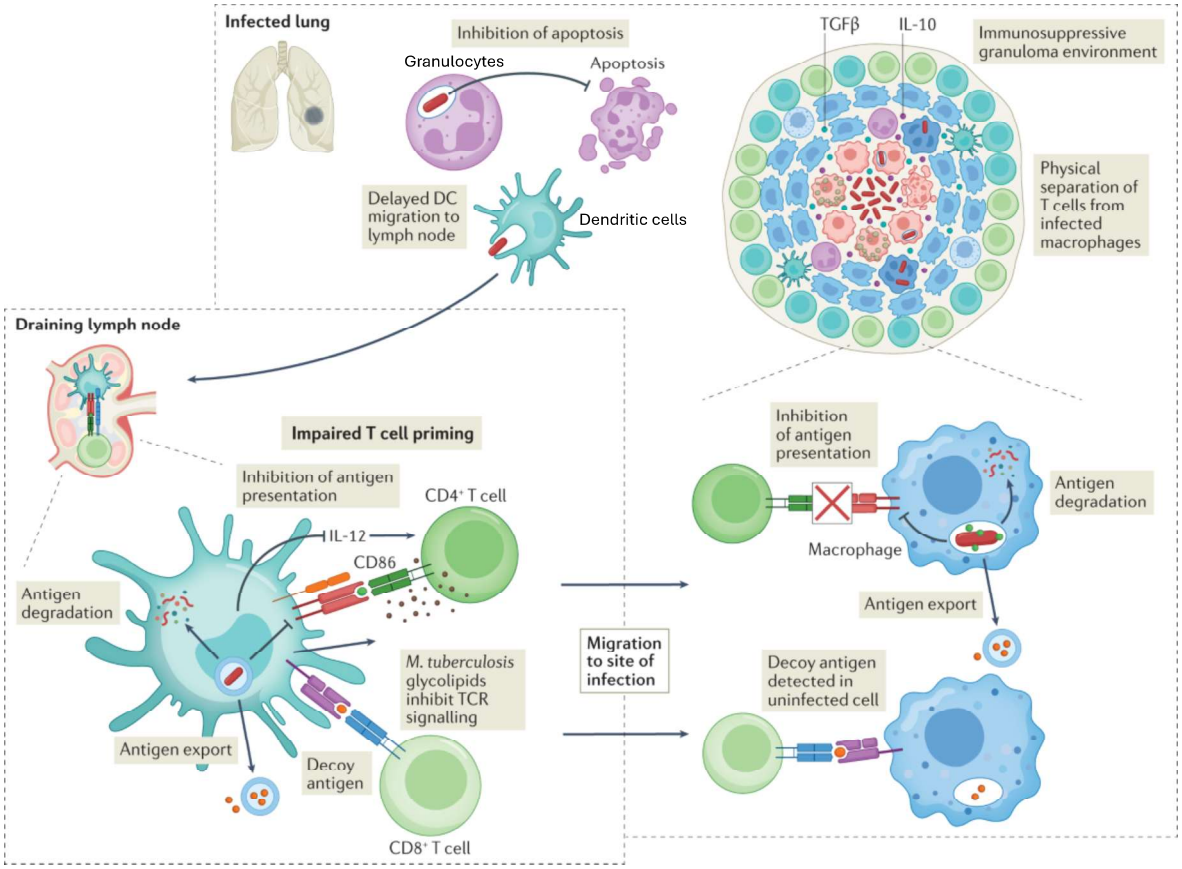

Figure 6. *M. tuberculosis* subverts adaptive immunity through multiple mechanisms. *M. tuberculosis* delays and weakens T cell responses through multiple evasion strategies, including diversion of antigens from immune recognition, degradation of immunogenic proteins, and presentation of decoy antigens. These mechanisms collectively create a window for bacterial establishment before effective T cell responses develop. Additionally, the granuloma's

immunosuppressive environment, marked by elevated transforming growth factor (TGF)-β and IL-10, along with the physical separation of T cells from infected macrophages further hinder effective immune responses. Reproduced from Chandra et al. (2022)[78].

CD4$^+$ T Cells and Their Central Role in Tuberculosis Protection

CD4$^+$ T cells are indispensable for host defence against *M. tuberculosis*[166,167]. Upon infection, dendritic cells migrate to the draining lymph nodes, where they present bacterial antigens to naïve CD4$^+$ T cells[96]. In the presence of IL-12, these T cells differentiate into T_H1 cells, which produce IFN-γ, a cytokine essential for activating macrophages and enhancing their microbicidal functions[166]. IFN-γ promotes phagolysosome fusion, nitric oxide production, and autophagy in infected macrophages, all of which are critical for controlling bacterial growth[168–171]. The importance of T_H1 cells is underscored by the severe susceptibility to mycobacterial infections observed in individuals with genetic deficiencies affecting T_H1 differentiation and IFN-γ production or signalling, a condition known as Mendelian susceptibility to mycobacterial disease (MSMD)[172].

Translating the established protective role of T_H1 cells into effective vaccines has proven challenging[173,174]. Recent studies have shown that intravenous BCG administration in non-human primates elicits more robust T_H1 responses that extensively infiltrate the lung tissue, achieving unprecedented protection (90% of animals protected, with 60% showing sterile immunity)[175]. When compared to conventional intradermal BCG, this striking efficacy underscores the importance of quickly establishing a specialised immune environment in the lung for effective *M. tuberculosis* clearance[175,176]. These findings may help to explain why vaccination strategies focused solely on boosting IFN-γ production have failed to surpass the centuries-old BCG's reported protection[177,178], and why excessive T_H1 responses can paradoxically exacerbate immunopathology in some cases[179].

In addition to T_H1 cells, CD4$^+$ T cells can differentiate into T_H17 cells in response to IL-6, IL-1β, and IL-23[180]. T_H17 cells produce IL-17, which recruits neutrophils to the site of infection[181–183]. While this response can be protective, excessive IL-17 production and neutrophil recruitment can lead to tissue damage, highlighting the dual role of T_H17 cells in tuberculosis immunity[181–186].

CD4$^+$ T cells most likely are multifunctional, co-producing multiple cytokines simultaneously, such as IFN-γ, TNF-α, and IL-2[187]. Multifunctional T cells have been associated with protective immunity and are more prevalent in latent infection than in active

tuberculosis[188]. Although their role is not fully understood, these cells have been widely studied in the context of vaccine development as markers of effective immune responses[189].

The clinical relevance of $CD4^+$ T cells is further illustrated by the heightened susceptibility to *M. tuberculosis* in HIV-positive individuals and CD4-deficient mice, where the lack of $CD4^+$ T cells impairs granuloma formation and increases the incidence of extrapulmonary disease due to uncontrolled bacterial replication and dissemination[190,191]. Adding to the protective role of $CD4^+$ T cells, there is a subset of individuals dubbed resisters. These individuals display no evidence of infection (TST/IGRA-), even when heavily exposed to *M. tuberculosis*[192–194]. This resister phenotype has recently been associated with an enriched T_H17 and regulatory T cell signature, which may contribute to sterilisation[55,69]. The factors driving these heterogeneous patterns of T cell differentiation and why they arise in some individuals but not in others remain unclear. Understanding these factors could lead to the development of vaccines that emulate natural resistance.

The Role of $CD8^+$ T Cells

$CD8^+$ T cells also play a role in the immune response to *M. tuberculosis*, though their contribution is less understood than that of $CD4^+$ T cells[195,196]. Activated $CD8^+$ T cells produce IFN-γ and granulocyte-macrophage colony-stimulating factor (GM-CSF), both of which contribute to bacterial control[197–199]. $CD8^+$ T cells can also directly kill infected cells through the release of perforin, granzymes, and granulysin, the latter of which has direct antimicrobial activity against *M. tuberculosis*[200–202]. Studies in mouse models have shown that $CD8^+$ T cell depletion during chronic infection leads to increased bacterial burdens, suggesting their importance in long-term infection control[197]. Further evidence supporting the protective role of $CD8^+$ T cells came from a recent study on tuberculosis resisters, where this phenotype was observed in individuals with well-controlled HIV infection[203]. These tuberculosis resisters displayed a higher abundance of lymphocytes, particularly $CD8^+$ T cells coexpressing granulysin, granzyme B, and perforin[203].

B cells and Antibodies

The role of B cells and antibodies in tuberculosis has been less studied and remains controversial[204]. Early experiments in mouse models suggested that B cell depletion had minimal impact on infection control[205]. However, recent human studies indicate that B cells

may contribute to immunity[206,207]. For example, individuals with latent infection and active tuberculosis exhibit distinct *M. tuberculosis*-specific antibody profiles[76]. Antibodies from latently infected individuals have been shown to enhance phagolysosome maturation, inflammasome activation, and macrophage killing of intracellular bacteria, suggesting a protective role for humoral immunity[76]. Additionally, B cells expressing antigen-specific B cell receptors migrate to the lung during infection, where they may participate in the local immune response[79].

1.5.3. IMMUNE MEDIATORS IN TUBERCULOSIS

A tightly regulated network of cytokines, chemokines, and other soluble factors balance pathogen control and the risk of immunopathology in tuberculosis. Key mediators, such as IL-1β, TNF-α, IFN-γ, IFN-β, nitric oxide, and IL-10, shape the immune landscape, ensuring a delicate equilibrium between protection and pathology[115,208,209]. IL-1β and its regulatory mechanisms are a focal point of this thesis, and will therefore be further discussed below.

IL-1β is a potent pro-inflammatory cytokine primarily produced by myeloid cells, including macrophages and dendritic cells, in response to *M. tuberculosis* infection[210]. Its production is tightly regulated at multiple levels[211]. Initially, PRR, such as TLR, detect bacterial components, triggering nuclear factor-kappa B (NF-κB) signalling and the transcription of *Il1b*, which is then translated into pro-IL-1β[212–214]. However, pro-IL-1β is biologically inactive and requires proteolytic cleavage by caspase-1, which is activated by the NLRP3 inflammasome[215]. Once NLRP3 is activated by the presence of diverse signals that disrupt cellular homeostasis[216], the inflammasome assembles and promotes the cleavage and secretion of mature IL-1β, which drives macrophage activation, neutrophil recruitment, and granuloma formation during the early stages of infection[217–219]. These IL-1β regulatory processes are essential for containing *M. tuberculosis*, as demonstrated by the increased susceptibility of humans with impaired IL-1 signalling and of IL-1β-deficient mice[220,221]. However, at later stages of infection, uncontrolled IL-1β production becomes detrimental. The continuous influx of neutrophils not only promotes tissue damage but also provides a niche for *M. tuberculosis* to grow and spread, exacerbating disease progression[222,223]. Thus, the inflammasome and IL-1β must be carefully regulated during *M. tuberculosis* infection to prevent excessive inflammation. One such regulatory mechanism involves the metabolic reprogramming of macrophages upon infection. The glycolytic pathway plays a crucial role in IL-1β production, as the transcription of *Il1b* is tightly linked

to the glycolytic shift induced by *M. tuberculosis* infection[224,225]. The metabolic rewiring of macrophages in response to *M. tuberculosis* infection is also shaped by multiple variables, such as cellular ontogeny[123], bacterial viability status[226], and infecting *M. tuberculosis* strain[227]. All these variables can have distinct impacts on IL-1β production. The role of immunometabolism in the context of tuberculosis will be discussed later in this introduction. IL-1β is also tightly regulated by multiple immune mediators, with type I IFNs (IFN-α/β) and IL-10 playing key roles in this regulation[228,229], as detailed below.

Type I IFNs, often induced by *M. tuberculosis* through the cGAS-stimulator of IFN genes (STING) pathway[230], and in some cases through TLR4 signalling[109], are critical for modulating immune responses. While type I IFNs are traditionally associated with antiviral immunity, their role in tuberculosis is complex and context-dependent[231]. In the early stages of infection, type I IFNs can suppress inflammasome activation by inducing nitric oxide and IL-10 production, preventing excessive IL-1β release and neutrophil recruitment, which could otherwise exacerbate tissue damage. However, it is important to mention that excessive type I IFNs signalling has been linked to detrimental outcomes in tuberculosis, including increased bacterial burden and immunopathology[73,110,208]. For example, type I IFNs can promote macrophage necrosis, impair T_H1 responses, induce NETs formation, and suppress protective IL-1 signalling, creating an environment favourable for bacterial persistence[153,156,232–235]. This dual role of type I IFNs in balancing inflammation while potentially undermining protective immunity highlights their complex contribution to tuberculosis pathogenesis.

IL-10, produced by macrophages, dendritic cells, and regulatory T cells, acts as a potent anti-inflammatory cytokine in the context of tuberculosis[236]. IL-10 downregulates the expression of pro-inflammatory cytokines, including IL-1β, TNF-α, and IL-12, and inhibits the activation of macrophages and dendritic cells[237]. In the context of tuberculosis, IL-10 helps to prevent excessive inflammation and tissue damage by suppressing inflammasome activity and IL-1β production[236]. However, high levels of IL-10 can also suppress protective immunity, promoting *M. tuberculosis* survival and chronic infection[236]. For instance, IL-10 inhibits the production of IL-12, a cytokine essential for T_H1 differentiation and IFN-γ production, thereby impairing macrophage activation and bacterial control[238]. Recent findings have also suggested that IL-10 overexpression during the early stages of *M. tuberculosis* infection contributes to the accumulation of $CD4^+$ T cells with limited capacity to migrate to the lung parenchyma, impairing effective bacterial clearance[239]. To sum up, IL-10 prevents immunopathology but can also hinder effective pathogen clearance.

Similarly to type I IFNs and IL-10, nitric oxide is a critical mediator of IL-1β in tuberculosis. Produced by inducible nitric oxide synthase (iNOS) in macrophages, nitric oxide directly kills *M. tuberculosis* by generating reactive nitrogen intermediates that damage bacterial components[223]. It also enhances phagolysosome fusion and autophagy, further restricting bacterial survival[223]. Beyond its antimicrobial effects, nitric oxide regulates inflammation by inhibiting NF-κB and NLRP3 inflammasome activation through S-nitrosylation, preventing excessive IL-1β release and neutrophil recruitment, which could otherwise exacerbate tissue damage[222,240].

The intricate interplay of immune mediators, such as IL-1β, type I IFNs, IL-10, and nitric oxide (*Figure 7*), highlights the complexity of the host response to *M. tuberculosis*. While these mediators are essential for balancing protection and pathology, their dysregulation can lead to either excessive inflammation or bacterial persistence. Understanding these mechanisms not only provides insights into tuberculosis pathogenesis but also underscores the need to explore how *M. tuberculosis* exploits these pathways to evade immune detection and establish chronic infection. This sets the stage for examining the pathogen's strategies to subvert host immunity, a critical aspect of tuberculosis biology.

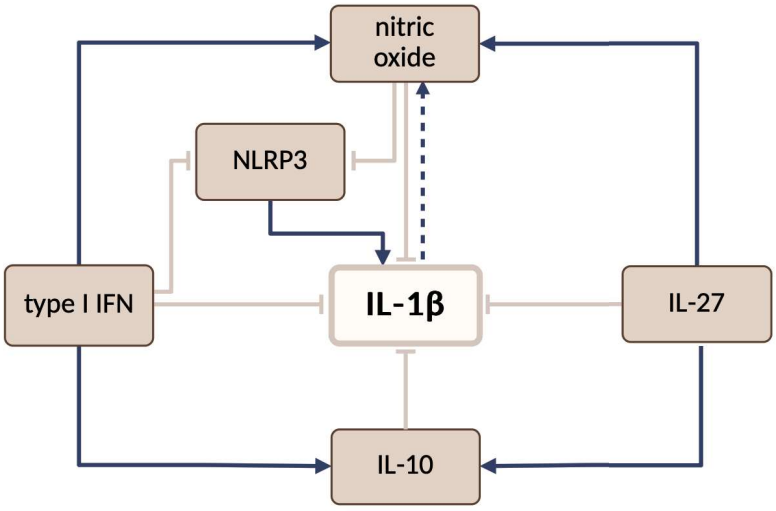

Figure 7. Immune mediators involved in the regulation of IL-1β production. IL-1β production is tightly regulated to balance host protection and immunopathology. Type I IFNs and IL-27 suppress IL-1β directly or indirectly via IL-10 and iNOS-derived nitric oxide production. Created in BioRender.

1.6. THE PATHOGEN BEHIND TUBERCULOSIS

M. tuberculosis, the causative agent of tuberculosis, is a slow-growing, aerobic, and facultative intracellular bacillus[241]. As a member of the *Mycobacterium* genus, it is classified as an acid-fast bacteria with a thick, waxy cell wall[241,242]. This cell wall is composed primarily of peptidoglycans and a complex layer of lipids, including mycolic acids, which contribute to its virulence and resistance to drugs, posing a significant challenge for treatment[243].

M. tuberculosis possesses a single, circular chromosome, with approximately 10% of its genome encoding proteins involved in immune evasion and immunopathogenesis[78,244]. The bacteria can metabolically adapt to diverse host environments[245,246], allowing it to infect and persist within phagocytic cells such as macrophages and neutrophils, as explained above. Its slow growth rate contributes to the chronic nature of tuberculosis and the lengthy treatment regimens required to eradicate the infection[43]. These adaptations, combined with its ability to evade host immune responses, make *M. tuberculosis* a formidable pathogen that has persisted for millennia.

1.6.1. THE EVOLUTION AND DIVERSITY OF THE *MYCOBACTERIUM TUBERCULOSIS* COMPLEX

The *Mycobacterium tuberculosis* complex (MTBC) comprises a group of phylogenetically related bacteria, which includes *M. tuberculosis*, a primarily human-adapted pathogen without any known environmental or animal reservoir, but also other species, such as *M. bovis* (which infects cattle), *Mycobacterium caprae* (goats), *Mycobacterium pinnipedii* (seals), *Mycobacterium microti* (rodents), and *Mycobacterium orygis* (oryx)[247,248]. These pathogens share a high degree of genetic similarity (99.9%), yet they exhibit distinct host preferences and pathogenic profiles, reflecting their adaptation to different ecological niches[248,249].

Recent advances in whole-genome sequencing have enabled the identification of ten distinct human-adapted lineages (*Figure 8*), that can be further divided into sublineages[250–255]. The human-adapted MTBC lineages can be broadly categorised as "ancient" (L1, L5-L10) or "modern" (L2-L4) lineages, based on the genomic deletion of the tuberculosis-specific deletion 1 (TbD1) locus in “modern” lineages, which may confer enhanced bacterial resistance to oxidative and hypoxic stressors[256–259]. Additionally, the human-adapted MTBC lineages and sublineages can be classified as "generalists" with a broad global distribution or "specialists" which are largely confined to specific geographic regions[260–264]. Generalist

lineages, such as L4, have been associated with high adaptability and the ability to infect genetically diverse human populations[253,265]. In contrast, specialist lineages, such as L5 and L6 (historically referred to as *Mycobacterium africanum*), appear to be adapted to specific human populations in West Africa[266–270].

The global expansion of MTBC lineages closely mirrors human migration patterns. Phylogenomic studies indicate that the spread of *M. tuberculosis* accompanied the out-of-Africa migration of modern humans, with subsequent diversification linked to major historical transitions, such as the Neolithic revolution and later colonial migrations[249,265,271]. For instance, L2 is thought to have expanded with the spread of agriculture in East Asia, while L4 was shaped by colonial expansion and trade routes[3,271].

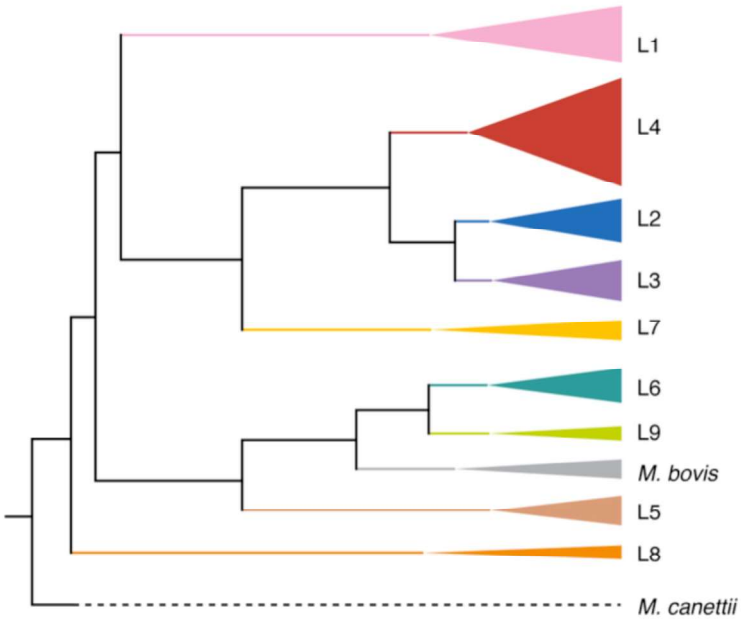

Figure 8. Phylogeny of *M. tuberculosis* lineages. Phylogenetic tree depicting the evolutionary relationships among 9 lineages of *M. tuberculosis* (depicted in colour) and one animal-adapted MTBC lineage, *M. bovis* (depicted in grey). The recently characterised lineage 10 is not included. The tree is rooted with *Mycobacterium canetti*, a member of the MTBC often regarded as a close relative of the MTBC's common ancestor. Genomic deletions, such as TbD1, serve as molecular markers for lineage distinction. Reproduced from Koleske et al. (2023)[272].

1.6.2. THE IMPACT OF BACTERIAL DIVERSITY ON TUBERCULOSIS OUTCOMES

Despite the high genetic conservation among *M. tuberculosis* lineages, several studies demonstrate the impact of the pathogen's genetic diversity on the diverse clinical

manifestations of tuberculosis, as well as on inducing different immune responses in the host[273,274].

Impact on Tuberculosis Presentation and Transmission

Regarding the impact of *M. tuberculosis* in disease presentation, several studies suggest that strains from L1 are more likely to cause extrapulmonary disease than strains from other lineages[275,276]. This is reinforced by the presence of the full-length type VII-secreted effector EsxM in L1 strains, which has been shown to promote macrophage migration and dissemination[277]. In contrast, “modern” lineages (L2, L3, and L4) carry a truncated version of EsxM and have lost the TbD1 region, a deletion linked to improved survival in hypoxic conditions, such as those found in granulomas[259,277]. This adaptation may contribute to the success of modern lineages in causing pulmonary disease and their widespread transmission[278]. Yet, when looking at studies conducted with strains from L2, the association with disease presentation is not as clear. While some studies in the United States seem to indicate lower rates of extrapulmonary disease with L2 strains, studies in the United Kingdom show an increased prevalence of this disease presentation[276,279]. It is worth noting that L2 strains are generally considered hypervirulent, although variability between sublineages can be observed[280,281]. In direct contrast, L6 strains are generally considered less virulent and are associated with slower progression from infection to active tuberculosis[282]. Studies focusing on tuberculosis caused by L4 strains, specifically the Latin American-Mediterranean (LAM) sublineage, suggest an association between infection with these strains and the presence of lung consolidations[283]. Similarly, individuals infected with L2 strains exhibit significantly more cavitation[284].

Since *M. tuberculosis* is an airborne pathogen, pulmonary tuberculosis plays a prominent role in transmission. Consequently, an increased transmission potential is associated with strains from lineages more prone to cause pulmonary damage or cavitation[285]. Epidemiological studies suggest that *M. tuberculosis* strains from "modern" lineages are more transmissible than those from "ancient" lineages[286]. For example, in the Netherlands, epidemiological data demonstrated lower transmission rates for L1, L5, and L6 strains compared to L4 strains[283]. A lower transmissibility of L5 and L6 strains has also been reported in several regions of West Africa[268,287]. However, there are some conflicting reports. In the Gambia, even though the progression to active disease was slower for strains from L6 when compared to strains from “modern” lineages, the varied lineages presented no difference in transmissibility[282]. These differential transmission dynamics between

lineages may be shaped by the host niche. Recent evidence points to bacterial strains belonging to geographically restricted lineages transmitting more efficiently among sympatric hosts (individuals from the same geographical region)[288]. In macrophage in vitro infections, allopatric host-pathogen interactions (when host and pathogen do not share a common geographical area) resulted in decreased infection rates, as compared to sympatric interactions[288]. This host-pathogen sympatry is also apparent in a study conducted in Vietnam where L2 strains preferentially infected individuals carrying polymorphisms in the gene encoding TLR2[289], and in a genome-to-genome study that identified an association between an intronic variation in the gene encoding flotellin-1 (FLOT1) and a highly transmissible sublineage L2 strain[290]. Notably, this sympatry between the host and the pathogen appears to be disrupted in HIV-positive individuals[291].

In summary, although the contribution of *M. tuberculosis* genetic diversity to the establishment of tuberculosis and bacterial transmission is evident, the extent to which host-pathogen interactions are shaped by factors like geographical sympatry and immune status, influencing transmission dynamics, remains unclear. Further research is needed to establish robust causal links and elucidate the underlying mechanisms for the differential transmission patterns.

Impact on the Immune Response

Due to the low genetic diversity of *M. tuberculosis*, the active role of the pathogen in regulating the host immune response was long underestimated and considered irrelevant. Recently, the genetic differences between *M. tuberculosis* strains and the resulting immunological and clinical phenotypes have been increasingly explored. Progressively, our understanding of the influence of *M. tuberculosis* diversity on the activation of immune mediators and how this relates to the establishment of infection and disease progression has advanced significantly[285,292].

One of the first studies showing an impact of *M. tuberculosis* phylogeny on macrophage responses to infection demonstrated that not only do these macrophages respond differently to different bacterial strains, but also that strains belonging to “modern” *M. tuberculosis* lineages generally induce lower inflammatory responses compared to “ancient” *M. tuberculosis* strains[257]. Aligning with this data, another study showed that, when compared to “modern” lineages, some “ancient” lineages exhibited impaired bacterial replication in macrophages due to defective upregulation of virulence factors like sulfolipids and phthiocerol dimycocerosates (PDIM), which are critical for immune evasion, such as

masking pathogen-associated molecular patterns (PAMPs) and suppressing TLR2 signalling[293,294]. Additionally, conserved genes in the intracellular transcriptome of both "modern" and "ancient" lineages were linked to essential *M. tuberculosis* pathways: stress responses, cell wall remodelling, and lipid metabolism[293]. Complementing these findings, recent data also indicate that different MTBC lineages display distinct capacities to accumulate triglyceride-rich lipid droplets, a phenotype linked to bacterial dormancy, with higher accumulation observed in L2 strains and reduced levels in L3 strains[295]. In line with this, in studies using the C3HeB/FeJ mouse model, *M. tuberculosis* clinical isolates stratified by transmission potential revealed that low-transmission strains induced higher lipid droplet accumulation, greater bacterial burden, and diffuse inflammatory lung pathology. In contrast, high-transmission strains were associated with reduced lipid droplet formation and the development of organised, caseating granulomas, a lesion type more conducive to transmission[296,297].

The impact of *M. tuberculosis* strain diversity on the recognition of the pathogen by innate immune cells has also been described. For example, a study from our laboratory showed that despite the importance of TLR2 for recognising *M. tuberculosis* and subsequently initiating an inflammatory response in infected macrophages, some clinical isolates additionally activate TLR4, enhancing the production of type I IFNs[109], a molecule with a detrimental role in tuberculosis[231]. Still related to differential macrophage activation, some hypervirulent *M. tuberculosis* Beijing (L2) strains have been shown to actively suppress apoptosis while promoting necrosis in infected macrophages, effectively evading a key antimicrobial defence mechanism[298,299]. Notably, a recent study from our laboratory showed that certain L4 *M. tuberculosis* clinical isolates have a greater ability to activate the inflammasome and consequently induce IL-1β production compared to others[300]. Moreover, we linked the ability to evade inflammasome activation with greater tuberculosis severity in patients[300]. Two of these clinical isolates, *M. tuberculosis* 4I2 (mild disease) and 6C4 (severe disease), are the focus of the work developed in this thesis. It is worth noting that it is now evident that differences in immune response resulting from *M. tuberculosis* diversity are not solely determined by bacterial phylogeny, as even within strains of the same lineage or sublineage, immunological profiles can vary. The major challenge now is to identify the molecular determinants of these variations, which will enable the development of tailored therapies.

In comparison to the innate immune system, the impact of *M. tuberculosis* diversity on the adaptive immune response is much less studied. Nevertheless, recent evidence points to "modern" lineages being associated with weaker $CD4^+$ and $CD8^+$ T cell activation,

creating favourable conditions for their proliferation and undermining granuloma integrity[295]. As a broader immune subversion strategy, *M. tuberculosis* evolved to hyperconserve T cell epitopes, as opposed to most pathogens that take advantage of T cell evasion[301,302]. However, even within this general strategy, there is already some evidence of T cell responses being affected by *M. tuberculosis* strain variability. For instance, certain *M. tuberculosis* strains, specifically L6 strains, presented an attenuated T cell response to ESAT-6 antigens[303]. It is also tempting to speculate that given that T cell differentiation in the lymph nodes depends on the microenvironment, different strains might influence the quality of the T_H cell response through microenvironment modulation generated by the dendritic cell responses. While, to date, there is no conclusive evidence of lineage-specific immune modulation of dendritic cells by *M. tuberculosis*, the pathogen can broadly subvert dendritic cell functions by impairing dendritic cell maturation and disrupting efficient antigen presentation[78,304,305].

A final note regarding the modulation of the immune response by different clinical isolates of *M. tuberculosis* concerns the interaction between the immune system and drug-resistant bacteria. Although this area of extreme clinical relevance is still very new, it is already evident that the acquisition of drug-resistance mutations alters the interaction of the 'new' bacteria with the host[306]. Understanding these changes, as well as their molecular bases, is critical for the discovery and adjustment of new immunomodulatory therapies.

The growing knowledge of the differences associated with the various lineages of *M. tuberculosis* undoubtedly brings new challenges to the study of tuberculosis, with implications across all the aforementioned fronts. It is likely that a universally applicable preventive or treatment solution for tuberculosis may not be feasible, but instead, solutions tailored to the most prevalent bacteria in a given geographical region may be necessary. For progress in this field of study, the diversity of *M. tuberculosis* must be systematically incorporated into all aspects of tuberculosis research, alongside host diversity and the resulting interaction between the two.

1.7. FUELLING THE FIGHT: HOW METABOLISM SHAPES IMMUNITY

Mounting an immune response is energetically demanding[307]. For immune cells such as macrophages and T cells, the activation process requires substantial biosynthetic activity, including the production of cytokines, chemokines, antimicrobial peptides, and antigen-presenting machinery[308,309]. This heightened demand is met through metabolic reprogramming, allowing immune cells to rapidly shift to an activated state[310]. Typically,

resting cells rely on OXPHOS and the tricarboxylic acid (TCA) cycle to maintain homeostasis[310]. Upon activation, immune cells, namely macrophages, can undergo a metabolic switch to aerobic glycolysis (Warburg effect), characterised by increased glucose uptake and lactate production even in the presence of oxygen[310]. This metabolic reprogramming is not just a consequence of activation; it also drives effector functions[311].

The metabolic interplay becomes significantly more complex in *M. tuberculosis* infection. *M. tuberculosis* exhibits remarkable metabolic flexibility that allows it to adapt and persist in hostile host environments such as granulomas, which are characterised by nutrient deprivation, hypoxia, and immune pressure[104,245]. The pathogen can adapt using multiple strategies: utilisation of diverse carbon and nitrogen sources, resistance to oxidative stress, and active manipulation of host cell metabolic pathways[102,245]. Of particular importance is the bacteria's ability to subvert macrophage metabolism, creating a more permissive intracellular niche that favours bacterial survival over clearance[81,123]. This metabolic manipulation effectively skews the immune response toward tolerance rather than eradication[81,123]. Adding further complexity, host-derived immunometabolites (intermediates and byproducts of metabolic pathways) can serve dual roles in *M. tuberculosis* infection. While these molecules normally promote inflammatory responses and pathogen clearance, *M. tuberculosis* has evolved mechanisms to sense and use them for its own benefit, enhancing bacterial survival and immune evasion[312].

The metabolic state of the host immune system is also influenced by the stage of tuberculosis infection, whether active disease, reinfection, or latency[313,314]. For example, during early infection, macrophages adopt a glycolytic phenotype, while in chronic or latent stages, metabolic reprogramming may favour lipid storage and immune suppression[313,314]. Understanding how these dynamic metabolic shifts correlate with immune responses and bacterial persistence is crucial for understanding tuberculosis pathogenesis.

1.7.1. MACROPHAGE METABOLISM AND TUBERCULOSIS CONTROL

Macrophages, as previously mentioned, serve as both primary defence cells and key cellular niches for *M. tuberculosis* survival[81]. Upon *M. tuberculosis* infection, macrophages undergo a rapid metabolic shift from OXPHOS to aerobic glycolysis[224,315]. This shift, mediated by PRR activation and transcription factor hypoxia-inducible factor 1-alpha (HIF-1α) stabilisation[314], supports the production of key inflammatory mediators such as IL-1β, TNF-α, and nitric oxide, fuelling a self-amplifying loop of metabolic activation and

inflammation[316,317]. Increased glycolytic flux also provides a rapid source of adenosine triphosphate (ATP) and essential metabolic intermediates required for immune activation[314,318]. Importantly, this Warburg-like metabolic shift is not limited to macrophages. Upon antigen recognition, T cells also engage in aerobic glycolysis to support rapid proliferation, clonal expansion, and acquisition of effector functions, highlighting a conserved mechanism of immune activation across cell types[309,319].

In parallel, mitochondrial metabolism remains critical for coordinating immune responses during *M. tuberculosis* infection. While pyruvate generated in resting macrophages generally enters the TCA cycle via conversion to acetyl-CoA, in *M. tuberculosis*-infected cells, pyruvate is preferentially converted into lactate, and the TCA cycle is disrupted[320]. One hallmark of this rewiring is the accumulation of specific intermediates, notably succinate, citrate, and itaconate, that mediate immune signalling[320]. Succinate accumulates due to inhibition of succinate dehydrogenase (SDH) or increased anaplerotic flux from glutamine[321,322]. Elevated succinate stabilises HIF-1α and supports IL-1β production[323]. Citrate is exported from the mitochondria and cleaved by ATP citrate lyase into acetyl-CoA[324], which not only fuels histone acetylation and transcriptional activation of inflammatory genes but also contributes to fatty acids and cholesterol biosynthesis[325,326]. Citrate also serves as a precursor for itaconate, a metabolite produced by the mitochondrial enzyme immune-responsive gene 1 (IRG1)[327]. Itaconate represents a central immunometabolite during tuberculosis infection, with multiple described immune functions[312]. Itaconate can exert direct antimicrobial activity by inhibiting *M. tuberculosis* isocitrate lyase, an enzyme essential for the bacteria's glyoxylate shunt which allows it to utilise host-derived fatty acids[312]. Additionally, itaconate modulates inflammation by acting as a regulator of the nuclear factor erythroid 2-related factor 2 (NRF2) pathway, reducing mitochondrial reactive oxygen species (ROS) production and limiting NLRP3 inflammasome activation[312,328]. This anti-inflammatory effect helps prevent excessive tissue damage during chronic infection[312,328]. Moreover, itaconate inhibits SDH, thus promoting succinate accumulation and creating feedback loops that regulate both pro- and anti-inflammatory signals[312,329].

Glycolytic and TCA cycle intermediates are also involved in amino acid biosynthesis[330]. These amino acids can, in turn, replenish TCA cycle intermediates to support sustained immune activation or metabolic rewiring[330]. For example, in activated macrophages, arginine is converted by iNOS into nitric oxide, a potent antimicrobial effector molecule[313]. Tryptophan is another amino acid involved in the regulation of hyperinflammation[313,331]. While macrophages use amino acid metabolism to fuel immune responses, *M. tuberculosis*

can scavenge host-derived amino acids as nitrogen sources to support intracellular survival[321,332], highlighting the metabolic competition between the pathogen and the host.

Although macrophage activation causes a shift towards glycolysis, mitochondrial OXPHOS remains functionally relevant, particularly during the later stages of infection or in alternatively activated macrophages (associated with anti-inflammatory responses)[333]. OXPHOS, driven by reducing coenzymes from the TCA cycle, such as nicotinamide adenine dinucleotide (NADH) and flavin adenine dinucleotide ($FADH_2$), ensures long-term ATP production and supports immune resolution[334]. These mitochondrial functions are especially important in sustaining cell viability, supporting autophagy, phagosome maturation, antigen presentation, and ROS generation, which are essential for antimicrobial activity and inflammasome activation[314,333,335]. The shift from glycolysis to OXPHOS also correlates with a change in cytokine profile, from pro-inflammatory mediators like IL-1β and TNF-α to anti-inflammatory cytokines such as IL-10 and TGF-β[336]. Disruption of mitochondrial function, whether through pathogen-induced damage or excessive ROS, can impair immune responses and lead to increased bacterial persistence[337].

Fatty acid metabolism adds another layer of complexity to this metabolic network. In macrophages, fatty acids are both an energy source and precursors for signalling molecules[338]. FAO can feed acetyl-CoA into the TCA cycle, supporting OXPHOS and ATP production, particularly under nutrient-limited conditions or in the resolution phase of infection, and is typically associated with anti-inflammatory macrophage phenotypes[338]. *M. tuberculosis*-infected macrophages in the lung, particularly within granulomas, frequently adopt a lipid-rich or foamy phenotype[339,340]. These cells accumulate lipid droplets and store neutral lipids, such as triglycerides and cholesterol esters, which can be mobilised through β-oxidation under stress conditions[339]. This lipid accumulation is modulated, in part, by the *M. tuberculosis* virulence factor ESAT-6[341,342]. While FAO supports energy production and the synthesis of immunoregulatory lipids such as prostaglandins, the lipid-rich environment can be subverted by *M. tuberculosis*[314]. The bacteria can catabolise host lipids through its own β-oxidation and methylcitrate pathways to sustain its intracellular survival and persistence[338]. Furthermore, *M. tuberculosis*-induced formation of foamy macrophages contributes to granuloma caseation, a nutrient- and oxygen-limited environment (*Figure 9*)[104,343]. This hypoxic environment within the granuloma induces a shift to dormancy in *M. tuberculosis*, mediated by the DosR regulon, allowing the pathogen to persist in a non-replicating state[245].

While much progress has been made in understanding immunometabolic pathways during *M. tuberculosis* infection, the macrophage metabolic reprogramming is not yet fully

understood. Notably, macrophages of different ontogenies respond differently to *M. tuberculosis* infection (*Figure 9*), suggesting that developmental origin and tissue localisation shape metabolic outcomes[123,344]. Alveolar macrophages reside in the alveolar space, where they are chronically exposed to surfactant lipids[123,344]. This environment promotes a metabolism skewed toward FAO and OXPHOS, contributing to a regulatory and anti-inflammatory profile[123,344]. Consequently, alveolar macrophages tend to be more permissive to early *M. tuberculosis* replication[123,344]. In contrast, interstitial macrophages exhibit a stronger pro-inflammatory phenotype and undergo a more pronounced shift toward glycolysis upon activation, supporting robust cytokine production and enhanced bactericidal activity[123,344].

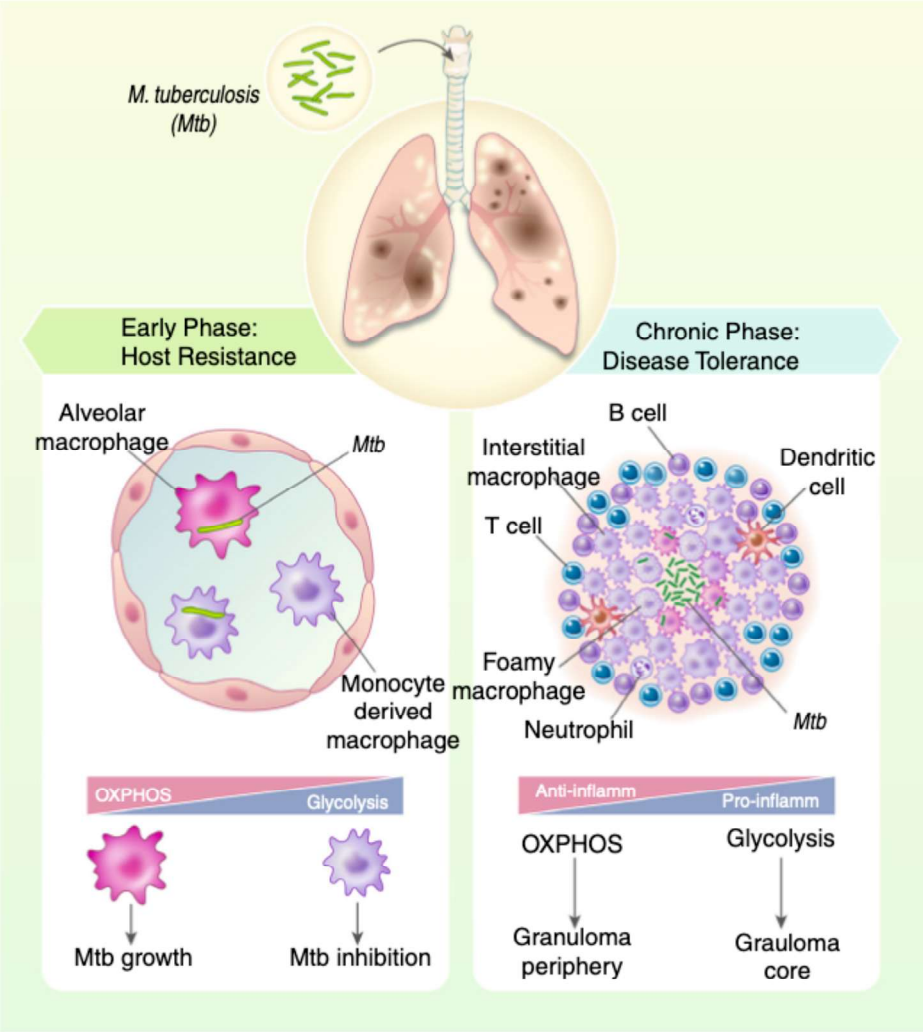

Figure 9. Macrophage metabolic dynamics during *M. tuberculosis* infection. The immune response to *M. tuberculosis* is intricately linked to metabolic changes within immune cells at various stages of infection. Alveolar macrophages depend on OXPHOS and FAO and are permissive to *M. tuberculosis*. In contrast, interstitial macrophages rely on glycolysis, which enhances their pro-inflammatory responses. As *M. tuberculosis* infection persists and the granuloma forms, a specialised

microenvironment is formed, where macrophages closer to the core undergo glycolysis to suppress bacterial replication, and peripheral macrophages use OXPHOS and FAO to modulate inflammation and tissue repair. The presence of foamy macrophages rich in lipids supports bacterial persistence and regulates inflammatory responses. The balance of these metabolic pathways within granulomas determines the efficiency of bacterial control and the preservation of lung tissue integrity. Reproduced from Sheedy & Divangahi (2020)[340].

In sum, macrophage metabolism during *M. tuberculosis* infection is a dynamic and highly coordinated process, with interconnected pathways that control the amplitude and nature of immune responses. Glycolysis enables rapid energy generation and immune activation; the TCA cycle, through intermediates like succinate, citrate, and itaconate, regulates inflammatory outputs; OXPHOS provides sustained energy and supports cell viability and resolution of inflammation; and FAO promotes both energy production and immune modulation, while also representing a nutrient source for the pathogen[320]. The cumulative effect of these metabolic programs determines whether macrophages adopt a bactericidal or permissive phenotype, influencing the outcome of tuberculosis infection[320]. Understanding and targeting this immunometabolic landscape offers promising opportunities for host-directed therapies that could enhance antimicrobial responses without exacerbating immunopathology.

1.7.2. THE IMPORTANCE OF BACTERIA VIABILITY IN IMMUNOMETABOLIC REPROGRAMMING

Infection triggers reciprocal metabolic adaptations that govern the balance between host immunity and pathogen persistence. The ability of *M. tuberculosis* to adapt its metabolic state to different host microenvironments is essential for its persistence and pathogenicity[245]. Likewise, host immune cells undergo extensive metabolic reprogramming to respond to infection[315]. Capturing these dynamics in experimental systems is key to uncovering mechanisms of immunity, persistence, and disease progression in tuberculosis. However, the models used to study these host-pathogen interactions vary widely in complexity and physiological relevance, and these differences significantly influence the metabolic responses observed experimentally.

Infection with live virulent *M. tuberculosis* ensures the presence of several bacterial mechanisms, including bacterial replication, activation of secretion systems such as ESX-

1, manipulation of host cell death pathways, and the ability to sense and respond to changes in the intracellular environment[345]. These evasion mechanisms can drive specific metabolic adaptations in infected cells, including shifts in glycolysis, OXPHOS, lipid metabolism, and redox balance[346]. Overall, infection with live virulent *M. tuberculosis* allows for dynamic, bidirectional interactions between host and pathogen. Temporal dynamics are often missed in models that lack bacterial viability cues. However, using live *M. tuberculosis* presents some logistical and financial constraints, as it requires biosafety level 3 (BSL-3) containment. As a result, many researchers rely on alternative models that are safer and more accessible, at the cost of biological complexity[347].

Among these alternative models often used are:

- Inactivated bacteria (e.g., heat-killed, irradiated, sonicated *M. tuberculosis*);
- Attenuated strains like *M. bovis* BCG and *M. tuberculosis* H37Ra;
- Pathogen-derived materials (e.g., protein lysates, conditioned media, or pathogen-derived soluble factors);
- Ligands that mimic PAMPs (e.g., lipopolysaccharide (LPS), Pam3CysSerLys4, Poly(I:C), CpG oligodeoxynucleotide)[347].

Each of these systems presents distinct limitations. Inactivated *M. tuberculosis* retain structural PAMPs but lack viability signals and active secretion of virulence factors[347]. BCG infection models, while live, lack key virulence determinants like the ESX-1 secretion system, crucial for many immunometabolic effects[121]. Pathogen-derived components and ligands that mimic PAMPs only activate individual PRR or specific signalling cascades without additional bacterial complexity. These simplified models often fail to reproduce the full spectrum of metabolic responses observed during live *M. tuberculosis* infection, particularly the virulence-dependent suppression or fine-tuning of metabolic pathways, leading to misinterpretation of host responses and affecting translational relevance. For example, inflammasome activation and IL-1β maturation (critical components of protective immunity in tuberculosis) are modulated by the bacteria's ESX-1 secretion system, which is absent in some of these models[348].

While it is still the consensus that *M. tuberculosis* triggers a glycolytic shift in macrophages[224,315,349], several studies have highlighted some differences in how different stimuli affect macrophage metabolism[226,315,350]. For example, in comparison to the more inflammatory phenotype induced by heat-killed *M. tuberculosis* H37Rv, macrophages infected with live bacteria promoted a more attenuated glycolytic and TCA cycle shift[226]. Similarly, both live H37Rv and H37Ra macrophage infection induced lower lactate

production compared to heat-killed and γ-irradiated strains[225]. Underlying differences were associated with the sustained expression of microRNA-21 in macrophages infected with live bacteria[225]. This miRNA directly targeted the glycolytic enzyme phosphofructokinase, suppressing glycolysis and limiting IL-1β production[225]. In line with these findings, macrophage infection with live *M. tuberculosis* was also associated with the activation of type I IFNs signalling, which correlated with reduced glycolysis and mitochondrial respiration when compared to stimulation with heat-killed bacteria[351]. The ability of live *M. tuberculosis* to restrain macrophage glycolysis appears to be an active immune evasion mechanism. Supporting this, *M. tuberculosis* infection was shown to increase macrophage-derived hydrogen sulfide (H_2S), which also inhibits glycolysis[350]. Mice deficient in cystathionine γ-lyase, an H_2S-producing enzyme, displayed enhanced glycolytic flux and lower bacterial burden[350]. *M. tuberculosis* infection has also been reported to impact the TCA cycle, particularly through the accumulation of succinate, a metabolite that bridges metabolic and inflammatory signalling[352], as it has been associated with HIF-1α stabilisation and subsequent IL-1β production[323]. While this link has been well-documented in LPS-stimulated macrophages, evidence from live *M. tuberculosis* infections is more limited. In a study using live *M. tuberculosis*, although succinate was detected in infected macrophages, its levels were not significantly altered compared to uninfected controls[315]. All of these discrepancies reinforce the idea that *M. tuberculosis* exploits metabolic dampening to its advantage.

Strain virulence also plays a significant role. In a study where macrophages were infected with virulent clinical isolates of *M. tuberculosis*, glucose uptake, ATP production, acetyl-CoA and cytoplasmic citrate levels, and fatty acids and cholesterol biosynthesis were reported to be elevated[353]. However, all these features were diminished in infections with the attenuated H37Ra strain[353]. Likewise, macrophage infection with drug-resistant W-Beijing strains induced a less effective glycolytic phenotype and limited IL-1β production than infection with drug-susceptible *M. tuberculosis* strains[227]. These resistant bacterial strains overexpressed PDIM, a cell wall lipid, and induced a strong IFN-β response (considered detrimental in tuberculosis)[227].

Importantly, recent in vivo studies suggest that metabolic responses to *M. tuberculosis* are not static. A biphasic response has been described in C57BL/6 mice, with an early glycolytic phase driven by HIF-1α and a later phase with a shift to oxidative metabolism[333]. A temporal pattern was also observed in granulomas, where HIF-1α expression was initially generally high in early inflammatory macrophages but restricted to foamy macrophages in later stages[354]. Pharmacologic inhibition of HIF-1α improved disease outcomes when

administered during later stages of infection but not during early infection, underscoring the context- and time-dependent nature of macrophage metabolic responses[354]. Supporting this complexity, alveolar and interstitial macrophages exhibit distinct metabolic profiles that influence *M. tuberculosis* infection outcomes, with alveolar macrophages contributing to a permissive environment for *M. tuberculosis* replication, and interstitial macrophages promoting bacterial restriction[123,344].

Despite their limitations, reductionist models remain valuable tools for studying tuberculosis. They are especially useful for dissecting early immune signalling events, identifying individual metabolic pathways involved in infection, and generating mechanistic insights that can be further validated using more complex systems. These models provide an essential foundation for hypothesis generation and allow for targeted investigation of specific host or bacterial factors[347]. However, their limitations must be acknowledged, and findings from these systems must be interpreted within the context of their constraints. Overreliance on simplified stimuli can obscure the full scope of metabolic reprogramming that occurs during live infection, particularly the nuanced, time- and strain-dependent metabolic shifts that shape host-pathogen dynamics.

Ultimately, integrating insights from across this spectrum of models, ranging from single agonists to live *M. tuberculosis* infection, will be critical for building a comprehensive understanding of tuberculosis pathogenesis. While no single model captures all aspects of the disease, recognising their respective strengths and limitations allows for experimental design that balances safety, feasibility, and physiological relevance. Only by appreciating how stimulus choice and bacterial viability influence metabolic outcomes can we accurately map the host responses that underpin immunity, bacterial persistence, and disease progression in tuberculosis.

REFERENCES

1. Frith, J. History of Tuberculosis. Part 1 - Phthisis, consumption and the White Plague. *JMVH* **22**, (2014).

2. Hershkovitz, I. *et al.* Tuberculosis origin: The Neolithic scenario. *Tuberculosis (Edinb)* **95 Suppl 1**, S122–S126 (2015).

3. Perrin, P. Human and tuberculosis co-evolution: An integrative view. *Tuberculosis (Edinb)* **95 Suppl 1**, S112–S116 (2015).

4. Daniel, T. M. The history of tuberculosis. *Respir Med* **100**, 1862–1870 (2006).

5. Buzic, I. & Giuffra, V. The paleopathological evidence on the origins of human tuberculosis: a review. *J Prev Med Hyg* **61**, (2020).

6. Stead, W. W. The origin and erratic global spread of tuberculosis. How the past explains the present and is the key to the future. *Clin Chest Med* **18**, 65–77 (1997).

7. Barberis, I., Bragazzi, N. L., Galluzzo, L. & Martini, M. The history of tuberculosis: from the first historical records to the isolation of Koch's bacillus. *J Prev Med Hyg* **58**, 9–12 (2017).

8. Karakousis, P. C. & Mooney, G. Respiratory Isolation for Tuberculosis: A Historical Perspective. *J Infect Dis* **231**, 3–9 (2025).

9. Koch, R. *The Aetiology of Tuberculosis*. (National Tuberculosis Association, New York, 1932).

10. Huang, Y., Ai, L., Wang, X., Sun, Z. & Wang, F. Review and Updates on the Diagnosis of Tuberculosis. *J Clin Med* **11**, 5826 (2022).

11. Lobo, N. *et al.* 100 years of Bacillus Calmette-Guérin immunotherapy: from cattle to COVID-19. *Nat Rev Urol* **18**, 611–622 (2021).

12. Keshavjee, S. & Farmer, P. E. Tuberculosis, drug resistance, and the history of modern medicine. *N Engl J Med* **367**, 931–936 (2012).

13. Zumla, A., Nahid, P. & Cole, S. T. Advances in the development of new tuberculosis drugs and treatment regimens. *Nat Rev Drug Discov* **12**, 388–404 (2013).

14. Dye, C. & Williams, B. G. The population dynamics and control of tuberculosis. *Science* **328**, 856–861 (2010).

15. Gandhi, N. R. *et al.* Multidrug-resistant and extensively drug-resistant tuberculosis: a threat to global control of tuberculosis. *Lancet* **375**, 1830–1843 (2010).

16. Smith, I. Mycobacterium tuberculosis pathogenesis and molecular determinants of virulence. *Clin Microbiol Rev* **16**, 463–496 (2003).

17. Finn McQuaid, C. *et al.* The potential impact of COVID-19-related disruption on tuberculosis burden. *Eur Respir J* **56**, (2020).

18. Geneva: World Health Organization. *Global Tuberculosis Report 2024*. https://www.who.int/publications/i/item/9789240101531 (2024).

19. Lefebvre, N. & Falzon, D. Risk factors for death among tuberculosis cases: analysis of European surveillance data. *Eur Respir J* **31**, 1256–1260 (2008).

20. Dheda, K., Barry, C. E. & Maartens, G. Tuberculosis. *Lancet* **387**, 1211–1226 (2016).

21. Pai, M. *et al.* Tuberculosis. *Nat Rev Dis Primers* **2**, (2016).

22. Bastos, H. N., Osório, N. S., Gagneux, S., Comas, I. & Saraiva, M. The Troika Host-Pathogen-Extrinsic Factors in Tuberculosis: Modulating Inflammation and Clinical Outcomes. *Front Immunol* **8**, (2018).

23. Aaron, L. *et al.* Tuberculosis in HIV-infected patients: a comprehensive review. *Clin Microbiol Infect* **10**, 388–398 (2004).

24. Fogel, N. Tuberculosis: a disease without boundaries. *Tuberculosis (Edinb)* **95**, 527–531 (2015).

25. Lange, C. *et al.* 100 years of *Mycobacterium bovis* bacille Calmette-Guérin. *Lancet Infect Dis* **22**, e2–e12 (2022).

26. Andersen, P. & Scriba, T. J. Moving tuberculosis vaccines from theory to practice. *Nat Rev Immunol* **19**, 550–562 (2019).

27. Pitt, J. M., Blankley, S., McShane, H. & O'Garra, A. Vaccination against tuberculosis: how can we better BCG? *Microb Pathog* **58**, 2–16 (2013).

28. Ernst, J. D. Mechanisms of *M. tuberculosis* Immune Evasion as Challenges to TB Vaccine Design. *Cell Host Microbe* **24**, 34–42 (2018).

29. Fletcher, H. A. Sleeping Beauty and the Story of the Bacille Calmette-Guérin Vaccine. *mBio* **7**, (2016).

30. World Health Organization. *Implementing the End TB Strategy: The Essentials*. *https://iris.who.int/handle/10665/206499* https://iris.who.int/handle/10665/206499 (2015).

31. Hatherill, M., Tait, D. & McShane, H. Clinical Testing of Tuberculosis Vaccine Candidates. *Microbiol Spectr* **4**, (2016).

32. Martin, C., Aguilo, N., Marinova, D. & Gonzalo-Asensio, J. Update on TB Vaccine Pipeline. *Applied Sciences 2020, Vol. 10, Page 2632* **10**, 2632 (2020).

33. Seddon, J. A. *et al.* The impact of BCG vaccination on tuberculin skin test responses in children is age dependent: evidence to be considered when screening children for tuberculosis infection. *Thorax* **71**, 932–939 (2016).

34. Furin, J., Cox, H. & Pai, M. Tuberculosis. *Lancet* **393**, 1642–1656 (2019).

35. Sousa, J. & Saraiva, M. Paradigm changing evidence that alter tuberculosis perception and detection: Focus on latency. *Infect Genet Evol* **72**, 78–85 (2019).

36. Delogu, G. & Goletti, D. The spectrum of tuberculosis infection: new perspectives in the era of biologics. *J Rheumatol Suppl* **91**, 11–16 (2014).

37. Mukherjee, S., Perveen, S., Negi, A. & Sharma, R. Evolution of tuberculosis diagnostics: From molecular strategies to nanodiagnostics. *Tuberculosis (Edinb)* **140**, (2023).

38. Detjen, A. K. *et al.* Xpert MTB/RIF assay for the diagnosis of pulmonary tuberculosis in children: a systematic review and meta-analysis. *Lancet Respir Med* **3**, 451–461 (2015).

39. World Health Organization. *Xpert MTB/RIF Implementation Manual : Technical and Operational 'How-to': Practical Considerations*. (2014).

40. Nuermberger, E. L. & Chaisson, R. E. Restocking the tuberculosis drug arsenal. *Nat Med* **30**, 642–643 (2024).

41. Garton, N. J. *et al.* Cytological and transcript analyses reveal fat and lazy persister-like bacilli in tuberculous sputum. *PLoS Med* **5**, 0634–0645 (2008).

42. Egorova, A., Salina, E. G. & Makarov, V. Targeting Non-Replicating *Mycobacterium tuberculosis* and Latent Infection: Alternatives and Perspectives (Mini-Review). *Int J Mol Sci* **22**, (2021).

43. Connolly, L. E., Edelstein, P. H. & Ramakrishnan, L. Why is long-term therapy required to cure tuberculosis? *PLoS Med* **4**, 435–442 (2007).

44. Colangeli, R. *et al. Mycobacterium tuberculosis* progresses through two phases of latent infection in humans. *Nat Commun* **11**, (2020).

45. Dheda, K. *et al.* Recent controversies about MDR and XDR-TB: Global implementation of the WHO shorter MDR-TB regimen and bedaquiline for all with MDR-TB? *Respirology* **23**, 36–45 (2018).

46. Farhat, M. *et al.* Drug-resistant tuberculosis: a persistent global health concern. *Nat Rev Microbiol* **22**, 617–635 (2024).

47. Akbari Aghababa, A. H., Nasiri, M. J., Pakzad, P. & Mirsamadi, E. S. Delamanid and bedaquiline resistance patterns in *Mycobacterium tuberculosis* in Iran: A cross-sectional analysis. *New Microbes New Infect* **60–61**, (2024).

48. Sazali, M. F. *et al.* Improving Tuberculosis Medication Adherence: The Potential of Integrating Digital Technology and Health Belief Model. *Tuberc Respir Dis (Seoul)* **86**, 82–93 (2023).

49. Singh, V. Tuberculosis treatment-shortening. *Drug Discov Today* **29**, (2024).

50. Harisinghani, M. G. *et al.* Tuberculosis from head to toe. *Radiographics* **20**, 449–470 (2000).

51. Scriba, T. J., Maseeme, M., Young, C., Taylor, L. & Leslie, A. J. Immunopathology in human tuberculosis. *Sci Immunol* **9**, eado5951 (2024).

52. Pieters, J. Entry and survival of pathogenic mycobacteria in macrophages. *Microbes Infect* **3**, 249–255 (2001).

53. Verrall, A. J. *et al.* Early Clearance of *Mycobacterium tuberculosis* Is Associated With Increased Innate Immune Responses. *J Infect Dis* **221**, 1342–1350 (2020).

54. Behr, M. A., Edelstein, P. H. & Ramakrishnan, L. Is *Mycobacterium tuberculosis* infection life long? *BMJ* **367**, (2019).

55. Andrews, J. R. Recasting resistance to *Mycobacterium tuberculosis*. *Nat Immunol* **25**, 1316–1318 (2024).

56. Russell, D. G. *Mycobacterium tuberculosis*: here today, and here tomorrow. *Nat Rev Mol Cell Biol* **2**, 569–577 (2001).

57. Kiazyk, S. & Ball, T. Latent tuberculosis infection: An overview. *Can Commun Dis Rep* **43**, 62–66 (2017).

58. BañUls, A. L., Sanou, A., Van Anh, N. T. & Godreuil, S. *Mycobacterium tuberculosis*: ecology and evolution of a human bacterium. *J Med Microbiol* **64**, 1261–1269 (2015).

59. Houben, R. M. G. J. & Dodd, P. J. The Global Burden of Latent Tuberculosis Infection: A Re-estimation Using Mathematical Modelling. *PLoS Med* **13**, (2016).

60. Schwalb, A. *et al.* Estimating the Global Burden of Viable *Mycobacterium Tuberculosis* Infection [pre-print]. *Posted on The Lancet* (2024) doi:10.2139/SSRN.5017943.

61. Behr, M. A., Edelstein, P. H. & Ramakrishnan, L. Rethinking the burden of latent tuberculosis to reprioritize research. *Nat Microbiol* **9**, 1157–1158 (2024).

62. Menzies, N. A. *et al.* Progression from latent infection to active disease in dynamic tuberculosis transmission models: a systematic review of the validity of modelling assumptions. *Lancet Infect Dis* **18**, e228–e238 (2018).

63. Vynnycky, E. & Fine, P. E. M. Lifetime risks, incubation period, and serial interval of tuberculosis. *Am J Epidemiol* **152**, 247–263 (2000).

64. Esmail, H., Barry, C. E., Young, D. B. & Wilkinson, R. J. The ongoing challenge of latent tuberculosis. *Philos Trans R Soc Lond B Biol Sci* **369**, (2014).

65. Tiemersma, E. W., van der Werf, M. J., Borgdorff, M. W., Williams, B. G. & Nagelkerke, N. J. D. Natural history of tuberculosis: duration and fatality of untreated pulmonary tuberculosis in HIV negative patients: a systematic review. *PLoS One* **6**, (2011).

66. Barry, C. E. *et al.* The spectrum of latent tuberculosis: rethinking the biology and intervention strategies. *Nat Rev Microbiol* **7**, 845–855 (2009).

67. Lin, P. L. & Flynn, J. L. The End of the Binary Era: Revisiting the Spectrum of Tuberculosis. *J Immunol* **201**, 2541–2548 (2018).

68. Cadena, A. M., Fortune, S. M. & Flynn, J. L. Heterogeneity in tuberculosis. *Nat Rev Immunol* **17**, 691–702 (2017).

69. Sun, M. *et al.* Specific CD4+ T cell phenotypes associate with bacterial control in people who 'resist' infection with *Mycobacterium tuberculosis*. *Nat Immunol* **25**, 1411–1421 (2024).

70. Henry Boom, W., Schaible, U. E. & Achkar, J. M. The knowns and unknowns of latent *Mycobacterium tuberculosis* infection. *J Clin Invest* **131**, (2021).

71. Drain, P. K. *et al.* Incipient and Subclinical Tuberculosis: a Clinical Review of Early Stages and Progression of Infection. *Clin Microbiol Rev* **31**, (2018).

72. Auld, S. C. *et al.* Research Roadmap for Tuberculosis Transmission Science: Where Do We Go From Here and How Will We Know When We're There? *J Infect Dis* **216**, S662–S668 (2017).

73. Berry, M. P. R. *et al.* An interferon-inducible neutrophil-driven blood transcriptional signature in human tuberculosis. *Nature* **466**, 973–977 (2010).

74. Singhania, A. *et al.* A modular transcriptional signature identifies phenotypic heterogeneity of human tuberculosis infection. *Nat Commun* **9**, (2018).

75. Tabone, O. *et al.* Blood transcriptomics reveal the evolution and resolution of the immune response in tuberculosis. *J Exp Med* **218**, (2021).

76. Lu, L. L. *et al.* A Functional Role for Antibodies in Tuberculosis. *Cell* **167**, 433-443.e14 (2016).

77. Coussens, A. K. *et al.* Classification of early tuberculosis states to guide research for improved care and prevention: an international Delphi consensus exercise. *Lancet Respir Med* **12**, 484–498 (2024).

78. Chandra, P., Grigsby, S. J. & Philips, J. A. Immune evasion and provocation by *Mycobacterium tuberculosis*. *Nat Rev Microbiol* **20**, 750–766 (2022).

79. O'Garra, A. *et al.* The immune response in tuberculosis. *Annu Rev Immunol* **31**, 475–527 (2013).

80. Nair, V. R. *et al.* Microfold Cells Actively Translocate *Mycobacterium tuberculosis* to Initiate Infection. *Cell Rep* **16**, 1253–1258 (2016).

81. Cohen, S. B. *et al.* Alveolar Macrophages Provide an Early *Mycobacterium tuberculosis* Niche and Initiate Dissemination. *Cell Host Microbe* **24**, 439-446.e4 (2018).

82. Cadena, A. M., Flynn, J. L. & Fortune, S. M. The Importance of First Impressions: Early Events in *Mycobacterium tuberculosis* Infection Influence Outcome. *mBio* **7**, (2016).

83. Killick, K. E. *et al.* Receptor-mediated recognition of mycobacterial pathogens. *Cell Microbiol* **15**, 1484–1495 (2013).

84. van der Wel, N. *et al. M. tuberculosis* and *M. leprae* translocate from the phagolysosome to the cytosol in myeloid cells. *Cell* **129**, 1287–1298 (2007).

85. Houben, D. *et al.* ESX-1-mediated translocation to the cytosol controls virulence of mycobacteria. *Cell Microbiol* **14**, 1287–1298 (2012).

86. Maertzdorf, J. *et al. Mycobacterium tuberculosis* Invasion of the Human Lung: First Contact. *Front Immunol* **9**, (2018).

87. Van Crevel, R., Ottenhoff, T. H. M. & Van der Meer, J. W. M. Innate immunity to *Mycobacterium tuberculosis*. *Clin Microbiol Rev* **15**, 294–309 (2002).

88. Delogu, G., Sali, M. & Fadda, G. The biology of mycobacterium tuberculosis infection. *Mediterr J Hematol Infect Dis* **5**, (2013).

89. Scordo, J. M., Knoell, D. L. & Torrelles, J. B. Alveolar Epithelial Cells in *Mycobacterium tuberculosis* Infection: Active Players or Innocent Bystanders? *J Innate Immun* **8**, 3–14 (2016).

90. Eum, S. Y. *et al.* Neutrophils are the predominant infected phagocytic cells in the airways of patients with active pulmonary TB. *Chest* **137**, 122–128 (2010).

91. Wolf, A. J. *et al. Mycobacterium tuberculosis* infects dendritic cells with high frequency and impairs their function in vivo. *J Immunol* **179**, 2509–2519 (2007).

92. Mayer-Barber, K. D. Granulocytes subsets and their divergent functions in host resistance to *Mycobacterium tuberculosis* - a 'tipping-point' model of disease exacerbation. *Curr Opin Immunol* **84**, (2023).

93. Bohrer, A. C. *et al.* Eosinophils are part of the granulocyte response in tuberculosis and promote host resistance in mice. *J Exp Med* **218**, (2021).

94. Dallenga, T. & Schaible, U. E. Neutrophils in tuberculosis--first line of defence or booster of disease and targets for host-directed therapy? *Pathog Dis* **74**, (2016).

95. Mihret, A. The role of dendritic cells in *Mycobacterium tuberculosis* infection. *Virulence* **3**, (2012).

96. Wolf, A. J. *et al.* Initiation of the adaptive immune response to *Mycobacterium tuberculosis* depends on antigen production in the local lymph node, not the lungs. *J Exp Med* **205**, 105–115 (2008).

97. Marino, S. *et al.* Dendritic cell trafficking and antigen presentation in the human immune response to *Mycobacterium tuberculosis*. *J Immunol* **173**, 494–506 (2004).

98. Cooper, A. M. Cell-mediated immune responses in tuberculosis. *Annu Rev Immunol* **27**, 393–422 (2009).

99. Jasenosky, L. D., Scriba, T. J., Hanekom, W. A. & Goldfeld, A. E. T cells and adaptive immunity to *Mycobacterium tuberculosis* in humans. *Immunol Rev* **264**, 74–87 (2015).

100. Pagán, A. J. & Ramakrishnan, L. Immunity and Immunopathology in the Tuberculous Granuloma. *Cold Spring Harb Perspect Med* **5**, (2014).

101. Ramakrishnan, L. Revisiting the role of the granuloma in tuberculosis. *Nat Rev Immunol* **12**, 352–366 (2012).

102. Russell, D. G. Who puts the tubercle in tuberculosis? *Nat Rev Microbiol* **5**, 39–47 (2007).

103. Huynh, K. K., Joshi, S. A. & Brown, E. J. A delicate dance: host response to mycobacteria. *Curr Opin Immunol* **23**, 464–472 (2011).

104. Krueger, G., Faisal, S. & Dorhoi, A. Microenvironments of tuberculous granuloma: advances and opportunities for therapy. *Front Immunol* **16**, 1575133 (2025).

105. Martin, C. J., Carey, A. F. & Fortune, S. M. A bug's life in the granuloma. *Semin Immunopathol* **38**, 213–220 (2016).

106. Lin, P. L. *et al.* Sterilization of granulomas is common in active and latent tuberculosis despite within-host variability in bacterial killing. *Nat Med* **20**, 75–79 (2014).

107. Liu, C. H., Liu, H. & Ge, B. Innate immunity in tuberculosis: host defense vs pathogen evasion. *Cell Mol Immunol* **14**, 963–975 (2017).

108. Chai, Q., Zhang, Y. & Liu, C. H. *Mycobacterium tuberculosis*: An Adaptable Pathogen Associated With Multiple Human Diseases. *Front Cell Infect Microbiol* **8**, (2018).

109. Carmona, J. *et al. Mycobacterium tuberculosis* Strains Are Differentially Recognized by TLRs with an Impact on the Immune Response. *PLoS One* **8**, (2013).

110. Moreira-Teixeira, L. *et al.* Type I IFN Inhibits Alternative Macrophage Activation during *Mycobacterium tuberculosis* Infection and Leads to Enhanced Protection in the Absence of IFN-γ Signaling. *J Immunol* **197**, 4714–4726 (2016).

111. Reiling, N. *et al.* Cutting edge: Toll-like receptor (TLR)2- and TLR4-mediated pathogen recognition in resistance to airborne infection with Mycobacterium tuberculosis. *J Immunol* **169**, 3480–3484 (2002).

112. Hölscher, C. *et al.* Containment of aerogenic *Mycobacterium tuberculosis* infection in mice does not require MyD88 adaptor function for TLR2, -4 and -9. *Eur J Immunol* **38**, 680–694 (2008).

113. Means, T. K. *et al.* Human Toll-Like Receptors Mediate Cellular Activation by *Mycobacterium tuberculosis*. *The Journal of Immunology* **163**, 3920–3927 (1999).

114. Means, T. K. *et al.* Differential effects of a Toll-like receptor antagonist on *Mycobacterium tuberculosis*-induced macrophage responses. *J Immunol* **166**, 4074–4082 (2001).

115. Giacomini, E. *et al.* Infection of human macrophages and dendritic cells with *Mycobacterium tuberculosis* induces a differential cytokine gene expression that modulates T cell response. *J Immunol* **166**, 7033–7041 (2001).

116. Watson, R. O. *et al.* The Cytosolic Sensor cGAS Detects *Mycobacterium tuberculosis* DNA to Induce Type I Interferons and Activate Autophagy. *Cell Host Microbe* **17**, 811–819 (2015).

117. Wassermann, R. *et al. Mycobacterium tuberculosis* Differentially Activates cGAS- and Inflammasome-Dependent Intracellular Immune Responses through ESX-1. *Cell Host Microbe* **17**, 799–810 (2015).

118. Mishra, B. B. *et al. Mycobacterium tuberculosis* protein ESAT-6 is a potent activator of the NLRP3/ASC inflammasome. *Cell Microbiol* **12**, 1046–1063 (2010).

119. Behar, S. M., Divangahi, M. & Remold, H. G. Evasion of innate immunity by *Mycobacterium tuberculosis*: is death an exit strategy? *Nat Rev Microbiol* **8**, 668–674 (2010).

120. Russell, D. G. *Mycobacterium tuberculosis* and the intimate discourse of a chronic infection. *Immunol Rev* **240**, 252–268 (2011).

121. Wong, K.-W. The Role of ESX-1 in *Mycobacterium tuberculosis* Pathogenesis. *Microbiol Spectr* **5**, (2017).

122. Ahmad, F. *et al.* Macrophage: A Cell With Many Faces and Functions in Tuberculosis. *Front Immunol* **13**, (2022).

123. Huang, L., Nazarova, E. V., Tan, S., Liu, Y. & Russell, D. G. Growth of *Mycobacterium tuberculosis* in vivo segregates with host macrophage metabolism and ontogeny. *J Exp Med* **215**, 1135–1152 (2018).

124. Zheng, W. *et al. Mycobacterium tuberculosis* resides in lysosome-poor monocyte-derived lung cells during chronic infection. *PLoS Pathog* **20**, (2024).

125. Pisu, D., Johnston, L., Mattila, J. T. & Russell, D. G. The frequency of CD38+ alveolar macrophages correlates with early control of *M. tuberculosis* in the murine lung. *Nat Commun* **15**, 8522 (2024).

126. Röszer, T. Understanding the Biology of Self-Renewing Macrophages. *Cells* **7**, (2018).

127. Guilliams, M. *et al.* Alveolar macrophages develop from fetal monocytes that differentiate into long-lived cells in the first week of life via GM-CSF. *J Exp Med* **210**, 1977–1992 (2013).

128. Agudelo, C. W., Samaha, G. & Garcia-Arcos, I. Alveolar lipids in pulmonary disease. A review. *Lipids Health Dis* **19**, (2020).

129. Lim, P. N., Cervantes, M. M., Pham, L. K. & Rothchild, A. C. Alveolar macrophages: novel therapeutic targets for respiratory diseases. *Expert Rev Mol Med* **23**, (2021).

130. Guirado, E., Schlesinger, L. S. & Kaplan, G. Macrophages in Tuberculosis: Friend or Foe. *Semin Immunopathol* **35**, 563 (2013).

131. Srivastava, S., Ernst, J. D. & Desvignes, L. Beyond macrophages: the diversity of mononuclear cells in tuberculosis. *Immunol Rev* **262**, 179–192 (2014).

132. Goenka, A., Casulli, J. & Hussell, T. *Mycobacterium tuberculosis* Joyrides Alveolar Macrophages into the Pulmonary Interstitium. *Cell Host Microbe* **24**, 331–333 (2018).

133. Small, P. L. C., Ramakrishnan, L. & Falkow, S. Remodeling schemes of intracellular pathogens. *Science* **263**, 637–639 (1994).

134. Simeone, R. *et al.* Phagosomal rupture by *Mycobacterium tuberculosis* results in toxicity and host cell death. *PLoS Pathog* **8**, (2012).

135. Davis, J. M. & Ramakrishnan, L. The role of the granuloma in expansion and dissemination of early tuberculous infection. *Cell* **136**, 37–49 (2009).

136. Ravesloot-Chavez, M. M., Van Dis, E. & Stanley, S. A. The Innate Immune Response to *Mycobacterium tuberculosis* Infection. *Annu Rev Immunol* **39**, 611–637 (2021).

137. Sia, J. K., Georgieva, M. & Rengarajan, J. Innate Immune Defenses in Human Tuberculosis: An Overview of the Interactions between *Mycobacterium tuberculosis* and Innate Immune Cells. *J Immunol Res* **2015**, (2015).

138. Martineau, A. R. *et al.* Neutrophil-mediated innate immune resistance to mycobacteria. *J Clin Invest* **117**, 1988–1994 (2007).

139. Lowe, D. M., Redford, P. S., Wilkinson, R. J., O'Garra, A. & Martineau, A. R. Neutrophils in tuberculosis: friend or foe? *Trends Immunol* **33**, 14–25 (2012).

140. Kolaczkowska, E. & Kubes, P. Neutrophil recruitment and function in health and inflammation. *Nat Rev Immunol* **13**, 159–175 (2013).

141. Amulic, B., Cazalet, C., Hayes, G. L., Metzler, K. D. & Zychlinsky, A. Neutrophil function: from mechanisms to disease. *Annu Rev Immunol* **30**, 459–489 (2012).

142. Dorhoi, A. & Kaufmann, S. H. E. Versatile myeloid cell subsets contribute to tuberculosis-associated inflammation. *Eur J Immunol* **45**, 2191–2202 (2015).

143. Gupta, N., Kumar, R. & Agrawal, B. New Players in Immunity to Tuberculosis: The Host Microbiome, Lung Epithelium, and Innate Immune Cells. *Front Immunol* **9**, (2018).

144. Eruslanov, E. B. *et al.* Neutrophil responses to *Mycobacterium tuberculosis* infection in genetically susceptible and resistant mice. *Infect Immun* **73**, 1744–1753 (2005).

145. Lovewell, R. R., Baer, C. E., Mishra, B. B., Smith, C. M. & Sassetti, C. M. Granulocytes act as a niche for *Mycobacterium tuberculosis* growth. *Mucosal Immunol* **14**, 229–241 (2021).

146. Marzo, E. *et al.* Damaging role of neutrophilic infiltration in a mouse model of progressive tuberculosis. *Tuberculosis (Edinb)* **94**, 55–64 (2014).

147. Keller, C. *et al.* Genetically determined susceptibility to tuberculosis in mice causally involves accelerated and enhanced recruitment of granulocytes. *Infect Immun* **74**, 4295–4309 (2006).

148. Condos, R., Rom, W. N., Liu, Y. M. & Schluger, N. W. Local immune responses correlate with presentation and outcome in tuberculosis. *Am J Respir Crit Care Med* **157**, 729–735 (1998).

149. Lowe, D. M. *et al.* Neutrophilia independently predicts death in tuberculosis. *Eur Respir J* **42**, 1752–1757 (2013).

150. Kimmey, J. M. *et al.* Unique role for ATG5 in neutrophil-mediated immunopathology during *M. tuberculosis* infection. *Nature* **528**, 565–569 (2015).

151. Nandi, B. & Behar, S. M. Regulation of neutrophils by interferon-γ limits lung inflammation during tuberculosis infection. *J Exp Med* **208**, 2251–2262 (2011).

152. Moreira-Teixeira, L. *et al.* Mouse transcriptome reveals potential signatures of protection and pathogenesis in human tuberculosis. *Nat Immunol* **21**, 464–476 (2020).

153. Moreira-Teixeira, L. *et al.* Type I IFN exacerbates disease in tuberculosis-susceptible mice by inducing neutrophil-mediated lung inflammation and NETosis. *Nat Commun* **11**, (2020).

154. Gern, B. H. *et al.* CD4-mediated immunity shapes neutrophil-driven tuberculous pathology. *bioRxiv* 2024.04.12.589315 (2024) doi:10.1101/2024.04.12.589315.

155. Cavalcante-Silva, L. H. A. *et al. Mycobacterium tuberculosis* in a Trap: The Role of Neutrophil Extracellular Traps in Tuberculosis. *Int J Mol Sci* **24**, 11385 (2023).

156. Chowdhury, C. S. *et al.* Type I IFN-mediated NET release promotes *Mycobacterium tuberculosis* replication and is associated with granuloma caseation. *Cell Host Microbe* **32**, 2092-2111.e7 (2024).

157. Hilda, J. N., Das, S., Tripathy, S. P. & Hanna, L. E. Role of neutrophils in tuberculosis: A bird's eye view. *Innate Immun* **26**, 240 (2019).

158. Lyadova, I. V. Neutrophils in Tuberculosis: Heterogeneity Shapes the Way? *Mediators Inflamm* **2017**, (2017).

159. Fulton, S. A. *et al.* Inhibition of major histocompatibility complex II expression and antigen processing in murine alveolar macrophages by *Mycobacterium bovis* BCG and the 19-kilodalton mycobacterial lipoprotein. *Infect Immun* **72**, 2101–2110 (2004).

160. Srivastava, S., Grace, P. S. & Ernst, J. D. Antigen Export Reduces Antigen Presentation and Limits T Cell Control of *M. tuberculosis*. *Cell Host Microbe* **19**, 44–54 (2016).

161. Georgieva, M., Sia, J. K., Bizzell, E., Madan-Lala, R. & Rengarajan, J. *Mycobacterium tuberculosis* GroEL2 Modulates Dendritic Cell Responses. *Infect Immun* **86**, (2018).

162. Sutiwisesak, R. *et al.* A natural polymorphism of *Mycobacterium tuberculosis* in the esxH gene disrupts immunodomination by the TB10.4-specific CD8 T cell response. *PLoS Pathog* **16**, (2020).

163. Blomgran, R., Desvignes, L., Briken, V. & Ernst, J. D. *Mycobacterium tuberculosis* inhibits neutrophil apoptosis, leading to delayed activation of naive CD4 T cells. *Cell Host Microbe* **11**, 81–90 (2012).

164. Gern, B. H. *et al.* TGFβ restricts expansion, survival, and function of T cells within the tuberculous granuloma. *Cell Host Microbe* **29**, 594-606.e6 (2021).

165. Gautam, U. S. *et al.* In vivo inhibition of tryptophan catabolism reorganizes the tuberculoma and augments immune-mediated control of *Mycobacterium tuberculosis*. *Proc Natl Acad Sci U S A* **115**, E62–E71 (2018).

166. North, R. J. & Jung, Y. J. Immunity to tuberculosis. *Annu Rev Immunol* **22**, 599–623 (2004).

167. Orme, I. M., Andersen, P. & Boom, W. H. T cell response to *Mycobacterium tuberculosis*. *J Infect Dis* **167**, 1481–1497 (1993).

168. Flynn, J. L. & Chan, J. Immunology of tuberculosis. *Annu Rev Immunol* **19**, 93–129 (2001).

169. Gutierrez, M. G. *et al.* Autophagy is a defense mechanism inhibiting BCG and *Mycobacterium tuberculosis* survival in infected macrophages. *Cell* **119**, 753–766 (2004).

170. Macmicking, J. D. *et al.* Identification of nitric oxide synthase as a protective locus against tuberculosis. *Proc Natl Acad Sci U S A* **94**, 5243–5248 (1997).

171. Scanga, C. A. *et al.* The inducible nitric oxide synthase locus confers protection against aerogenic challenge of both clinical and laboratory strains of *Mycobacterium tuberculosis* in mice. *Infect Immun* **69**, 7711–7717 (2001).

172. Casanova, J. L. & Abel, L. Genetic dissection of immunity to mycobacteria: the human model. *Annu Rev Immunol* **20**, 581–620 (2002).

173. Liu, X., Li, H., Li, S., Yuan, J. & Pang, Y. Maintenance and recall of memory T cell populations against tuberculosis: Implications for vaccine design. *Front Immunol* **14**, (2023).

174. Li, F. *et al.* Tuberculosis Vaccines and T Cell Immune Memory. *Vaccines (Basel)* **12**, (2024).

175. Darrah, P. A. *et al.* Prevention of tuberculosis in macaques after intravenous BCG immunization. *Nature* **577**, 95–102 (2020).

176. Peters, J. M. *et al.* High-dose intravenous BCG vaccination induces enhanced immune signaling in the airways. *Sci Adv* **11**, (2025).

177. Tameris, M. D. *et al.* Safety and efficacy of MVA85A, a new tuberculosis vaccine, in infants previously vaccinated with BCG: a randomised, placebo-controlled phase 2b trial. *Lancet* **381**, 1021–1028 (2013).

178. Liu, X. *et al.* A multistage mycobacterium tuberculosis subunit vaccine LT70 including latency antigen Rv2626c induces long-term protection against tuberculosis. *Hum Vaccin Immunother* **12**, 1670–1677 (2016).

179. Sakai, S. *et al.* CD4 T Cell-Derived IFN-γ Plays a Minimal Role in Control of Pulmonary *Mycobacterium tuberculosis* Infection and Must Be Actively Repressed by PD-1 to Prevent Lethal Disease. *PLoS Pathog* **12**, (2016).

180. Khader, S. A. *et al.* IL-23 compensates for the absence of IL-12p70 and is essential for the IL-17 response during tuberculosis but is dispensable for protection and antigen-specific IFN-gamma responses if IL-12p70 is available. *J Immunol* **175**, 788–795 (2005).

181. Cruz, A. *et al.* Cutting edge: IFN-gamma regulates the induction and expansion of IL-17-producing CD4 T cells during mycobacterial infection. *J Immunol* **177**, 1416–1420 (2006).

182. Cruz, A. *et al.* Pathological role of interleukin 17 in mice subjected to repeated BCG vaccination after infection with *Mycobacterium tuberculosis*. *J Exp Med* **207**, 1609–1616 (2010).

183. Torrado, E. & Cooper, A. M. IL-17 and Th17 cells in tuberculosis. *Cytokine Growth Factor Rev* **21**, 455–462 (2010).

184. Harrington, L. E. *et al.* Interleukin 17-producing CD4+ effector T cells develop via a lineage distinct from the T helper type 1 and 2 lineages. *Nat Immunol* **6**, 1123–1132 (2005).

185. Park, H. *et al.* A distinct lineage of CD4 T cells regulates tissue inflammation by producing interleukin 17. *Nat Immunol* **6**, 1133–1141 (2005).

186. Scriba, T. J. *et al.* Sequential inflammatory processes define human progression from *M. tuberculosis* infection to tuberculosis disease. *PLoS Pathog* **13**, (2017).

187. Wilkinson, K. A. & Wilkinson, R. J. Polyfunctional T cells in human tuberculosis. *Eur J Immunol* **40**, 2139–2142 (2010).

188. Qin, S. *et al.* Multifunctional T cell response in active pulmonary tuberculosis patients. *Int Immunopharmacol* **99**, (2021).

189. Zeng, G., Zhang, G. & Chen, X. Th1 cytokines, true functional signatures for protective immunity against TB? *Cell Mol Immunol* **15**, 206–215 (2018).

190. Havlir, D. V. & Barnes, P. F. Tuberculosis in patients with human immunodeficiency virus infection. *N Engl J Med* **340**, 367–373 (1999).

191. Mogues, T., Goodrich, M. E., Ryan, L., LaCourse, R. & North, R. J. The relative importance of T cell subsets in immunity and immunopathology of airborne *Mycobacterium tuberculosis* infection in mice. *J Exp Med* **193**, 271–280 (2001).

192. Baliashvili, D. *et al.* Resistance to *Mycobacterium tuberculosis* Infection Among Household Contacts: A Multinational Study. *Clin Infect Dis* **73**, 1037–1045 (2021).

193. Gutierrez, J., Kroon, E. E., Möller, M. & Stein, C. M. Phenotype Definition for 'Resisters' to *Mycobacterium tuberculosis* Infection in the Literature-A Review and Recommendations. *Front Immunol* **12**, (2021).

194. Simmons, J. D. *et al.* Immunological mechanisms of human resistance to persistent *Mycobacterium tuberculosis* infection. *Nat Rev Immunol* **18**, 575–589 (2018).

195. Nunes-Alves, C. *et al.* Human and Murine Clonal CD8+ T Cell Expansions Arise during Tuberculosis Because of TCR Selection. *PLoS Pathog* **11**, (2015).

196. Booty, M. G., Nunes-Alves, C., Carpenter, S. M., Jayaraman, P. & Behar, S. M. Multiple Inflammatory Cytokines Converge To Regulate CD8+ T Cell Expansion and Function during Tuberculosis. *J Immunol* **196**, 1822–1831 (2016).

197. Rothchild, A. C. *et al.* Role of Granulocyte-Macrophage Colony-Stimulating Factor Production by T Cells during *Mycobacterium tuberculosis* Infection. *mBio* **8**, (2017).

198. Lin, P. L. & Flynn, J. A. L. CD8 T cells and *Mycobacterium tuberculosis* infection. *Semin Immunopathol* **37**, 239–249 (2015).

199. Silva, B. D. de S., Trentini, M. M., da Costa, A. C., Kipnis, A. & Junqueira-Kipnis, A. P. Different phenotypes of CD8+ T cells associated with bacterial load in active tuberculosis. *Immunol Lett* **160**, 23–32 (2014).

200. Cho, S. *et al.* Antimicrobial activity of MHC class I-restricted CD8+ T cells in human tuberculosis. *Proc Natl Acad Sci U S A* **97**, 12210–12215 (2000).

201. Serbina, N. V., Liu, C.-C., Scanga, C. A. & Flynn, J. L. CD8+ CTL from lungs of *Mycobacterium tuberculosis*-infected mice express perforin in vivo and lyse infected macrophages. *J Immunol* **165**, 353–363 (2000).

202. Stenger, S. *et al.* An antimicrobial activity of cytolytic T cells mediated by granulysin. *Science* **282**, 121–125 (1998).

203. Dallmann-Sauer, M. *et al. Mycobacterium tuberculosis* resisters despite HIV exhibit activated T cells and macrophages in their pulmonary alveoli. *J Clin Invest* **135**, (2025).

204. Rijnink, W. F., Ottenhoff, T. H. M. & Joosten, S. A. B-Cells and Antibodies as Contributors to Effector Immune Responses in Tuberculosis. *Front Immunol* **12**, (2021).

205. Phuah, J. Y., Mattila, J. T., Lin, P. L. & Flynn, J. L. Activated B cells in the granulomas of nonhuman primates infected with *Mycobacterium tuberculosis*. *Am J Pathol* **181**, 508–514 (2012).

206. Li, H. & Javid, B. Antibodies and tuberculosis: finally coming of age? *Nat Rev Immunol* **18**, 591–596 (2018).

207. Loxton, A. G. Bcells and their regulatory functions during Tuberculosis: Latency and active disease. *Mol Immunol* **111**, 145–151 (2019).

208. Domingo-Gonzalez, R., Prince, O., Cooper, A. & Khader, S. A. Cytokines and Chemokines in *Mycobacterium tuberculosis* Infection. *Microbiol Spectr* **4**, (2016).

209. Cavalcanti, Y. V. N., Brelaz, M. C. A., Neves, J. K. D. A. L., Ferraz, J. C. & Pereira, V. R. A. Role of TNF-Alpha, IFN-Gamma, and IL-10 in the Development of Pulmonary Tuberculosis. *Pulm Med* **2012**, (2012).

210. Eder, C. Mechanisms of interleukin-1beta release. *Immunobiology* **214**, 543–553 (2009).

211. Silvério, D., Gonçalves, R., Appelberg, R. & Saraiva, M. Advances on the Role and Applications of Interleukin-1 in Tuberculosis. *mBio* **12**, (2021).

212. Lopez-Castejon, G. & Brough, D. Understanding the mechanism of IL-1β secretion. *Cytokine Growth Factor Rev* **22**, 189–195 (2011).

213. Mayer-Barber, K. D. & Yan, B. Clash of the Cytokine Titans: counter-regulation of interleukin-1 and type I interferon-mediated inflammatory responses. *Cell Mol Immunol* **14**, 22–35 (2017).

214. Dubois, H., Wullaert, A. & Lamkanfi, M. General Strategies in Inflammasome Biology. *Curr Top Microbiol Immunol* **397**, 1–22 (2016).

215. Sims, J. E. & Smith, D. E. The IL-1 family: regulators of immunity. *Nat Rev Immunol* **10**, 89–102 (2010).

216. Liston, A. & Masters, S. L. Homeostasis-altering molecular processes as mechanisms of inflammasome activation. *Nat Rev Immunol* **17**, 208–214 (2017).

217. Jayaraman, P. *et al.* IL-1β promotes antimicrobial immunity in macrophages by regulating TNFR signaling and caspase-3 activation. *J Immunol* **190**, 4196–4204 (2013).

218. Van Den Eeckhout, B., Tavernier, J. & Gerlo, S. Interleukin-1 as Innate Mediator of T Cell Immunity. *Front Immunol* **11**, 621931 (2021).

219. Lamkanfi, M. & Dixit, V. M. Mechanisms and functions of inflammasomes. *Cell* **157**, 1013–1022 (2014).

220. Juffermans, N. P. *et al.* Interleukin-1 signaling is essential for host defense during murine pulmonary tuberculosis. *J Infect Dis* **182**, 902–908 (2000).

221. Yamada, H., Mizumo, S., Horai, R., Iwakura, Y. & Sugawara, I. Protective role of interleukin-1 in mycobacterial infection in IL-1 alpha/beta double-knockout mice. *Lab Invest* **80**, 759–767 (2000).

222. Mishra, B. B. *et al.* Nitric oxide controls the immunopathology of tuberculosis by inhibiting NLRP3 inflammasome-dependent processing of IL-1β. *Nat Immunol* **14**, 52–60 (2013).

223. Mishra, B. B. *et al.* Nitric oxide prevents a pathogen-permissive granulocytic inflammation during tuberculosis. *Nat Microbiol* **2**, (2017).

224. Gleeson, L. E. *et al.* Cutting Edge: *Mycobacterium tuberculosis* Induces Aerobic Glycolysis in Human Alveolar Macrophages That Is Required for Control of Intracellular Bacillary Replication. *J Immunol* **196**, 2444–2449 (2016).

225. Hackett, E. E. *et al. Mycobacterium tuberculosis* Limits Host Glycolysis and IL-1β by Restriction of PFK-M via MicroRNA-21. *Cell Rep* **30**, 124-136.e4 (2020).

226. Cumming, B. M., Addicott, K. W., Adamson, J. H. & Steyn, A. J. C. *Mycobacterium tuberculosis* induces decelerated bioenergetic metabolism in human macrophages. *Elife* **7**, (2018).

227. Howard, N. C. *et al. Mycobacterium tuberculosis* carrying a rifampicin drug resistance mutation reprograms macrophage metabolism through cell wall lipid changes. *Nat Microbiol* **3**, 1099–1108 (2018).

228. Takeda, K. & Akira, S. Toll-like receptors in innate immunity. *Int Immunol* **17**, 1–14 (2005).

229. McNab, F. W. *et al.* Type I IFN induces IL-10 production in an IL-27-independent manner and blocks responsiveness to IFN-γ for production of IL-12 and bacterial killing in *Mycobacterium tuberculosis*-infected macrophages. *J Immunol* **193**, 3600–3612 (2014).

230. Cheng, Y. & Schorey, J. S. *Mycobacterium tuberculosis*-induced IFN-β production requires cytosolic DNA and RNA sensing pathways. *J Exp Med* **215**, 2919–2935 (2018).

231. Lúcia Moreira-Teixeira, Mayer-Barber, K., Sher, A. & O'Garra, A. Type I interferons in tuberculosis: Foe and occasionally friend. *J Exp Med* **215**, 1273–1285 (2018).

232. Dorhoi, A. *et al.* Type I IFN signaling triggers immunopathology in tuberculosis-susceptible mice by modulating lung phagocyte dynamics. *Eur J Immunol* **44**, 2380–2393 (2014).

233. Zhang, L., Jiang, X., Pfau, D., Ling, Y. & Nathan, C. F. Type I interferon signaling mediates *Mycobacterium tuberculosis*-induced macrophage death. *J Exp Med* **218**, (2021).

234. Ji, D. X. *et al.* Type I interferon-driven susceptibility to *Mycobacterium tuberculosis* is mediated by IL-1Ra. *Nat Microbiol* **4**, 2128–2135 (2019).

235. Mayer-Barber, K. D. *et al.* Host-directed therapy of tuberculosis based on interleukin-1 and type I interferon crosstalk. *Nature* **511**, 99–103 (2014).

236. Redford, P. S., Murray, P. J. & O'Garra, A. The role of IL-10 in immune regulation during *M. tuberculosis* infection. *Mucosal Immunol* **4**, 261–270 (2011).

237. Saraiva, M. & O'Garra, A. The regulation of IL-10 production by immune cells. *Nat Rev Immunol* **10**, 170–181 (2010).

238. Branchett, W. J., Saraiva, M. & O'Garra, A. Regulation of inflammation by Interleukin-10 in the intestinal and respiratory mucosa. *Curr Opin Immunol* **91**, (2024).

239. Ferreira, C. M. *et al.* Early IL-10 promotes vasculature-associated CD4+ T cells unable to control *Mycobacterium tuberculosis* infection. *JCI Insight* **6**, (2021).

240. Braverman, J. & Stanley, S. A. Nitric Oxide Modulates Macrophage Responses to *Mycobacterium tuberculosis* Infection through Activation of HIF-1α and Repression of NF-κB. *J Immunol* **199**, 1805–1816 (2017).

241. Koch, A. & Mizrahi, V. *Mycobacterium tuberculosis*. *Trends Microbiol* **26**, 555–556 (2018).

242. Fu, L. M. & Fu-Liu, C. S. Is *Mycobacterium tuberculosis* a closer relative to Gram-positive or Gram-negative bacterial pathogens? *Tuberculosis* **82**, 85–90 (2002).

243. Brennan, P. J. & Nikaido, H. The envelope of mycobacteria. *Annu Rev Biochem* **64**, 29–63 (1995).

244. Cole, S. T. *et al.* Deciphering the biology of *Mycobacterium tuberculosis* from the complete genome sequence. *Nature* **393**, 537–544 (1998).

245. Russell, D. G. *et al.* Mycobacterium tuberculosis wears what it eats. *Cell Host Microbe* **8**, 68–76 (2010).

246. Galagan, J. E. Genomic insights into tuberculosis. *Nat Rev Genet* **15**, 307–320 (2014).

247. Brosch, R. *et al.* A new evolutionary scenario for the *Mycobacterium tuberculosis* complex. *Proc Natl Acad Sci U S A* **99**, 3684–3689 (2002).

248. Brites, D. *et al.* A New Phylogenetic Framework for the Animal-Adapted *Mycobacterium tuberculosis* Complex. *Front Microbiol* **9**, (2018).

249. Brites, D. & Gagneux, S. Co-evolution of *Mycobacterium tuberculosis* and Homo sapiens. *Immunol Rev* **264**, 6–24 (2015).

250. Gagneux, S. Ecology and evolution of *Mycobacterium tuberculosis*. *Nat Rev Microbiol* **16**, 202–213 (2018).

251. Ngabonziza, J. C. S. *et al.* A sister lineage of the *Mycobacterium tuberculosis* complex discovered in the African Great Lakes region. *Nat Commun* **11**, (2020).

252. Coscolla, M. *et al.* Phylogenomics of *Mycobacterium africanum* reveals a new lineage and a complex evolutionary history. *Microb Genom* **7**, 1–14 (2021).

253. Stucki, D. *et al. Mycobacterium tuberculosis* lineage 4 comprises globally distributed and geographically restricted sublineages. *Nat Genet* **48**, 1535–1543 (2016).

254. Guyeux, C. *et al.* Newly Identified *Mycobacterium africanum* Lineage 10, Central Africa. *Emerg Infect Dis* **30**, 560–563 (2024).

255. Napier, G. *et al.* Robust barcoding and identification of *Mycobacterium tuberculosis* lineages for epidemiological and clinical studies. *Genome Med* **12**, (2020).

256. Krishnan, N. *et al. Mycobacterium tuberculosis* lineage influences innate immune response and virulence and is associated with distinct cell envelope lipid profiles. *PLoS One* **6**, (2011).

257. Portevin, D., Gagneux, S., Comas, I. & Young, D. Human macrophage responses to clinical isolates from the *Mycobacterium tuberculosis* complex discriminate between ancient and modern lineages. *PLoS Pathog* **7**, (2011).

258. Saelens, J. W., Viswanathan, G. & Tobin, D. M. Mycobacterial Evolution Intersects With Host Tolerance. *Front Immunol* **10**, (2019).

259. Bottai, D. *et al.* TbD1 deletion as a driver of the evolutionary success of modern epidemic *Mycobacterium tuberculosis* lineages. *Nat Commun* **11**, (2020).

260. Coscolla, M. & Gagneux, S. Consequences of genomic diversity in *Mycobacterium tuberculosis*. *Semin Immunol* **26**, 431–444 (2014).

261. Firdessa, R. *et al.* Mycobacterial lineages causing pulmonary and extrapulmonary tuberculosis, Ethiopia. *Emerg Infect Dis* **19**, 460–463 (2013).

262. Reed, M. B. *et al.* Major *Mycobacterium tuberculosis* lineages associate with patient country of origin. *J Clin Microbiol* **47**, 1119–1128 (2009).

263. Vasconcellos, S. E. G. *et al.* Distinct genotypic profiles of the two major clades of *Mycobacterium africanum*. *BMC Infect Dis* **10**, (2010).

264. Hershberg, R. *et al.* High functional diversity in *Mycobacterium tuberculosis* driven by genetic drift and human demography. *PLoS Biol* **6**, 2658–2671 (2008).

265. Gagneux, S. *et al.* Variable host-pathogen compatibility in *Mycobacterium tuberculosis*. *Proc Natl Acad Sci U S A* **103**, 2869–2873 (2006).

266. Yeboah-Manu, D. *et al.* Spatio-Temporal Distribution of *Mycobacterium tuberculosis* Complex Strains in Ghana. *PLoS One* **11**, (2016).

267. Gehre, F. *et al.* The first phylogeographic population structure and analysis of transmission dynamics of M. africanum West African 1-combining molecular data from Benin, Nigeria and Sierra Leone. *PLoS One* **8**, (2013).

268. Groenheit, R. *et al.* The Guinea-Bissau family of *Mycobacterium tuberculosis* complex revisited. *PLoS One* **6**, (2011).

269. De Jong, B. C. *et al.* Use of spoligotyping and large sequence polymorphisms to study the population structure of the *Mycobacterium tuberculosis* complex in a cohort study of consecutive smear-positive tuberculosis cases in The Gambia. *J Clin Microbiol* **47**, 994–1001 (2009).

270. Homolka, S. *et al.* High genetic diversity among *Mycobacterium tuberculosis* complex strains from Sierra Leone. *BMC Microbiol* **8**, (2008).

271. Comas, I. *et al.* Out-of-Africa migration and Neolithic coexpansion of *Mycobacterium tuberculosis* with modern humans. *Nat Genet* **45**, 1176–1182 (2013).

272. Koleske, B. N., Jacobs, W. R. & Bishai, W. R. The *Mycobacterium tuberculosis* genome at 25 years: lessons and lingering questions. *J Clin Invest* **133**, (2023).

273. Niemann, S., Merker, M., Kohl, T. & Supply, P. Impact of Genetic Diversity on the Biology of *Mycobacterium tuberculosis* Complex Strains. *Microbiol Spectr* **4**, (2016).

274. Peters, J. S. *et al.* Genetic Diversity in *Mycobacterium tuberculosis* Clinical Isolates and Resulting Outcomes of Tuberculosis Infection and Disease. *Annu Rev Genet* **54**, 511–537 (2020).

275. Séraphin, M. N. *et al.* Association between *Mycobacterium tuberculosis* lineage and site of disease in Florida, 2009-2015. *Infect Genet Evol* **55**, 366–371 (2017).

276. Click, E. S., Moonan, P. K., Winston, C. A., Cowan, L. S. & Oeltmann, J. E. Relationship between *Mycobacterium tuberculosis* phylogenetic lineage and clinical site of tuberculosis. *Clin Infect Dis* **54**, 211–219 (2012).

277. Saelens, J. W. *et al.* An ancestral mycobacterial effector promotes dissemination of infection. *Cell* **185**, 4507-4525.e18 (2022).

278. Sweeney, M. I., Carranza, C. E. & Tobin, D. M. Understanding *Mycobacterium tuberculosis* through its genomic diversity and evolution. *PLoS Pathog* **21**, e1012956 (2025).

279. Pareek, M. *et al.* Ethnicity and mycobacterial lineage as determinants of tuberculosis disease phenotype. *Thorax* **68**, 221–229 (2013).

280. De Souza, G. A. *et al.* Using a label-free proteomics method to identify differentially abundant proteins in closely related hypo- and hypervirulent clinical *Mycobacterium tuberculosis* Beijing isolates. *Mol Cell Proteomics* **9**, 2414–2423 (2010).

281. Hanekom, M. *et al. Mycobacterium tuberculosis* Beijing genotype: a template for success. *Tuberculosis (Edinb)* **91**, 510–523 (2011).

282. De Jong, B. C. *et al.* Progression to active tuberculosis, but not transmission, varies by *Mycobacterium tuberculosis* lineage in The Gambia. *J Infect Dis* **198**, 1037–1043 (2008).

283. Nebenzahl-Guimaraes, H., Verhagen, L. M., Borgdorff, M. W. & Van Soolingena, D. Transmission and Progression to Disease of *Mycobacterium tuberculosis* Phylogenetic Lineages in The Netherlands. *J Clin Microbiol* **53**, 3264–3271 (2015).

284. Thwaites, G. *et al.* Relationship between *Mycobacterium tuberculosis* genotype and the clinical phenotype of pulmonary and meningeal tuberculosis. *J Clin Microbiol* **46**, 1363–1368 (2008).

285. Coscolla, M. Biological and Epidemiological Consequences of MTBC Diversity. *Adv Exp Med Biol* **1019**, 95–116 (2017).

286. Buu, T. N. *et al.* Increased transmission of *Mycobacterium tuberculosis* Beijing genotype strains associated with resistance to streptomycin: a population-based study. *PLoS One* **7**, (2012).

287. Niobe-Eyangoh, S. N. *et al.* Genetic biodiversity of *Mycobacterium tuberculosis* complex strains from patients with pulmonary tuberculosis in Cameroon. *J Clin Microbiol* **41**, 2547–2553 (2003).

288. Gröschel, M. I. *et al.* Differential rates of *Mycobacterium tuberculosis* transmission associate with host-pathogen sympatry. *Nat Microbiol* **9**, 2113–2127 (2024).

289. Caws, M. *et al.* The influence of host and bacterial genotype on the development of disseminated disease with *Mycobacterium tuberculosis*. *PLoS Pathog* **4**, (2008).

290. Luo, Y. *et al.* Paired analysis of host and pathogen genomes identifies determinants of human tuberculosis. *Nat Commun* **15**, 10393 (2024).

291. Fenner, L. *et al.* HIV infection disrupts the sympatric host-pathogen relationship in human tuberculosis. *PLoS Genet* **9**, (2013).

292. Tientcheu, L. D. *et al.* Immunological consequences of strain variation within the *Mycobacterium tuberculosis* complex. *Eur J Immunol* **47**, 432–445 (2017).

293. Homolka, S., Niemann, S., Russell, D. G. & Rohde, K. H. Functional genetic diversity among *Mycobacterium tuberculosis* complex clinical isolates: delineation of conserved core and lineage-specific transcriptomes during intracellular survival. *PLoS Pathog* **6**, 1–17 (2010).

294. Dulberger, C. L., Rubin, E. J. & Boutte, C. C. The mycobacterial cell envelope - a moving target. *Nat Rev Microbiol* **18**, 47–59 (2020).

295. Arbués, A. *et al.* Soluble immune mediators orchestrate protective in vitro granulomatous responses across *Mycobacterium tuberculosis* complex lineages. *Elife* **13**, (2025).

296. Lovey, A. *et al.* Early alveolar macrophage response and IL-1R-dependent T cell priming determine transmissibility of *Mycobacterium tuberculosis* strains. *Nat Commun* **13**, (2022).

297. Verma, S. *et al.* Transmission phenotype of *Mycobacterium tuberculosis* strains is mechanistically linked to induction of distinct pulmonary pathology. *PLoS Pathog* **15**, (2019).

298. Parwati, I., van Crevel, R. & van Soolingen, D. Possible underlying mechanisms for successful emergence of the *Mycobacterium tuberculosis* Beijing genotype strains. *Lancet Infect Dis* **10**, 103–111 (2010).

299. Sohn, H. *et al.* Induction of cell death in human macrophages by a highly virulent Korean Isolate of *Mycobacterium tuberculosis* and the virulent strain H37Rv. *Scand J Immunol* **69**, 43–50 (2009).

300. Sousa, J. *et al. Mycobacterium tuberculosis* associated with severe tuberculosis evades cytosolic surveillance systems and modulates IL-1β production. *Nat Commun* **11**, (2020).

301. Coscolla, M. *et al. M. tuberculosis* T Cell Epitope Analysis Reveals Paucity of Antigenic Variation and Identifies Rare Variable TB Antigens. *Cell Host Microbe* **18**, 538–548 (2015).

302. Comas, Ĩ. *et al.* Human T cell epitopes of *Mycobacterium tuberculosis* are evolutionarily hyperconserved. *Nat Genet* **42**, 498–503 (2010).

303. De Jong, B. C. *et al. Mycobacterium africanum* elicits an attenuated T cell response to early secreted antigenic target, 6 kDa, in patients with tuberculosis and their household contacts. *J Infect Dis* **193**, 1279–1286 (2006).

304. Kim, H. & Shin, S. J. Pathological and protective roles of dendritic cells in *Mycobacterium tuberculosis* infection: Interaction between host immune responses and pathogen evasion. *Front Cell Infect Microbiol* **12**, (2022).

305. Ankley, L., Thomas, S. & Olive, A. J. Fighting Persistence: How Chronic Infections with *Mycobacterium tuberculosis* Evade T Cell-Mediated Clearance and New Strategies To Defeat Them. *Infect Immun* **88**, (2020).

306. Bobba, S. & Khader, S. A. Rifampicin drug resistance and host immunity in tuberculosis: more than meets the eye. *Trends Immunol* **44**, 712–723 (2023).

307. Buck, M. D., Sowell, R. T., Kaech, S. M. & Pearce, E. L. Metabolic Instruction of Immunity. *Cell* **169**, 570–586 (2017).

308. Ogger, P. P. & Byrne, A. J. Macrophage metabolic reprogramming during chronic lung disease. *Mucosal Immunol* **14**, 282–295 (2021).

309. Slack, M., Wang, T. & Wang, R. T cell metabolic reprogramming and plasticity. *Mol Immunol* **68**, 507–512 (2015).

310. Zhang, X. *et al.* Metabolic substrate utilization in stress-induced immune cells. *Intensive Care Med Exp* **8**, (2020).

311. Ganeshan, K. & Chawla, A. Metabolic regulation of immune responses. *Annu Rev Immunol* **32**, 609–634 (2014).

312. Kim, J. K., Park, E. J. & Jo, E. K. Itaconate, Arginine, and Gamma-Aminobutyric Acid: A Host Metabolite Triad Protective Against Mycobacterial Infection. *Front Immunol* **13**, (2022).

313. Qualls, J. E. & Murray, P. J. Immunometabolism within the tuberculosis granuloma: amino acids, hypoxia, and cellular respiration. *Semin Immunopathol* **38**, 139–152 (2016).

314. Howard, N. C. & Khader, S. A. Immunometabolism during *Mycobacterium tuberculosis* Infection. *Trends Microbiol* **28**, 832–850 (2020).

315. Vrieling, F. *et al.* Analyzing the impact of *Mycobacterium tuberculosis* infection on primary human macrophages by combined exploratory and targeted metabolomics. *Sci Rep* **10**, (2020).

316. Nagao, A., Kobayashi, M., Koyasu, S., Chow, C. C. T. & Harada, H. HIF-1-Dependent Reprogramming of Glucose Metabolic Pathway of Cancer Cells and Its Therapeutic Significance. *Int J Mol Sci* **20**, (2019).

317. Li, C., Wang, J., Xu, J. F., Pi, J. & Zheng, B. Roles of HIF-1α signaling in *Mycobacterium tuberculosis* infection: New targets for anti-TB therapeutics? *Biochem Biophys Res Commun* **711**, (2024).

318. Kumar, R. *et al.* Immunometabolism of Phagocytes During *Mycobacterium tuberculosis* Infection. *Front Mol Biosci* **6**, (2019).

319. Russell, S. L. *et al.* Compromised Metabolic Reprogramming Is an Early Indicator of CD8+ T Cell Dysfunction during Chronic *Mycobacterium tuberculosis* Infection. *Cell Rep* **29**, 3564-3579.e5 (2019).

320. Park, J. H., Shim, D., Kim, K. E. S., Lee, W. & Shin, S. J. Understanding Metabolic Regulation Between Host and Pathogens: New Opportunities for the Development of Improved Therapeutic Strategies Against *Mycobacterium tuberculosis* Infection. *Front Cell Infect Microbiol* **11**, (2021).

321. Borah, K. *et al.* Intracellular *Mycobacterium tuberculosis* Exploits Multiple Host Nitrogen Sources during Growth in Human Macrophages. *Cell Rep* **29**, 3580-3591.e4 (2019).

322. Adolph, C., McNeil, M. B. & Cook, G. M. Impaired Succinate Oxidation Prevents Growth and Influences Drug Susceptibility in *Mycobacterium tuberculosis*. *mBio* **13**, e01672-22 (2022).

323. Tannahill, G. M. *et al.* Succinate is an inflammatory signal that induces IL-1β through HIF-1α. *Nature* **496**, 238–242 (2013).

324. Gleeson, L. E. *et al.* Cigarette Smoking Impairs the Bioenergetic Immune Response to *Mycobacterium tuberculosis* Infection. *Am J Respir Cell Mol Biol* **59**, 572–579 (2018).

325. Huang, Y., Zhu, C., Pan, L. & Zhang, Z. The role of *Mycobacterium tuberculosis* acetyltransferase and protein acetylation modifications in tuberculosis. *Front Cell Infect Microbiol* **13**, 1218583 (2023).

326. Wilburn, K. M., Fieweger, R. A. & VanderVen, B. C. Cholesterol and fatty acids grease the wheels of *Mycobacterium tuberculosis* pathogenesis. *Pathog Dis* **76**, fty021 (2018).

327. Li, Y. *et al.* Blockage of citrate export prevents TCA cycle fragmentation via Irg1 inactivation. *Cell Rep* **38**, (2022).

328. Hooftman, A. & O'Neill, L. A. J. The Immunomodulatory Potential of the Metabolite Itaconate. *Trends Immunol* **40**, 687–698 (2019).

329. Lampropoulou, V. *et al.* Itaconate Links Inhibition of Succinate Dehydrogenase with Macrophage Metabolic Remodeling and Regulation of Inflammation. *Cell Metab* **24**, 158–166 (2016).

330. Chandel, N. S. Amino Acid Metabolism. *Cold Spring Harb Perspect Biol* **13**, (2021).

331. Sorgdrager, F. J. H., Naudé, P. J. W., Kema, I. P., Nollen, E. A. & De Deyn, P. P. Tryptophan Metabolism in Inflammaging: From Biomarker to Therapeutic Target. *Front Immunol* **10**, (2019).

332. Agapova, A. *et al.* Flexible nitrogen utilisation by the metabolic generalist pathogen *Mycobacterium tuberculosis*. *Elife* **8**, (2019).

333. Shi, L. *et al.* Infection with *Mycobacterium tuberculosis* induces the Warburg effect in mouse lungs. *Sci Rep* **5**, (2015).

334. Cortassa, S., Aon, M. A. & Sollott, S. J. Control and Regulation of Substrate Selection in Cytoplasmic and Mitochondrial Catabolic Networks. A Systems Biology Analysis. *Front Physiol* **10**, (2019).

335. Shi, L., Jiang, Q., Bushkin, Y., Subbian, S. & Tyagi, S. Biphasic Dynamics of Macrophage Immunometabolism during *Mycobacterium tuberculosis* Infection. *mBio* **10**, (2019).

336. Refai, A., Gritli, S., Barbouche, M. R. & Essafi, M. *Mycobacterium tuberculosis* Virulent Factor ESAT-6 Drives Macrophage Differentiation Toward the Pro-inflammatory M1 Phenotype and Subsequently Switches It to the Anti-inflammatory M2 Phenotype. *Front Cell Infect Microbiol* **8**, (2018).

337. Faas, M. M. & de Vos, P. Mitochondrial function in immune cells in health and disease. *Biochim Biophys Acta Mol Basis Dis* **1866**, (2020).

338. Laval, T., Chaumont, L. & Demangel, C. Not too fat to fight: The emerging role of macrophage fatty acid metabolism in immunity to *Mycobacterium tuberculosis*. *Immunol Rev* **301**, 84–97 (2021).

339. Knight, M., Braverman, J., Asfaha, K., Gronert, K. & Stanley, S. Lipid droplet formation in *Mycobacterium tuberculosis* infected macrophages requires IFN-γ/HIF-1α signaling and supports host defense. *PLoS Pathog* **14**, (2018).

340. Sheedy, F. J. & Divangahi, M. Targeting immunometabolism in host defence against *Mycobacterium tuberculosis*. *Immunology* **162**, 145–159 (2021).

341. Singh, V., Kaur, C., Chaudhary, V. K., Rao, K. V. S. & Chatterjee, S. *M. tuberculosis* Secretory Protein ESAT-6 Induces Metabolic Flux Perturbations to Drive Foamy Macrophage Differentiation. *Sci Rep* **5**, (2015).

342. Singh, V. *et al. Mycobacterium tuberculosis*-driven targeted recalibration of macrophage lipid homeostasis promotes the foamy phenotype. *Cell Host Microbe* **12**, 669–681 (2012).

343. Kim, H. & Shin, S. J. Revolutionizing control strategies against *Mycobacterium tuberculosis* infection through selected targeting of lipid metabolism. *Cell Mol Life Sci* **80**, (2023).

344. Pisu, D., Huang, L., Grenier, J. K. & Russell, D. G. Dual RNA-Seq of Mtb-Infected Macrophages In Vivo Reveals Ontologically Distinct Host-Pathogen Interactions. *Cell Rep* **30**, 335-350.e4 (2020).

345. Parbhoo, T., Mouton, J. M. & Sampson, S. L. Phenotypic adaptation of *Mycobacterium tuberculosis* to host-associated stressors that induce persister formation. *Front Cell Infect Microbiol* **12**, 956607 (2022).

346. Llibre, A. *et al.* Host Immune-Metabolic Adaptations Upon Mycobacterial Infections and Associated Co-Morbidities. *Front Immunol* **12**, (2021).

347. Cumming, B. M., Pacl, H. T. & Steyn, A. J. C. Relevance of the Warburg Effect in Tuberculosis for Host-Directed Therapy. *Front Cell Infect Microbiol* **10**, (2020).

348. Dorhoi, A. *et al.* Activation of the NLRP3 inflammasome by *Mycobacterium tuberculosis* is uncoupled from susceptibility to active tuberculosis. *Eur J Immunol* **42**, 374–384 (2012).

349. Lachmandas, E. *et al.* Rewiring cellular metabolism via the AKT/mTOR pathway contributes to host defence against *Mycobacterium tuberculosis* in human and murine cells. *Eur J Immunol* **46**, 2574–2586 (2016).

350. Rahman, M. A. *et al.* Hydrogen sulfide dysregulates the immune response by suppressing central carbon metabolism to promote tuberculosis. *Proc Natl Acad Sci U S A* **117**, 6663–6674 (2020).

351. Olson, G. S. *et al.* Type I interferon decreases macrophage energy metabolism during mycobacterial infection. *Cell Rep* **35**, (2021).

352. Mcgettrick, A. F. & O'Neill, L. A. J. NLRP3 and IL-1β in macrophages as critical regulators of metabolic diseases. *Diabetes Obes Metab* **15 Suppl 3**, 19–25 (2013).

353. Mehrotra, P. *et al.* Pathogenicity of *Mycobacterium tuberculosis* is expressed by regulating metabolic thresholds of the host macrophage. *PLoS Pathog* **10**, (2014).

354. Baay-Guzman, G. J. *et al.* Dual role of hypoxia-inducible factor 1 α in experimental pulmonary tuberculosis: its implication as a new therapeutic target. *Future Microbiol* **13**, 785–798 (2018).

CHAPTER 2

AIMS

CHAPTER 2

AIMS

Tuberculosis remains the deadliest infectious disease worldwide, causing around 1.25 million deaths annually. Despite considerable research efforts, the host-pathogen interactions that determine tuberculosis severity remain poorly understood. The heterogeneity of tuberculosis outcomes is affected by host factors and *Mycobacterium tuberculosis* diversity. In our research group, we have characterised a cohort of 681 tuberculosis patients and identified *M. tuberculosis* clinical isolates associated with either mild (4I2) or severe (6C4) disease outcomes. Previous work from our group revealed that these isolates elicit distinct levels of interleukin (IL)-1β, a cytokine essential for host resistance, in macrophages.

This thesis aims to dissect the interplay between host susceptibility, bacterial diversity, and immune responses during tuberculosis by addressing the following key questions:

1) Metabolic determinants of inflammasome activation: Given the striking differences in IL-1β production between macrophages infected with *M. tuberculosis* 4I2 and 6C4, we aimed to determine whether this differential response was linked to distinct metabolic reprogramming. Metabolic shifts in glycolysis, tricarboxylic acid (TCA) cycle intermediates, mitochondrial reactive oxygen species (ROS) production, and electron transport chain (ETC) assembly have been associated with NLR family pyrin domain containing 3 (NLRP3) inflammasome activation and IL-1β secretion. Here, we investigated whether *M. tuberculosis* 4I2 and 6C4 differentially rewired macrophage metabolism and if these metabolic adaptations were required for inflammasome activation and IL-1β production.

2) Host susceptibility and immune signatures of tuberculosis severity: To model tuberculosis severity in vivo and identify immune mechanisms that distinguish mild from severe disease, we used C3HeB/FeJ (susceptible) and C57BL/6 (resistant) mice. These mouse strains differ in their lung pathology and immune signatures, with C3HeB/FeJ mice more accurately recapitulating human tuberculosis. Our objective was to characterise the initial immune

responses in the lungs of susceptible and resistant mice during infection with clinically relevant *M. tuberculosis* isolates, as well as identify immune signatures associated with tuberculosis severity.

This thesis combines macrophage-focused in vitro studies with in vivo murine models to shed light on the molecular and immunological mechanisms influencing the severity of tuberculosis. Gaining insight into the host-pathogen interaction will be instrumental in identifying novel therapeutic targets and biomarkers to improve tuberculosis control strategies.

CHAPTER 3

EXPERIMENTAL RESULTS

GENETICALLY DIVERSE *MYCOBACTERIUM TUBERCULOSIS* ISOLATES MANIPULATE INFLAMMASOME AND INTERLEUKIN 1β SECRETION INDEPENDENTLY OF MACROPHAGE METABOLIC REWIRING

The research presented in this chapter was partially funded by a European Society of Clinical Microbiology and Infectious Diseases (ESCMID) Research Grant 2022 awarded to Ana Isabel Fernandes.

This chapter has been published in *The Journal of Infectious Diseases*.

GENETICALLY DIVERSE *MYCOBACTERIUM TUBERCULOSIS* ISOLATES MANIPULATE INFLAMMASOME AND IL-1β SECRETION INDEPENDENTLY OF MACROPHAGE METABOLIC REWIRING

Ana Isabel Fernandes[1,2], Alexandre Jorge Pinto[1], Diogo Silvério[1,2], Ulrike Zedler[3], Carolina Ferreira[4,5], Iola F. Duarte[6], Ricardo Silvestre[4,5], Anca Dorhoi[3,7], Margarida Saraiva[1,8]

1 Instituto de Investigação e Inovação em Saúde, University of Porto, Porto, Portugal

2 Doctoral Program in Molecular and Cell Biology, Instituto de Ciências Biomédicas Abel Salazar, University of Porto, Porto, Portugal

3 Institute of Immunology, Friedrich-Loeffler-Institut, Greifswald-Insel Riems, Germany

4 Life and Health Sciences Research Institute, School of Medicine, University of Minho, Braga, Portugal

5 ICVS/3B's-PT Government Associate Laboratory, Braga, Portugal

6 CICECO-Aveiro Institute of Materials, Department of Chemistry, University of Aveiro, Aveiro, Portugal

7 Faculty of Mathematics and Natural Sciences, University of Greifswald, Greifswald, Germany

8 Instituto de Biologia Molecular e Celular, University of Porto, Porto, Portugal

Published in:

https://doi.org/10.1093/infdis/jiae583 **The Journal of Infectious Diseases** 2024

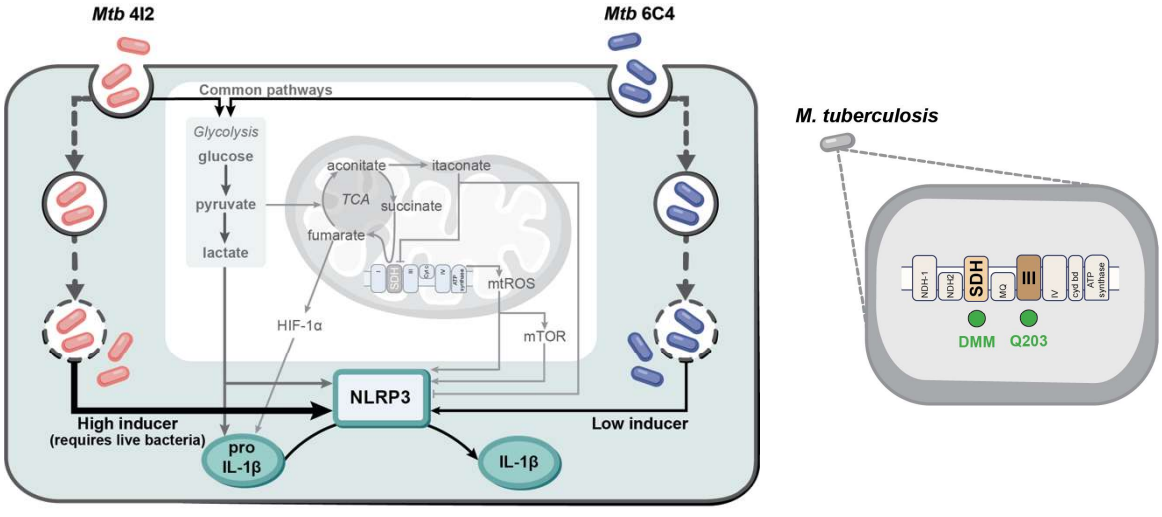

The Journal of Infectious Diseases
MAJOR ARTICLE

Genetically Diverse *Mycobacterium tuberculosis* Isolates Manipulate Inflammasome and Interleukin 1β Secretion Independently of Macrophage Metabolic Rewiring

Ana Isabel Fernandes,[1,2] Alexandre Jorge Pinto,[1] Diogo Silvério,[1,2,a] Ulrike Zedler,[3] Carolina Ferreira,[4,5] Iola F. Duarte,[6] Ricardo Silvestre,[4,5] Anca Dorhoi,[3,7] and Margarida Saraiva[1,8]

[1]Instituto de Investigação e Inovação em Saúde, Universidade do Porto, Porto, Portugal; [2]Doctoral Program in Molecular and Cell Biology, Instituto de Ciências Biomédicas Abel Salazar, Universidade do Porto, Porto, Portugal; [3]Institute of Immunology, Friedrich-Loeffler-Institut, Greifswald-Insel Riems, Germany; [4]Life and Health Sciences Research Institute (ICVS), School of Medicine, University of Minho, Braga, Portugal; [5]ICVS/3B's-PT Government Associate Laboratory, Braga, Portugal; [6]CICECO-Aveiro Institute of Materials, Department of Chemistry, University of Aveiro, Aveiro, Portugal; [7]Faculty of Mathematics and Natural Sciences, University of Greifswald, Greifswald, Germany; and [8]Instituto de Biologia Molecular e Celular, University of Porto, Porto, Portugal

The diversity of *Mycobacterium tuberculosis* impacts the outcome of tuberculosis. We previously showed that *M. tuberculosis* isolates obtained from patients with severe disease induced low inflammasome activation and interleukin 1β (IL-1β) production by infected macrophages. Here we questioned whether this differential modulation of macrophages by *M. tuberculosis* isolates depended on distinct metabolic reprogramming. We found that the macrophage metabolic landscape was similar regardless of the infecting *M. tuberculosis* isolate. Paralleling single–Toll-like receptor (TLR) activated macrophages, glycolysis inhibition during infection impaired IL-1β secretion. However, departing from TLR -based models, in infected macrophages, IL-1β secretion was independent of mitochondrial metabolic changes and hypoxia-inducible factor 1α (HIF-1α). Additionally, we found an unappreciated impact of a host metabolic inhibitor on the pathogen, and show that inflammasome activation and IL-1β production by macrophages require metabolically active bacteria. Our study highlights the potential confounding effect of host metabolic inhibitors on the pathogen and uncoupling of *M. tuberculosis*-inflammasome modulation from the host metabolic reprogramming.

Keywords. *Mycobacterium tuberculosis*; immunometabolism; inflammasome; macrophage.

Lay Summary. *Mycobacterium tuberculosis* is the causative agent of tuberculosis and the top infectious killer in the world, with around 1.3 million deaths reported annually. The genetic variability of this pathogen can shape its interaction with the host and modulate disease outcomes. We previously found that *M. tuberculosis* clinical isolates from patients with severe forms of tuberculosis evade cytosolic surveillance systems in macrophages. Here, we explored whether this evasion tactic was linked to metabolic alterations in the infected macrophages. We found that different *M. tuberculosis* isolates induced similar metabolic changes in infected macrophages. Additionally, we demonstrate that both host glycolysis and pathogen's metabolism were pivotal for maximum interleukin 1β (IL-1β) production. These findings highlight the complexity of macrophage-pathogen interactions and emphasize that bacterial metabolism should be considered in metabolic studies and may be amenable to therapeutic intervention against tuberculosis.

The metabolic reprogramming of immune cells is central to the immune response [1]. There has been a growing interest in understanding metabolic reprogramming during tuberculosis, a disease that claims over 1.3 million lives annually [2]. In experimental infections, *Mycobacterium tuberculosis* shifts the lung immune cell metabolism from oxidative phosphorylation towards glycolysis [3]. Several studies also support the metabolic reprogramming of *M. tuberculosis*-infected macrophages to fuel antimicrobial responses [3–6], although this metabolic shift is not ubiquitous amongst immune cells [7]. Monocyte-derived macrophages upregulate glycolysis, and alveolar macrophages β-oxidation and fatty acid uptake [3, 8, 9]. Furthermore, recent studies suggest an impact of the pathogen's natural diversity on the metabolic rewiring of the infected cells [10, 11].

The accumulation of tricarboxylic acid (TCA) cycle intermediates, assembly of the electron transport chain (ETC) and mitochondrial reactive oxygen species (ROS) production are linked to NLRP3 activation and interleukin 1β (IL-1β)

Received 25 June 2024; editorial decision 18 November 2024; accepted 19 November 2024; published online 21 November 2024

[a]Current affiliation: ENZIfarma SA, Vila Nova de Gaia, Portugal.

Correspondence: Margarida Saraiva, PhD, Instituto de Investigacao e Inovacao em Saude, Universidade do Porto, Rua Alfredo Allen 208, 4200-135 Porto, Portugal, (margarida.saraiva@i3s.up.pt).

The Journal of Infectious Diseases®

© The Author(s) 2024. Published by Oxford University Press on behalf of Infectious Diseases Society of America.
This is an Open Access article distributed under the terms of the Creative Commons Attribution-NonCommercial-NoDerivs licence (https://creativecommons.org/licenses/by-nc-nd/4.0/), which permits non-commercial reproduction and distribution of the work, in any medium, provided the original work is not altered or transformed in any way, and that the work is properly cited. For commercial re-use, please contact reprints@oup.com for reprints and translation rights for reprints. All other permissions can be obtained through our RightsLink service via the Permissions link on the article page on our site—for further information please contact journals.permissions@oup.com.

https://doi.org/10.1093/infdis/jiae583

production [12–14]. Given the key role of IL-1β in host resistance to *M. tuberculosis* [15], the mechanisms leading to inflammasome activation, particularly NLRP3 and AIM2, in response to this pathogen have attracted much attention [16]. Several *M. tuberculosis*-encoded proteins and lipids activate the NLRP3 inflammasome, whereas *M. tuberculosis* DNA activates AIM2 [16]. Counteracting the protective role of inflammasomes, *M. tuberculosis* has developed several mechanisms to evade NLRP3 activation [16], including action of the *M. tuberculosis*-encoded serine-threonine kinase PknF [17], the serine hydrolase Hip1 [18], and of Rv3364c [19]. We previously showed that *M. tuberculosis* isolates obtained from severe tuberculosis cases evaded macrophage cytosolic surveillance systems, while those from mild tuberculosis activated the inflammasome, thus inducing high levels of IL-1β in macrophages [20]. Here, we questioned whether distinct *M. tuberculosis* isolates differentially rewired the macrophage metabolism. We show that irrespective of their ability to induce IL-1β, the *M. tuberculosis* isolates under study similarly altered the macrophage metabolic profiles. We show that maximum IL-1β production depended on the macrophage glycolytic shift and on metabolically active bacteria. However, unlike single-Toll-like receptor (TLR) agonists [21–23], *M. tuberculosis* infection uncoupled mitochondrial metabolic alterations from inflammasome activation and IL-1β secretion. Collectively, our study highlights the importance of examining metabolic/inflammatory networks using live *M. tuberculosis* and shows the potential impact of host metabolic inhibitors on the pathogen, offering new perspectives on the immunometabolic control of cytokine responses in tuberculosis.

METHODS

Animals, Reagents, and Bacterial Stocks

C57BL/6 mice (male/female, 8–12 weeks) were maintained under specific-pathogen-free conditions at Instituto de Investigação e Inovação em Saúde or Friedrich-Loeffler-Institut. Myeloid-restricted hypoxia-inducible factor (Hif)$1a^{fl/fl}$-LysMcre$^{+/+}$ (mHIF-$1\alpha^{-/-}$), C57BL/6NJ-Acod$1^{em1(IMPC)J}$/J (IRG$1^{-/-}$), and matched C57BL/6 were provided by Dr Ricardo Silvestre and Dr Agostinho Carvalho, Life and Health Sciences Research Institute, School of Medicine, University of Minho, Portugal. Experiments followed Animal Research: Reporting of *In Vivo* Experiments (ARRIVE) guidelines, complying with European Union Directive 2010/63/EU, German Animal Welfare, and Portuguese *Direção Geral de Alimentação e Veterinária* (DGAV) regulations.

All reagents and resources are listed in Supplementary Table 1.

M. tuberculosis were cultured in Middlebrook 7H9 medium with 10% oleic albumin dextrose catalase (OADC) and 0.2% glycerol, and aliquoted stocks stored at −80°C. The bacteria concentration was calculated by colony-forming units enumeration.

Bone Marrow-Derived Macrophages Generation

Mouse bone marrow cells (tibias and femurs) were plated at 0.5×10^6 cells/mL in Petri dishes in complete Dulbecco's Modified Eagle's Medium (cDMEM) with 20% L-cell conditioned medium (LCCM) or recombinant macrophage colony-stimulating factor (M-CSF), and maintained at 37°C, 5% CO_2. Fresh medium was added on day 4, and cells harvested and plated in cDMEM on day 7. For glucose-free conditions, bone marrow-derived macrophages (BMDM) were preincubated with DMEM without glucose 2 hours before infection. For extracellular acidification rate (ECAR) assays, bone marrow suspensions from cryopreserved stocks were differentiated as above.

Alveolar Macrophages and Bone Marrow Monocytes Isolation and Infection

Alveolar macrophages were obtained by flushing phosphate-buffered saline (PBS)-2% fetal bovine serum (FBS) into the trachea of euthanized mice. Bone marrow monocytes were purified using EasySep Mouse Monocyte Isolation Kit. Cells were infected in media without antibiotics (multiplicity of infection [MOI] = 2, BMDM; MOI = 1, alveolar macrophages and monocytes). Cell pellets or culture supernatants were recovered for RNA, protein analysis, or metabolomics. Supernatants were filter sterilized.

Chemical Inhibitors or Agonists

Chemical inhibitors and agonists 2-deoxy-glucose (2-DG), dimethyl malonate (DMM), mitoTEMPO, and rapamycin were added to BMDM 2 hours before infection. Except for rapamycin, inhibitors were maintained throughout the experiment. Bacteria were treated overnight with 2-DG, DMM, or Q203 and pelleted by centrifugation before infection.

mRNA Analysis

Total RNA was extracted with TripleXtractor, converted to cDNA, and subjected to real-time PCR, with SYBR Green. Target gene mRNA expression was normalized to ubiquitin. Oligonucleotide sequences are in Supplementary Table 2.

IL-1β Quantification

IL-1β was quantified using a commercially available enzyme-linked immunosorbent assay (ELISA).

High-Performance Liquid Chromatography

Glucose and lactate were quantified in culture supernatants by high-performance liquid chromatography; HyperREZ XP Carbohydrate H + 8μM. The mobile phase (0.0025 M H_2SO_4) was refiltered and degasified for 30 minutes. Analysis was conducted with running protocol (sensitivity 8): 15 minutes at a

constant flux of 0.7 mL/min at 54°C. Peaks were detected in a refractive index detector (IOTA 2, Reagents). Integration was performed using Gilson Uniprot Software.

Extracellular Flux Analysis

BMDM were incubated overnight in Cell-Tak coated XFp plates, at 1×10^6 cells/mL in cDMEM. *M. tuberculosis* were cultured as above and the concentration of disaggregated clumps adjusted in cDMEM. cDMEM was replaced with XF DMEM medium 1 hour before the assay. ECAR readings were monitored with XFp extracellular flux analyzer, while glucose, oligomycin, and 2-DG were sequentially added. BMDM were fixed in 4% paraformaldehyde (PFA) overnight and stained with 4′,6-diamidino-2-phenylindole (DAPI). Images were acquired and analyzed on Cell Insight CX7 High-Content Screening. ECAR values were normalized with total cell numbers.

THP1-ASC-GFP Differentiation, Infection, and Speck Quantification

THP1-ASC-GFP cells maintained in complete Roswell Park Memorial Institute medium (RPMI) 1640 with Zeocin and penicillin-streptomycin, were differentiated with phorbol 12-myristate 13-acetate (PMA) for 24 hours, rested for 4 days without PMA, and infected (MOI = 1). For ASC specks detection, infected cells were fixed in 4% PFA and stained with PhenoVue Hoechst 33342 and HCS CellMask Deep Red. Images were acquired in Operetta CLS High-Content Analysis System (20× water, NA 1.0) and analyzed with Harmony software.

Nuclear Magnetic Resonance-Based Metabolomics

At 24 hours postinfection, supernatants were collected and cells were washed and extracted using a biphasic extraction with methanol/chloroform/water (1:1:0.7) [24]. Resulting polar extracts were dried in a SpeedVac concentrator. Collected supernatants (including cell-free medium) underwent a protein-precipitation using cold methanol. Resulting supernatants were vacuum-dried. Cell-free medium was used to assess metabolite consumption and excretion by BMDM. For nuclear magnetic resonance (NMR) analysis, dried samples were resuspended in 600 mL of deuterated PBS (100 mM, pH 7.4) containing 0.1 mM 3-(trimethylsilyl) propanoic acid (TSP-d_4), and 550 mL of each sample was transferred to 5-mm NMR tubes. Samples were analyzed in a Bruker Avance III HD 500 NMR spectrometer, at 500.13 MHz for ^{1}H observation, at 298 K, using a 5-mm TXI probe. Standard 1D ^{1}H spectra with water presaturation (pulse program "noesypr1d", Bruker library) were acquired and processed. Metabolite assignment was based on matching spectral information to reference spectra available in Chenomx (Edmonton), BBIOREFCODE-2–0–0 (Bruker Biospin), and the Human Metabolome Database [25]. Principal component analysis (PCA) was performed in MetaboAnalyst.

In Silico Study of *M. tuberculosis* SDH-1

The 3D structure of *M. tuberculosis* SDH-1 was predicted with amino acid sequences (NCBI protein database: flavoprotein subunit [NP_214762.1], iron-sulfur subunit [NP_217836.1], and membrane anchor subunit [NP_214763.1]) exported to ColabFold (https://colab.research.google.com/github/sokrypton/ColabFold/blob/main/AlphaFold2.ipynb#scrollTo = kOblAo-xetgx) [26]. Models for each domain were individually built against pdb100 templates, and the 5 best models relaxed using AMBER software. The best models were analyzed, and superpositioned with *Mycobacterium smegmatis* SDH-1 (PDB: 7D6 V) using PyMOL Molecular Graphics System. PubChem structures used: ubiquinone-1 (compound identification [CID] 4462), DMM (CID 7943), malonate (CID 9084), and succinate (CID 160419).

Statistical Analysis

Results are represented as mean ± SD or in box-and-whiskers plots (Tukey method). Data were analyzed using GraphPad Prism. Sample size (n) is in figure legends. Normality and log normality were assessed using Shapiro-Wilk or D'Agostino-Pearson tests and outliers with Grubbs test. Statistical significance was defined as $P \leq .05$.

RESULTS

Genetically Distinct *M. tuberculosis* Clinical Isolates Elicit Similar Glycolytic Reprogramming in Macrophages

In our previous study [20], we stratified the tuberculosis severity at presentation for 681 adult patients with pulmonary tuberculosis and investigated how *M. tuberculosis* isolates recovered from patients with mild, moderate, or severe tuberculosis interacted with host cells. We found that *M. tuberculosis* isolates recovered from cases with mild disease consistently induced robust IL-1β responses in macrophages across multiple donors, whereas bacteria recovered from severe tuberculosis cases did not [20]. *M. tuberculosis* isolates 4I2 (high IL-1β inducer; mild tuberculosis) and 6C4 (low IL-1β inducer; severe tuberculosis) were selected from our larger collection of isolates as prototypes of such differences (Figure 1*A*). Given the link between macrophage metabolic reprogramming and inflammasome activation [1, 23], we questioned whether these *M. tuberculosis* clinical isolates might differentially control the macrophage metabolic shift with an impact on IL-1β release.

We first evaluated whether glycolysis affected IL-1β production by BMDM infected with either clinical isolate. Glycolysis inhibition with 2-DG, a nonmetabolizable glucose analogue (Figure 1*B*), abrogated IL-1β secretion and lowered *Il1b* expression in infected BMDM (Figure 1*C*), irrespective of the *M. tuberculosis* isolate. Similar data were observed in infected BMDM cultures deprived of glucose (Figure 1*D*). BMDM infected in the presence of 2-DG or the absence of glucose also showed a significant decrease in lactate, a glycolysis by-product

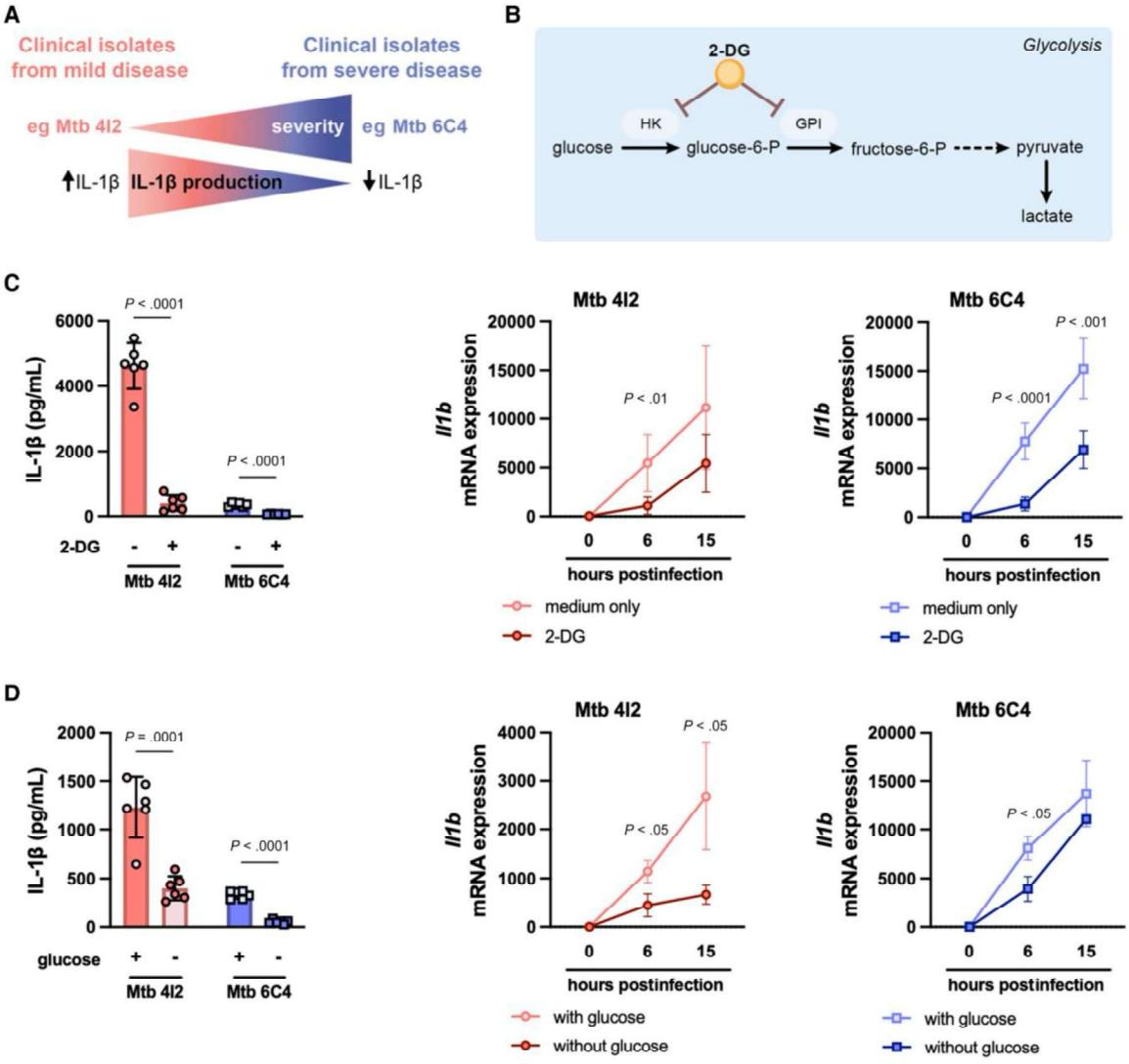

Figure 1. Glucose consumption contributes to IL-1β production by infected macrophages. *A*, Inverse correlation between disease severity and IL-1β production in cells infected with *Mycobacterium tuberculosis* 4I2 and *M. tuberculosis* 6C4, as described in Sousa et al [20]. *B*, 2-DG inhibitory action within the glycolytic pathway. *C* and *D*, Mouse BMDM were left untreated (–) or pretreated (+) for 2 hours with 2-DG (*C*) or incubated with DMEM without glucose (*D*) and subsequently infected at a multiplicity of infection of 2 with either clinical isolate. 2-DG and absence of glucose were maintained for the duration of the experiment. The amount of secreted IL-1β was quantified in the cell culture supernatants 24 hours postinfection. Six and 15 hours postinfection, cell cultures were lysed and the levels of *Il1b* determined by real-time PCR. Represented is the mean ± SD of triplicate wells for 2 experiments (*C*) or 1 experiment representative of 2 (*D*). Statistical analysis was performed using 2-tailed unpaired Student *t* test. Abbreviations: 2-DG, 2-deoxy-glucose; BMDM, bone marrow-derived macrophages; DMEM, Dulbecco's Modified Eagle's Medium; GPI, glucose-6-phosphate isomerase; HK, hexokinase; IL-1β, interleukin 1β; Mtb, *M. tuberculosis*.

(Supplementary Figure 1*A*). Downstream inhibition of the pentose phosphate pathway with 6-animonicotinamide (Supplementary Figure 1*B*) did not significantly impact IL-1β secretion by infected BMDM (Supplementary Figure 1*C*). Importantly, none of the inhibitors altered cell viability (Supplementary Figure 1*D*). Also, the presence of 2-DG or the absence of glucose during infection did not alter bacteria phagocytosis (Supplementary Figure 1*E*).

Given that BMDM infected with *M. tuberculosis* 4I2 or 6C4 required glycolysis to produce IL-1β, we questioned if the glycolytic shift induced by either isolate differed. Compared to noninfected cells, *M. tuberculosis*-infected BMDM showed increased glucose consumption and lactate production, with similar lactate/glucose

ratios (Figure 2A). Consistently, gene expression for glucose transporters and glycolytic enzymes increased in both infections, with only *Slc2a1* and *Hk2* showing higher expression in *M. tuberculosis* 6C4 infections at the later time point (Figure 2B). ECAR assays confirmed a comparable increase in glycolysis, glycolytic capacity, and glycolytic reserve in *M. tuberculosis* 4I2- and 6C4-infected BMDM (Figure 2C). Together, these data indicate a common glycolytic response to live *M. tuberculosis* infection despite downstream strain-specific differences in inflammasome activation and IL-1β production.

IL-1β Production by Infected Macrophages Is Independent of Mitochondrial ROS and mTOR

Because the differences in IL-1β secretion by *M. tuberculosis* 4I2- or 6C4-infected macrophages were not related to differential glycolysis, we investigated the contribution of other metabolic pathways. The oxidation of succinate, a TCA intermediate that accumulates in bacterial infections [27, 28], can lead to mitochondrial depolarization, mitochondrial ROS production, and activation of the mTOR pathway, all converging to inflammasome activation [22, 29] (Figure 3A). To assess the impact of mitochondrial metabolic alterations in IL-1β production by *M. tuberculosis*-infected macrophages, we inhibited succinate dehydrogenase (SDH) with DMM (Figure 3A). DMM markedly decreased IL-1β protein in infected BMDM, irrespective of the *M. tuberculosis* clinical isolate (Figure 3B), but did not affect *Il1b* transcription (Figure 3B). This suggests an effect of DMM in NLRP3 inhibition through the mitochondrial respiratory chain (Figure 3A). However, macrophage staining with Mitotracker Red CMXRos revealed no major alterations in mitochondrial membrane potential between the 2 infections (Supplementary Figure 2A). Additionally, mitochondrial ROS sequestration with mitoTEMPO (Figure 3C) or mTOR blockade with rapamycin (Figure 3D) did not impact IL-1β secretion or *Il1b* transcription. None of the mitochondrial inhibitors altered cell viability (Supplementary Figure 2B), nor bacteria uptake (Supplementary Figure 2C). As a control, mitoTEMPO and rapamycin reduced IL-1β secretion by BMDM stimulated with lipopolysaccharide (LPS) + ATP (Supplementary Figure 2D and 2E), a condition that induces IL-1β secretion in a mitochondrial ROS-dependent way [29, 30]. Thus, IL-1β secretion by *M. tuberculosis*-infected BMDM may be independent of ETC alterations, unlike what has been reported in single-TLR–based systems [14, 23].

As for BMDM, only inhibition of glycolysis (with 2-DG or in medium without glucose) or of SDH (with DMM) lowered IL-1β secretion in *M. tuberculosis* 4I2-infected mouse alveolar macrophages or bone marrow monocytes, and macrophages differentiated from the human monocytic cell line THP1 (Figure 4A–C). Consistent with this, a decrease in inflammasome activation was detected in *M. tuberculosis* 4I2-infected THP1-ASC-GFP reporter cells upon glycolysis or SDH inhibition, whereas mitochondrial ROS sequestration and mTOR inhibition resulted in a sustained percentage of ASC-speck–positive cells (Figure 4D and Supplementary Figure 3).

Collectively, our findings suggest that canonical pathways linking mitochondrial metabolism and inflammasome activation operate differently upon complex stimuli (live *M. tuberculosis*) when compared to single-TLR stimulation.

M. tuberculosis Clinical Isolates Elicit Similar Metabolomic Profiles in Infected Macrophages

To elucidate why SDH inhibition decreased IL-1β secretion in infected macrophages, we performed an extracellular (cell culture supernatants) and intracellular (cell extracts) NMR metabolomic analysis. This included BMDM cultures (noninfected, infected with *M. tuberculosis* 4I2 or 6C4), and bacterial cultures obtained under the same conditions but without host cells. The baseline levels for different metabolites were defined in medium alone, with deviations above or below representing respectively excretion or consumption.

PCA of the extracellular metabolome (Figure 5A) showed infected cells clustering together, suggesting a similar macrophage metabolic reprogramming in both *M. tuberculosis* infections. As above, *M. tuberculosis*-infected BMDM consumed more glucose and secreted more lactate than noninfected macrophages, irrespective of the infecting clinical isolate (Figure 5B). This was accompanied by a slight increase in pyruvate consumption and no effect on fructose (Figure 5B). Infected BMDM cultures also showed increased itaconate and glutamate release, again with no differences between *M. tuberculosis* isolates (Figure 5B). Most of the detected metabolites were similar between the 2 infections and the isolates cultured in the absence of BMDM, and mainly unaffected as compared to the culture medium (Figure 5B and Supplementary Figure 4).

The intracellular metabolome PCA plot showed some separation between cellular and bacteria-only conditions (Figure 5C). However, infected cells clustered together, supporting that no substantial metabolic differences exist between infections with the 2 clinical isolates. Consistent with the extracellular metabolome data and descriptions for other bacterial infections [31–33], we detected an increase of itaconate and alanine in infected cells (Figure 5D). We did not detect an intracellular accumulation of succinate or ATP + ADP upon infection (Figure 5D). Other detected metabolites were also similarly modulated, irrespectively of the *M. tuberculosis* isolate (Supplementary Figure 4).

In essence, both infections induced similar macrophage metabolic alterations, including a glycolytic shift and an increase in TCA cycle by-products, which did not include succinate.

IL-1β Production by *M. tuberculosis*-Infected Macrophages Is Independent of HIF-1α and IRG1 Activity

Succinate is linked to the stabilization of HIF-1α, a transcription factor for *Il1b* [21, 34], while itaconate is associated to

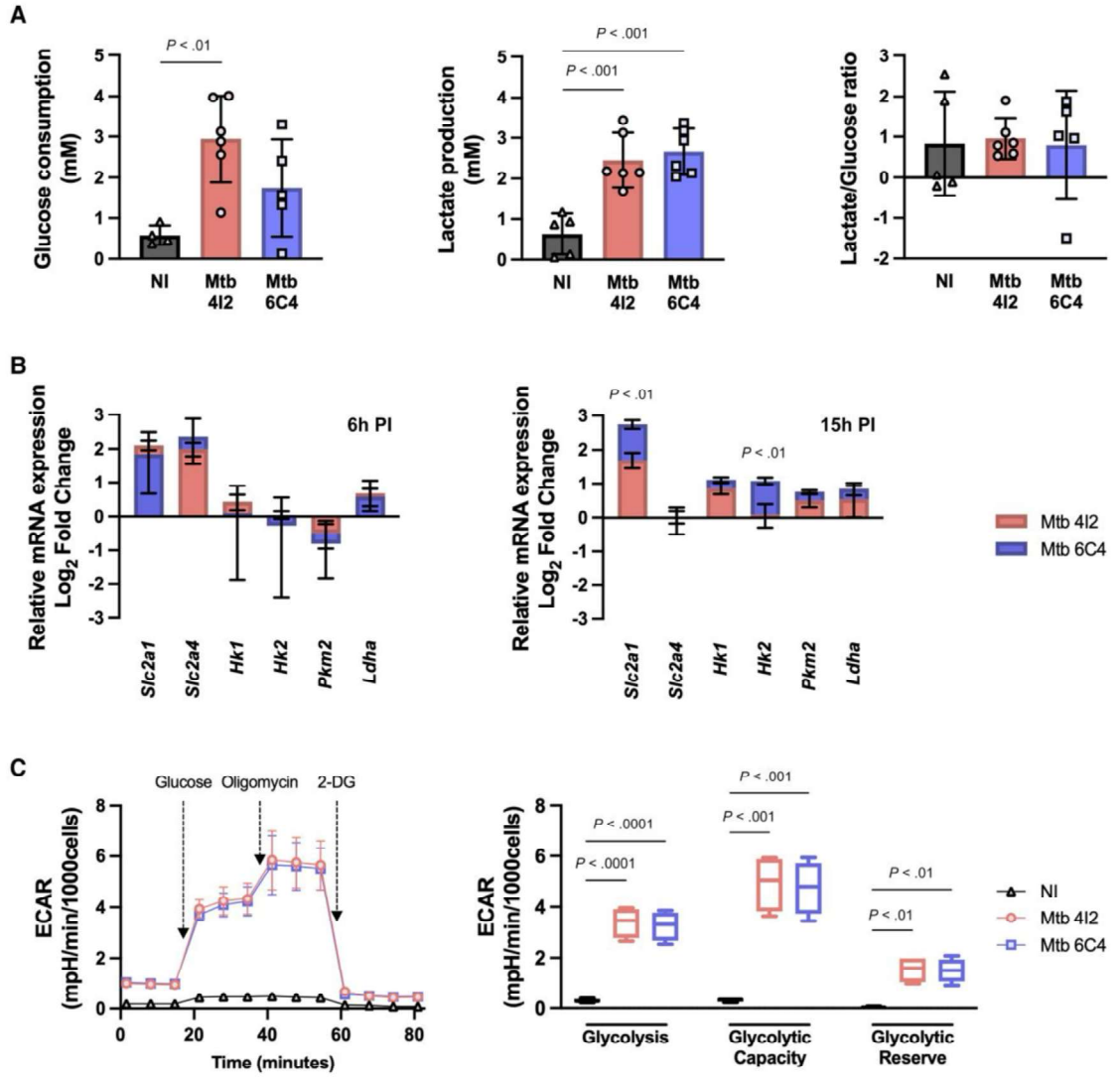

Figure 2. Glycolysis does not differ between the 2 *Mycobacterium tuberculosis* clinical isolates. *A* and *B*, BMDM from C57BL/6 mice were infected at an MOI of 2 with either clinical isolate. *A*, Glucose consumption and lactate production were measured through HPLC in the supernatant of infected cultures after 24 hours, and the lactate/glucose ratio was calculated based on these values. *B*, Six and 15 hours postinfection, cell cultures were lysed and the expression of the indicated genes determined by real-time PCR. Data are represented in $\log_2$ (fold change), with 0 representing noninfected macrophages. *C*, BMDM infected at MOI of 2 for 24 hours were submitted to glycolysis stress test. ECAR was measured with an XFp Analyzer. Glycolysis, glycolytic capacity, and glycolytic reserve were calculated. Represented is the mean ± SD of triplicate (*A* and *B*) or duplicate (*C*) wells for 2 experiments (*A* and *C*) or 1 experiment representative of 2 (*B*). For ECAR assays (*C*) data are also represented in a box and whiskers plot (Tukey method). Statistical analysis was performed using 1-way ANOVA (*A* and *C*) or 2-tailed unpaired Student *t* test (*B*). Abbreviations: 2-DG, 2-deoxy-glucose; BMDM, bone marrow-derived macrophages; ECAR, extracellular acidification rate; HPLC, high-performance liquid chromatography; IL-1β, interleukin 1β; MOI, multiplicity of infection; Mtb, *M. tuberculosis*; NI, noninfected; PI, postinfection.

SDH and NLRP3 inhibition [12, 35] (Figure 6*A*). Thus, we tested the contribution of these pathways to IL-1β production by *M. tuberculosis*-infected macrophages. When compared to wild-type mice, infection of mHIF1α$^{-/-}$ BMDM with either *M. tuberculosis* isolate yielded no effect on IL-1β protein levels, with only minor differences in *Il1b* mRNA (Figure 6*B*). Similarly, lack of IRG1 [36], the enzyme that converts aconitate into itaconate, showed no impact on IL-1β secretion or *Il1b* transcription (Figure 6*C*). With exception for the effect of DMM, our data show that the TCA cycle and IL-1β production may be uncoupled in certain systems.

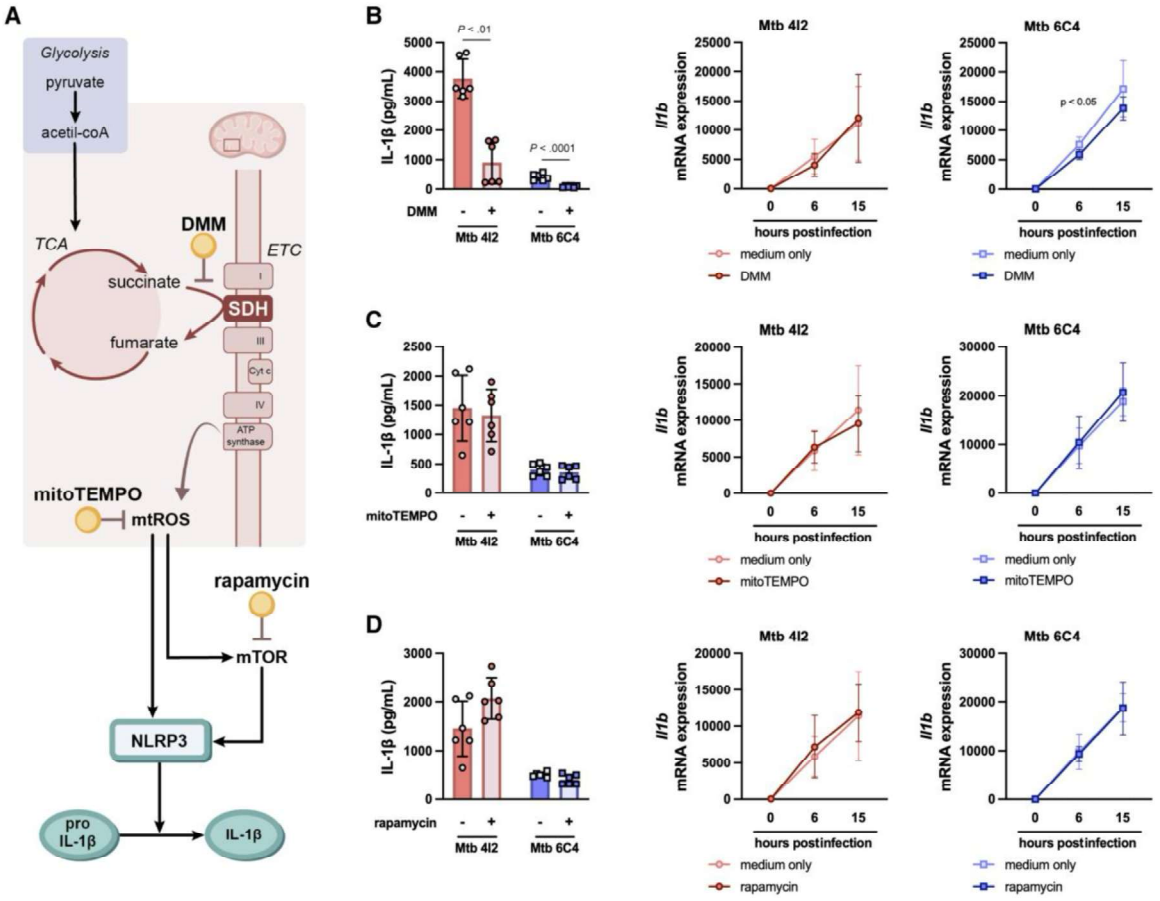

Figure 3. DMM inhibits inflammasome activation and IL-1β production independently of mitochondrial ROS and mTOR. *A*, DMM, mitoTEMPO, and rapamycin inhibitory action within the metabolic pathway. *B–D*, BMDM from C57BL/6 mice were left untreated (–) or pretreated (+) for 2 hours with DMM (*B*), mitoTEMPO (*C*), or rapamycin (*D*) and subsequently infected with either clinical isolate at a multiplicity of infection of 2. The inhibitors were maintained in the cultures throughout the incubation period, with exception of rapamycin which was only present for 2 hours. The amount of secreted IL-1β was quantified in the cell culture supernatants 24 hours postinfection. Six and 15 hours postinfection, cell cultures were lysed and *Il1b* expression measured by real-time PCR. Represented is the mean ± SD of triplicate wells for 2 experiments. Statistical analysis was performed using 2-tailed unpaired Student *t* test. Abbreviations: BMDM, bone marrow-derived macrophages; DMM, dimethyl malonate; ETC, electron transport chain; IL-1β, interleukin 1β; Mtb, *M. tuberculosis*; mTOR, mammalian target of rapamycin; mtROS, mitochondrial reactive oxygen species; SDH, succinate dehydrogenase; TCA, tricarboxylic acid.

DMM Acts on the Pathogen to Inhibit IL-1β Secretion by Infected Macrophages

The effect of DMM on IL-1β was posttranscriptional, not related to the usual host metabolic players, and involved inflammasome inhibition (Figures 3–6), which paralleled the outcome of inhibiting of the bacterial metabolism with rifampicin during infection [20]. So, we hypothesized that DMM might primarily interfere with the bacterial, not the host, metabolism.

M. tuberculosis encodes 3 SDH enzymes: SDH-1 (Rv0247c to Rv0249c), SDH-2 (Rv3316 to Rv3319), and fumarate reductase (Rv1552 to Rv1555) [37, 38]. We focused on SDH-1, which is highly homologous to the *M. smegmatis*-encoded molecule and has a published structure and predicted electron transfer mechanism [39]. The structure of *M. tuberculosis* SDH-1 was predicted using ColabFold [26] and superpositioned with the resolved structure of *M. smegmatis* SDH-1 containing the ligand ubiquinone-1 (instead of menaquinone, PDB: 7D6 V; Figure 7A, left). The electron transfer pathway in *M. tuberculosis* SDH-1 is likely similar to that of *M. smegmatis* SDH-1, predicted to occur from succinate oxidation in the flavoprotein domain (shown in cyan; Figure 7A, left and middle) to the quinone binding site (in green; Figure 7A, left and middle), through redox centers (in yellow; Figure 7A, left and middle) [39]. Furthermore, the redox centers arrangement is similar to the mammalian SDH [40], and likely inhibited by the same small molecules, that is DMM. Thus, DMM may bind directly

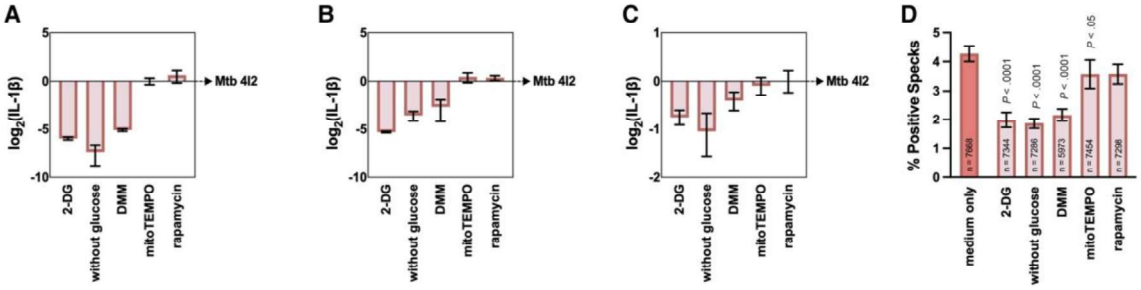

Figure 4. The impact of metabolic inhibitors on IL-1β is not cell specific. *A*, Alveolar macrophages, (*B*) bone-marrow-derived monocytes from C57BL/6 mice, and (*C*) THP1-ASC-GFP macrophages were left untreated (–) or pretreated (+) with the indicated inhibitors for 2 hours and infected with *Mycobacterium tuberculosis* 4I2 at an MOI of 1 for 24 hours. The inhibitors were maintained in the cultures throughout the incubation period, with exception of rapamycin which was only present for 2 hours. The amount of secreted IL-1β was quantified in the cell culture supernatants. Data are represented in $\log_2$ (fold change), with 0 representing macrophages infected with *M. tuberculosis* 4I2. *D*, Phorbol 12-myristate 13-acetate (PMA)-differentiated THP-1-ASC-GFP were treated with inhibitors for 2 hours as indicated in the figure and infected with *M. tuberculosis* 4I2 at an MOI of 1 and the percentage of speck-positive cells determined 6 hours postinfection. Represented is the mean ± SD of triplicate wells for 1 experiment (*A* and *D*) or 2 experiments (*B* and *C*). For immunofluorescence, 60 fields per replicate (total number of cells indicated in each bar) were acquired and analyzed. Statistical analysis was performed using 1-way ANOVA (*D*). Abbreviations: 2-DG, 2-deoxy-glucose; DMM, dimethyl malonate; IL-1β, interleukin 1β; MOI, multiplicity of infection; Mtb, *M. tuberculosis*.

to the SDH quinone-binding domain (Figure 7*A*, middle and right), or be converted into malonate competing for the SDH succinate binding site (Figure 7*A*, middle and right) [41].

To distinguish the impact of DMM on the host versus bacteria, we compared macrophages, pretreated with inhibitors, during infection (affecting the host, and potentially the pathogen) versus pretreating the pathogen with inhibitors and washing it out before infection (targeting mainly the pathogen; Figure 7*B*). As before (Figure 1), BMDM exposure to 2-DG highly impacted IL-1β secretion (Figure 7*B*), whereas pretreating *M. tuberculosis* with 2-DG did not, showing a host-specific effect for 2-DG (Figure 7*B*). In contrast, DMM impacted IL-1β secretion similarly for both experimental conditions (Figure 7*B*) suggesting that affecting the bacteria was enough to decrease IL-1β secretion. The effect of DMM was more pronounced in *M. tuberculosis* 4I2 than in isolate 6C4, fitting in with our previous data for differential inflammasome activation by these *M. tuberculosis* isolates [20]. In turn, Q203, a specific inhibitor of the *M. tuberculosis* respiratory chain [42], only impacted pathogen-mediated IL-1β secretion (Figure 7*B*). Of note, BMDM infected with DMM-treated bacteria showed no differences in *Il1b* transcript when compared to DMM-treated BMDM (Supplementary Figure 5*A*), further supporting its post-transcriptional effect. Lastly, pretreatment of *M. tuberculosis* 4I2 with DMM or Q203 decreased the activation of the host inflammasome measured in THP1-ASC-GFP reporter cells, unlike pretreatment with 2-DG (Figure 7*C* and Supplementary Figure 5*B*).

Collectively, these data suggest that DMM inhibits pathogen metabolism by targeting bacterial SDH. Given the high similarity of SDH across *M. tuberculosis* isolates, DMM is likely effective against all isolates. However, for isolates like 4I2, which require metabolic activity to activate the host inflammasome, DMM subsequently reduces host IL-1β production. In summary (Figure 7*D*), our results position the macrophage glycolytic shift promoted by *M. tuberculosis* infection and the bacterial metabolism as critical for IL-1β production, with no apparent contribution of the host TCA cycle and ETC, contrasting previously described findings for single-TLR agonists.

DISCUSSION

M. tuberculosis diversity significantly impacts host-pathogen interactions and tuberculosis outcomes, with closely related strains employing distinct and highly effective mechanisms to subvert host responses [20, 43–45]. Several studies have shown that *M. tuberculosis* infection shifts macrophage metabolism from oxidative phosphorylation to glycolysis [4, 5, 46, 47], but other investigations report that *M. tuberculosis* infection decelerates or limits the host metabolism [6, 46, 48, 49]. Whether genetically diverse isolates modulate this process remained largely unexplored [6, 7]. Here, we investigated the metabolic adaptation of macrophages to infection with genetically diverse clinical isolates that distinctly modulate NLRP3 activation and IL-1β production in a host-independent manner [20].

We report that despite downstream strain-specific differences in inflammasome activation and IL-1β production, the 2 *M. tuberculosis* clinical isolates elicited similar glycolytic responses in macrophages, indicating a shared bioenergetic profile. This suggests that while bacterial genetic variation affects macrophage cytokine responses, the energetic requirements to mount this initial immune response are conserved.

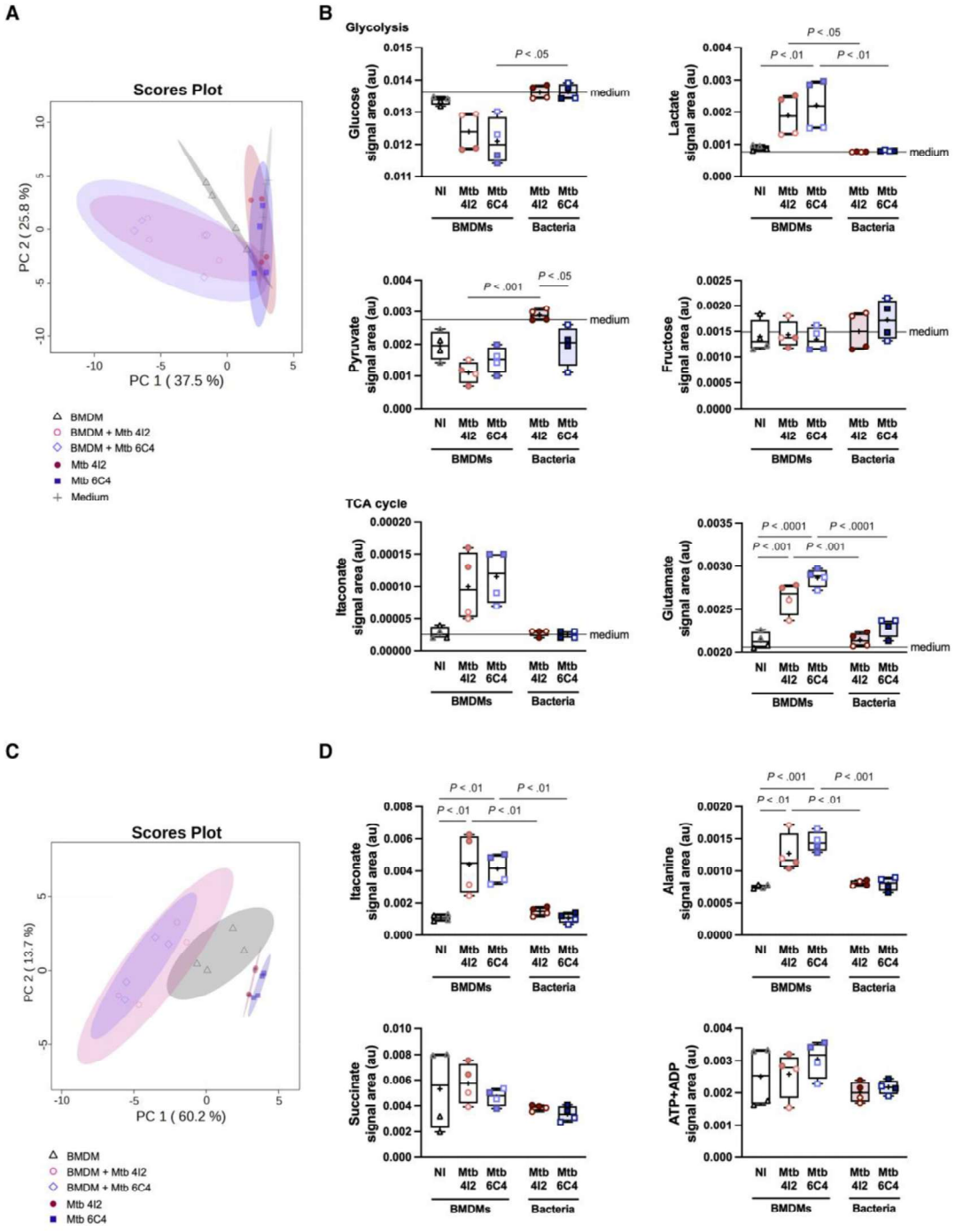

Figure 5. NMR-based metabolomic analysis of macrophages infected with *Mycobacterium tuberculosis* clinical isolate 4I2 or 6C4 reveals similar metabolic profiles. *A*, PCA of spectral data from the culture supernatants of noninfected BMDM, macrophages infected with *M. tuberculosis* 4I2 or 6C4 for 24 hours at a multiplicity of infection of 2, and *M. tuberculosis* 4I2 or 6C4 cultured in similar medium but in the absence of host cells. *B*, Representative metabolites consumed and excreted in the tested conditions. Variations are expressed in relation to media only. *C*, PCA of spectral data recorded for intracellular aqueous extracts in the same conditions as in (*A*). *D*, Relative intracellular levels of representative metabolites across the tested conditions. Represented are box and whisker plots (Tukey method) of duplicate wells for 2 experiments. Each replicate is a pool of 24 wells in a 24-well plate. Statistical analysis was performed using 1-way ANOVA. Abbreviations: au, arbitrary unit; BMDM, bone-marrow derived macrophages; Mtb, *M. tuberculosis*; NI, noninfected; PCA, principal component analysis; TCA, tricarboxylic acid.

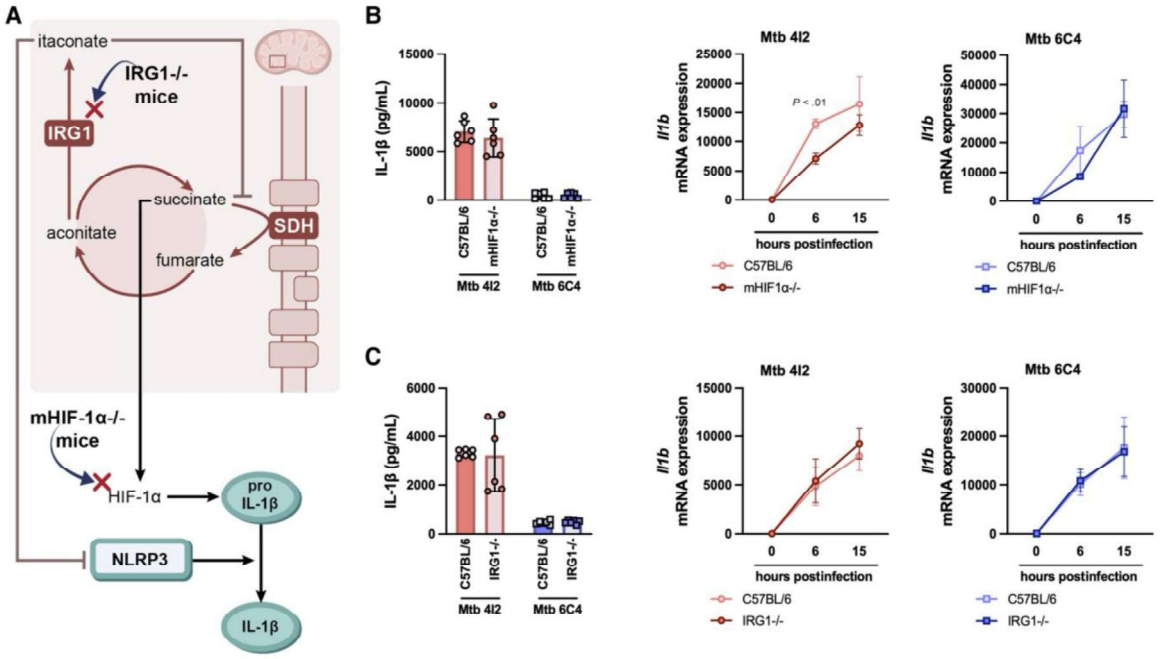

Figure 6. IL-1β production by *Mycobacterium tuberculosis*-infected macrophages is independent of HIF-1α and IRG1 activity. *A*, HIF-1α and IRG1 pathways and their impact on IL-1β regulation. *B* and *C*, BMDM from C57BL/6 and mHIF-1α$^{-/-}$ (*B*) or IRG1$^{-/-}$ (*C*) mice were infected with either clinical isolate at a multiplicity of infection of 2 for 24 hours. The amount of secreted IL-1β was quantified in the cell culture supernatants 24 hours postinfection. Six and 15 hours postinfection, cell cultures were lysed and the *Il1b* expression measured by real-time PCR. Represented is the mean ± SD of triplicate wells for 2 experiments (*B* and *C*) or 1 experiment (*B*) representative of 2. Statistical analysis was performed using a 2-tailed unpaired Student *t* test. Abbreviations: BMDM, bone-marrow derived macrophages; HIF-1α, hypoxia-inducible factor 1 subunit α; IL-1β, interleukin 1β; IRG1, immune responsive gene 1; Mtb, *M. tuberculosis*; PCR, polymerase chain reaction; SDH, succinate dehydrogenase.

Additionally, our study underpins the glycolytic pathway as a crucial regulator of IL-1β production during *M. tuberculosis* infection, impacting both *Il1b* transcription and NLRP3 activation. We also investigated the interplay between the TCA cycle and inflammasome activation in infected macrophages, as DMM significantly decreased IL-1β production in these cells due to posttranscriptional modulation. However, surprisingly, mitochondrial ROS sequestration, mTOR inhibition, or HIF-1α deletion did not impact IL-1β secretion. Departing from current immunometabolic models based on single-TLR activation [12, 21, 22], our findings suggest that during macrophage infection with live *M. tuberculosis*, inflammasome activation may be uncoupled from the TCA cycle. Further supporting the hypothesis that canonical pathways conventionally linked to inflammasome activation may operate differently under single (eg, LPS) versus complex stimuli (eg, live *M. tuberculosis*), metabolomic analyses revealed overwhelmingly similar macrophage metabolic profiles in response to both *M. tuberculosis* isolates. Our observations, indicating that the differential activation of the inflammasome and subsequent IL-1β production in macrophages infected with distinct *M. tuberculosis* isolates are not linked to differential metabolic requirements, contradict our original hypothesis. Future investigations should explore alternative molecular mechanisms at play in infected cells. Promising avenues include examining the dynamics of phagolysosome formation or rupture induced by these different isolates, as well as potential alterations in macrophage autophagic flux. These findings open new research perspectives on the immunometabolic control of cytokine responses.

The evidence that DMM inhibited inflammasome activation and IL-1β production without the contribution of common host pathways was puzzling. We hypothesized that DMM may interfere with pathogen metabolism rather than macrophage metabolic adaptation to infection. Combining structural prediction of the *M. tuberculosis* SDH with stimulation of macrophages with *M. tuberculosis* preexposed to DMM, we concluded that this was indeed the case. It remains to be established whether DMM affects mycobacterial replication or the production/abundance of virulence factors (ie, PDIM, PknF, or ESX-1 components) needed for NLRP3 activation. It will be important to further investigate the molecular pathways triggered in the pathogen, as both our previous [20] and current study show that inflammasome activation and high IL-1β induction in infected macrophages depended on the presence of live, metabolically active bacteria.

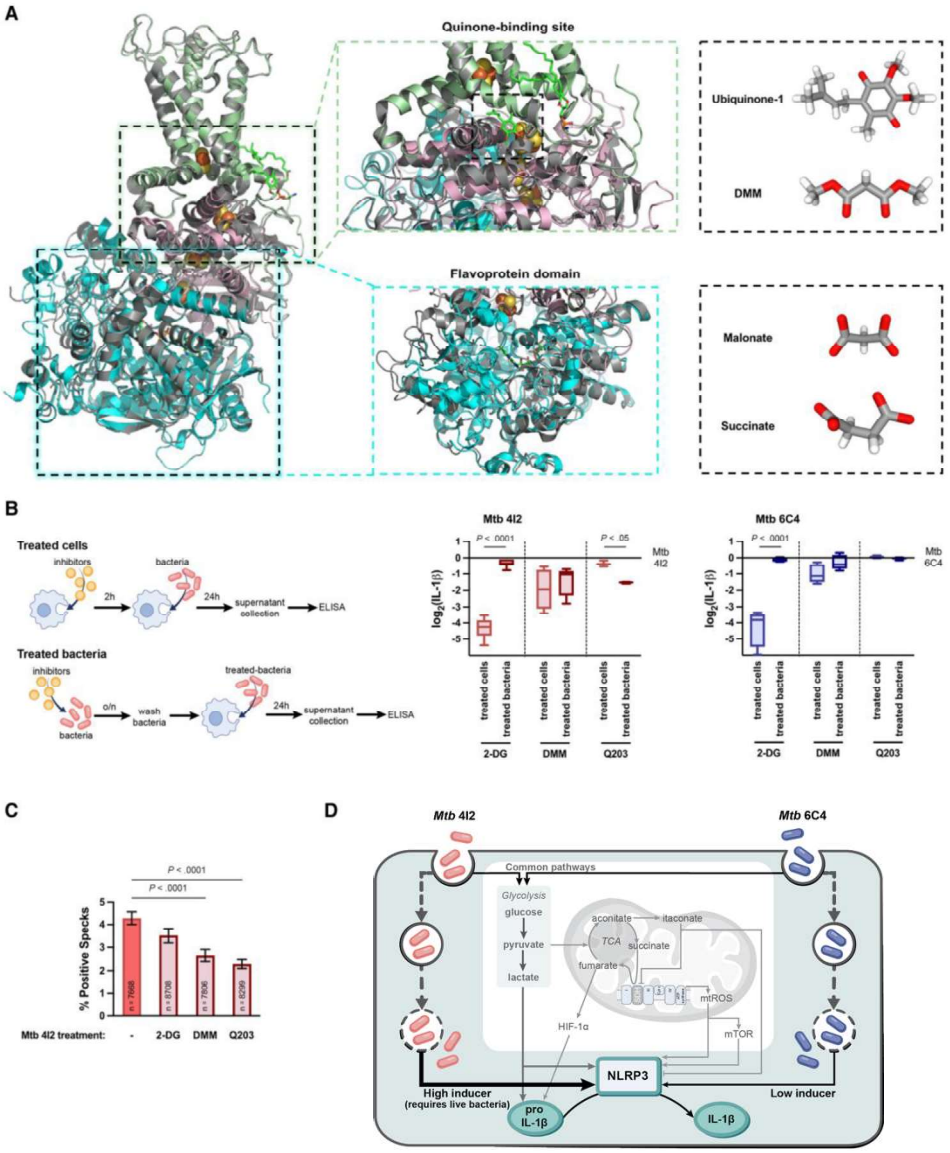

Figure 7. Infection of macrophages with *Mycobacterium tuberculosis* 4I2 exposed to DMM results in reduced inflammasome activation and IL-1β production. *A*, *M. tuberculosis* SDH-1 protein structure predicted with ColabFold. Flavoprotein domain (represented in cyan), iron-sulfur domain (represented in pink), and membrane anchor domain (represented in green) are superpositioned with SDH-1 from *Mycobacterium smegmatis* in complex with ubiquinone-1 (7D6V, grey). Redox centers (represented in yellow/orange) include the flavin-adenine nucleotide (FAD), the [2Fe-2S], [4Fe-4S], [3Fe-4S] iron-sulfur cluster, and the Rieske-type [2Fe-2S] cluster. Ubiquinone-1 (CID 4462), DMM (CID 7943), malonate (CID 9084), and succinate (CID 160419) structures were extracted from PubChem. *B*, Schematic representation of the protocol for treating bacteria or macrophages with metabolic inhibitors. *M. tuberculosis* 4I2 and 6C4 or C57BL/6 BMDM were pretreated with the indicated inhibitors according to the protocol. Treated macrophages were infected with nontreated bacteria and nontreated macrophages were infected with treated bacteria, at an MOI of 2 for 24 hours. The amount of secreted IL-1β was quantified in the cell culture supernatants. Data are represented in $\log_2$ (fold change), with 0 representing nontreated macrophages infected with nontreated *M. tuberculosis* 4I2 or 6C4. *C*, THP1-ASC-GFP macrophages were infected with treated *M. tuberculosis* 4I2, at an MOI of 1 for 6 hours and the percentage of speck-positive cells was determined for the different conditions. Represented are box and whiskers plots (Tukey method) (*B*), or the mean ± SD (*C*) of triplicate wells for 2 experiments (*B*) or 1 experiment (*C*). For immunofluorescence, 60 fields (total number of cells indicated in each bar) per replicate were acquired and analyzed. Statistical analysis was performed using 1-way ANOVA. *D*, Model of the macrophage immunometabolic adaptation during *M. tuberculosis* infection and its interaction with the inflammasome activation and IL-1β secretion. Common pathways triggered in response to *M. tuberculosis* 4I2 or 6C4 are shown in the center. The pathways leading to distinct activation of the NLRP3 inflammasome by these clinical isolates remain unknown. Abbreviations: 2-DG, 2-deoxy-glucose; BMDM, bone-marrow derived macrophages; CID, PubChem compound identification; DMM, dimethyl malonate; ELISA, enzyme-linked immunosorbent assay; HIF-1α, hypoxia-inducible factor 1α; IL-1β, interleukin 1β; MOI, multiplicity of infection; Mtb, *M. tuberculosis*; mTOR, mammalian target of rapamycin; mtROS, mitochondrial reactive oxygen species; o/n, overnight; SDH, succinate dehydrogenase; TCA, tricarboxylic acid.

In conclusion, our study demonstrates that observations from experiments with single bacteria-derived moieties may not be valid in context of live organisms and that during *M. tuberculosis* infection IL-1β production primarily relies on bacteria-specific mechanisms. These findings are critical for in-depth and accurate understanding of the infectious process and its metabolic regulation. Furthermore, the impact of host-designed metabolic inhibitors on the pathogen raises awareness of conserved biological pathways and could facilitate the design of new therapies.

Supplementary Data

Supplementary materials are available at *The Journal of Infectious Diseases* online (http://jid.oxfordjournals.org/). Supplementary materials consist of data provided by the author that are published to benefit the reader. The posted materials are not copyedited. The contents of all supplementary data are the sole responsibility of the authors. Questions or messages regarding errors should be addressed to the author.

Notes

Author contributions. A. I. F., I. F. D., R. S., A. D., and M. S. contributed conceptualization. A. I. F., A. J. P., I. F. D., A. D., and M. S. performed formal analysis. I. F. D., R. S., and M. S. acquired funding. A. I. F., A. J. P., D. S., U. Z., C. F., I. F. D., and M. S. performed investigations. M. S. contributed project administration. I. F. D., R. S., A. D., and M. S. contributed resources. R. S., A. D., and M. S. contributed supervision. A. I. F., A. J. P., and M. S. contributed visualization and wrote the draft. All authors contributed writing review and editing.

Acknowledgements. We thank Drs Gil Castro, Tiago Beites, and Joana Couto for critically reading the manuscript. The authors thank the support from the Instituto de Investigação e Inovação em Saúde scientific platforms animal facility, translational cytometry, and biosciences screening, a member of PT-OPENSCREEN (NORTE-01-0145-FEDER-085468), and Portuguese platform of BioImaging (PPBI; PPBI-POCI-01-0145-FEDER-022122).

Financial support. This work was supported by the Portuguese Foundation for Science and Technology (FCT; grant numbers PTDC/SAU-INF/1172/2021 and CEECIND/00241/2017 to M. S., CEECIND/02387/2018 to I. F. D, and 10.54499/2020.00185.CEECIND/CP1600/CT0004 to R. S.). A. I. F. was supported by the FCT (grant number 2020.05949.BD PhD scholarship); the European Federation of Immunological Societies-Immunology Letters (short-term fellowship); and the European Society of Clinical Microbiology and Infectious Diseases (research grant 2022). D. S. was supported by the FCT (grant number SFRH/BD/143536/2019 PhD fellowship). This work was also supported by the project CICECO-Aveiro Institute of Materials UIDB/50011/2020 (DOI 10.54499/UIDB/50011/2020), UIDP/50011/2020 (DOI 10.54499/UIDP/50011/2020) and LA/P/0006/2020 (DOI 10.54499/LA/P/0006/2020), financed by national funds through the FCT/MEC (PIDDAC), and projects 10.54499/UIDB/50026/2020, 10.54499/UIDP/50026/2020 and 10.54499/LA/P/0050/2020. The NMR spectrometer is part of the National NMR Network, partially supported by Infrastructure Project number 022161, cofinanced by *Fundo Europeu de Desenvolvimento Regional* (FEDER) through COMPETE 2020, *Programa Operacional Competitividade e Internacionalização* (POCI), and PORL, and FCT through PIDDAC.

Potential conflicts of interest. All authors: No reported conflicts. All authors have submitted the ICMJE Form for Disclosure of Potential Conflicts of Interest. Conflicts that the editors consider relevant to the content of the manuscript have been disclosed.

References

1. Van den Bossche J, O'Neill LA, Menon D. Macrophage immunometabolism: where are we (going)? Trends Immunol **2017**; 38:395–406.
2. World Health Organization. Global tuberculosis report 2023. https://iris.who.int/. Accessed 1 September 2024.
3. Shi L, Salamon H, Eugenin EA, Pine R, Cooper A, Gennaro ML. Infection with *Mycobacterium tuberculosis* induces the Warburg effect in mouse lungs. Sci Rep **2015**; 5:18176.
4. Gleeson LE, Sheedy FJ, Palsson-McDermott EM, et al. Cutting edge: *Mycobacterium tuberculosis* induces aerobic glycolysis in human alveolar macrophages that is required for control of intracellular bacillary replication. J Immunol **2016**; 196:2444–9.
5. Lachmandas E, Beigier-Bompadre M, Cheng SC, et al. Rewiring cellular metabolism via the AKT/mTOR pathway contributes to host defence against *Mycobacterium tuberculosis* in human and murine cells. Eur J Immunol **2016**; 46:2574–86.
6. Mendonca LE, Pernet E, Khan N, et al. Human alveolar macrophage metabolism is compromised during *Mycobacterium tuberculosis* infection. Front Immunol **2023**; 13:1044592.
7. Kumar R, Singh P, Kolloli A, et al. Immunometabolism of phagocytes during *Mycobacterium tuberculosis* infection. Front Mol Biosci **2019**; 6:105.
8. Huang L, Nazarova EV, Tan S, Liu Y, Russell DG. Growth of *Mycobacterium tuberculosis* in vivo segregates with host macrophage metabolism and ontogeny. J Exp Med **2018**; 215:1135–52.
9. Pisu D, Huang L, Grenier JK, Russell DG. Dual RNA-Seq of Mtb-infected macrophages in vivo reveals ontologically distinct host-pathogen interactions. Cell Rep **2020**; 30:335–50.e4.
10. Howard NC, Marin ND, Ahmed M, et al. *Mycobacterium tuberculosis* carrying a rifampicin drug resistance mutation

reprograms macrophage metabolism through cell wall lipid changes. Nat Microbiol **2018**; 3:1099–108.
11. Mehrotra P, Jamwal SV, Saquib N, et al. Pathogenicity of *Mycobacterium tuberculosis* is expressed by regulating metabolic thresholds of the host macrophage. PLoS Pathog **2014**; 10:e1004265.
12. Hooftman A, Angiari S, Hester S, et al. The immunomodulatory metabolite itaconate modifies NLRP3 and inhibits inflammasome activation. Cell Metab **2020**; 32:468–78.e7.
13. Garaude J, Acín-Pérez R, Martínez-Cano S, et al. Mitochondrial respiratory-chain adaptations in macrophages contribute to antibacterial host defense. Nat Immunol **2016**; 17:1037–45.
14. Billingham LK, Stoolman JS, Vasan K, et al. Mitochondrial electron transport chain is necessary for NLRP3 inflammasome activation. Nat Immunol **2022**; 23:692–704.
15. Silvério D, Gonçalves R, Appelberg R, Saraiva M. Advances on the role and applications of interleukin-1 in tuberculosis. mBio **2021**; 12:e0313421.
16. Rastogi S, Briken V. Interaction of mycobacteria with host cell inflammasomes. Front Immunol **2022**; 13:791136.
17. Rastogi S, Ellinwood S, Augenstreich J, Mayer-Barber KD, Briken V. *Mycobacterium tuberculosis* inhibits the NLRP3 inflammasome activation via its phosphokinase PknF. PLoS Pathog **2021**; 17:e1009712.
18. Madan-Lala R, Peixoto KV, Re F, Rengarajan J. *Mycobacterium tuberculosis* hip1 dampens macrophage proinflammatory responses by limiting toll-like receptor 2 activation. Infect Immun **2011**; 79:4828–38.
19. Danelishvili L, Everman JL, McNamara MJ, Bermudez LE. Inhibition of the plasma-membrane-associated serine protease cathepsin G by *Mycobacterium tuberculosis* Rv3364c suppresses caspase-1 and pyroptosis in macrophages. Front Microbiol **2012**; 2:281.
20. Sousa J, Cá B, Maceiras AR, et al. *Mycobacterium tuberculosis* associated with severe tuberculosis evades cytosolic surveillance systems and modulates IL-1β production. Nat Commun **2020**; 11:1949.
21. Tannahill GM, Curtis AM, Adamik J, et al. Succinate is an inflammatory signal that induces IL-1β through HIF-1α. Nature **2013**; 496:238–42.
22. Mills EL, Kelly B, Logan A, et al. Succinate dehydrogenase supports metabolic repurposing of mitochondria to drive inflammatory macrophages. Cell **2016**; 167: 457–70.e13.
23. Zotta A, O'Neill LAJ, Yin M. Unlocking potential: the role of the electron transport chain in immunometabolism. Trends Immunol **2024**; 45:259–73.
24. Carrola J, Bastos V, Jarak I, et al. Metabolomics of silver nanoparticles toxicity in HaCaT cells: structure–activity relationships and role of ionic silver and oxidative stress. Nanotoxicology **2016**; 10:1105–17.
25. Wishart DS, Feunang YD, Marcu A, et al. HMDB 4.0: the human metabolome database for 2018. Nucleic Acids Res **2018**; 46:D608–17.
26. Mirdita M, Schütze K, Moriwaki Y, Heo L, Ovchinnikov S, Steinegger M. ColabFold: making protein folding accessible to all. Nat Methods **2022**; 19:679–82.
27. Rosenberg G, Yehezkel D, Hoffman D, et al. Host succinate is an activation signal for *Salmonella* virulence during intracellular infection. Science **2021**; 371:400–5.
28. Riquelme SA, Prince A. Airway immunometabolites fuel *Pseudomonas aeruginosa* infection. Respir Res **2020**; 21: 326.
29. Li X, Zhang X, Pan Y, et al. mTOR regulates NLRP3 inflammasome activation via reactive oxygen species in murine lupus. Acta Biochim Biophys Sin (Shanghai) **2018**; 50: 888–96.
30. Wu KKL, Long KK, Lin H, et al. The APPL1-rab5 axis restricts NLRP3 inflammasome activation through early endosomal-dependent mitophagy in macrophages. Nat Commun **2021**; 12:6637.
31. Schuster EM, Epple MW, Glaser KM, et al. TFEB induces mitochondrial itaconate synthesis to suppress bacterial growth in macrophages. Nat Metab **2022**; 4: 856–66.
32. Jiang Q, Qiu Y, Kurland IJ, et al. Glutamine is required for M1-like polarization of macrophages in response to *Mycobacterium tuberculosis* infection. mBio **2022**; 13: e0127422.
33. Borah K, Beyß M, Theorell A, et al. Intracellular *Mycobacterium tuberculosis* exploits multiple host nitrogen sources during growth in human macrophages. Cell Rep **2019**; 29:3580–91.e4.
34. Jiang M, Chen Z, Li H, et al. Succinate and inosine coordinate innate immune response to bacterial infection. PLoS Pathog **2022**; 18:e1010796.
35. Lampropoulou V, Sergushichev A, Bambouskova M, et al. Itaconate links inhibition of succinate dehydrogenase with macrophage metabolic remodeling and regulation of inflammation. Cell Metab **2016**; 24:158–66.
36. Price JV, Russo D, Ji DX, et al. IRG1 and inducible nitric oxide synthase act redundantly with other interferon-gamma-induced factors to restrict intracellular replication of *Legionella pneumophila*. mBio **2019**; 10: e02629-19.
37. Hartman T, Weinrick B, Vilchèze C, et al. Succinate dehydrogenase is the regulator of respiration in *Mycobacterium tuberculosis*. PLoS Pathog **2014**; 10:e1004510.
38. Cook GM, Hards K, Vilchèze C, Hartman T, Berney M. Energetics of respiration and oxidative phosphorylation in mycobacteria. Microbiol Spectr **2014**; 2:10.1128/microbiolspec.MGM2-0015-2013.

39. Zhou X, Gao Y, Wang W, et al. Architecture of the mycobacterial succinate dehydrogenase with a membrane-embedded Rieske FeS cluster. Proc Natl Acad Sci U S A **2021**; 118:e2022308118.
40. Sun F, Huo X, Zhai Y, et al. Crystal structure of mitochondrial respiratory membrane protein complex II. Cell **2005**; 121:1043–57.
41. Dervartanian DV, Veeger C. Studies on succinate dehydrogenase I. Spectral properties of the purified enzyme and formation of enzyme-competitive inhibitor complexes. Biochim Biophys Acta **1964**; 92:233–47.
42. Hasenoehrl EJ, Wiggins TJ, Berney M. Bioenergetic inhibitors: antibiotic efficacy and mechanisms of action in *Mycobacterium tuberculosis*. Front Cell Infect Microbiol **2021**; 10:611683.
43. Tientcheu LD, Koch A, Ndengane M, Andoseh G, Kampmann B, Wilkinson RJ. Immunological consequences of strain variation within the *Mycobacterium tuberculosis* complex. Eur J Immunol **2017**; 47:432–45.
44. Peters JS, Ismail N, Dippenaar A, et al. Genetic diversity in *Mycobacterium tuberculosis* clinical isolates and resulting outcomes of tuberculosis infection and disease. Annu Rev Genet **2020**; 54:511–37.
45. Carmona J, Cruz A, Moreira-Teixeira L, et al. *Mycobacterium tuberculosis* strains are differentially recognized by TLRs with an impact on the immune response. PLoS One **2013**; 8:e67277.
46. Cumming BM, Addicott KW, Adamson JH, Steyn AJ. *Mycobacterium tuberculosis* induces decelerated bioenergetic metabolism in human macrophages. Elife **2018**; 7: e30169.
47. Vrieling F, Kostidis S, Spaink HP, et al. Analyzing the impact of *Mycobacterium tuberculosis* infection on primary human macrophages by combined exploratory and targeted metabolomics. Sci Rep **2020**; 10:7085.
48. Pacl HT, Chinta KC, Reddy VP, et al. NAD(H) homeostasis underlies host protection mediated by glycolytic myeloid cells in tuberculosis. Nat Commun **2023**; 14: 5472.
49. Hackett EE, Charles-Messance H, O'Leary SM, et al. *Mycobacterium tuberculosis* limits host glycolysis and IL-1β by restriction of PFK-M via microRNA-21. Cell Rep **2020**; 30:124–36.e4.

CHAPTER 3

SUPPLEMENTARY INFORMATION

SUPPLEMENTARY FIGURES

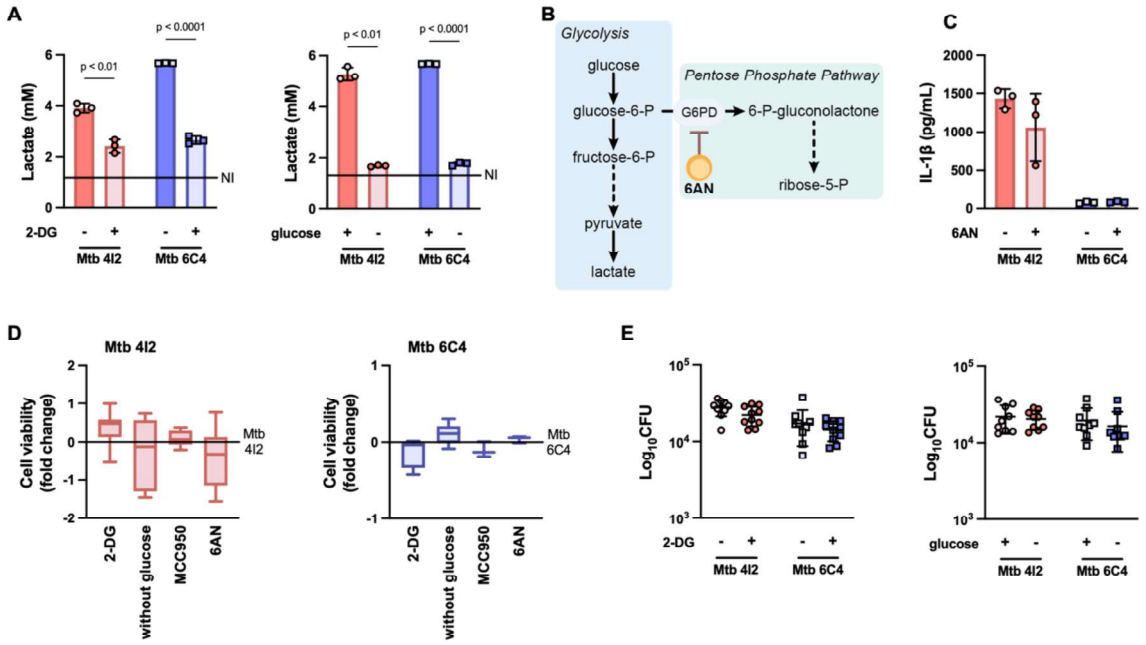

Supplementary Figure 1. C57BL/6 BMDM were pre-treated for 2 hours with 2-DG (A, D, E), DMEM without glucose (A, D, E), or 6AN (C-D) and subsequently infected with either *M. tuberculosis* clinical isolate. The amount of secreted (A) lactate or (C) IL-1β was quantified in the cell culture supernatants 24 hours post-infection. (B) 6AN inhibitory action within the pentose phosphate pathway. (D) Cell viability was measured 24 hours post-infection by ORANGU cell counting solution colourimetric assay. Data are represented in $\log_2$(fold change), with 0 representing macrophages infected with *M. tuberculosis* 4I2 or 6C4. (E) The effect of 2-DG or glucose absence in the internalisation of *M. tuberculosis* 4I2 or 6C4 by BMDM was measured 4 hours post-infection by CFU enumeration. Represented is the mean ± SD (A, C, E) or box and whisker plots (Tukey's method) (D) of triplicate wells for one experiment representative of two (A) or two experiments (C-E). Statistical analysis was performed using a two-tailed unpaired Student's t-test. 2-DG, 2-deoxy-glucose; 6AN, 6-aminonicotinamide; G6PD, glucose-6-phosphate dehydrogenase; Mtb, *M. tuberculosis*; NI, non-infected.

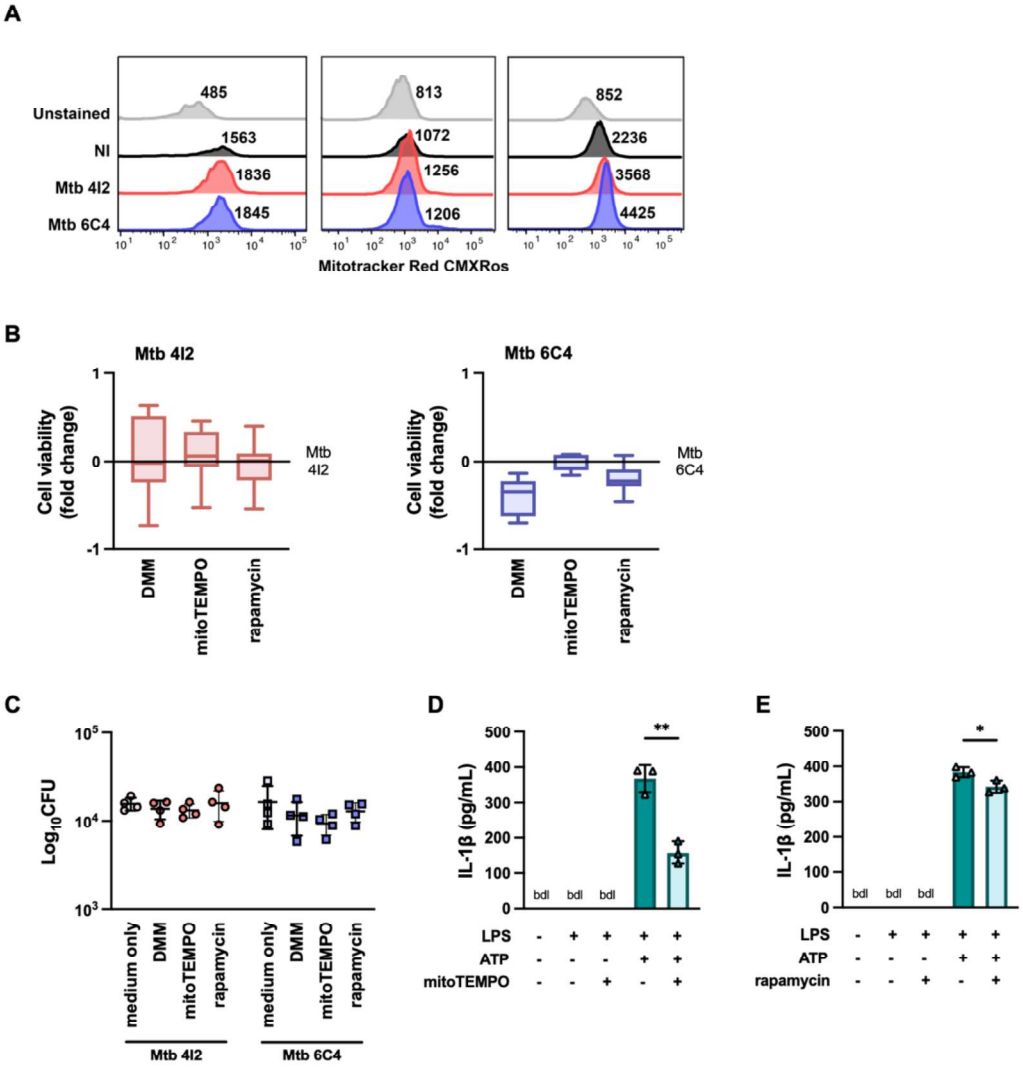

Supplementary Figure 2. C57BL/6 BMDM were infected with either clinical isolate at an MOI of 2. (A) 24 hours post-infection, BMDM were stained with Mitotracker Red CMXRos and MFI were analysed and are represented in the figure. Three independent experiments are shown and each replicate is a pool of 5 wells in a 24 well-plate. (B) Cell viability for BMDM pre-treated for 2 hours with the indicated inhibitors measured 24 hours post-infection using a colourimetric assay. Data are represented in $\log_2$(fold change), with 0 representing macrophages infected with *M. tuberculosis* 4I2 (right panel) or 6C4 (left panel). (C) The effect of DMM, mitoTEMPO or rapamycin on phagocytosis of *M. tuberculosis* 4I2 or 6C4 by BMDM was measured at 4 hours post-infection by CFU enumeration. (D, E) The activity of mitoTEMPO (D) or rapamycin (E) was validated in LPS+ATP-stimulated BMDM. The cells were stimulated as indicated in the figure in the presence (+) or absence (-) of the inhibitors and IL-1β was measured in the culture supernatants. Represented is a box and whisker plots (Tukey's method) (B) or the mean ± SD (C-E) of triplicate wells for one experiment. bdl, below detection level; DMM, dimethyl malonate; LPS, lipopolysaccharide; Mtb, *M. tuberculosis*; NI, non-infected; p.i., post-infection.

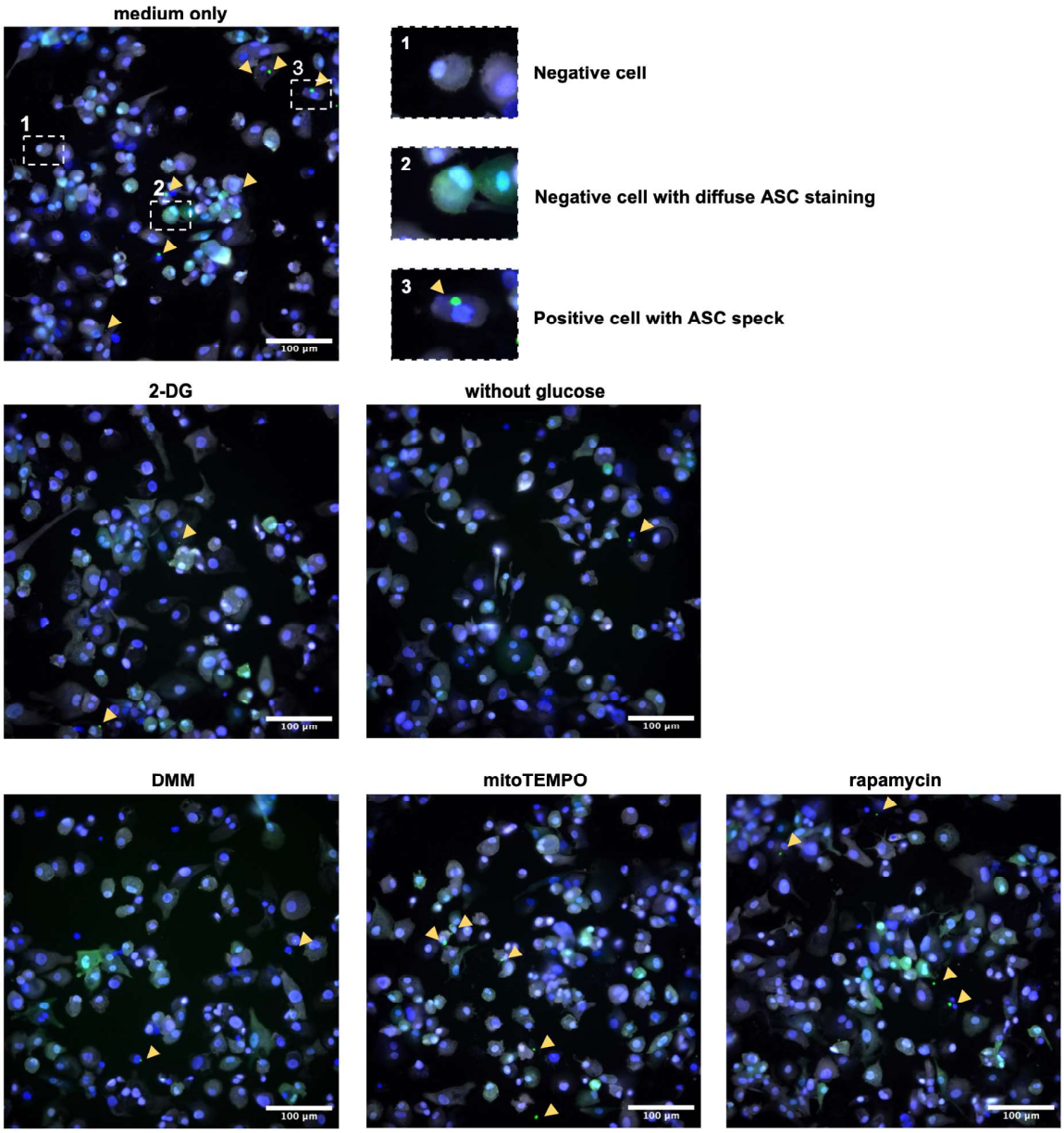

Supplementary Figure 3. Representative images of THP1-ASC-GFP cell cultures used for the quantifications shown in *Figure 4D*. Nuclei are stained blue, cytoplasms in grey and ASC-specks in green. The arrows point to ASC specks. Representative images of a negative cell (1), negative cell with diffuse ASC staining (2) and positive cell with ASC speck (3) are also shown. Scale bars, 100µm. 2-DG, 2-deoxy-glucose; DMM, dimethyl malonate.

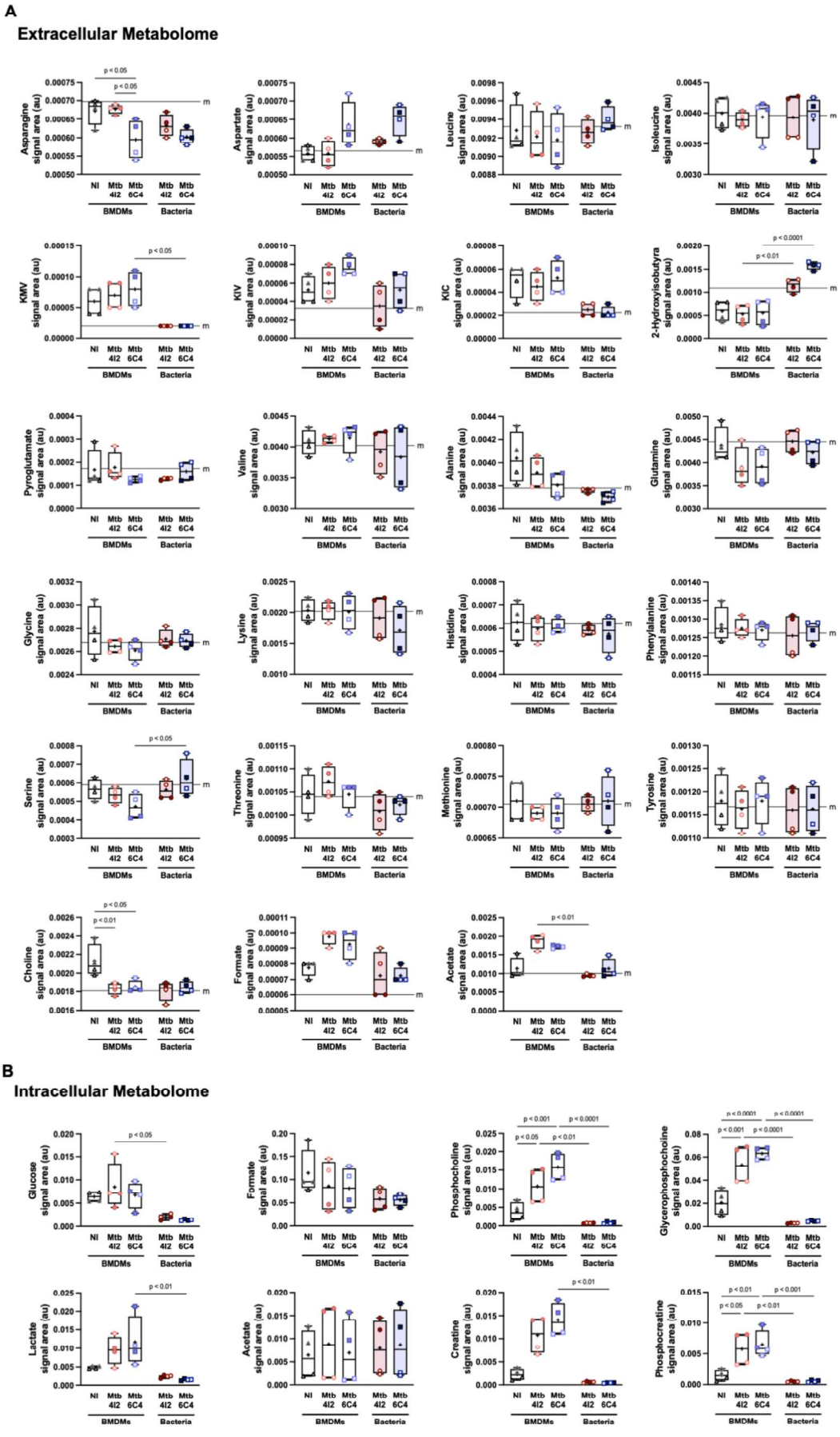

Supplementary Figure 4. *Legend on the next page.*

Supplementary Figure 4 continued. C57BL/6 BMDM were infected with *M. tuberculosis* 4I2 or 6C4 or left uninfected and 24 hours later the supernatant and cellular extract recovered for NMR metabolomics. In parallel, *M. tuberculosis* 4I2 and 6C4 cultures were also recovered. (A) Metabolites consumed and excreted among the tested conditions. Variations are expressed in relation to acellular media. (B) Relative intracellular levels of metabolites. Represented are box and whisker plots (Tukey's method) of duplicate wells for two experiments. Each replicate is a pool of 24 wells in a 24 well-plate. Statistical analysis was performed using One-way ANOVA. au, arbitrary unit; BMDM, bone marrow-derived macrophages; Mtb, *M. tuberculosis*; m, medium; NI, non-infected.

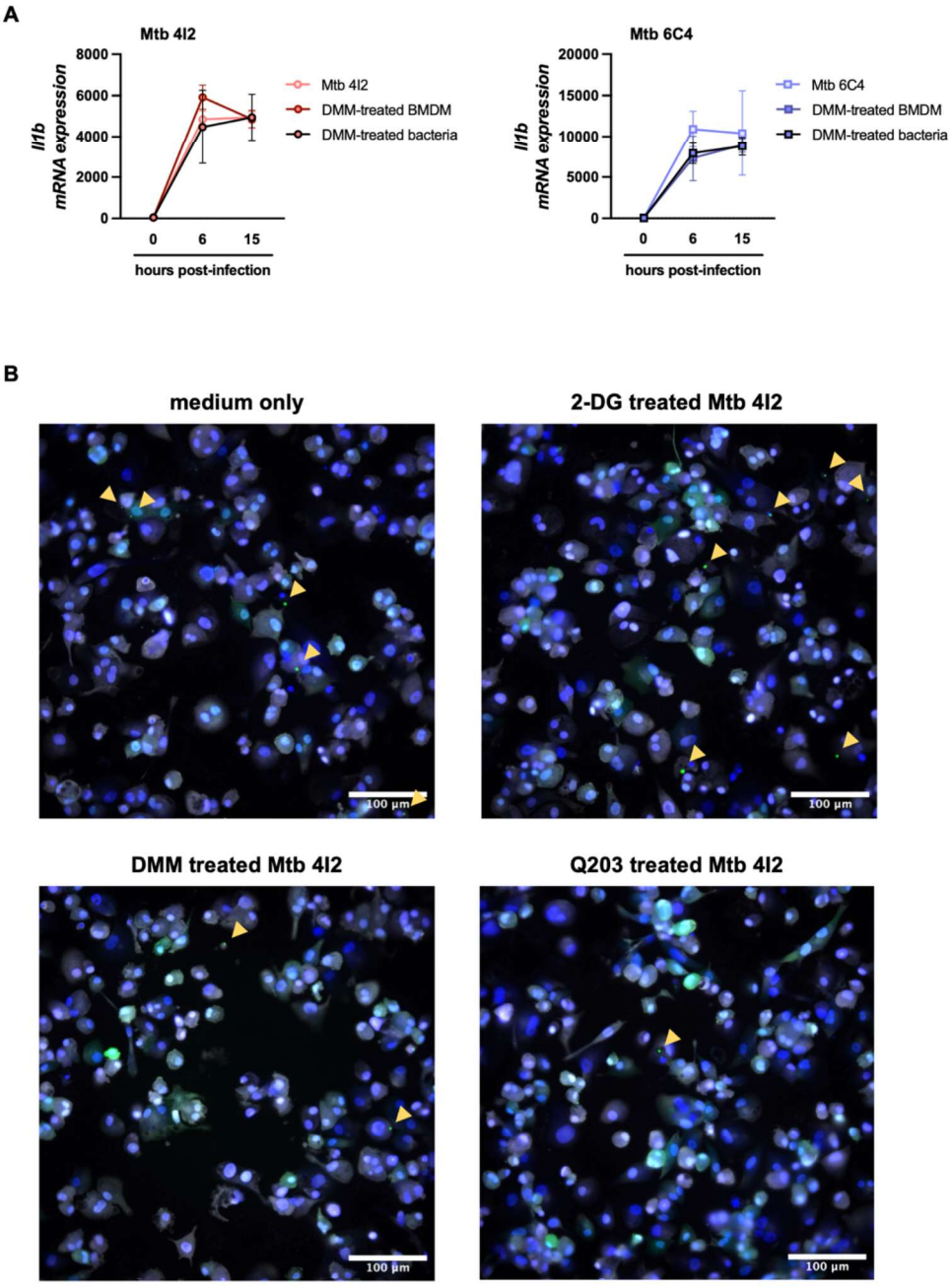

Supplementary Figure 5. (A) *M. tuberculosis* clinical isolates or BMDM from C57BL/6 mice were treated with DMM prior to infection according to the protocol in *Figure 7B*. Treated macrophages were infected with non-treated bacteria and non-treated macrophages were infected with treated bacteria, at an MOI of 2 for 6 hours and 15 hours. At the indicated timepoints, cell cultures were lysed and the expression of *Il1b* measured by real-time PCR. Represented is the mean ± SD of triplicate wells for one experiment. Statistical analysis was performed using a two-tailed unpaired Student's t-test. (B) Representative images of THP1-ASC-GFP cell cultures used for the quantifications shown in *Figure 7C*. Nuclei are stained blue, cytoplasms in grey and ASC-specks in green. The arrows point to ASC specks. Scale bars, 100 µm. 2-DG, 2-deoxy-glucose; BMDM, bone marrow-derived macrophage; DMM, dimethyl malonate; Mtb, *M. tuberculosis*.

SUPPLEMENTARY TABLES

Supplementary Table 1. List of materials and resources.

Materials and resources	Concentration	Supplier
Reagents		
Middlebrook 7H9		BD Biosciences
Middlebrook 7H11		BD Biosciences
cDMEM		
- DMEM		Gibco
- Foetal bovine serum (FBS)	10%	Gibco
- Sodium pyruvate	1%	Gibco
- HEPES	1%	Gibco
- L-glutamine	1%	Gibco
Mouse recombinant M-CSF	40 $ng.mL^{-1}$	BioLegend
Cryopreservation medium		
- FBS	90%	Gibco
- DMSO	10%	PanReac AppliChem
cRPMI		
- RPMI 1640		Gibco
- FBS	10%	Gibco
- Sodium pyruvate	1%	Gibco
- HEPES	1%	Gibco
- L-glutamine	1%	Gibco
- Penicillin-Streptomycin	100 $U.mL^{-1}$	Gibco
XF DMEM medium		
- XF DMEM medium without phenol red		Agilent
- L-glutamine	2 mM	Agilent
Paraformaldehyde (PFA)	4%	Bio-Optica
Zeocin	100 $\mu g.mL^{-1}$	InvivoGen
Phorbol 12-myristate 13-acetate (PMA)	100 nM	Sigma
PhenoVue Hoechst 33342	10 $\mu g.mL^{-1}$	Revvity
HCS CellMask Deep Red	10 $\mu g.mL^{-1}$	Thermo Fisher Scientific
Lipopolysaccharide (LPS)	500 $ng.mL^{-1}$ 100 $ng.mL^{-1}$	Sigma-Aldrich
ATP	5 mM	InvivoGen
EasySep™ Mouse Monocyte Isolation kit		STEMCELL Technologies
TripleXtractor		GriSP
ProtoScript First Strand cDNA Synthesis kit		New England Biolabs
iTaq Universal SYBR Green Supermix		Applied Biosystems
Mouse IL-1 beta ELISA		Invitrogen
Cell-Tak		Corning
Orangu™		Cell Guidance Systems
Lactate Assay Kit		Merck
Mitotraker Red CMXRos		Invitrogen

Supplementary Table 1. *Continued.*

Materials and resources	Concentration	Supplier
Chemical inhibitors or agonists		
Glucose	10 mM	Agilent
Oligomycin	2 μM	Agilent
2-deoxy glucose (2-DG)	50 mM 5 mM	Sigma Merck
Dimethyl malonate (DMM)	10 mM	Merck
MitoTEMPO	5 μM	Merck
Rapamycin	10 nM	Merck
Q203	0.28 nM	MedChemExpress
Material and Equipment		
XFp plates		Agilent
XFp extracellular analyser		Agilent
Cell Insight CX7 High-Content Screening		Thermo Fisher Scientific
Operetta CLS High-Content Analysis System		Revvity
Accuri C6 Plus		BD Biosciences
Cell lines		
THP1-ASC-GFP		InvivoGen
Software		
Harmony		Revvity
PyMOL Molecular Graphics Systems		Schröndinger, LLC
GraphPad prism 10		Dotmatics
FlowJo v10.10.0		BD Biosciences

Supplementary Table 2. List of oligonucleotide sequences.

Gene name	Oligonucleotide sequence (5'-3')	Provider
Ubiquitin	Forward: TGGCTATTAATTATTGGGTCTGCAT Reverse: GCAAGTGGCTAGAGTGCAGAGTAA	Invitrogen
Il1b	Forward: ACCTTCCAGGATGAGGACATGA Reverse: AACGTCACACACCAGCAGGTTA	Invitrogen
Slc2a1 (*Glut1*)	Forward: CCAGCTGGGAATCGTCGTT Reverse: AAGTCTGCATTGCCCATGAT	Merck
Slc2a4 (*Glut4*)	Forward: ACATACCTGACAGGGCAAG Reverse: CGCCCTTAGTTGGTCAGAA	Merck
Hk1	Forward: CGGAATGGGGAGCCTTTGG Reverse: GCCTTCCTTATCCGTTTCAATGG	Merck
Hk2	Forward: TGATCGCCTGCTTATTCACGG Reverse: AACCGCCTAGAAATCTCCAGA	Merck
Pkm2	Forward: GCCGCCTGGACATTGACTC Reverse: CCATGAGAGAAATTCAGCCGAG	Merck
Ldha	Forward: ACGCAGACAAGGAGCAGTGGAA Reverse: ATGCTCTCAGCCAAGTCTGCCA	Merck
Ndufa9	Forward: TGGGAGAGAAGGAAGTGAGAAG Reverse: CACAGCAAGAAACCAACGATAA	Merck
Sdha	Forward: AATTAAGGCAAATGCTGGAGAA Reverse: TGCATGTTTAGGCGTAGTTCTG	Merck
McIIIcI	Forward: GGCTACTTTTTGGAACATCTGG Reverse: GCCCCAATACTCTCTACCTCCT	Merck
McIIIcII	Forward: AGAGAGCAGAATGGAGACAACC Reverse: AGCACCAAGAAGATGCTGAAGT	Merck

Supplementary Methods

Cell viability and Lactate quantification

At 24h post-infection cell monolayers were incubated with Orangu™ for 1-3 hours at 37 ºC and absorbance read (450 nm) for viability quantification; culture supernatants were collected and lactate detected using the Lactate Assay Kit.

Intracellular M. tuberculosis quantification

Four hours after BMDM infection with Mtb clinical isolates at an MOI of 2, extracellular bacteria were washed with PBS and cell monolayers lysed with saponin for CFU enumeration in Middlebrook 7H11 agar supplemented with 10% OADC. CFU were determined after 21 days of incubation at 37 ºC.

Stimulation of BMDM with LPS and ATP

BMDM were primed with LPS (100 $ng.mL^{-1}$) for 20 hours, followed by treatment with mitoTEMPO (5 μM) for 30 min and ATP (3 mM) stimulation for 4 hours, in the presence of mitoTEMPO (34). For the rapamycin assay, BMDM were pre-treated with rapamycin (10 nM) for 1 hour and primed with LPS (500 $ng.mL^{-1}$) for 3 hours. The medium was then replaced, and cells were stimulated with ATP (5 mM) for an additional 30 min (33). IL-1β was measured in the culture supernatant.

Mitochondrial membrane potential quantification

24 h post-infection, BMDM were incubated at 37 ºC with 5 μM of CMXRos dye for 30 min in the dark, harvested, fixed in 4% PFA for 20 min, and acquired in Accuri C6 Plus. Analyses were with FlowJo v10.10.0.

CHAPTER 4

EXPERIMENTAL RESULTS

TWO MICE, TWO FATES: HOW HOST DIVERSITY SHAPES IMMUNE RESPONSES TO *MYCOBACTERIUM TUBERCULOSIS*

Part of this chapter has been submitted for publication, specifically data from *Figure 1* and *Figure 2*.

TYPE I IFN IMPEDES EARLY BACTERIAL CONTROL IN TB-RESISTANT AND -SUSCEPTIBLE MICE AND ACTIVATES NEUTROPHILS TO RESTRICT LUNG MACROPHAGE-T CELL INTERACTIONS

William J. Branchett[1], Evangelos Stavropoulos[1], Jessica Shields[1], Alaa Al-Dibouni[1], Marcos Cardoso[2], **Ana Isabel Fernandes**[2,3], Lúcia Moreira-Teixeira[1], Hubert Slawinski[1], Ania Mikolajczak[1], Angela Rodgers[1], Margarida Saraiva[2] and Anne O'Garra[1,4]

[1] The Francis Crick Institute, London, UK

[2] Instituto de Investigação e Inovação em Saúde, University of Porto, Porto, Portugal

[3] Doctoral Program in Molecular and Cell Biology, Instituto de Ciências Biomédicas Abel Salazar, University of Porto, Porto, Portugal

[4] National Heart and Lung Institute, Imperial College London, London, UK

Under final revision:
Journal of Experimental Medicine

CHAPTER 4

EXPERIMENTAL RESULTS

TWO MICE, TWO FATES: HOW HOST DIVERSITY SHAPES IMMUNE RESPONSES TO *MYCOBACTERIUM TUBERCULOSIS*

Ana Isabel Fernandes[1,2], Marcos Cardoso[1], Diogo Silvério[1,2], Rute Gonçalves[1,2], Margarida Saraiva[1,*]

[1] Instituto de Investigação e Inovação em Saúde, University of Porto, Porto, Portugal

[2] Doctoral Program in Molecular and Cell Biology, Instituto de Ciências Biomédicas Abel Salazar, University of Porto, Porto, Portugal

Unpublished data

[*]Corresponding author: Margarida Saraiva (margarida.saraiva@i3s.up.pt)

GRAPHICAL ABSTRACT

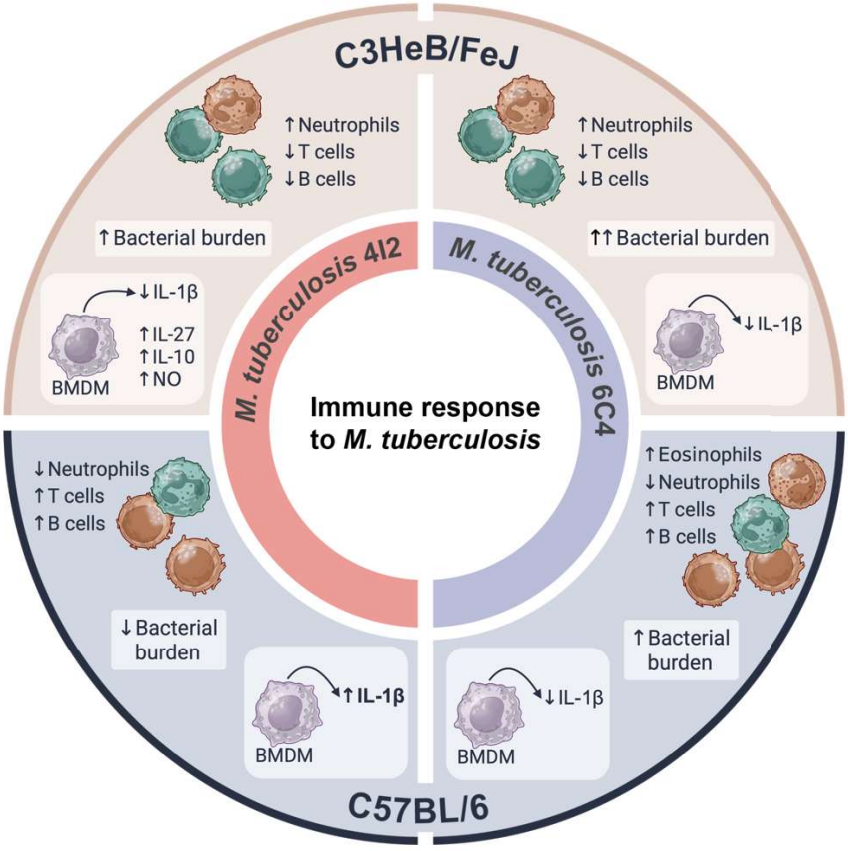

ABSTRACT

Approximately 1.25 million deaths are attributed to tuberculosis each year, making it one of the major causes of mortality worldwide. Tuberculosis results from a complex interplay between the host and the pathogen, *Mycobacterium tuberculosis*. The progression and severity of the disease are thought to be determined by early immune events in the lung, although the precise underlying molecular pathways remain unclear.

To investigate the impact of host genetic factors on immune responses to *M. tuberculosis*, we used the tuberculosis-susceptible C3HeB/FeJ mouse strain alongside the more resistant C57BL/6 strain. As expected, infection in C3HeB/FeJ mice resulted in more structured lung lesions dominated by neutrophils and higher bacterial loads at the peak infection, whereas C57BL/6 mice exhibited more diffuse lesions with stronger recruitment of adaptive immune cells, with a corresponding lower bacterial burden. Interestingly, these differences in immune response were consistent across different *M. tuberculosis* clinical isolates, indicating that host genetic background plays a dominant role in shaping this response. Additionally, interleukin (IL)-1β production was impaired in C3HeB/FeJ mice compared to C57BL/6 mice, indicating a compromised inflammatory response that may heighten their susceptibility. Mechanistically, our current findings suggest a possible role for IL-27, IL-10, and nitric oxide signalling in limiting IL-1β responses in C3HeB/FeJ mice.

Overall, our study highlights the significance of the host genetic background in shaping immune responses to *M. tuberculosis.* Given the heterogeneity of tuberculosis outcomes in both animal models and human populations, refining these disease models is essential. This could improve strategies for identifying novel therapeutic targets that modulate immune pathways for better disease control.

KEYWORDS: *Mycobacterium tuberculosis,* disease severity, immune response, mouse models, IL-1β signalling.

INTRODUCTION

With over 10 million new cases and 1.25 million deaths documented in 2023, tuberculosis has reclaimed its status as the world's deadliest infectious disease[1]. Despite global efforts to control this disease, tuberculosis remains a significant public health challenge, partly due to its highly heterogeneous clinical presentation[2,3]. Upon infection with *Mycobacterium tuberculosis*, the main causative agent of tuberculosis, outcomes can vary: some individuals clear the infection, many remain asymptomatic, a subset progresses to active disease[4–7]. Among patients with active tuberculosis, manifestations can range from mild to severe pulmonary infection to disseminated forms of the disease[8–10]. The precise mechanisms driving tuberculosis progression are still poorly understood.

Early lung immune events are critical determinants of tuberculosis progression, shaping both bacterial control and inflammation-mediated pathology[2,11–15]. However, deciphering these early immune dynamics in human patients remains challenging due to difficulties in pinpointing the onset of infection and the limited access to human lung tissue. Thus, experimental models that recapitulate human tuberculosis progression and its underlying diversity are essential for dissecting the host-pathogen interactions that shape disease severity. To address this knowledge gap, we leveraged the mouse model.

Mouse aerosol infection models offer a tractable system for studying tuberculosis pathogenesis under controlled conditions[16]. C3HeB/FeJ mice, which carry the susceptible sst1 allele, can develop necrotic lesions and lung cavitation, and exhibit blood and lung signatures akin to those observed in human tuberculosis, making them an excellent model of disease susceptibility[9,17]. In contrast, C57BL/6 mice are considered tuberculosis-resistant, with non-necrotic lesions containing few neutrophils and the ability to mount effective immune responses, making them a well-established model for studying protective mechanisms in tuberculosis[18–20]. Comparing these two mouse strains can reveal immune mechanisms underlying resistance or susceptibility and assess how early immune events contributed to differential disease outcomes. For example, increased susceptibility in C3HeB/FJ mice has been linked to a sustained type I interferon (IFNs) response, increased neutrophil activation, and pulmonary NETosis, which promote bacterial growth[9,21]. Additionally, C3HeB/FeJ mice displayed diminished B cell and T cell responses, which were more abundant in C57BL/6 mice, reinforcing their role in early immune control[9].

Beyond host factors, the genetic diversity of *M. tuberculosis* undoubtedly influences tuberculosis severity[3,21,22]. *M. tuberculosis* belongs to the *Mycobacterium tuberculosis* complex, comprised of 10 lineages phylogeographically linked to the human population

distribution[3,23,24]. Despite the high genetic similarity within this complex, different strains of *M. tuberculosis* evoke different immune responses and clinical manifestations of tuberculosis[3]. Our previous work demonstrated that *M. tuberculosis* isolates recovered from pulmonary tuberculosis patients with different clinical presentations exhibit distinct immune modulatory properties[25]. In a cohort of over 600 pulmonary tuberculosis patients, clinical isolates associated with mild presentations, such as *M. tuberculosis* 4I2, triggered robust inflammasome activation and interleukin (IL)-1β secretion (a key cytokine in host resistance), whereas those linked to severe disease, i.e. *M. tuberculosis* 6C4, evaded macrophage cytosolic surveillance systems, leading to lower/impaired IL-1β production[25]. While the molecular mechanisms underlying the differential inflammasome activation are still under investigation, this phenotype appears to be host-independent, highlighting that bacterial virulence traits directly manipulate immune activation and disease trajectory.

In this study, we investigated if the differential outcomes of tuberculosis observed in patients infected with the selected isolates[25] were recapitulated using the mouse model. We compared the different immune responses elicited by *M. tuberculosis* 4I2 and 6C4 in C57BL/6 and C3HeB/FeJ mice. We were able to successfully discriminate the two *M. tuberculosis* clinical isolates, with differences being more pronounced in C57BL/6 mice, where *M. tuberculosis* 6C4-infected animals presented higher bacterial burdens and histopathology than *M. tuberculosis* 4I2-infected mice. In accordance with prior observations using reference strains of *M. tuberculosis*[9], C3HeB/FeJ mice exhibited higher bacterial burdens and neutrophil-predominant lung infiltrates, while C57BL/6 mice developed more diffuse lesions with stronger adaptive immune cell recruitment. These immune responses persisted across both *M. tuberculosis* infections, underscoring the significant role of host genetics in shaping disease progression. Moreover, we found that *M. tuberculosis*-infected C3HeB/FeJ mice displayed impaired IL-1β production in the lung, a phenotype also observed at the macrophage level, particularly with the high IL-1β inducer *M. tuberculosis* 4I2. Decreased levels of IL-1β were accompanied by increased levels of IL-27, IL-10, and nitric oxide, suggesting a potential mechanism for the heightened susceptibility of C3HeB/FeJ mice to *M. tuberculosis* infection. This study provides preliminary yet foundational insights into the interplay between host genetics, bacterial diversity, and immune responses in tuberculosis. By identifying key immune mediators involved in differential outcomes, we may offer potential biomarkers for an earlier detection of disease progression. Additionally, understanding how *M. tuberculosis* strains differentially modulate immune pathways could inform patient stratification strategies and guide host-directed therapies, with the ultimate goal of improving patient outcomes.

MATERIALS AND METHODS

Ethics statement

Animals. All animal experiments were approved by the i3S Animal Ethics Committee and licensed by the Portuguese National Authority for Animal Health – Direção Geral de Alimentação e Veterinária (DGAV Ref #018413/2021-11-24), following the European Directive 2010/63/EU and Portuguese legislation (Decreto-Lei 113/2013). Experiments were conducted at the AAALAC-accredited i3S Animal Facility, adhering to the 3Rs principle (Replacement, Reduction, and Refinement) and following FELASA recommendations. All experiments complied with Animal Research: Reporting of in Vivo Experiments (ARRIVE) guidelines (https://arriveguidelines.org).

Biosafety Measures. All *M. tuberculosis* manipulations were carried out under biosafety level 3 conditions at i3S, in compliance with national regulations, transposing EU directives 90/679/CEE, 93/88/CEE, and 95/30/CE. Personnel handling *M. tuberculosis* received specialised biosafety level 3 training.

Bacteria stocks growth and quantification

M. tuberculosis clinical isolates 4I2 and 6C4, obtained from the sputum of patients enrolled in a cohort of 681 culture-confirmed tuberculosis cases diagnosed at *Centro Hospitalar São João* (CHUSJ), Porto, Portugal, between 2007 and 2013, were initially characterised in a study by Sousa et al[25,26].

Bacterial stocks were propagated in Middlebrook 7H9 liquid medium supplemented with 10% Oleic Albumin Dextrose Catalase (OADC) growth supplement and 0.2% glycerol. Bacteria were collected during the exponential growth phase, aliquoted, and stored at -80 °C. Five frozen vials were thawed, serially diluted, and plated on 7H11 agar supplemented with 10% OADC and 0.5% glycerol to determine viable bacterial counts. Colony-forming units (CFU) were enumerated after incubation at 37 °C for 21 to 28 days. For required experiments, bacterial aliquots were thawed just before use and diluted to the appropriate concentration.

Reagents

All reagents and resources are listed in *Supplementary Table 1*.

Animals

C57BL/6 and C3HeB/FeJ mice were bred and housed under specific-pathogen-free (SPF) conditions at the i3S animal facility. Both male and female mice, aged between 8 and 12 weeks at the start of the experiments, were used. The mice were kept in individually ventilated cages fitted with HEPA filters and maintained in rooms with controlled temperatures (20–24 °C), humidity (45–65%), and a 12:12 light/dark cycle. Water and a standardised synthetic diet (Envigo Teklad Global Rodent Diet, 2014S) were provided ad libitum. Mice were humanely euthanised by CO_2 asphyxiation or intraperitoneal injection of sodium pentobarbital, with efforts made to minimise suffering. For infection experiments, the animals were housed in the i3S Animal Biosafety Level 3 facility under containment conditions.

Aerosol infection and animal monitoring

Mice were infected with *M. tuberculosis* clinical isolates via aerosol inhalation using a Glas-Col exposure system, mimicking the natural route of infection. Three days post-infection, CFU enumeration in lung homogenates from three mice was used to determine infection doses (values are provided in the figure legends)[27,28]. Infected animals were monitored weekly, which included weight measurements and assessments of general clinical signs (e.g., appearance, behaviour, hydration, and respiratory movement). A humane endpoint (HEP) was defined as a weight loss of ≥20%, a lack of responsiveness to physical stimulation, or severe dyspnoea.

Processing of lung tissue and bronchoalveolar lavage

At the indicated time points, infected and non-infected mice were euthanised by intraperitoneal injection of a lethal dose of sodium pentobarbital. All procedures were performed aseptically.

Bronchoalveolar lavage was collected by inserting a catheter in the trachea of the euthanised mice and injecting phosphate-buffered saline (PBS) with 2% foetal bovine serum (FBS) and 2 mM ethylenediaminetetraacetic acid (EDTA). The PBS was flushed into the lungs and then aspirated multiple times[29,30]. Cells were counted using the trypan blue exclusion assay. Half of the recovered fluid was used to assess the bacterial burden. The remaining volume was stained for multiparametric flow cytometry.

The lungs were perfused with PBS to remove circulating blood. The right upper lobe was excised for histological analysis. The remaining lobes were enzymatically digested using 0.1% Collagenase D (prepared in Hanks' Balanced Salt Solution - HBSS 1x) at 37 °C, followed by mechanical disruption in complete Dulbecco's Modified Eagle Medium (DMEM, high glucose, GlutaMAX™ supplement, pyruvate supplemented with 10% FBS and 1% HEPES; cDMEM), and filtered through a 70 µm mesh. From the total volume (12 mL), 1 mL of the single-cell suspensions was used for bacterial burden determination, while the remaining volume was centrifuged. The resulting supernatants were filtered and stored at -80 °C for subsequent cytokine analysis. The cell pellet was incubated with ammonium-chloride-potassium (ACK) buffer (0.15 M NH4Cl, 10 mM KHCO3, and 0.1 mM EDTA) for red blood cell lysis. Cells were then counted using the trypan blue exclusion assay and used for flow cytometry and ribonucleic acid (RNA) analysis. Cell pellets for gene expression analysis by real-time polymerase chain reaction (PCR) were stored in TripleXtractor reagent at -80 °C until RNA extraction[27,28].

Histological and morphometric analysis

After lung perfusion with PBS, the right upper lobe was excised and fixed in 10% phosphate-buffered formalin for one week. The fixed tissues were then embedded in paraffin, and 3 µm sections were prepared for histological analysis. For histopathological examination, the lung sections were stained with haematoxylin and eosin (H&E). Images were acquired using a NanoZoomer 2.0-HT Whole Slide Imager, Digital Pathology Slide Scanner[27,28]. Pathological scoring (lesion score) was performed blindly based on the parameters detailed in *Supplementary Table 2*. A quantitative morphometric analysis of lung pathology (% lesion area) was conducted using ilastik (Interactive Learning and Segmentation Toolkit)[31] and CellProfiler[32]. Probability maps for the entire lung structure and lesion areas were generated in ilastik and subsequently analysed in CellProfiler. Representative images of this pipeline can be found in *Supplementary Figure 1*.

Bacterial burden determination by CFU enumeration

For in vivo experiments, after lysing host cells with 0.1% saponin, *M. tuberculosis* from lung and bronchoalveolar lavage cell suspensions was serially diluted and plated on 7H11 agar supplemented with 10% OADC, 0.5% glycerol, and MGIT PANTA antibiotic[27,28]. CFU were tallied after incubation at 37 °C for 21 to 28 days.

For in vitro experiments, four hours after bone marrow-derived macrophages (BMDM) infection with *M. tuberculosis* clinical isolates at a multiplicity of infection of 2 bacteria:1 cell (MOI of 2), extracellular bacteria were removed by washing with PBS. To assess bacterial internalisation, infected cells were lysed with 0.1% saponin, and the bacterial burden was determined by colony-forming unit enumeration on Middlebrook 7H11 agar plates supplemented with 10% OADC. Plates were incubated at 37 °C for 21 to 28 days before CFU determination. To assess the BMDM bacterial control, fresh medium was added following the 4 hour wash, and cells were incubated for 4 days before lysis with 0.1% saponin and CFU enumeration as described above.

Immune cell population analysis by flow cytometry

Lung cell suspensions were stained for surface antigens for 30 minutes at 4 °C and fixed in 4% paraformaldehyde for 20 minutes. Dead cells were excluded from the analyses using a viability dye. To assess immune cell recruitment and infiltration, multiparametric flow cytometry was employed to analyse both myeloid and lymphoid populations in lung and bronchoalveolar lavage[27]. All samples were acquired using a BD LSRFortessa flow cytometer, and data analysis was performed in FlowJo. The gating strategy is illustrated in *Supplementary Figure 2*.

Bone marrow-derived macrophage generation

Mouse BMDM were differentiated from bone marrow precursors in the presence of 20% L929 cell-conditioned media (LCCM). Tibias and femurs were aseptically collected from mice, and the bone marrow was flushed using cDMEM. Bone marrow cells were counted and plated in 100 mm Petri dishes at a concentration of 0.5×10^6 cells/mL in cDMEM supplemented with 20% LCCM. The cells were maintained at 37 °C with 5% CO_2. On day 4, additional cDMEM supplemented with 20% LCCM was added to support differentiation. On day 7, fully differentiated BMDM were harvested, counted, and plated for further

experiments. For downstream analysis, 5×10^5 or 1×10^5 cells were plated in 24-well and 96-well plates, respectively, and allowed to rest overnight before infection or stimulation[25,30].

Alveolar macrophages isolation

Alveolar macrophages were obtained from the bronchoalveolar lavage by flushing PBS with 2% FBS and 2 mM EDTA into the trachea of euthanised mice, as described above. The resulting cell pellet was treated with ACK buffer for red blood cell lysis. Alveolar macrophage purity was assessed by flow cytometry, with the cell suspensions considered pure if the alveolar macrophage ($CD45^+/CD11c^+SiglecF^+$) content exceeded 95%. The cells were plated in complete Roswell Park Memorial Institute 1640 medium (RPMI with 10% FBS, 1% sodium pyruvate, 1% HEPES, and 1% L-glutamine; cRPMI) containing Penicillin-Streptomycin (100 U/mL), and allowed to adhere overnight in a 37 °C humidified incubator with 5% CO_2. The media with antibiotics were washed out prior to infection with *M. tuberculosis*[29,30].

In vitro infections

Before infection, mycobacterial clumps were disaggregated with a 25G needle. For BMDM infection, an MOI of 2 was used[25]. Alveolar macrophages were infected at an MOI of 1[30]. At various time points, cell pellets or culture supernatants were used for protein, viability, intracellular cytokine analysis, and CFU enumeration. Culture supernatants were filter-sterilised before further processing. For specific experiments, MCC950 (1 μM) was added to BMDM 2 hours prior to infection and maintained for the duration of the experiment[25,30].

Stimulation of BMDM with LPS and ATP

BMDM were primed with lipopolysaccharide (LPS, 100 ng/mL) for 20 hours, followed by stimulation with adenosine triphosphate (ATP, 3 mM) for 4 hours[30]. Cell culture supernatants were subsequently collected for cytokine measurement.

Cytokine quantification

Cytokine levels were measured in the supernatants of lung cell suspensions and in vitro cultures using a commercially available bead-based multiplex immunoassay. The LEGENDplex™ multiplex assay, analysed by flow cytometry on the BD Accuri C6 Plus, allowed simultaneous detection of IL-1α, IL-1β, IL-6, IL-10, IL-12p70, IL-17A, IL-23, IL-27, monocyte chemoattractant protein-1 (MCP-1, also known as C-C motif chemokine ligand 2, CCL2), IFN-β, IFN-γ, tumour necrosis factor (TNF)-α, and granulocyte-macrophage colony-stimulating factor (GM-CSF). Data was analysed using the LEGENDplex™ Cloud-based Data Analysis Software. Alternatively, when specified in figure legends, IL-1β production was quantified via a commercially available enzyme-linked immunosorbent assay (ELISA).

RNA extraction, cDNA, and real-time analysis

Total RNA from mouse lung cells was extracted with TripleXtractor reagent, according to the manufacturer's instructions and quantified using the NanoDrop 1000 Spectrophotometer. Glycogen was used to enhance RNA precipitation and recovery. Complementary deoxyribonucleic acid (cDNA) was synthesised in a T100 Thermal Cycler using the ProtoScript First-Strand cDNA Synthesis kit. Real-time PCR assays were performed using a CFX384 Real-Time PCR Detection System. Target gene RNA expression was quantified by real-time PCR using iTaq Universal SYBR Green Supermix and normalised using *ubiquitin* and *gapdh* as reference genes. The relative gene expression was determined using the $2^{-\Delta\Delta Ct}$ method[25,28,30]. The oligonucleotide sequences used are listed in *Supplementary Table 3*. The specificity of amplification was confirmed by melting curve analysis.

Nitric oxide quantification

The production of nitric oxide was quantified by measuring nitrite accumulation in the culture supernatants of BMDM using a standard Griess reaction. Equal parts culture supernatant was mixed with Griess reagent (1% sulfanilamide and 0.1% N-(1-naphthyl) ethylenediamine dihydrochloride in 2% H3PO4). After a 10 minute incubation in the dark at room temperature, the reaction yielded a pink azo dye. Absorbance was measured at 550 nm using the Synergy 2 spectrophotometer.

Cell viability quantification

Twenty-four hours post-infection, Orangu™ was added to cells and incubated at 37 °C for 1 to 3 hours, following the manufacturer's instructions. Absorbance was read at 450 nm.

Statistical analysis

Results are shown as mean ± standard error of the mean (SEM) or represented in box and whisker plots (Tukey's method). Data were analysed using GraphPad Prism software, version 10.0. References to "n" and the statistical tests applied are provided in the figure legends. Each dataset was tested for normality and log-normality with the Shapiro-Wilk or D'Agostino-Pearson tests and for outliers using Grubbs's test. Based on this information, parametric or nonparametric statistical tests were used for multiple corrections and correlations. Differences were considered significant at $p \leq 0.05$ and indicated in the figures.

RESULTS AND DISCUSSION

Host responses to *M. tuberculosis* infection diverge in C3HeB/FeJ and C57BL/6 mice

In order to model and decipher immune signatures of tuberculosis severity, we infected mice with *M. tuberculosis* clinical isolates associated with distinct disease presentations in human tuberculosis patients: *M. tuberculosis* 4I2 (mild/high IL-1β inducer) and 6C4 (severe/low IL-1β inducer)[25]. We infected the tuberculosis-susceptible C3HeB/FeJ and the more tuberculosis-resistant C57BL/6 mice[9] via aerosol with an infection dose of approximately 500 CFU/lung and monitored the establishment and progression of disease 15- and 30-days post-infection by assessing tissue pathology, immune cell infiltration, bacterial burden, and the overall health of the animals.

We started by assessing pulmonary disease severity, as shown in *Figure 1A*. During the early timepoint (15 days post-infection), when *M. tuberculosis* infection is dominated primarily by innate immunity[2], the histological features of infected animals were comparable to those of non-infected animals, with minimal immune cell infiltrations (*Figure 1A*). By day 30, when the adaptive immunity is already engaged[2], lesions were more pronounced across all infections, displaying both myeloid and lymphoid infiltrates (*Figure 1A*, identified with green and black arrows). Most lesions appeared to be perivascular or peribronchiolar (*Figure 1A*, identified with asterisks). At this time point, differences between mouse strains became apparent, as granulocyte infiltrates were more common in C3HeB/FeJ mice (*Figure 1A*), consistent with previous reports for these mouse strains[9]. In contrast, lesions in C57BL/6 mice presented more lymphocytic lesions (*Figure 1A*). Particularly in *M. tuberculosis* 4I2 infections, lung lesions in C3HeB/FeJ mice were more organised, whereas in C57BL/6 mice, they appeared to be more diffuse (*Figure 1A*). Furthermore, as compared to *M. tuberculosis* 4I2, infection with *M. tuberculosis* 6C4 led to more extensive pathology in both mouse strains (*Figure 1A*), aligning with the radiographic data of the tuberculosis patients[25]. Morphometric analysis of the lung sections confirmed these differences in lesion severity, revealing a greater percentage of affected lung area in mice infected with *M. tuberculosis* 6C4 than in those infected with isolate 4I2, particularly in C57BL/6 mice (*Figure 1B*), despite their classification as tuberculosis-resistant. This trend was also reflected in the lung lesion score (*Figure 1C*) and lung cellularity (*Figure 1D*). Future studies should incorporate later time points and immunofluorescence analysis to provide a more detailed characterisation of lesion progression, including changes in cellular composition and their spatial organisation.

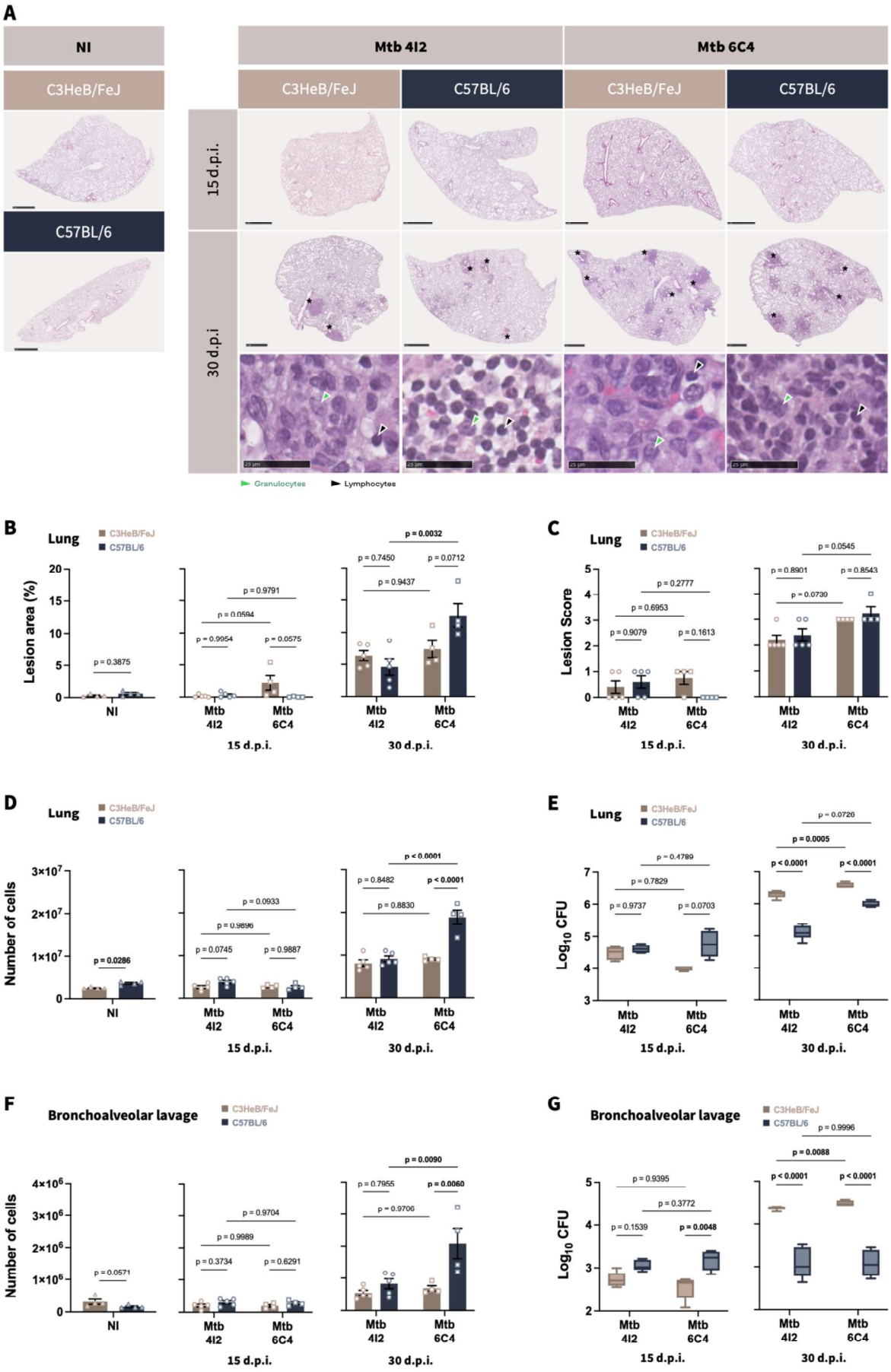

Figure 1. *Figure legend on the next page.*

Figure 1 continued. The impact of *M. tuberculosis* 4I2 and 6C4 infection in the lungs of infected susceptible and resistant mice. C3HeB/FeJ and C57BL/6 mice were infected via aerosol with *M. tuberculosis* 4I2 or 6C4. The infection doses for the experiments used in this figure were 460 ± 34 CFU/lung (*M. tuberculosis* 4I2, n = 5 for each condition) and 448 ± 29 CFU/lung (*M. tuberculosis* 6C4, n = 4 for each condition). Infected and non-infected (n = 4 for each condition) animals were 9.0 ± 0.2 weeks old at the start of the experiment. At the indicated time points, lungs were collected for histological analysis, total cell number quantification, and CFU enumeration. ***(A)*** Representative images of H&E-stained lung slices for each experimental group. The scale bar corresponds to 1 mm (25 μm in close-up images). Asterisks indicate perivascular or peribronchiolar lesions, green arrows point to granulocytes, and black arrows to lymphocytes. ***(B)*** Lung pathology, defined as the percentage of cell infiltrates, was determined using morphometric analysis of H&E-stained lung slices. ***(C)*** The histopathological features *(Supplementary Table 2)* in the mice's lungs were assessed, and a relative score was assigned. ***(D)*** Lung cell suspensions were prepared, and the total cell numbers were determined with trypan blue. ***(E)*** The bacterial burden in infected mice's lungs was assessed through CFU enumeration. ***(F)*** At the indicated time points, bronchoalveolar lavage was collected, and the total cell numbers for each mouse were quantified with trypan blue. ***(G)*** The bacterial burden in the bronchoalveolar lavage was assessed by CFU enumeration. ***(B-G)*** Each dot represents an individual mouse, and the mean ± SEM is shown for each group. C3HeB/FeJ mice are represented in light brown and C57BL/6 mice in dark blue. Statistical analysis was performed using an unpaired *t*-test or two-way ANOVA with Tukey's multiple comparison test. Differences between groups were considered significant if $p < 0.05$. ***Abbreviations:*** d.p.i., days post-infection; Mtb, *M. tuberculosis*; NI, non-infected.

Lung bacterial burden further highlighted differences in disease progression between the two mouse strains. At 15 days post-infection, no statistically significant differences were observed (*Figure 1E*). Still, C57BL/6 mice tended to display a higher bacterial burden than C3HeB/FeJ mice specially when infected with the severe clinical isolate (*M. tuberculosis* 6C4; *Figure 1E*). This suggests that the tuberculosis-susceptible C3HeB/FeJ mice may surprisingly exhibit better early control of *M. tuberculosis* than the more resistant C57BL/6 mice. However, by day 30, this tendency reversed. CFU enumeration showed that C3HeB/FeJ mice exhibited significantly higher bacterial burdens than infected C57BL/6 mice, regardless of the infecting clinical isolate (*Figure 1E*), indicating a less effective bacterial control over time in C3HeB/FeJ mice. This pattern in bacterial burden persisted independently of the initial infection dose, with C3HeB/FeJ mice showing higher bacterial loads with an infection dose of 1000 CFU/lung (*Supplementary Figure 3A*).

We also compared the cellularity and bacterial burden in the bronchoalveolar lavage of the infected animals at the same time points. Paralleling the lung findings,

bronchoalveolar lavage cellularity was markedly higher in C57BL/6 mice, especially following *M. tuberculosis* 6C4 infection, suggesting a more robust immune cell recruitment (*Figure 1F*). Also, accompanying data from the lung, C57BL/6 mice displayed higher bacterial burdens in the bronchoalveolar lavage at early time points (*Figure 1G*). However, by day 30 post-infection, bacterial burdens in the bronchoalveolar lavage of C57BL/6 mice remained stable, regardless of the infecting isolate, suggesting a more effective containment of bacteria (*Figure 1G*). In contrast, in C3HeB/FeJ mice, bacterial burdens in the bronchoalveolar lavage increased exponentially from day 15 to day 30 post-infection (*Figure 1G*).

Overall, despite the aforementioned marked differences in infection dynamics, both mouse strains gained weight throughout the infection and displayed no overt signs of disease, irrespective of the infecting isolate (*Supplementary Figure 3B*).

Taken together, our data reveal that the tuberculosis-resistant C57BL/6 and tuberculosis-susceptible C3HeB/FeJ mice exhibit distinct infection dynamics to the tested *M. tuberculosis* clinical isolates. Clear differences in bacterial burden and lung pathology were observed between the two mouse strains, irrespective of the infecting isolate. However, C57BL/6 mice appear to differentiate more clearly between the two clinical isolates, with lung pathology and bacterial burden being higher with *M. tuberculosis* 6C4 (*Figure 1*), recapitulating human disease[25]. To further explore these differences in bacterial burden and immune responses, we next investigated immune cell recruitment in infected mice

Differential cell recruitment profile in *M. tuberculosis*-infected C3HeB/FeJ and C57BL/6 mice

The progression of *M. tuberculosis* infection and disease outcome are strongly linked to the host immune response[2], which, in turn, can be influenced by the characteristics of the host and the infecting bacteria[3,16,25,33]. To characterise the mature immune cell populations in the lung throughout infection with *M. tuberculosis* 4I2 and 6C4, we infected C3HeB/FeJ and C57BL/6 mice and performed multiparametric flow cytometry at different time points (see *Supplementary Figure 2* for gating strategy).

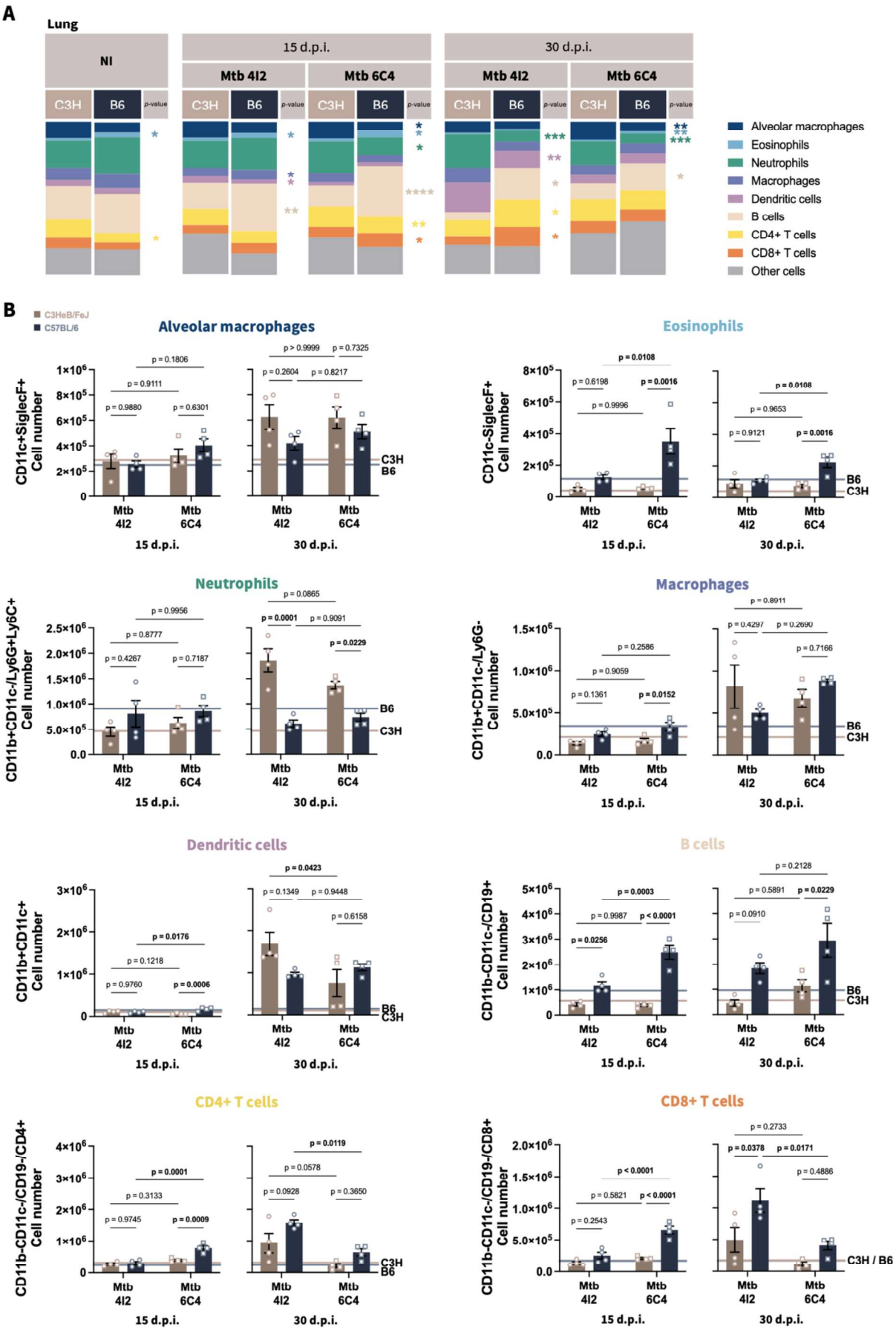

Figure 2. *Figure legend on the next page.*

Figure 2 continued. Immune cell recruitment in the lungs of C3HeB/FeJ and C57BL/6 mice upon infection with *M. tuberculosis*. C3HeB/FeJ and C57BL/6 mice were infected via aerosol with *M. tuberculosis* 4I2 or 6C4. The infection doses for the experiments used in this figure were 460 ± 34 CFU/lung (*M. tuberculosis* 4I2) and 429 ± 24 CFU/lung (*M. tuberculosis* 6C4). Infected and non-infected animals were 9.0 ± 0.2 weeks old at the beginning of the experiment. At the specified time points, lungs were collected (n = 4 for each condition). ***(A)*** Cell frequencies for mature immune cell populations in the lung were determined through flow cytometry, employing the gating strategy outlined in *Supplementary Figure 2*. Statistical analysis was performed using unpaired *t*-test. Differences between groups were considered significant if $p < 0.05$ and represented in the graphs (* $p < 0.05$, ** $p < 0.01$, *** $p < 0.001$, **** $p < 0.0001$). Alveolar macrophages are represented in dark blue, eosinophils in light blue, neutrophils in green, macrophages in dark purple, dendritic cells in light purple, B cells in beige, $CD4^+$ T cells in yellow, $CD8^+$ T cells in orange, and other cells in grey. ***(B)*** Total cell numbers of the populations indicated in *(A)*. The mean for non-infected animals for each strain is represented by a line. Each dot represents an individual mouse, and data is expressed as mean ± SEM. C3HeB/FeJ macrophages are shown in light brown and C57BL/6 in dark blue. Statistical analysis was performed using two-way ANOVA with Tukey's multiple comparison test. Differences between groups were considered significant if $p < 0.05$. ***Abbreviations:*** B6, C57BL/6; C3H, C3HeB/FeJ; CD, cluster of differentiation; d.p.i., days post-infection; Mtb, *M. tuberculosis*; NI, non-infected.

Non-infected animals from each mouse strain served as a baseline, and only minor differences were noted between the two mice in the non-infected condition. $CD4^+$ T cell frequencies were slightly more elevated in C3HeB/FeJ mice (*Figure 2A*), although this was not reflected at the cell number level (*Supplementary Figure 4*). In C57BL/6 mice, both the frequency and total number of eosinophils ($CD11c^-SiglecF^+$) were increased (*Figure 2* and *Supplementary Figure 4*).

At 15 days post-infection and for both mouse strains infected with *M. tuberculosis* 4I2, the immune cell populations in the lungs were comparable to those in non-infected animals (*Figure 2*). In contrast, infection with *M. tuberculosis* 6C4 led to an early immune cell infiltration in C57BL/6 mice, with a significant increase in the number of eosinophils and lymphocytes ($CD19^+$ B cells, $CD4^+$ T cells, and $CD8^+$ T cells; *Figure 2B*). In fact, eosinophil numbers peaked at this timepoint (*Figure 2B*). While lymphocytes, such as $CD4^+$ T cells, are well-established as key players in protective immunity[9,34], the role of eosinophils is still controversial. Recent evidence places eosinophils as protective for the host and required for optimal bacterial control[35]. However, these granulocytes may also exhibit detrimental effects due to their aggressive inflammatory properties, which can cause tissue damage and exacerbate the disease[36,37]. Future studies should attempt to address the possible role

of this influx of eosinophils to the lungs of C57BL/6 mice infected with the severe clinical isolate (*M. tuberculosis* 6C4) and expand these findings to other *M. tuberculosis* isolates.

Analysis of the lung 30 days post-infection revealed a generalised and substantial increase in alveolar macrophages ($CD11c^{+}SiglecF^{+}$), interstitial macrophages ($CD11b^{+}CD11c^{+}/Ly6G^{-}$), and dendritic cells ($CD11b^{+}CD11c^{+}$), independently of the mouse or bacterial strain (*Figure 2B*). At this time point, we detected more substantial differences between the mouse strains. Neutrophils ($CD11b^{+}CD11c^{-}/Ly6G^{-}Ly6C^{+}$), both frequency and cell numbers, were exceedingly more prevalent in C3HeB/FeJ mice, regardless of the infecting clinical isolate (*Figure 2*). In contrast, C57BL/6 mice displayed a higher frequency and cell numbers of lymphocytes (*Figure 2*). These findings align with previous reports[9,38,39] and indicate that C3HeB/FeJ mice mount a robust innate immune response dominated by neutrophils, suggesting a more inflammatory phenotype normally associated with tissue damage. Conversely, the C57BL/6 mice engage in a more adaptive immune-driven response, with a higher presence of T and B cells, potentially contributing to improved bacterial control later during infection.

M. tuberculosis initiates infection in the airways. To assess the immune cell populations present in the alveolar space, we also performed flow cytometry on bronchoalveolar lavage samples. Lung suspensions from non-infected mice were predominantly composed of alveolar macrophages (*Supplementary Figure 5*). A similar alveolar space composition was observed 15 days post-infection (*Supplementary Figure 5*). By day 30 post-infection, cell frequencies in the bronchoalveolar lavage largely mirrored findings in the lung, with higher neutrophil percentages in C3HeB/FeJ and increased lymphocyte levels in C57BL/6 (*Supplementary Figure 5*). These findings reinforce the notion that during the first 30 days of *M. tuberculosis* infection, C3HeB/FeJ mice strongly trigger innate immune responses where neutrophils are prevalent, while C57BL/6 mice develop a more robust adaptive immune response. Collectively, these findings support the divergent immune cell recruitment between C3HeB/FeJ and C57BL/6 mice, which likely contributes to tissue damage vs improved bacterial control, respectively.

Future studies should address immune cell populations that were not fully characterised in this study, which are indicated in *Figure 2A* as other cells. These include subsets of dendritic cells, monocytes and macrophages, and T cells. Beyond immune cells, non-hematopoietic $CD45^{-}$ populations, such as epithelial and endothelial cells, should also be examined, as these are crucial for immune cell migration, recruitment, and granuloma formation[40–43]. Additionally, the spatial organisation of the immune cells in the lung and longitudinal changes in immune response warrant further investigation. These directions

will enhance our understanding of the complex interactions shaping tuberculosis pathogenesis.

C3HeB/FeJ and C57BL/6 mice have divergent IL-1β profiles

Most of the differences seen in the immune cell profiles stemmed from variations in host genetics, which likely contribute to differing susceptibility to *M. tuberculosis* infection, irrespectively of the infecting isolate. However, our findings show that C57BL/6 mice display differences in CFU and pathology with respect to the two clinical isolates, suggesting that bacterial diversity also influences the immune response and tuberculosis outcome. To delve deeper into this issue, we next assessed IL-1β production in the lungs of these mice, as *M. tuberculosis* 4I2 and 6C4 are known to elicit distinct IL-1β responses in macrophages, with *M. tuberculosis* 4I2 prompting greater IL-1β levels through an NLR family pyrin domain containing 3 (NLRP3) inflammasome-dependent mechanism[25].

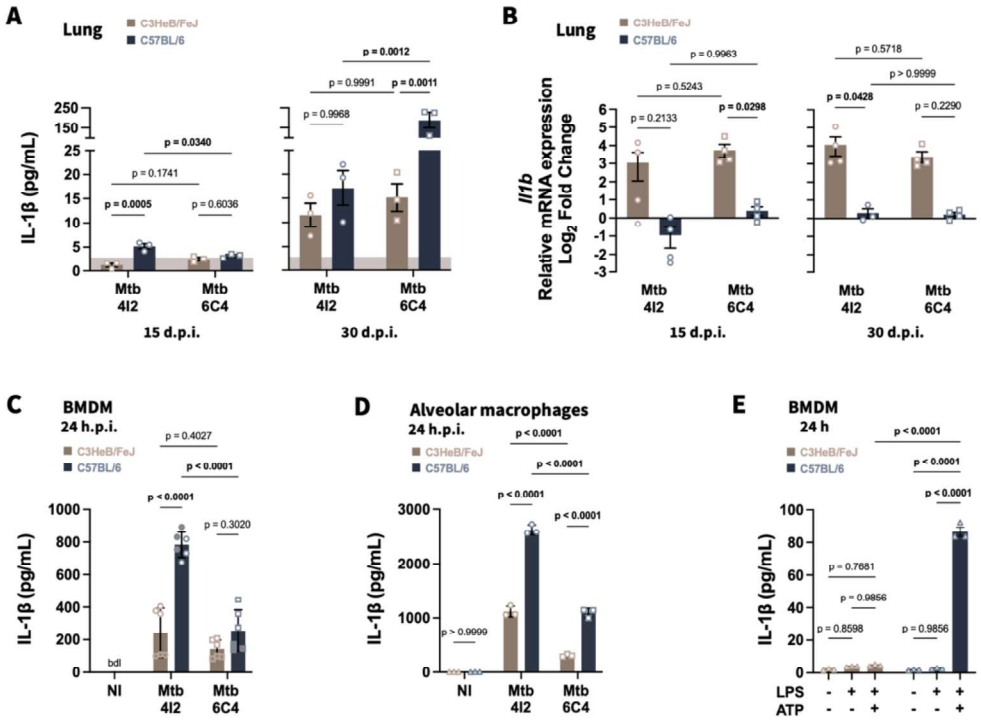

Figure 3. IL-1β production in C3HeB/FeJ and C57BL/6 mice. C3HeB/FeJ and C57BL/6 mice were infected via aerosol with *M. tuberculosis* 4I2 or 6C4. ***(A)*** The infection doses for the experiments depicted in this figure were 1077 ± 103 CFU/lung (*M. tuberculosis* 4I2) and 857 ± 13 CFU/lung (*M. tuberculosis* 6C4). Infected and non-infected animals were 9.8 ± 0.2 weeks old at the start of the experiment. At the specified time points, lung supernatants were collected (n = 3 for each condition), and the amount of secreted IL-1β was quantified through a bead-based immunoassay. Each dot represents an individual mouse, and values within the tinted brown area were below the detection

level and extrapolated. ***(B)*** The infection doses for the experiments used in this figure were 460 ± 34 CFU/lung (*M. tuberculosis* 4I2) and 448 ± 29 CFU/lung (*M. tuberculosis* 6C4). Infected and non-infected animals were 9.1 ± 0.2 weeks old at the start of the experiment. At the indicated time points, lungs were collected (n = 4 for each condition). The expression of the gene encoding *Il1b* in the lung was determined by real-time PCR and represented as fold change, with the respective non-infected animal serving as a baseline and each dot representing an individual mouse. ***(C-E)*** The amounts of secreted IL-1β were quantified through an immune-based immunoassay in the cell culture supernatants 24 hours after stimulation. ***(C)*** Mouse BMDM were infected at an MOI of 2 with either *M. tuberculosis* 4I2 or 6C4. Represented are triplicate wells of three experiments. ***(D)*** Mouse alveolar macrophages were infected at an MOI of 1 with either clinical isolate. Represented are triplicate wells of one experiment. ***(E)*** Mouse BMDM stimulated with LPS (100 ng/mL, 20 hours) followed by ATP (3 mM, 4 hours). Represented are triplicate wells of one experiment. Data are expressed as mean ± SEM. C3HeB/FeJ macrophages are shown in light brown and C57BL/6 in dark blue. Statistical analysis was performed using two-way ANOVA with Tukey's multiple comparison test. Differences between groups were considered significant if $p < 0.05$. ***Abbreviations:*** bdl, below detection level; BMDM, bone marrow-derived macrophages; d.p.i., days post-infection; h.p.i., hours post-infection; IL, interleukin; Mtb, *M. tuberculosis*; NI, non-infected.

IL-1β production was measured in the lung supernatant, and the expression of the *Il1b gene* was quantified by qPCR in lung cells. By day 15 post-infection, C57BL/6 mice infected with *M. tuberculosis* 4I2 already exhibited significantly higher IL-1β levels compared to the other infections (*Figure 3A*). In contrast, C3HeB/FeJ mice failed to upregulate IL-1β protein production in response to *M. tuberculosis* 4I2 at this early stage (*Figure 3A*). By day 30 post-infection, increased cell recruitment and inflammation likely played a more prominent role in dictating IL-1β production, as the bacterial strain influence was not as evident. At this time-point, C3HeB/FeJ mice displayed lower IL-1β protein levels than C57BL/6 mice, irrespective of the infecting strain (*Figure 3A*). Interestingly, the relative expression of the *Il1b* gene was higher in infected C3HeB/FeJ than C57BL/6 mice at both time points, for infection with either *M. tuberculosis* strain (*Figure 3B*).

The discrepancy between the high expression of the *Il1b* gene and the reduced IL-1β production by infected C3HeB/FeJ mice prompted us to investigate whether IL-1β production was affected in the macrophages of these mice. As previously reported[25], C57BL/6 BMDM infected with *M. tuberculosis* 4I2 secreted more IL-1β than those infected with *M. tuberculosis* 6C4 (*Figure 3C*). In C3HeB/FeJ BMDM, IL-1β levels were significantly lower than those secreted by infected C57BL/6 BMDM, 24 hours post-infection (*Figure 3C*), suggesting, indeed, a possible deficiency in IL-1β secretion in C3HeB/FeJ mice.

This differential IL-1β production by infected C3HeB/FeJ vs C57BL/6 mice extended beyond BMDM, as C3HeB/FeJ alveolar macrophages infected with either *M. tuberculosis* isolate exhibited significantly lower IL-1β secretion than C57BL/6 alveolar macrophages (*Figure 3D*). Nevertheless, *M. tuberculosis* 4I2 induced higher IL-1β secretion in C3HeB/FeJ macrophages than *M. tuberculosis* 6C4, mirroring the pattern previously reported in C57BL/6. These findings raise important questions regarding what strain- or host-specific mechanisms underlie IL-1β production and how they contribute to disease outcomes.

To assess if differences in IL-1β production were linked to increased apoptosis in C3HeB/FeJ macrophages or other issues in protein production, we assess the viability of BMDM and alveolar macrophages from both mouse strains upon infection with either *M. tuberculosis* clinical isolate. Notably, BMDM from C3HeB/FeJ showed increased cell viability under all conditions as compared to C57BL/6 BMDM (*Supplementary Figure 6A*). In the case of alveolar macrophages, this difference was only seen for non-infected C3HeB/FeJ (*Supplementary Figure 6B*). Thus, C3HeB/FeJ BMDM are more viable than C57BL/6 BMDM, possibly due to reduced pyroptosis in C3HeB/FeJ macrophages, a form of inflammatory cell death driven by NLRP3 inflammasome activation[44,45].

We also tried to determine whether the observed differences in IL-1β secretion were linked to bacterial infection dynamics, specifically by assessing whether the infection rate and bacterial persistence in BMDM of either mouse strain were affected. However, no differences in CFU enumeration were found between infected C3HeB/FeJ and C57BL/6 BMDM, 4 hours and 4 days after infection (*Supplementary Figure 6C*).

To further investigate the mechanisms driving IL-1β production, we examined the role of the NLRP3 inflammasome. In both mice strains, maximal IL-1β secretion relied on NLRP3 inflammasome activation, although this was more evident in C57BL/6 BMDM (*Supplementary Figure 6D*). We also stimulated BMDM with LPS, a potent activator of the innate immune response[46], and ATP, a canonical NLRP3 inflammasome activator[47]. Notably, unlike what was observed for C57BL/6 BMDM, stimulation of C3HeB/FeJ BMDM with LPS+ATP did not result in an increase in IL-1β secretion (*Figure 3E*), reinforcing a host-specific defect in IL-1 signalling in C3HeB/FeJ mice.

Given the undeniable protective role of IL-1 signalling against tuberculosis[48], this defective IL-1β response likely contributes to the higher susceptibility observed in C3HeB/FeJ mice. This impairment in IL-1β production may disrupt immune cell recruitment and pathogen control, ultimately shaping the disease outcome. Additionally, as the *M.*

tuberculosis clinical isolates differ in their dependence on IL-1β for immune evasion or persistence[25], unravelling this host-pathogen interplay could provide crucial insights into tuberculosis progression. However, the underlying mechanism for this IL-1β deficiency in C3HeB/FeJ mice remains unclear. Excessive type I IFNs, previously described in *M. tuberculosis* infected C3HeB/FeJ mice, is a known suppressor of IL-1β and could be a key factor in this regulation, along with other immune mediators[9,48–50].

Potential candidates for the modulation of IL-1β in C3HeB/FeJ mice

Several host mechanisms that regulate IL-1β have been described in the context of tuberculosis, the most notable being type I IFNs[51]. Type I IFNs have continuously been implicated in tuberculosis pathogenesis, both promoting and suppressing host defence mechanisms[49]. Type I IFNs can directly downregulate *Il1b* transcription[52] or indirectly through the anti-inflammatory cytokine IL-10[18]. IL-10 is a key anti-inflammatory cytokine that dampens pro-inflammatory responses and is frequently upregulated in tuberculosis, where it has been associated with bacterial persistence[18]. Another key immune mediator of IL-1β is nitric oxide, a reactive nitrogen species produced by inducible nitric oxide synthase (iNOS), that can inhibit the NLRP3 inflammasome, limiting the cleavage of pro-IL-1β into its active form[53]. Nitric oxide has a prominent role in tuberculosis pathogenesis, as it can, similarly to type I IFNs and IL-10, inhibit IL-1β-driven neutrophil recruitment, which, if uncontrolled, can become detrimental to the host[54]. Although not commonly discussed in the context of tuberculosis, IL-27 is another immune mediator that can suppress IL-1β, as it shares signalling pathways with type I IFNs and IL-10 and can exert complementary immunosuppressive effects[55–57].

To further elucidate possible mechanisms explaining the differential IL-1β production of C3HeB/FeJ and C57BL/6 macrophages in response *to M. tuberculosis* infection, we analysed a panel of immune mediators previously implicated in the regulation of IL-1β. The secretion of IFN-β (a member of the type I IFNs family) by BMDM was higher in response to *M. tuberculosis* 4I2 infection than with *M. tuberculosis* 6C4, independently of the host genetic background (*Figure 4A*). This difference, previously reported for C57BL/6 macrophages[25], was now confirmed to also occur in C3HeB/FeJ macrophages, suggesting that production of this cytokine by BMDM in response *to M. tuberculosis* was primarily influenced by the infecting bacterial strain rather than by the host.

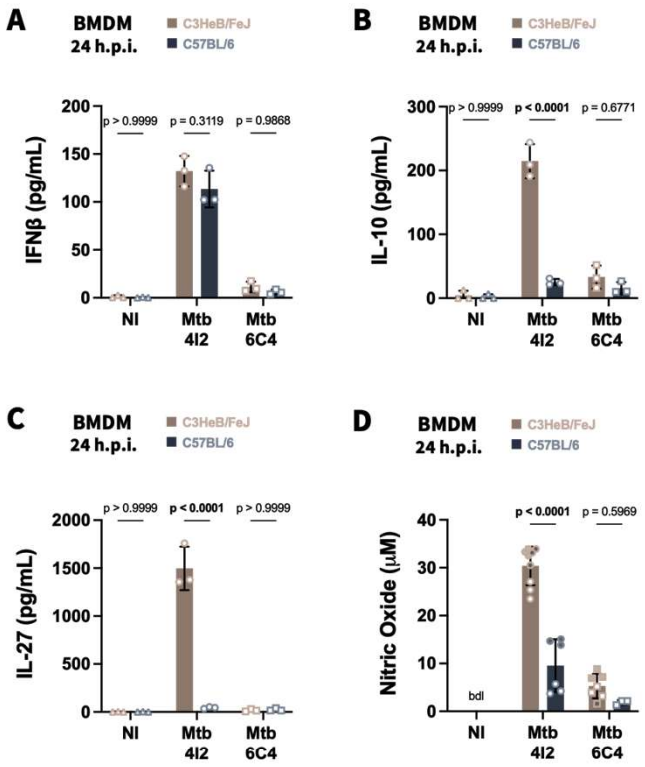

Figure 4. Potential candidates for the modulation of IL-1β in C3HeB/FeJ macrophages. ***(A-C)*** Mouse BMDM were infected at a multiplicity of infection of 2 with either *M. tuberculosis* 4I2 or 6C4. The amounts of secreted immune mediators were quantified in the cell culture supernatants 24 hours post-infection through a bead-based immunoassay. ***(D)*** Nitric oxide was quantified using Greiss reagent. Data are expressed as mean ± SEM. Triplicate wells for ***(A-C)*** one or ***(D)*** three experiments are represented. C3HeB/FeJ are shown in light brown and C57BL/6 in dark blue. Statistical analysis was performed using two-way ANOVA with Tukey's multiple comparison test. Differences between groups were considered significant if $p < 0.05$. ***Abbreviations:*** bdl, below detection level; BMDM, bone marrow-derived macrophages; h.p.i., hours post-infection; IFNβ, interferon-β; IL, interleukin; Mtb, *M. tuberculosis*; NI, non-infected.

Conversely, immune mediators such as IL-10 (*Figure 4B*), IL-27 (*Figure 4C*), and nitric oxide (*Figure 4D*) exhibited an inverse pattern to IL-1β, with infected C3HeB/FeJ macrophages secreting higher levels than C57BL/6 macrophages. Due to their role in IL-1β regulation, IL-10, IL-27, and nitric oxide emerged as potential candidates for the deficient IL-1β response observed in C3HeB/FeJ macrophages.

Several other pro-inflammatory cytokines, including TNF-α, IL-1α, IL-6, IL-23, GM-CSF, and IL-12p70, were measured in the supernatant of infected BMDM. We observed higher secretion levels in infected C57BL/6 BMDM compared to C3HeB/FeJ, mirroring the pattern observed with IL-1β (*Supplementary Figure 7*). This may suggest a broader

suppression of pro-inflammatory responses beyond just IL-1β in C3HeB/FeJ macrophages. The exception to this pattern was CCL2, a chemokine associated with increased disease severity[58].

The reduced IL-1β response in C3HeB/FeJ mice aligns with their increased susceptibility to tuberculosis and may result from bacterial evasion strategies or host-specific regulatory mechanisms[48]. Our preliminary data suggest that IL-10, IL-27, and iNOS signalling may play a crucial role in restricting IL-1β responses in C3HeB/FeJ macrophages. To elucidate the contribution of these immune mediators to disease susceptibility, future studies should assess whether these immune mediators are similarly altered in vivo and explore whether pharmacologically targeting these pathways would impact IL-1β production and mitigate disease severity. Moreover, expanding these observations to LPS- and ATP-stimulated BMDMs could provide broader insights into whether these immune regulatory patterns are specific to *M. tuberculosis* infection or represent a more general immune response mechanism intrinsic to C3HeB/FeJ macrophages.

CONCLUSIONS

Tuberculosis remains a global health crisis that affects millions of people every year[1]. Our exploratory study underscores the intricate relationship between host genetics, pathogen diversity, and immune responses in shaping tuberculosis outcomes. Using the tuberculosis-resistant C57BL/6 and tuberculosis-susceptible C3HeB/FeJ mice, we observed distinct immune response profiles to infection with *M. tuberculosis* clinical isolates, suggesting that host genetic background plays a central role in regulating immune responses to *M. tuberculosis*, potentially overriding pathogen-driven immune modulation.

Nonetheless, our findings also revealed key differences attributable to the infecting *M. tuberculosis* clinical isolates. Notably, infection with *M. tuberculosis* 6C4 resulted in a more severe disease phenotype, characterised by higher bacterial burdens, more extensive lung pathology, and increased immune cell infiltration. This aligns with previous observations of *M. tuberculosis* 6C4 being associated with severe tuberculosis in human patients[25]. In contrast, *M. tuberculosis* 4I2 induced a comparatively milder infection, with lower bacterial loads and lung pathology. The distinction between these two isolates was particularly evident in C57BL/6 mice. Collectively, these data suggest that bacterial virulence traits directly influence host immunity. Importantly, this clear stratification of disease severity depending on the infecting strain was less pronounced in C3HeB/FeJ mice, where the host-driven immune suppression mechanisms (such as elevated IL-27, IL-10, and nitric oxide) appeared to limit the capacity to distinguish between the two strains. Our study reinforces the importance of host-pathogen interactions in tuberculosis pathogenesis, shedding light on potential immune mechanisms that contribute to disease severity. While we provide an initial framework for understanding these dynamics, future research should focus on increasing the sample size and validating these findings, while exploring the mechanisms underlying disease susceptibility and discriminating host-driven immune regulation from pathogen-specific virulence strategies.

ACKNOWLEDGEMENTS

This work was financed through FCT – Fundação para a Ciência.e Tecnologia (PTDC/SAU-INF/1172/2021), and the La Caixa Foundation (HR21-00415). AIF, DS, and RG were funded by FCT through PhD grants references 2020.05949.BD, SFRH/BD/143536/2019, and 2022.12852.BD, respectively. MS was funded by FCT – Estímulo Individual ao Emprego Científico (2019-2025), reference CEECIND/00241/2017.

REFERENCES

1. World Health Organization. Global Tuberculosis Report. (2024).

2. O'Garra, A. et al. The immune response in tuberculosis. Annu Rev Immunol 31, 475–527 (2013).

3. Bastos, H. N., Osório, N. S., Gagneux, S., Comas, I. & Saraiva, M. The Troika Host-Pathogen-Extrinsic Factors in Tuberculosis: Modulating Inflammation and Clinical Outcomes. Front Immunol 8, (2018).

4. Fogel, N. Tuberculosis: a disease without boundaries. Tuberculosis (Edinb) 95, 527–531 (2015).

5. Barry, C. E. et al. The spectrum of latent tuberculosis: rethinking the biology and intervention strategies. Nat Rev Microbiol 7, 845–855 (2009).

6. Pai, M. et al. Tuberculosis. Nat Rev Dis Primers 2, (2016).

7. Singhania, A., Wilkinson, R. J., Rodrigue, M., Haldar, P. & O'Garra, A. The value of transcriptomics in advancing knowledge of the immune response and diagnosis in tuberculosis. Nat Immunol 19, 1159–1168 (2018).

8. Berry, M. P. R. et al. An interferon-inducible neutrophil-driven blood transcriptional signature in human tuberculosis. Nature 466, 973–977 (2010).

9. Moreira-Teixeira, L. et al. Mouse transcriptome reveals potential signatures of protection and pathogenesis in human tuberculosis. Nat Immunol 21, 464–476 (2020).

10. Cadena, A. M., Fortune, S. M. & Flynn, J. L. Heterogeneity in tuberculosis. Nat Rev Immunol 17, 691–702 (2017).

11. Cadena, A. M., Flynn, J. L. & Fortune, S. M. The Importance of First Impressions: Early Events in *Mycobacterium tuberculosis* Infection Influence Outcome. mBio 7, (2016).

12. Huang, L., Nazarova, E. V., Tan, S., Liu, Y. & Russell, D. G. Growth of *Mycobacterium tuberculosis* in vivo segregates with host macrophage metabolism and ontogeny. J Exp Med 215, 1135–1152 (2018).

13. Lowe, D. M., Redford, P. S., Wilkinson, R. J., O'Garra, A. & Martineau, A. R. Neutrophils in tuberculosis: friend or foe? Trends Immunol 33, 14–25 (2012).

14. Corleis, B. & Dorhoi, A. Early dynamics of innate immunity during pulmonary tuberculosis. Immunol Lett 221, 56–60 (2020).

15. Singhania, A. et al. A modular transcriptional signature identifies phenotypic heterogeneity of human tuberculosis infection. Nat Commun 9, (2018).

16. Kramnik, I. & Beamer, G. Mouse models of human TB pathology: roles in the analysis of necrosis and the development of host-directed therapies. Semin Immunopathol 38, 221–237 (2016).

17. Pichugin, A. V., Yan, B. S., Sloutsky, A., Kobzik, L. & Kramnik, I. Dominant role of the sst1 locus in pathogenesis of necrotizing lung granulomas during chronic tuberculosis infection and reactivation in genetically resistant hosts. Am J Pathol 174, 2190–2201 (2009).

18. Cooper, A. M., Mayer-Barber, K. D. & Sher, A. Role of innate cytokines in mycobacterial infection. Mucosal Immunol 4, 252–260 (2011).

19. Behar, S. M., Divangahi, M. & Remold, H. G. Evasion of innate immunity by *Mycobacterium tuberculosis*: is death an exit strategy? Nat Rev Microbiol 8, 668–674 (2010).

20. Flynn, J. L. & Chan, J. Immunology of tuberculosis. Annu Rev Immunol 19, 93–129 (2001).

21. Moreira-Teixeira, L. et al. Type I IFN Inhibits Alternative Macrophage Activation during *Mycobacterium tuberculosis* Infection and Leads to Enhanced Protection in the Absence of IFN-γ Signaling. J Immunol 197, 4714–4726 (2016).

22. Carmona, J. et al. *Mycobacterium tuberculosis* Strains Are Differentially Recognized by TLRs with an Impact on the Immune Response. PLoS One 8, (2013).

23. Koleske, B. N., Jacobs, W. R. & Bishai, W. R. The *Mycobacterium tuberculosis* genome at 25 years: lessons and lingering questions. J Clin Invest 133, (2023).

24. Guyeux, C. et al. Newly Identified *Mycobacterium africanum* Lineage 10, Central Africa. Emerg Infect Dis 30, 560–563 (2024).

25. Sousa, J. et al. *Mycobacterium tuberculosis* associated with severe tuberculosis evades cytosolic surveillance systems and modulates IL-1β production. Nat Commun 11, (2020).

26. Bastos, H. N. et al. A Prediction Rule to Stratify Mortality Risk of Patients with Pulmonary Tuberculosis. PLoS One 11, (2016).

27. Maceiras, A. R., Silvério, D., Gonçalves, R., Cardoso, M. S. & Saraiva, M. Infection with hypervirulent *Mycobacterium tuberculosis* triggers emergency myelopoiesis but not trained immunity. Front Immunol 14, (2023).

28. Fonseca, K. L. et al. Deficiency in the glycosyltransferase Gcnt1 increases susceptibility to tuberculosis through a mechanism involving neutrophils. Mucosal Immunol 13, 836–848 (2020).

29. Rothchild, A. C. et al. Alveolar macrophages generate a noncanonical NRF2-driven transcriptional response to *Mycobacterium tuberculosis* in vivo. Sci Immunol 4, (2019).

30. Fernandes, A. I. et al. Genetically diverse *Mycobacterium tuberculosis* isolates manipulate inflammasome activation and IL-1β secretion independently of macrophage metabolic rewiring. J Infect Dis (2024) doi:10.1093/INFDIS/JIAE583.

31. Berg, S. et al. ilastik: interactive machine learning for (bio)image analysis. Nat Methods 16, 1226–1232 (2019).

32. Lamprecht, M. R., Sabatini, D. M. & Carpenter, A. E. CellProfiler: free, versatile software for automated biological image analysis. Biotechniques 42, 71–75 (2007).

33. Gagneux, S. Ecology and evolution of *Mycobacterium tuberculosis*. Nat Rev Microbiol 16, 202–213 (2018).

34. Sakai, S., Mayer-Barber, K. D. & Barber, D. L. Defining Features of Protective CD4 T cell responses to *Mycobacterium tuberculosis*. Curr Opin Immunol 0, 137 (2014).

35. Bohrer, A. C. et al. Eosinophils are part of the granulocyte response in tuberculosis and promote host resistance in mice. J Exp Med 218, (2021).

36. Lasco, T. M. et al. Rapid accumulation of eosinophils in lung lesions in guinea pigs infected with *Mycobacterium tuberculosis*. Infect Immun 72, 1147–1149 (2004).

37. Prakash Babu, S., Narasimhan, P. B. & Babu, S. Eosinophil Polymorphonuclear Leukocytes in TB: What We Know so Far. Front Immunol 10, (2019).

38. Gern, B. H. et al. CD4-mediated immunity shapes neutrophil-driven tuberculous pathology. bioRxiv (2024) doi:10.1101/2024.04.12.589315.

39. Linge, I., Kondratieva, E. & Apt, A. Prolonged B-Lymphocyte-Mediated Immune and Inflammatory Responses to Tuberculosis Infection in the Lungs of TB-Resistant Mice. Int J Mol Sci 24, (2023).

40. Mantovani, A., Dinarello, C. A., Molgora, M. & Garlanda, C. Interleukin-1 and Related Cytokines in the Regulation of Inflammation and Immunity. Immunity 50, 778–795 (2019).

41. Dudek, M. et al. Lung epithelium and myeloid cells cooperate to clear acute pneumococcal infection. Mucosal Immunol 9, 1288–1302 (2016).

42. Bohrer, A. C., Tocheny, C., Assmann, M., Ganusov, V. V. & Mayer–Barber, K. D. Cutting Edge: IL-1R1 Mediates Host Resistance to *Mycobacterium tuberculosis* by Trans-Protection of Infected Cells. J Immunol 201, 1645–1650 (2018).

43. Cohen, S. B. et al. Alveolar Macrophages Provide an Early *Mycobacterium tuberculosis* Niche and Initiate Dissemination. Cell Host Microbe 24, 439-446.e4 (2018).

44. Bergsbaken, T., Fink, S. L. & Cookson, B. T. Pyroptosis: host cell death and inflammation. Nat Rev Microbiol 7, 99 (2009).

45. Rastogi, S., Ellinwood, S., Augenstreich, J., Mayer-Barber, K. D. & Briken, V. *Mycobacterium tuberculosis* inhibits the NLRP3 inflammasome activation via its phosphokinase PknF. PLoS Pathog 17, e1009712 (2021).

46. Zamyatina, A. & Heine, H. Lipopolysaccharide Recognition in the Crossroads of TLR4 and Caspase-4/11 Mediated Inflammatory Pathways. Front Immunol 11, (2020).

47. Di Virgilio, F. Liaisons dangereuses: P2X(7) and the inflammasome. Trends Pharmacol Sci 28, 465–472 (2007).

48. Silvério, D., Gonçalves, R., Appelberg, R. & Saraiva, M. Advances on the Role and Applications of Interleukin-1 in Tuberculosis. mBio 12, (2021).

49. Lúcia Moreira-Teixeira, Mayer-Barber, K., Sher, A. & O'Garra, A. Type I interferons in tuberculosis: Foe and occasionally friend. J Exp Med 215, 1273–1285 (2018).

50. Moreira-Teixeira, L. et al. Type I IFN exacerbates disease in tuberculosis-susceptible mice by inducing neutrophil-mediated lung inflammation and NETosis. Nat Commun 11, (2020).

51. Mayer-Barber, K. D. & Yan, B. Clash of the Cytokine Titans: counter-regulation of interleukin-1 and type I interferon-mediated inflammatory responses. Cell Mol Immunol 14, 22–35 (2017).

52. Novikov, A. et al. *Mycobacterium tuberculosis* triggers host type I IFN signaling to regulate IL-1β production in human macrophages. J Immunol 187, 2540–2547 (2011).

53. Mishra, B. B. et al. Nitric oxide controls the immunopathology of tuberculosis by inhibiting NLRP3 inflammasome-dependent processing of IL-1β. Nat Immunol 14, 52–60 (2013).

54. Mishra, B. B. et al. Nitric oxide prevents a pathogen-permissive granulocytic inflammation during tuberculosis. Nat Microbiol 2, (2017).

55. Gollnick, H., Barber, J., Wilkinson, R. J., Newton, S. & Garg, A. IL-27 inhibits anti-*Mycobacterium tuberculosis* innate immune activity of primary human macrophages. Tuberculosis (Edinb) 139, (2023).

56. Ritter, K., Rousseau, J. & Hölscher, C. Interleukin-27 in Tuberculosis: A Sheep in Wolf's Clothing? Front Immunol 12, (2022).

57. Iyer, S. S., Ghaffari, A. A. & Cheng, G. Lipopolysaccharide-mediated IL-10 transcriptional regulation requires sequential induction of type I IFNs and IL-27 in macrophages. J Immunol 185, 6599–6607 (2010).

58. Hasan, Z. et al. CCL2 responses to *Mycobacterium tuberculosis* are associated with disease severity in tuberculosis. PLoS One 4, (2009).

CHAPTER 4

SUPPLEMENTARY INFORMATION

SUPPLEMENTARY FIGURES

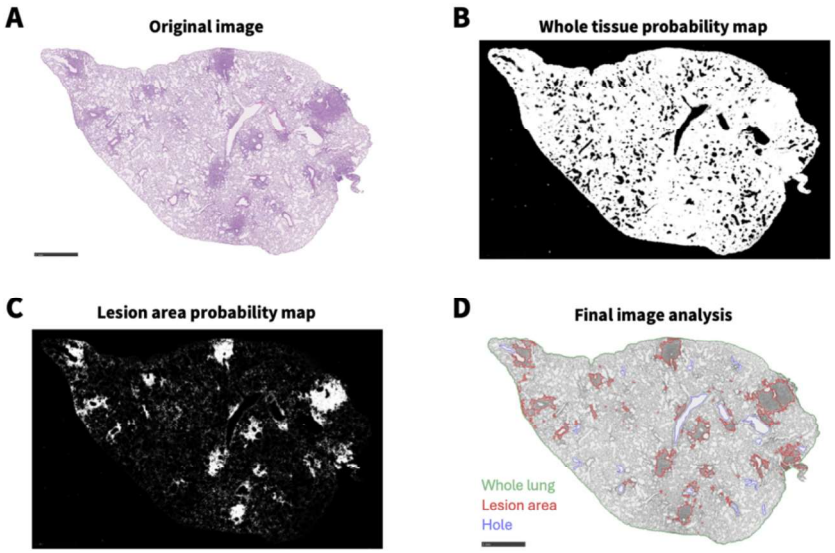

Supplementary Figure 1. Representative images obtained during morphometric analysis of lung histopathology. ***(A)*** Image of a mouse's lung slide stained with H&E. ***(B-C)*** Whole tissue and lesion probability maps with the background in black and the lung tissue and lesions in white. ***(D)*** Image output from the morphometric analysis used to calculate the percentage of lesion areas in the lung slices. The whole lung tissue, lung lesions, and holes are outlined in green, red, and blue, respectively.

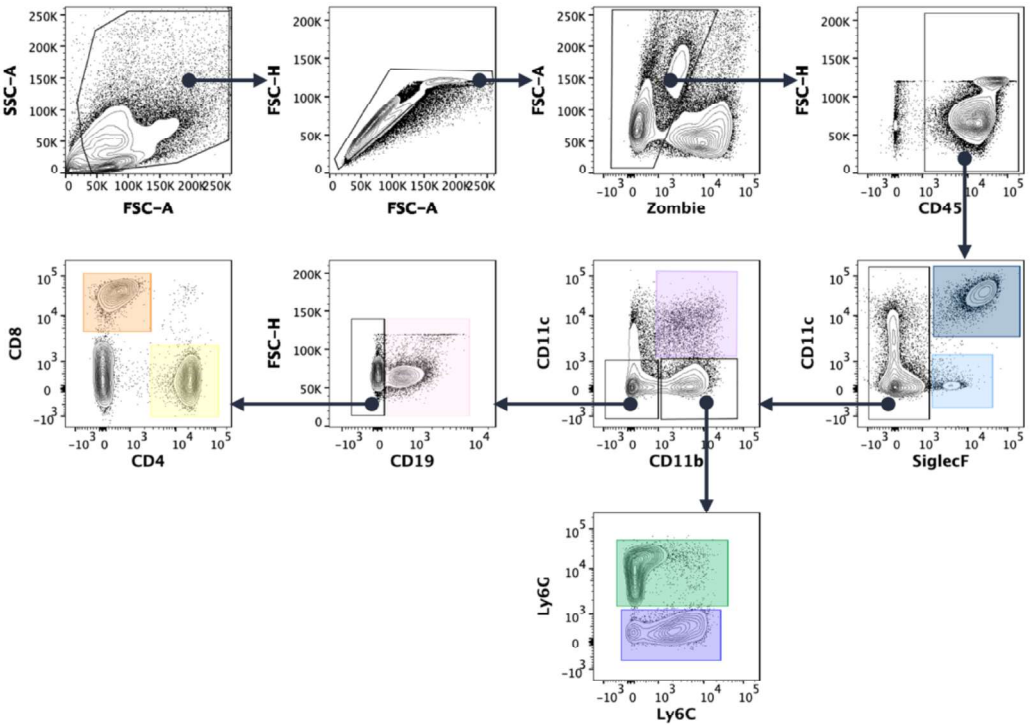

Supplementary Figure 2. Gating strategy for analysis of mature immune cell populations in the lung and bronchoalveolar lavage by flow cytometry. Tinted gates illustrate the cell populations represented and analysed in *Figure 2* and *Supplementary Figure 4A* (alveolar macrophages in dark blue, eosinophils in light blue, neutrophils in green, macrophages in dark purple, dendritic cells in light purple, B cells in beige, $CD4^+$ T cells in yellow, and $CD8^+$ T cells in orange). ***Abbreviations:*** CD, cluster of differentiation.

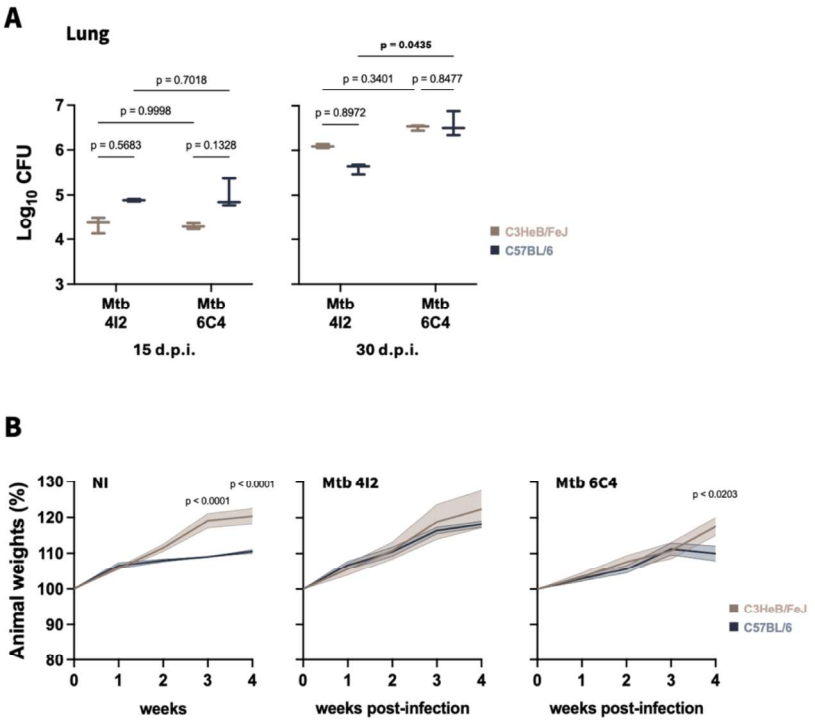

Supplementary Figure 3. Bacterial burden and weight variation over time in C3HeB/FeJ and C57BL/6 mice following *M. tuberculosis* infection. C3HeB/FeJ and C57BL/6 mice were infected via aerosol with *M. tuberculosis* 4l2 or 6C4. ***(A)*** Bacterial burdens in the lungs (n = 3 for each condition) of *M. tuberculosis*-infected mice 15- and 30-days post-infection, quantified by CFU enumeration. The infection doses for the experiments used in this figure were 920 ± 57 CFU/lung (*M. tuberculosis* 4l2) and 857 ± 13 CFU/lung (*M. tuberculosis* 6C4). Animals were 10.7 ± 0.3 weeks old at the beginning of the experiment. ***(B)*** Percentage of weight variation over time. Mice were weighed weekly. The infection doses for the experiments used in this figure were 460 ± 34 CFU/lung (*M. tuberculosis* 4l2, n = 10 for each condition) and 448 ± 29 CFU/lung (*M. tuberculosis* 6C4, n = 8 for each condition). Infected and non-infected animals (n = 4 for each condition) were 8.9 ± 0.2 weeks old. Represented are the mean ± SEM. C3HeB/FeJ mice are represented in light brown and C57BL/6 mice in dark blue. Statistical analysis was performed using a two-way ANOVA. Differences between groups were considered significant if $p < 0.05$. ***Abbreviations:*** d.p.i., days post-infection; Mtb, *M. tuberculosis*; NI, non-infected.

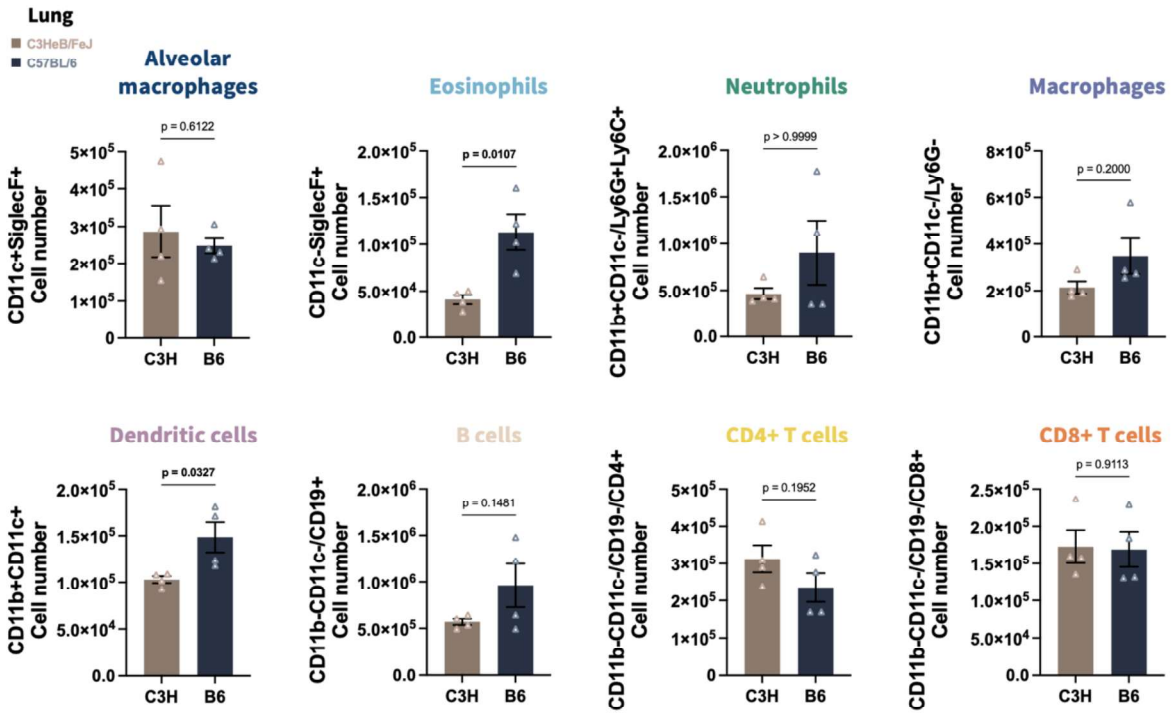

Supplementary Figure 4. Total cell numbers in the lungs of C3HeB/FeJ and C57BL/6 uninfected mice. Non-infected mice were 8.8 ± 0.2 weeks old at the beginning of the experiment. Lung cell numbers for mature immune cell populations were determined through flow cytometry (n = 4 for each condition), employing the gating strategy outlined in *Supplementary Figure 2*. Represented are the mean ± SEM. C3HeB/FeJ mice are represented in light brown and C57BL/6 mice in dark blue. Statistical analysis was performed using an unpaired *t*-test. Differences between groups were considered significant if $p < 0.05$. ***Abbreviations:*** B6, C57BL/6; C3H, C3HeB/FeJ; CD, cluster of differentiation.

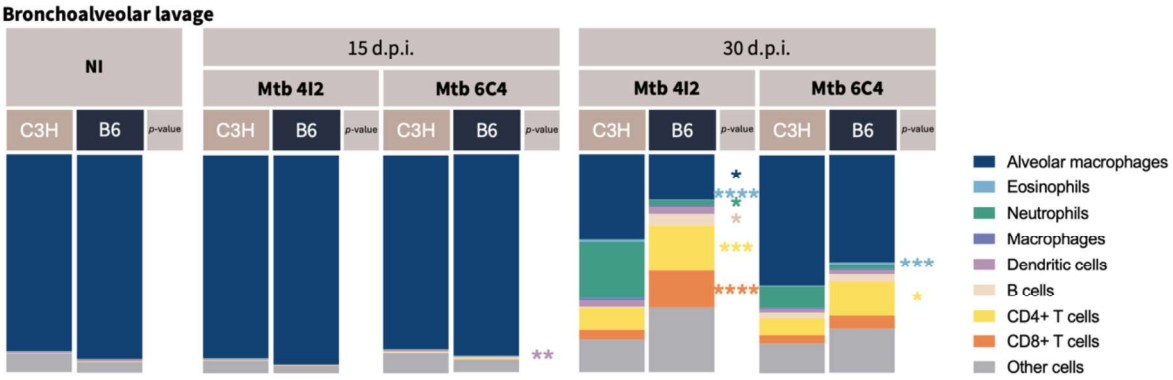

Supplementary Figure 5. The immune cell recruitment in the bronchoalveolar lavage of C3HeB/FeJ and C57BL/6 mice following *M. tuberculosis* infection mirrors alterations observed in the lung. C3HeB/FeJ and C57BL/6 mice were infected via aerosol with *M. tuberculosis* 4I2 or 6C4. The infection doses for the experiments used in this figure were 460 ± 34 CFU/lung (*M. tuberculosis* 4I2) and 403 ± 12 CFU/lung (*M. tuberculosis* 6C4). Infected and non-infected animals were 8.8 ± 0.2 weeks old at the beginning of the experiment. At the specified time points, bronchoalveolar lavage was collected (n = 4 for each condition). Cell frequencies for mature immune cell populations were determined through flow cytometry, employing the gating strategy outlined in *Supplementary Figure 2*. Statistical analysis was performed using an unpaired *t*-test. Differences between groups were considered significant if $p < 0.05$ and represented in the graphs (* $p < 0.05$, ** $p < 0.01$, *** $p < 0.001$, **** $p < 0.0001$). Alveolar macrophages are represented in dark blue, eosinophils in light blue, neutrophils in green, macrophages in dark purple, dendritic cells in light purple, B cells in beige, CD4+ T cells in yellow, CD8 T cells in orange, and other cells in grey. ***Abbreviations**:* B6, C57BL/6; C3H, C3HeB/FeJ; CD, cluster of differentiation; d.p.i., days post-infection; Mtb, *M. tuberculosis*; NI, non-infected.

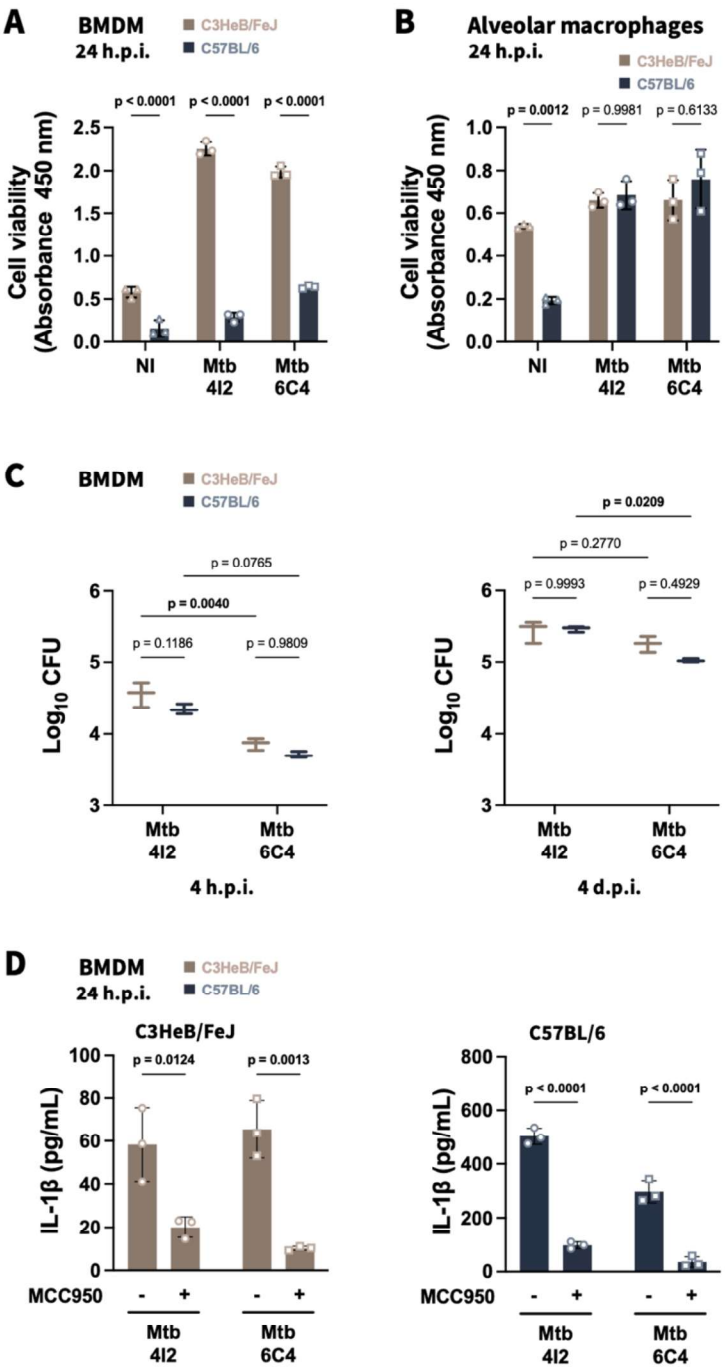

Supplementary Figure 6. *Legend on the next page.*

Supplementary Figure 6 continued. C3HeB/FeJ macrophages show increased viability compared to C57BL/6 macrophages and no differences in bacterial burden. Mouse BMDM and alveolar macrophages were infected with either clinical isolate at an MOI of 2 and 1, respectively. Cell viability in ***(A)*** BMDM and ***(B)*** alveolar macrophages was assessed 24 hours post-infection using the ORANGU cell counting solution colourimetric assay. ***(C)*** Differences in the bacterial burden of *M. tuberculosis* 4I2 or 6C4 in C3HeB/FeJ and C57BL/6 BMDM were measured 4 hours and 4 days post-infection by CFU enumeration. ***(D)*** Mouse BMDM were left untreated (−) or pretreated (+) for 2 hours with MCC950 (selective NLRP3 inflammasome inhibitor) and subsequently infected at an MOI of 2 with either clinical isolate. MCC950 were maintained for the duration of the experiment. The amount of secreted IL-1β was quantified in the cell culture supernatants 24 hours post-infection. Represented are ***(A,B,D)*** the mean ± SEM, or ***(C)*** box and whisker plots (Tukey's method) of triplicate wells for 1 experiment. C3HeB/FeJ mice are represented in light brown and C57BL/6 mice in dark blue. Statistical analysis was performed using two-way ANOVA with Tukey's multiple comparison test. Differences between groups were considered significant if $p < 0.05$. ***Abbreviations:*** BMDM, bone marrow-derived macrophages; d.p.i., days post-infection; h.p.i., hours post-infection; IL-1β, interleukin 1β; Mtb, *M. tuberculosis*; NI, non-infected; NLRP3, NLR family pyrin domain–containing-3.

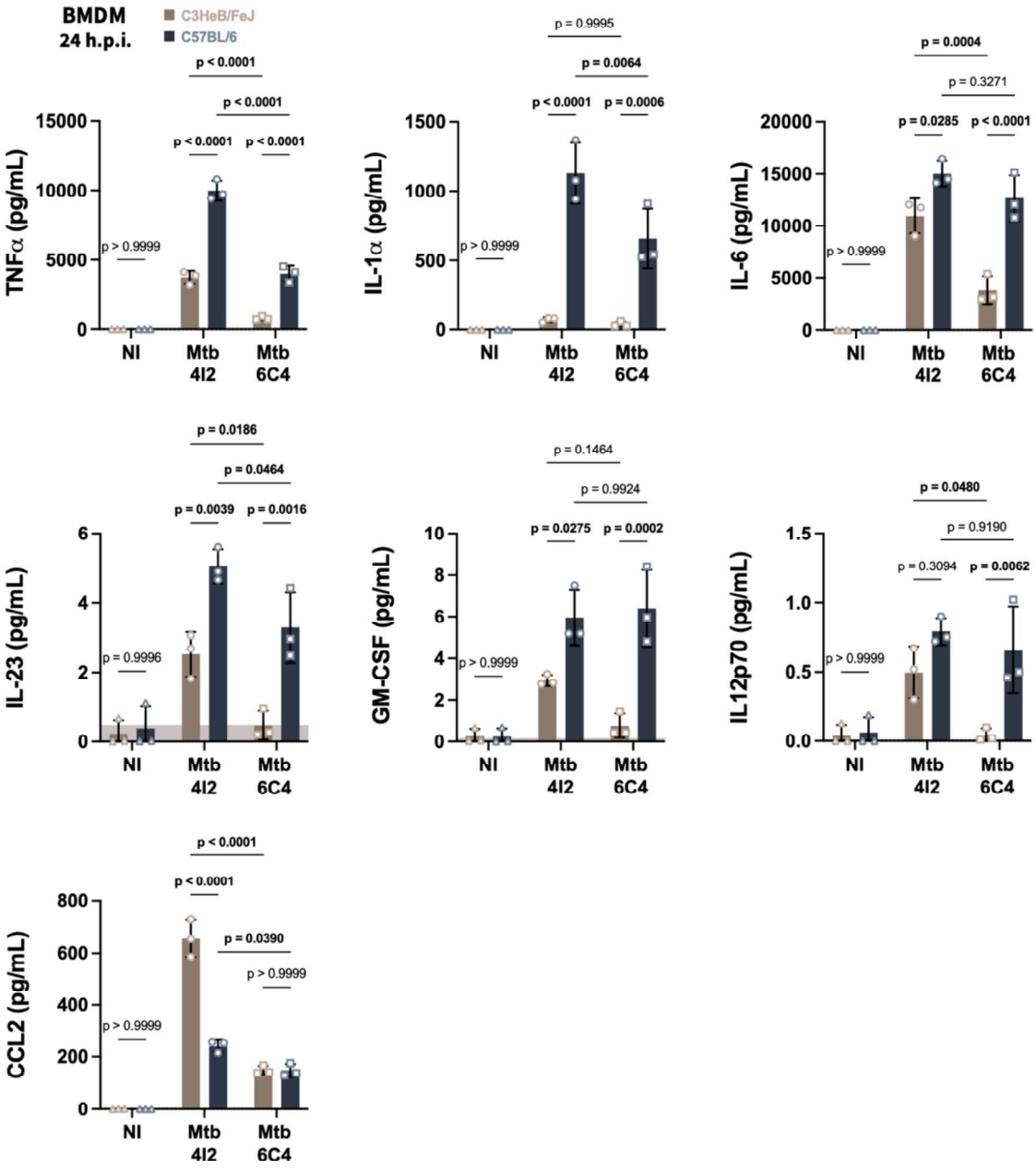

Supplementary Figure 7. C3HeB/FeJ macrophages exhibit a lower pro-inflammatory cytokine profile. Mouse BMDM were infected at an MOI of 2 with either *M. tuberculosis* 4I2 or 6C4. The amounts of secreted cytokines were quantified in the cell culture supernatants 24 hours post-infection through a bead-based immunoassay. Values within the tinted brown area were considered below the detection level and extrapolated. Represented are triplicate wells of one experiment. Data is expressed as mean ± SEM. C3HeB/FeJ macrophages are shown in light brown and C57BL/6 in dark blue. Statistical analysis was performed using two-way ANOVA with Tukey's multiple comparison test. Differences between groups were considered significant if $p < 0.05$. ***Abbreviations:*** BMDM, bone marrow-derived macrophages; CCL2, C-C motif chemokine ligand 2; GM-CSF, Granulocyte-macrophage colony-stimulating factor; h.p.i., hours post-infection; IL, interleukin; Mtb, *M. tuberculosis*; NI, non-infected; TNFα, tumour necrosis factor α.

SUPPLEMENTARY TABLES

Supplementary Table 1. List of materials and resources.

Reagents and resources	Supplier
Reagents	
Adenosine Triphosphate (ATP)	InvivoGen
Ammonium Chloride (NH_4CL)	Sigma-Aldrich
Bovine Serum Albumin	Sigma-Aldrich
Collagenase D	Merck
D(+)-Glucose Monohydrate	Merck
DIFCO™ Middlebrook 7H9 Broth	BD Biosciences
DIFCO™ Middlebrook 7H11 Agar	BD Biosciences
DMEM, High Glucose, GlutaMAX™ Supplement, Pyruvate	Gibco
Ethylenediaminetetraacetic Acid (EDTA)	Sigma-Aldrich
Foetal Bovine Serum (FBS) Heat Inactivated	Gibco
Formalin 10% Solution Neutral Buffered	Bio-Optica
Glycerol (for Molecular Biology >99%)	Merck
Glycogen	Merck
Hanks' Balanced Salt Solution (HBSS)	Gibco
HEPES Buffer Solution (1 M)	Gibco
iTaq™ Universal SYBR® Green Supermix	Bio-Rad
L-Glutamine	Gibco
LEGENDplex™ Mouse Inflammation Panel (13-plex)	BioLegend
Lipopolysaccharide (LPS)	Sigma-Aldrich
MGIT PANTA antibiotic	Quilaban
Mouse IL-1 beta Uncoated ELISA Kit	Invitrogen
N-(1-Naphthyl) Ethylenediamine Dihydrochloride	Sigma-Aldrich
Oleic Acid-Albumin from Bovine Serum	Sigma-Aldrich
Orangu™ Cell Counting Solution	Cell Guidance Systems
Penicillin-Streptomycin (10 000 $U\text{-}mL^{-1}$)	Gibco
Phosphate-Buffered Saline (PBS) 1x, pH 7.4	Gibco
Phosphoric Acid (H_3PO_4)	Merck
Potassium Bicarbonate ($KHCO_3$)	Sigma-Aldrich
ProtoScript® First Strand cDNA Synthesis Kit	New England Biolabs
Roswell Park Memorial Institute (RPMI) 1640	Gibco
Saponin from Quillaja Bark	Sigma-Aldrich
Sodium Chloride (NaCl)	Sigma-Aldrich
Sodium Hydroxyde (NaOH)	Sigma-Aldrich
Sodium Nitrite ($NaNO_2$)	Merck
Sodium Pyruvate (100 mM)	Merck
Sulfanilamide	Merck
TripleXtractor Reagent	GRiSP Research Solutions
Trypan Blue Stain (0.4%)	Gibco

Supplementary Table 1. *Continued.*

Reagents and resources	Supplier
Antibodies	
APC Anti-Mouse CD170 (Siglec-F, Clone S17007L, 1:200)	BioLegend
APC/Cyanine7 Anti-Mouse CD19 (Clone 6D5, 1:100)	BioLegend
APC/Cyanine7 Anti-Mouse Ly-6G (Clone 1A8, 1:200)	BioLegend
Brilliant Violet 510™ Anti-Mouse/human CD11b (Clone M1/70, 1:100)	BioLegend
Brilliant Violet 650™ Anti-Mouse CD8a (Clone 53-6.7, 1:200)	BioLegend
Brilliant Violet 785™ Anti-Mouse CD4 (Clone GK1.5, 1:200)	BioLegend
BD OptiBuild™ BV786 Rat Anti-Mouse Siglec-F (Clone E50-2440, 1:200)	BD Biosciences
FITC Anti-Mouse CD8a (Clone 5H10-1, 1:200)	BioLegend
Pacific Blue™ Anti-Mouse Ly-6C (Clone HK1.4, 1:300)	BioLegend
PE Anti-Mouse CD11b (Clone M1/70, 1:400)	BioLegend
PE Anti-Mouse CD45 (Clone 30-F11, 1:400)	BioLegend
PE/Cyanine7 Anti-Mouse CD11c (Clone N418, 1:200)	BioLegend
PerCP/Cyanine5.5 Anti-Mouse CD45 (Clone 30-F11, 1:400)	BioLegend
PerCP/Cyanine5.5 Anti-Mouse Ly-6G (Clone 1A8, 1:300)	BioLegend
TruStain FcX Anti-Mouse CD16/32 Antibody (Clone 93, 1:200)	BioLegend
Zombie AmCyan™ Fixable Viability Kit (1:500)	BioLegend
Zombie Green™ Fixable Viability Kit (1:500)	BioLegend
Chemical Inhibitors	
MCC950 (1 µM)	InvivoGen
Material and Equipment	
BD Accuri™ C6 Plus	BD Biosciences
BD LSRFortessa™	BD Biosciences
CFX384 Real-Time PCR Detection System	Bio-Rad
Glas-Col Inhalation Exposure System	Glas-Col
NanoDrop 1000 Spectrophotometer	Thermo Scientific
NanoZoomer 2.0-HT Whole Slide Imager, Digital Pathology Slide Scanner	Hamamatsu Photonics
Synergy 2	BioTek
T100 Thermal Cycler	Bio-Rad
Software	
CellProfiler™ v4.2.8	Lamprecht et al (2007) Biotechniques
CFX Manager™	Bio-Rad
FlowJo™ v10.10	BD Life Sciences
GraphPad Prism v10.0.0	Dotmatics
Interactive Learning and Segmentation Toolkit (ilastik) v1.4.0	Berg et al (2019) Nat. Methods
LEGENDplex™ Cloud-based Data Analysis	BioLegend with Qognit
NDP.view 2	Hamamatsu Photonics

Supplementary Table 2. Histological features used for qualitative analysis of the lung pathology.

Score	Description	Key Features
0	Normal	- No signs of inflammation or structural damage.
1	Initial signs of lesion	- Few small infiltrates of inflammatory cells; - Mainly composed of myeloid cells; - Perivascular location; - No additional damage.
2	Mild lesion	- Small but well-formed infiltrates of inflammatory cells; - Composed of myeloid and lymphoid cells; - Perivascular location; - No additional damage.
3	Moderate lesion	- Medium-sized lesions or multiple small lesions; - Composed of macrophages, granulocytes, and lymphocytes; - May show signs of congestion.
4	Severe lesion	- Multiple medium lesions or a few extensive ones; - Presence of multiple cell types; - Presence of necrotic areas, cellular debris, and congestion.
5	Extensive lesion	- Lungs almost entirely covered with lesions; - Presence of diverse cell types; - Necrotic ones at lesion centers; - Presence of congestion, edema, and damaged epithelium.

Supplementary Table 3. List of oligonucleotide sequences.

Gene name	Oligonucleotide sequence (5'-3')	Provider
Gapdh	Forward: CTGACGTGCCGCCTGGAGAAA Reverse: AGCCCCGGCATCGAAGGTGG	Invitrogen
Il1b	Forward: ACCTTCCAGGATGAGGACATGA Reverse: AACGTCACACACCAGCAGGTTA	Invitrogen
Ubiquitin	Forward: TGGCTATTAATTATTGGGTCTGCAT Reverse: GCAAGTGGCTAGAGTGCAGAGTAA	Invitrogen

CHAPTER 5

GENERAL DISCUSSION

CHAPTER 5

GENERAL DISCUSSION

Tuberculosis remains a persistent challenge in modern medicine, largely due to its remarkable heterogeneity, with clinical presentations ranging from mild to severe disease[1]. Understanding the factors that contribute to these divergent outcomes remains a key question in tuberculosis research. A previous study from our lab identified two *Mycobacterium tuberculosis* clinical isolates, 4I2 and 6C4, associated with mild and severe disease, respectively[2]. Notably, while *M. tuberculosis* 4I2 infection robustly induces inflammasome-mediated interleukin (IL)-1β, *M. tuberculosis* 6C4 infection efficiently evades the macrophage cytosolic surveillance systems, resulting in attenuated IL-1β levels[2]. These isolates provided an ideal system to investigate not only how bacterial diversity shapes host immunity and disease severity, but also how IL-1β shapes the response to *M. tuberculosis*, as its varying roles throughout infection.

Given the well-documented link between metabolism, inflammasome activation and IL-1β production[3], we first aimed to determine whether the differential IL-1β production observed upon infection with *M. tuberculosis* 4I2 and 6C4 was linked to distinct metabolic reprogramming in macrophages. Surprisingly, despite differences in inflammasome activation and IL-1β production, the metabolic landscape of macrophages infected with the two distinct *M. tuberculosis* clinical isolates was remarkably similar. Both high and low IL-1β-inducing isolates promoted a similar glycolytic shift in macrophages, with glycolysis being essential for IL-1β production regardless of the bacterial infecting strain. However, unlike models based on single Toll-like receptor (TLR) agonists, IL-1β production in *M. tuberculosis*-infected macrophages was independent of mitochondrial metabolic changes and hypoxia-inducible factor 1-alpha (HIF-1α), suggesting that the metabolic requirements for inflammasome activation in response to live *M. tuberculosis* differ from the more simplistic TLR-based models, like lipopolysaccharide (LPS) stimulation.

One of the most intriguing findings of this work was the discovery that the host metabolic inhibitor dimethyl malonate (DMM) primarily affected the pathogen. DMM reduced IL-1β, likely by inhibiting the bacterial succinate dehydrogenase (SDH), highlighting the importance of metabolically active bacteria in macrophage inflammasome activation. This

finding underscores the need to consider bacterial metabolism pathways in immunometabolic studies.

Although this work has advanced our understanding of macrophage responses to *M. tuberculosis*, a fundamental question still remains: What bacterial factors drive the observed differential inflammasome activation and IL-1β production in macrophages? Our intracellular metabolomics analysis provided a possible clue, as we found that trehalose levels, a bacterial metabolite, were elevated in *M. tuberculosis* 6C4 conditions, both in the presence and absence of host cells (*Appendix Figure 1*). Trehalose is a nonmammalian disaccharide that can play a dual role in tuberculosis pathogenesis. While it can enhance host defences through transcription factor EB (TFEB)-mediated autophagy[4,5], it is also involved in the biosynthesis of key glycolipids from the mycobacterial cell wall responsible for inhibiting phagosome maturation, contributing to immune evasion[6]. Additionally, trehalose serves as an energy reservoir during stress that supports *M. tuberculosis* persistence[7]. This duality raises intriguing questions: Does trehalose contribute to the immune evasion strategies in *M. tuberculosis* 6C4 infection? Could we target bacterial trehalose metabolism to enhance macrophage responses? Ongoing research in the lab is now focusing on dissecting these possibilities.

Building on the lab's macrophage-focused studies with *M. tuberculosis* 4I2 and 6C4, the second part of this thesis sought to model tuberculosis severity in the mouse model using these clinical isolates. We employed two previously characterised mouse models with distinct susceptibilities to tuberculosis: C3HeB/FeJ mice, which are highly tuberculosis-susceptible and develop caseating lung lesions, and C57BL/6 mice, which are relatively tuberculosis-resistant[8]. By infecting these mice with the two clinical isolates, we aimed to determine whether the differing severities observed in patients were similarly reflected in animal models, as well as to identify immune signatures associated with tuberculosis severity.

Our results revealed striking differences in disease progression between the two mouse strains. By day 30 post-infection, aligning with their classification as tuberculosis-susceptible, C3HeB/FeJ mice exhibited higher bacterial burdens than C57BL/6 mice, independently of the bacterial strain used. Lung pathology also differed between the mice strains, with C3HeB/FeJ mice presenting neutrophil-dominated lung lesions and C57BL/6 displaying more lymphocytic lesions. Interestingly, differences in lung pathology between infections with the two *M. tuberculosis* clinical isolates were more pronounced in C57BL/6 mice than in C3HeB/FeJ mice, suggesting that host susceptibility may mask some of the bacterial strains-specific immune signatures. In C57BL/6 mice, infection with the more

severe isolate (*M. tuberculosis* 6C4) led to increased disease severity, marked by a higher cell recruitment of lymphocytes and eosinophils to the lung. While lymphocytes are overall known for their protective role in tuberculosis[9], the role of eosinophils remains unclear[10,11]. In the context of *M. tuberculosis* 6C4 infection, do eosinophils help control infection, or do their strong inflammatory effects worsen lung damage, contributing to disease severity? Additionally, while our study provides a characterisation of immune cell recruitment, spatial localisation of immune populations within lung lesions remains to be explored. Immunofluorescence-based analysis of these immune mediators could provide a more comprehensive understanding of cytokine dynamics within granulomas. Given the difficulty in identifying the precise onset of infection in humans[1], future studies should also investigate long-term infection dynamics, particularly at later time points (6 to 10 weeks post-infection), to determine how early immune responses translate into chronic disease and what differences in tuberculosis outcomes may arise.

A particularly intriguing finding of this work was the impaired IL-1β production in C3HeB/FeJ mice, both observed in the mice's lungs and at the macrophage level. Given the well-established role of IL-1β in protective immunity against *M. tuberculosis*, this deficiency likely contributes to the increased disease susceptibility in these mice. Our data suggests this suppression in C3HeB/FeJ macrophages may be mediated by IL-10, IL-27, or nitric oxide. These findings raised several questions: Does the increased anti-inflammatory signalling contribute to an environment conducive to bacterial persistence and progressive tissue damage? Could therapeutic modulation of these pathways restore IL-1β-driven protection? Additionally, how do these immune mediators interact with other signalling pathways, such as type I interferons (IFNs)[12], which have been previously implicated in tuberculosis susceptibility in C3HeB/FeJ mice? To address these questions, ongoing research in the lab is focused on dissecting the impact of these regulatory networks on disease severity.

Ultimately, both studies reinforce the central role of IL-1β in tuberculosis immunity, highlighting how its production is shaped by both bacterial strain diversity and host genetics, an interplay with direct implications for disease severity (*Figure 1*). The immune network started to be unveiled here may offer potential biomarkers for disease severity stratification and may guide the development of host-directed therapies that modulate immune responses to improve patient outcomes. Future research should focus on validating these findings in human tuberculosis cohorts and exploring targets to enhance protective immune responses. By bridging findings from in vitro models to mouse models to human disease, we advance our understanding of tuberculosis heterogeneity and pave the way for deeper

mechanistic understanding and therapeutic innovation. With continued research, these insights may contribute to improved strategies for tuberculosis control and treatment, ultimately informing the design of novel host-directed therapies that mitigate disease severity and improve patient outcomes.

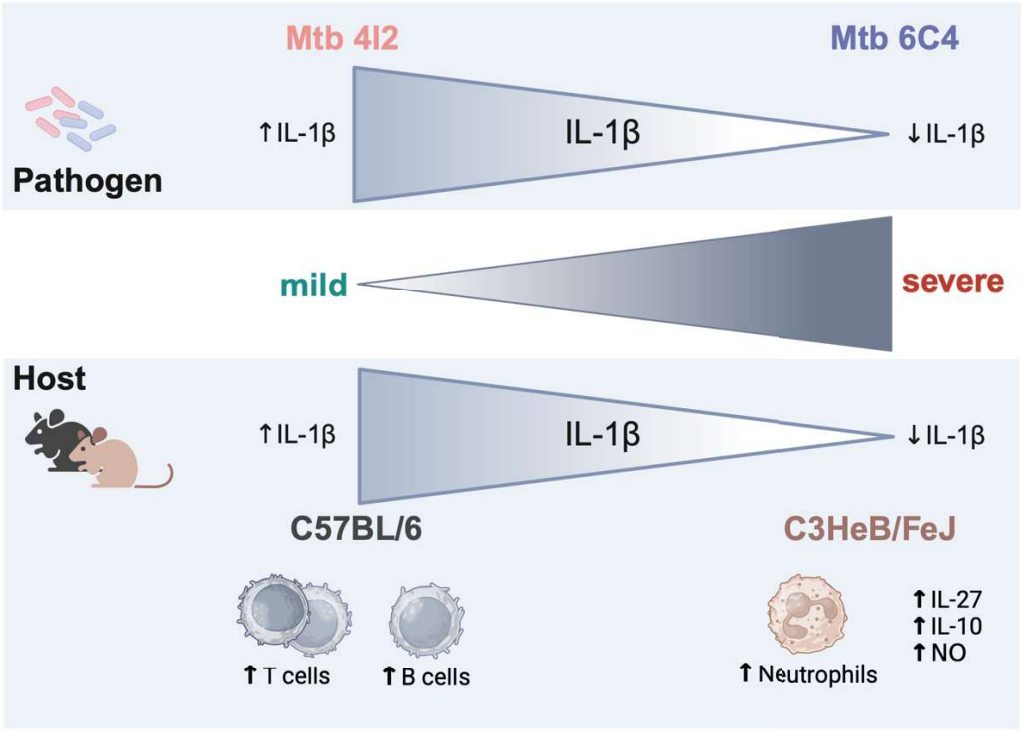

Figure 1. IL-1β modulation by the pathogen and the host shapes tuberculosis severity. IL-1β levels are differently regulated by both *M. tuberculosis* strain diversity and host genetics. Pathogen-driven modulation is evident with *M. tuberculosis* clinical isolates that induced lower levels of IL-1β, which correlated with increased disease severity in both human patients and mouse models. From the host perspective, relatively resistant C57BL/6 mice induced higher IL-1β levels and were associated with milder disease severity, driven by rapid accumulation of lymphocytes. In contrast, C3HeB/FeJ mice exhibited impaired IL-1β production, potentially linked to elevated IL-10, nitric oxide (NO), and IL-27, and were associated with increased disease severity accompanied by neutrophilic inflammation. Created in BioRender.

REFERENCES

1. Pai, M. et al. Tuberculosis. Nat Rev Dis Primers 2, (2016).

2. Sousa, J. et al. *Mycobacterium tuberculosis* associated with severe tuberculosis evades cytosolic surveillance systems and modulates IL-1β production. Nat Commun 11, (2020).

3. Haneklaus, M. & O'Neill, L. A. J. NLRP3 at the interface of metabolism and inflammation. Immunol Rev 265, 53–62 (2015).

4. Sharma, V. et al. Trehalose limits opportunistic mycobacterial survival during HIV co-infection by reversing HIV-mediated autophagy block. Autophagy 17, 476–495 (2021).

5. Jeong, S. J. et al. Trehalose causes low-grade lysosomal stress to activate TFEB and the autophagy-lysosome biogenesis response. Autophagy 17, 3740–3752 (2021).

6. Santamaria, C. et al. Trehalose dimycolate inhibits phagosome maturation and promotes intracellular *M. tuberculosis* growth via noncanonical SNARE interaction. bioRxiv (2024) doi:10.1101/2024.12.16.627577.

7. Kalera, K. et al. Targeting *Mycobacterium tuberculosis* Persistence through Inhibition of the Trehalose Catalytic Shift. ACS Infect Dis 10, 1391–1404 (2024).

8. Moreira-Teixeira, L. et al. Mouse transcriptome reveals potential signatures of protection and pathogenesis in human tuberculosis. Nat Immunol 21, 464–476 (2020).

9. Sakai, S., Mayer-Barber, K. D. & Barber, D. L. Defining Features of Protective CD4 T cell responses to *Mycobacterium tuberculosis*. Curr Opin Immunol 0, 137 (2014).

10. Bohrer, A. C. et al. Eosinophils are part of the granulocyte response in tuberculosis and promote host resistance in mice. J Exp Med 218, (2021).

11. Prakash Babu, S., Narasimhan, P. B. & Babu, S. Eosinophil Polymorphonuclear Leukocytes in TB: What We Know so Far. Front Immunol 10, (2019).

12. Moreira-Teixeira, L. et al. Type I IFN exacerbates disease in tuberculosis-susceptible mice by inducing neutrophil-mediated lung inflammation and NETosis. Nat Commun 11, (2020).

APPENDIX

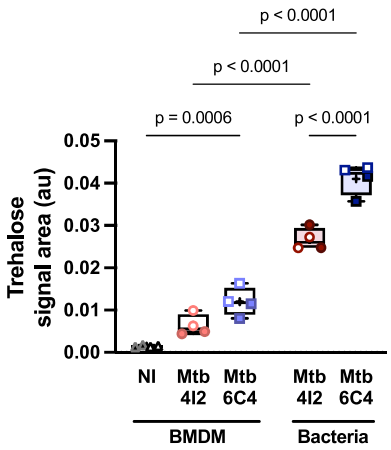

Figure 1. NMR-based metabolomics reveals increased levels of trehalose in *M. tuberculosis* 6C4 conditions. Relative intracellular levels of trehalose from intracellular aqueous extracts of non-infected BMDM, macrophages infected with *M. tuberculosis* 4I2 or 6C4 for 24 hours at an MOI of 2, and *M. tuberculosis* 4I2 or 6C4 cultured in similar medium but in the absence of host cells. Represented is a box and whisker plot (Tukey method) of duplicate wells for 2 experiments. Each replicate is a pool of 24 wells in a 24-well plate. Statistical analysis was performed using One-way ANOVA. ***Abbreviations:*** au, arbitrary units; BMDM, bone marrow-derived macrophages; MOI, multiplicity of infection; Mtb, *M. tuberculosis*; NI, non-infected.